


2022

Ammonia cycling and emerging particulate matter pollutants under arable land-use management: A modelling approach

Vivien Pohl

Technological University Dublin, vivienpohl@outlook.com

Follow this and additional works at: <https://arrow.tudublin.ie/engdoc>

 Part of the [Bioresource and Agricultural Engineering Commons](#), [Civil and Environmental Engineering Commons](#), and the [Environmental Health Commons](#)

Recommended Citation

Pohl, V. (2022). Ammonia cycling and emerging particulate matter pollutants under arable land-use management: A modelling approach. Technological University Dublin. DOI: 10.21427/M6ZZ-R957

This Theses, Ph.D is brought to you for free and open access by the Engineering at ARROW@TU Dublin. It has been accepted for inclusion in Doctoral by an authorized administrator of ARROW@TU Dublin. For more information, please contact arrow.admin@tudublin.ie, aisling.coyne@tudublin.ie, gerard.connolly@tudublin.ie.



This work is licensed under a [Creative Commons Attribution-NonCommercial-Share Alike 4.0 License](#)



Ammonia cycling and emerging particulate matter pollutants under arable land-use management: A modelling approach

By

Vivien Pohl

A thesis presented to

Technological University Dublin for the award of PhD

Prepared under the supervision of

Dr Alan Gilmer,

Dr David O'Connor,

Prof. John Cassidy,

Dr Eugene McGovern

& Dr Vivienne Byers

Water Innovation Research Centre, Environmental Sustainability and
Health Institute, Technological University Dublin, Grangegorman,
Dublin 7

School of Architecture, Building and Environment

July 2022

Abstract

Air quality monitoring in Ireland is under the jurisdiction of the Environmental Protection Agency in compliance with the Gothenburg Protocol, EU/national legislation, and the National Clean Air Strategy. Particulate Matter (PM) has been acknowledged as a key atmospheric pollutant, with serious public health impacts and no safe threshold of exposure in place to-date. Ammonia (NH_3) emissions are linked to the secondary production of PM through atmospheric reactions occurring with acidic atmospheric components such as sulfuric acid, nitric acid, and hydrochloric acid. These reactions result in the formation of ammonium sulfate, ammonium nitrate and ammonium chloride, among others. More than 95% of NH_3 emissions occurring in Ireland arise from agriculture, with minor contributions from transport and natural sources.

This study aims to advance knowledge and understanding of the role of arable agricultural practices and management in NH_3 enrichment and aid in mapping of the sources of PM production. The nature and contribution of NH_3 in the atmosphere to secondary PM in defined arable settings will be examined to provide greater insight into system dynamics facilitating emission control and mitigation measures to be implemented. This will be achieved through a review of existing literature and database assessment combined with the application of a localised field monitoring network in arable agricultural settings.

As Ireland currently has no active atmospheric NH_3 monitoring in place, reported emission levels can prove to be imprecise. And lead to over- and under-estimation of NH_3 gas emissions to the atmosphere from sources such as agriculture. By establishing

localized monitoring stations at emission sources, the precision of the estimated NH_3 concentrations in the atmosphere can be improved. This can also lead to improved understanding of PM dynamics and formation. This will be achieved by using a combination of active and passive sampling instruments for in-field atmospheric sample collection, which will then be analysed in the laboratory using ion chromatography. Additionally, to gain a fuller understanding of the dynamics of an agricultural system, background monitoring of soil properties and water nutrient enrichment will also be carried out.

The output of this project will build on existing theories of NH_3 , and PM dynamics established by previous research, and combine these with field data, including agricultural practices, NH_3 source production and PM generation, soil and water enrichment and quality background monitoring to synthesise a new mechanistic paradigm. This new understanding will be operationalised through the development of a conceptual model of NH_3 dynamics and PM generation, and agri-ecological interactions known as Conceptual Ammonia-aeroSol bIOspheric Simulation (CASIOS). The model builds on a Drivers, Pressures, State, Impacts, Responses framework, with an additional attribute introduced under the term 'Concept' which includes environmental conditions previously not considered under this paradigm.

Declaration

I certify that this thesis which I now submit for examination for the award of PhD, is entirely my own work and has not been taken from the work of others, save and to the extent that such work has been cited and acknowledged within the text of my work.

This thesis was prepared according to the regulations for graduate study by research of the Technological University Dublin and has not been submitted in whole or in part for another award in any other third level institution.

The work reported on in this thesis conforms to the principles and requirements of the Technological University Dublin's guidelines for ethics in research.

Technological University Dublin has permission to keep, lend or copy this thesis in whole or in part, on condition that any such use of the material of the thesis be duly acknowledged.

Signature _____ Date _____

Vivien Pohl

Acknowledgments

I would like to thank my supervisors, Dr Alan Gilmer, and Dr David O'Connor, who patiently guided me through my work, and without whom all this would not have been possible.

I would also like to thank Dr Vivienne Byers, Prof. John Cassidy and Dr Eugene McGovern who did not hesitate to lend a helping hand with this project when it was needed.

I am very grateful to the technical staff in Central Quad, who always were there to lend a helping hand when it was needed and for putting up with me in general.

I would like to express my gratitude to my family and friends who have put up with me and my lack of sanity throughout this entire process. Without your support, your continuous threats, and your knack for making me laugh even when I was ready to go on a rampage, this whole part of my life may not have even happened. From the bottom of my heart, thank you to all.

List of Abbreviations

ADM: Annual Denuder Method

ALPHA: Adapted Low-cost Passive High Absorption

AT: Air Temperature

ATP: Adenosine Triphosphate

BOD₅: Five Day Biological Oxygen Demand

C: Carbon

Ca: Calcium

CAN: Calcium Ammonium Nitrate

CEC: Cation Exchange Capacity

CEH: Centre for Ecology and Hydrology (United Kingdom)

CLRTAP: Convention on Long-Range Transboundary Air Pollution

CMIS: Chemical Ionization Mass Spectroscopy

CV: Coefficient of variation

1-D: 1 Dimensional

2-D: 2 Dimensional

3-D: 3 Dimensional

DELTA: DEnuder for Long-Term Atmospheric

DOAS: Differential Optical Absorption Spectroscopy

DO: Dissolved Oxygen

DPSIR: Drivers, Pressures, State, Impact and Responses

EC: Electronic Conductivity

EEA: European Environmental Agency

EMEP: European Monitoring and Evaluation Programme

EPA: Environmental Protection Agency

EU: European Union

HCl: Hydrochloric acid

HNO₂: Nitrous acid

HNO₃: Nitric acid

H₂SO₄: Sulfuric acid

ICP-MS: Inductively coupled plasma mass spectrometry

IC: Ion Chromatography

K: Potassium

kg: Kilogram

LHS: Left-Hand-Side

M: Molar

mins: minutes

Mg: Magnesium

mg/L: milligrams per liter

MSA: Methanesulfonic Acid

N: Nitrogen

N₂: Dinitrogen

N_r: Reactive nitrogen

Na: Sodium

NAMN: National Ammonia Monitoring Network

NEC: National Emissions Ceilings

NED: N-(1-naphthyl)-ethylenediamine dihydrochloride

NH₃: Ammonia

NH₃-N: Ammonia-Nitrogen

NH₄⁺: Ammonium

NH₄Cl: Ammonium chloride

NH₄⁺-N: Ammonium-Nitrogen

NO: Nitric oxide

NO_x: Nitrogen oxides

NO_x-N: Nitrogen Oxides-Nitrogen

NO₂⁻: Nitrite

NO₂-N: Nitrite-Nitrogen

NO₃⁻: Nitrate

NO₃-N: Nitrate-Nitrogen

(NH₄)₂SO₄: Ammonium sulfate

O: Oxygen

O₃: Ozone

OH⁻: Hydroxyl ion

P: Phosphorous

PM: Particulate Matter

PM_{2.5}: Fine particulate matter (particles with a diameter of $\leq 2.5 \mu\text{m}$)

PM₁₀: Coarse particulate matter (particles with a diameter of $\leq 10 \mu\text{m}$)

PO₄⁻: Phosphate

PPD: Particle Population Density

R_D: Rainfall depth

RH: Relative Humidity

RHS: Right-Hand-Side

S: Sulfur

SO₂: Sulfur dioxide

SOC: Soil Organic Content

SO_x: Sulfur oxides

TDS: Total Dissolved Solids

TD-LAS: Tunable Diode Laser Absorption Spectroscopy

TSP: Total Suspended Solids

UK: United Kingdom

UPW: Ultra-Pure Water

US EPA: United States Environmental Protection Agency

VCl_3 : Vanadium (III) Chloride

VOCs: Volatile Organic Compounds

v/v: volume per volume

WS: Wind Speed

w/v: weight per volume

XRF: X-Ray Fluorescence

μS : micro-siemens

$\mu\text{g/ml}$: microgram per milliliter

Table of Contents

Abstract.....	i
Declaration.....	iii
Acknowledgments.....	iv
List of Abbreviations	v
List of Tables	xv
List of Figures.....	xvi
Chapter 1: Introduction	
1.1 Introduction.....	1
1.2 Legislative Framework and Policy Relevance.....	2
1.3 Rationale	4
1.4 Aims and Objectives	6
Chapter 2: Literature Review	
2.1 Introduction.....	9
2.1.1 Search process.....	9
2.1.2 Inclusion and exclusion criteria	11
2.2 Introduction of Nitrogen	11
2.3 Biogeochemical Cycling of Nitrogen	13
2.4 Atmospheric Chemistry of Ammonia and Secondary Particulate Matter Formation	17
2.5 Deposition Processes Ammonia and Secondary Particulate Matter	22
2.5 Controlling factors of emission, transport, and deposition processes of ammonia and secondary particulate matter	31

2.6	Modelling the Soil-Water-Atmosphere Nexus in Ammonia and Particulate Matter dynamics	37
2.6.1	Direct source measurement: state-of-the-art techniques	39
2.6.2	Modelling of Ammonia and Particulate Matter	41
2.7	Concluding Remarks.....	47
Chapter 3: Methodology		13
3.1	Introduction.....	49
3.2	Site 1	51
3.3	Site 2	54
3.4	Site 3	55
3.5	Overview of Research Methods.....	56
3.6	Network Operation.....	63
3.7	Atmospheric Sampling and Analysis.....	67
3.7.1	Initial inspection and handling of filters for samplers	67
3.7.2	Quality Control and Validation.....	69
3.7.3	ALPHA passive sampler preparation.....	70
3.7.4	Extraction of ammonia from ALPHA passive sampler filters	72
3.7.5	DELTA II active sampler preparation.....	73
3.7.6	Degreasing of DELTA II denuders for sampling atmospheric gases.....	75
3.7.7	Coating solution for DELTA II denuders sampling atmospheric ammonia ..	76
3.7.8	Acid coating solution for filters sampling ammonium aerosols	76
3.7.9	Coating procedure for DELTA II filters	76
3.7.10	Coating procedure for DELTA II filters	77

3.7.11	Assembly of DELTA II active sampler sampling unit containing filters.....	77
3.7.12	Assembly of DELTA II active sampler train	78
3.7.13	Setting up DELTA II active samplers on site	79
3.7.14	Collection of exposed samples from each DELTA II active sampling unit...	80
3.7.15	Extraction of 5% w/v citric acid coated DELTA II denuders	80
3.7.16	Extraction of 12% w/v citric acid coated DELTA II filters	80
3.7.17	Ion chromatography analysis of extracts.....	81
3.7.18	Calculation of air concentration of ammonia and particulate matter	86
3.7.19	Imaging of particulate matter (DELTA II sampler)	88
3.8	Water Sampling and Analysis.....	89
3.8.1	Ammonia analysis in water using the phenate method	90
3.8.2	Nitrate and Nitrite analysis using the vanadium chloride method	91
3.8.3	Ortho-Phosphate analysis.....	94
3.8.4	Five-day biological oxygen demand	95
3.9	Soil Sampling and Analysis	97
3.9.1	Moisture content analysis of soil by gravimetric method	98
3.9.2	Elemental analysis of soil	99
3.9.3	Leaching study of soils	99
3.9.4	Design of precipitation simulations	101
3.9.5	Soil leachate analysis	91
3.10	Development of the CASIOS model.....	93
Chapter 4: Results and Discussion.....		
4.1	Introduction.....	97

4.2	Atmospheric Monitoring.....	97
4.2.1	Ion Chromatography method development and optimization.....	97
4.2.2	Atmospheric NH ₃ Concentrations (ALPHA samplers).....	101
4.2.3	Atmospheric NH ₃ and Aerosol NH ₄ ⁺ concentrations (DELTA II samplers).....	107
4.3	Water Analysis.....	114
4.3.1	Background monitoring of water pH	115
4.3.2	Background monitoring of water electrical conductivity and total dissolved solids	118
4.3.3	Background monitoring of water biological oxygen demand.....	123
4.3.4	Background monitoring of water dissolved oxygen concentrations	124
4.3.5	Background monitoring of ammonia concentrations in water	128
4.3.6	Background monitoring of nitrite and nitrate concentrations in water	132
4.3.7	Background monitoring of ortho-phosphate concentrations in water.....	136
4.4	Soil Analysis	138
4.4.1	Elemental analysis of soil by X-Ray Fluorescence.....	138
4.4.2	Ion Chromatography analysis of soil	140
4.4.3	Soil fertility analysis	142
4.4.4	Soil leaching study	145
4.5	Micro-meteorological monitoring.....	154
4.6	Discussion of Results.....	160
4.7	Conclusion	172
Chapter 5: Conceptual Model		
5.1	180

5.2	180
5.2.1 Drivers.....	180
5.2.2 Pressures	181
5.2.3 States	184
5.2.4 Impacts	185
5.2.5 Responses.....	186
Chapter 6: General Conclusion and Future Work.....	158
References.....	193
List of Publications	I
List of Employability and Discipline Skills.....	II

List of Tables

TABLE 3. 1 SAMPLING CARRIED OUT FOR EACH SITE DURING THE MONITORING PERIOD	57
TABLE 3. 2 DEFECT CRITERIA AND DESCRIPTION (STATE OF ALASKA DEPARTMENT OF ENVIRONMENTAL CONSERVATION, 2017)	69
TABLE 3. 3 CRITERIA FOR COATING SOLUTION	71
TABLE 3.4 DILUTION OF DIONEX™ METHANESULFONIC ACID CATION ELUENT CONCENTRATE WORKING STANDARD SOLUTION (0.4 M)	82
TABLE 3.5 COLUMN SPECIFICATIONS OF DIONEX IONPAC™ CS12A	82
TABLE 3.6 COLUMN SPECIFICATIONS OF DIONEX IONPAC™ CS16	83
TABLE 3.7 ION CHROMATOGRAPHY METHOD 1	84
TABLE 3.8 ION CHROMATOGRAPHY METHOD 2	84
TABLE 3.9 ION CHROMATOGRAPHY METHOD 3	84
TABLE 3.10 ION CHROMATOGRAPHY METHOD 4	85
TABLE 3.11 ION CHROMATOGRAPHY METHOD 5	85
TABLE 3.12 DIONEX™ COMBINED SIX CATION STANDARD.....	85
TABLE 3. 13 DILUTION CRITERIA OF BOD ₅ SAMPLES ADAPTED FROM DELZER & MCKENZIE, 1999.....	97
TABLE 3.14 RAINFALL SIMULATION CONDITIONS	105
TABLE 3.15 SLEET SNOW SIMULATION PARAMETERS	106
TABLE 3.16 CONCENTRATION OF ANIONS IN THERMO SCIENTIFIC SUPPLIED COMBINED SEVEN ANION STANDARD II	91
TABLE 3.17 ION CHROMATOGRAPHY METHOD	93
TABLE 4.1 MEAN NH ₃ CONCENTRATION (MGM ⁻³) AND SUMMARY OF STATISTICS FOR EACH SITE.....	102

TABLE 4.2 MEAN GASEOUS NH_3 AND AEROSOL NH_4^+ CONCENTRATIONS (MGM^{-3}) AND SUMMARY OF STATISTICS FOR EACH COMPONENT	107
TABLE 4.3 PPD AND AVERAGE PARTICLE SIZE REPRESENTATIVE OF EACH SEASON DURING THE MONITORING PERIOD	113
TABLE 4.4 ELEMENTAL ANALYSIS OF SOIL FROM SITES 1 AND 2	139
TABLE 4.5 COMPOSITION OF SOIL	140
TABLE 4.6 COMPOSITION OF SOIL PRE-TREATMENT	141
TABLE 4.7 ANNUAL AVERAGE AT MEASURED	157
TABLE 4.8 ANNUAL AVERAGE PRECIPITATION MEASURED	158
TABLE 4.9 ANNUAL AVERAGE SOIL AND WATER TEMPERATURE MEASURED.....	160

List of Figures

FIGURE 1.1 PROHIBITED PERIODS OF FERTILIZATION IN IRELAND.....	6
FIGURE 2.1 THE NITROGEN CYCLE-REACTIONS OVER THE ARROWS INDICATE THE CHEMICAL REACTION TAKING PLACE, TRANSFORMING ONE FORM OF N TO ANOTHER AND THE CHEMICAL SPECIES OVER THE ARROWS ARE THE REACTANTS SPECIES INVOLVED IN THE REACTION. (DARROUZET-NARDI, 2005).....	15
FIGURE 2.2 ABBREVIATED NITROGEN CYCLE, SHOWING THE ROLE OF AMMONIA (ADAPTED FROM DOYLE ET AL., (2017))	17
FIGURE 2.3 ENSEMBLE-MEAN PATTERN OF DRY DEPOSITION OF OXIDIZED FORMS OF N IN $\text{KG N HA}^{-1} \text{ A}^{-1}$ FOR THE YEAR OF 2001 (SHAW ET AL., 2014)	24
FIGURE 2.4 ENSEMBLE-MEAN PATTERN OF DRY DEPOSITION OF REDUCED FORMS OF N IN $\text{KG N HA}^{-1} \text{ A}^{-1}$ FOR THE YEAR OF 2001 (SHAW ET AL., 2014).....	24
FIGURE 2.5 RESISTANCE MODEL SCHEMATIC FOR BIDIRECTIONAL AMMONIA FLUX ADAPTED FROM PLEIM ET AL., (2013)	25
FIGURE 2.6 MODEL ESTIMATED N DEPOSITION FROM GLOBAL TOTAL N EMISSIONS, WITH AN ESTIMATED TOTAL OF 105 Tg N YR^{-1} (UNIT SCALE IN $\text{KG N HA}^{-1} \text{ YR}^{-1}$) FOR THE YEAR 2000 (DENTENER ET AL., 2006)	29
FIGURE 2.7 AN EXAMPLE OF A MULTI-LAYER 2-D MODEL SCHEMIATIC: THE SOIL-VEGETATION MODEL BY KATATA ET AL.,(2013)	44
FIGURE 3.1 MAP OF CHOSEN LOCATIONS FOR MONITORING IN IRELAND	51
FIGURE 3.2 MAP OF SITE 1	53
FIGURE 3.3 MAP OF SITE 2	55
FIGURE 3.4 MAP OF SITE 3	56

FIGURE 3.5 STATISTICAL ANALYSIS	60
FIGURE 3.6 ATMOSPHERIC WORKFLOW FROM SAMPLING TO MODELLING	61
FIGURE 3.7 WATER WORKFLOW FROM SAMPLING TO MODELLING.....	62
FIGURE 3.8 SOIL WORKFLOW FROM SAMPLING TO MODELLING	63
FIGURE 3.9 ALPHA PASSIVE SAMPLER UNITS	65
FIGURE 3.10 DELTA II DENUDER ACTIVE SAMPLER UNIT	66
FIGURE 3.11 ELEVATED SET-UP FOR MICROMETEOROLOGICAL STATIONS AT SITE 1 (RHS) AND SITE 2 (LHS)	67
FIGURE 3.12 DETAILED OUTLINE OF CEH ALPHA SAMPLER BODY ADAPTED FROM POSKITT, (2017)	72
FIGURE 3.13 COMPONENTS OF MONITORING ENCLOSURE OF LOW VOLTAGE DELTA II SAMPLER SYSTEM ADAPTED FROM TANG ET AL., 2017	73
FIGURE 3.14 DETAILS OF CONNECTION TO THE GAS METER (TANG ET AL., 2017)	74
FIGURE 3.15 DETAILS OF EXTERNAL SAMPLE HOLDER FOR SPECIATED COLLECTION OF AMMONIA GAS AND PARTICULATE AMMONIUM	74
FIGURE 3.16 DETAILS OF EXTERNAL SAMPLE HOLDER FOR SPECIATED COLLECTION OF REACTIVE GASES (NITRIC ACID, SULFUR DIOXIDE, HYDROCHLORIC ACID AND AMMONIA) AND PARTICULATES (NITRATE, SULFATE, CHLORIDE, AMMONIUM, SODIUM, CALCIUM AND MAGNESIUM)	75
FIGURE 3.17 DETAILED DIAGRAM OF AEROSOL SAMPLER COMPONENTS (LHS) AND THE ASSEMBLED AEROSOL SAMPLER (RHS) ADAPTED FROM TANG ET AL., 2017	78
FIGURE 3.18 ASSEMBLY OF FULL SAMPLING TRAIN, CONNECTED IN SERIES FOR THE SAMPLING OF NH ₃ AND PM.....	79
FIGURE 3.19 CONTINUOUS MONITORING OF WATER TEMPERATURE AT SITE 1 (LHS) AND SITE 2 (RHS). THE PROBE ATTACHED TO THE FLOATATION DEVICES ARE DEPICTED INSIDE THE RED SQUARES.....	89
FIGURE 3.20 COLOUR CHANGE OF SAMPLE WHEN INDOPHENOL BLUE IS FORMED BY A REACTION OF AMMONIA, HYPOCHLORITE AND PHENOL CATALYSED BY SODIUM NITROPRUSSIDE	91

FIGURE 3.21 SOIL TEMPERATURE PROBES AT SITE 1 (LHS) AND SITE 2 (RHS)	98
FIGURE 3.22 DESIGN OF RAIN SIMULATION CHAMBER.....	102
FIGURE 3.23 CANISTER PLACEMENT INSIDE THE RAIN SIMULATION CHAMBER FOR THE DURATION OF THE PROJECT.....	103
FIGURE 4.1 COMPARISON OF CHROMATOGRAMS DURING METHOD OPTIMIZATION: A) CHROMATOGRAM OF 2.5 MG/ML NH_4^+ STANDARD WITH CS12 COLUMN AND 15 MM ELUENT; B) CHROMATOGRAM OF 2.5 MG/ML NH_4^+ STANDARD WITH CS12 COLUMN AND 5 MM ELUENT; C) CHROMATOGRAM OF 2.5 MG/ML NH_4^+ STANDARD WITH CS16 COLUMN AND 30 MM ELUENT; D) CHROMATOGRAM OF 2.5 MG/ML NH_4^+ STANDARD WITH CS16 COLUMN AND 35 MM ELUENT .	100
FIGURE 4.2 CHROMATOGRAM OF 0.02 MG/ML NH_4^+	101
FIGURE 4.3 TIME-SERIES OF AMBIENT ATMOSPHERIC NH_3 CONCENTRATIONS MEASURED AT INDIVIDUAL SITE (A) AND THE AVERAGE CONCENTRATIONS MEASURED AT ACTIVE SITES (B) .	104
FIGURE 4.4 RELATIONSHIP BETWEEN ENVIRONMENTAL FACTORS AND ATMOSPHERIC NH_3 CONCENTRATIONS. A) AIR AND SOIL TEMPERATURE; B) PRECIPITATION	106
FIGURE 4.5 TIME-SERIES OF AMBIENT ATMOSPHERIC (GASEOUS) NH_3 AND AEROSOL NH_4^+ CONCENTRATIONS MEASURED DURING THE MONITORING PERIOD USING ALPHA AND DELTA II SAMPLERS.....	109
FIGURE 4.6 RELATIONSHIP BETWEEN ENVIRONMENTAL FACTORS AND AMBIENT ATMOSPHERIC NH_3 (GASEOUS) AND AEROSOL NH_4^+ CONCENTRATIONS. A) AIR AND SOIL TEMPERATURE; B) PRECIPITATION; C) WS; D) RH.....	111
FIGURE 4.7 PARTICULATE MATTER SAMPLES FROM EACH SEASON	112
FIGURE 4.8 SIZE DISTRIBUTION OF AEROSOLS REPRESENTATIVE OF EACH SEASON DURING THE MONITORING PERIOD	113
FIGURE 4.9 pH MEASURED AT SITE 1 (DENOTED S1) AND SITE 2 (DENOTED S2).....	116
FIGURE 4.10 RELATIONSHIP BETWEEN $\text{NH}_3\text{-N}$ AND pH, AND $\text{NO}_3\text{-N}$ AND pH AT SITE 1.....	117
FIGURE 4.11 RELATIONSHIP BETWEEN $\text{NH}_3\text{-N}$ AND pH, AND $\text{NO}_3\text{-N}$ AND pH AT SITE 2.....	117

FIGURE 4.12 RELATIONSHIP BETWEEN PH AND TEMPERATURE AT SITE 1 (LHS) AND SITE 2 (RHS)	118
FIGURE 4.13 ELECTRONIC CONDUCTIVITY MEASURED AT SITE 1 (DENOTED S1) AND SITE 2 (DENOTED S2).....	120
FIGURE 4.14 TDS MEASURED AT SITE 1 (DENOTED S1) AND SITE 2 (DENOTED S2).....	121
FIGURE 4.15 TDS-EC CORRELATION AT SITE 1 (LHS) AND SITE 2 (RHS).....	122
FIGURE 4.16 BOD ₅ VALUES MEASURED AT SITE 1 (DENOTED S1) AND SITE 2 (DENOTED S2).....	123
FIGURE 4.17 DO VALUES MEASURED AT SITE 1 (DENOTED S1) AND SITE 2 (DENOTED S2).....	125
FIGURE 4.18 RELATIONSHIP BETWEEN DO AND TEMPERATURE AT SITES 1 (LHS) AND 2 (RHS).....	126
FIGURE 4.19 RELATIONSHIP BETWEEN DO AND NUTRIENT LOADING: NH ₃ -N LOADING AND DO AT SITE 1 (TOP LHS); NH ₃ -N LOADING AND DO AT SITE 2 (TOP RHS); AND PO ₄ -P LOADING AND DO AT SITE 2 (BOTTOM MIDDLE).....	127
FIGURE 4.20 CONCENTRATION OF NH ₃ -N (MG/L) AT SITES 1 AND 2#.....	129
FIGURE 4.21 ALGAL BLOOM AT SITE 2, JULY 2020 (RHS), AND OCTOBER 2020 (LHS)	129
FIGURE 4.22 ALGAL BLOOMS AT SITES 1 (RHS) AND 2 (LHS).....	130
FIGURE 4.23 RELATIONSHIPS BETWEEN NH ₃ -N CONCENTRATION AND TEMPERATURE AT SITES 1 (TOP LHS) AND 2 (TOP LHS); AND NH ₃ -N CONCENTRATION AND DO AT SITES 1 (BOTTOM LHS) AND 2 (BOTTOM LHS).....	132
FIGURE 4.24 CONCENTRATION OF NO ₂ -N (MG/L) AT SITES 1 AND 2.....	133
FIGURE 4.25 CONCENTRATION OF NO ₃ -N (MG/L) AT SITES 1 AND 2.....	134
FIGURE 4.26 RELATIONSHIPS BETWEEN THE CONCENTRATION OF NO ₃ -N (MG/L) AND NH ₃ -N AT SITES 1 (TOP LHS) AND 2 (TOP RHS); AND THE CONCENTRATION OF NO ₂ -N (MG/L) AND NH ₃ -N AT SITES 1 (BOTTOM LHS) AND 2 (BOTTOM RHS).....	135
FIGURE 4.27 CONCENTRATION OF PO ₄ -P (MG/L) AT SITE 2	138
FIGURE 4.28 ELEMENTAL ANALYSIS OF SOILS FROM SITE 1 (LHS) AND SITE 2 (RHS).....	139
FIGURE 4.29 ION ANALYSIS OF SOILS FROM SITE 1 (DENOTED AS S1) AND SITE 2 (DENOTED S2) PRE-TREATMENT.....	142
FIGURE 4.30 MICRO-OXYMAX [®] RESPIROMETER	143

FIGURE 4.31 RQ (TOP) AND CO ₂ EVOLUTION RATE (BOTTOM) FOR SOILS ANALYSED IN TRIPLICATE FROM BOTH SITES 1 AND 2	144
FIGURE 4.32 MICROBIOLOGICAL ANALYSIS OF COMPOSITE SOILS FROM SITES 1 AND 2.....	145
FIGURE 4.33 CHANGES IN SOIL LEACHATE pH (TOP LHS), EC (TOP RHS) AND VOLUME (BOTTOM). S1 AND 2 REFER TO SITES 1 AND 2 RESPECTIVELY; ‘F’, ‘A’ AND ‘O’ REFER TO FREEZE-, AIR-, AND OVER-DRYING; AND ‘NR’ AND ‘SN’ REFER TO ‘NORMAL RAIN’ AND ‘SNOW’ RESPECTIVELY. ...	146
FIGURE 4.34 CHANGES LEACHATE EC AS A FUNCTION OF TEMPERATURE. S1 AND 2 REFER TO SITES 1 AND 2 RESPECTIVELY; ‘F’, ‘A’ AND ‘O’ REFER TO FREEZE-, AIR-, AND OVER-DRYING; AND ‘NR’ AND ‘SN’ REFER TO ‘NORMAL RAIN’ AND ‘SNOW’ RESPECTIVELY.....	147
FIGURE 4.35 IONIC FLUXES IN SOIL LEACHATE UNDER SYNTHETIC PRECIPITATION SIMULATION. S1 AND 2 REFER TO SITES 1 AND 2; AND ‘F’ AND ‘O’ REFER TO FREEZE- AND OVER-DRYING RESPECTIVELY.....	149
FIGURE 4.36 IONIC FLUXES IN SOIL LEACHATE UNDER NATURAL PRECIPITATION SIMULATION. S1 AND 2 REFER TO SITES 1 AND 2; AND ‘F’ AND ‘A’ REFER TO FREEZE- AND AIR-DRYING RESPECTIVELY.	150
FIGURE 4.37 TRACE ELEMENT FLUXES IN SOIL LEACHATE UNDER SYNTHETIC PRECIPITATION SIMULATION. S1 AND 2 REFER TO SITES 1 AND 2; AND ‘F’ AND ‘O’ REFER TO FREEZE- AND OVER-DRYING RESPECTIVELY.	152
FIGURE 4.38 TRACE ELEMENT FLUXES IN SOIL LEACHATE UNDER NATURAL PRECIPITATION SIMULATION. S1 AND 2 REFER TO SITES 1 AND 2; AND ‘F’ AND ‘A’ REFER TO FREEZE- AND AIR-DRYING RESPECTIVELY.	153
FIGURE 4.39 WIND ROSE FOR SITE 1 WIND SPEEDS AND WIND CLASS FREQUENCY DISTRIBUTIONS MEASURED DURING THE MONITORING PERIOD. RADIAL BARS REPRESENT PERCENTAGES OF WIND MEASUREMENTS FROM EACH DIRECTIONS, EACH SUBDIVIDED INTO SIX SPEED CATEGORIES: 0.5-2.1 MS ⁻¹ , 2.1-3.6 MS ⁻¹ , 3.6-5.7 MS ⁻¹ , 5.7-8.8 MS ⁻¹ , 8.8-11.1 MS ⁻¹ , AND >11.1 MS ⁻¹	156
FIGURE 4.40 AT (LHS) MEASURED AT SITES 1 AND 2 AND RH (RHS TOP) AND A COMPARISON OF RH AND AT (RHS BOTTOM) DURING THE MONITORING PERIOD.....	157
FIGURE 4.41 PRECIPITATION MEASURED AT SITES 1 AND 2 DURING THE MONITORING PERIOD.....	158

FIGURE 4.42 WATER AND SOIL TEMPERATURE MEASURED AT SITES 1 (LHS) AND 2 (RHS) 159

FIGURE 5.1 DECISION TREE FOR THE DEVELOPMENT OF THE CASIOS MODEL 175

FIGURE 5.2 CONCEPTUAL MODEL DEVELOPED FOR ARABLE AGRICULTURAL SYSTEM (CASIOS)..... 179

Chapter 1: Introduction

1.1 Introduction

Ammonia (NH_3) is a naturally occurring, highly reactive and highly soluble alkaline trace gas, originating from both natural and anthropogenic sources. In Ireland, one of the primary sources of NH_3 in the atmosphere is agriculture, e.g.: manures, slurries and synthetic fertilizer application (Kelleghan et al., 2019). Emission and deposition vary both spatially and temporally, resulting in emission “hot-spots” correlating to areas with a high density of agricultural activities and practices (Phillips, Arya, & Aneja, 2004). Additional emissions of NH_3 associated with agriculture include fertilizer production and biomass burning. Generally, NH_3 emitted to the atmosphere is either dry deposited back onto surfaces (for example to foliage), is wet deposited on to surfaces, or undergoes atmospheric reactions (transforming into different atmospheric species). NH_3 will also be converted to ammonium (NH_4^+) in the atmosphere which also undergoes the deposition processes mentioned above. From an environmental perspective, elevated concentrations of NH_3 can lead to deleterious impacts, including the formation of secondary particulate matter, acidification of ecosystems, biodiversity losses and eutrophication (Kelleghan et al., 2019). These impacts also have ramifications for human health, including premature mortality, decrease in lung functionality and increased cardiovascular problems (Hunt, Ferguson, Hurley, & Searl, 2016).

The Irish Environmental Protection Agency (EPA) currently monitors atmospheric particulate NH_4^+ at three representative sites (Carnsore, County Wexford; Oak Park, County Carlow and Malin, County Donegal) in agreement with the European Monitoring and Evaluation Programme (EMEP). However there is currently no continuous monitoring network in place for NH_3 gas concentration in Ireland (Leinert, McGovern, & Jennin, 2008). In contrast to Ireland, under the UK National Ammonia Monitoring

Network (NAMN), Northern Ireland has three continuous monitoring sites for NH_3 gas in the atmosphere. NH_3 is also a pollutant which is currently not covered by the CAFÉ Directive under ambient air quality (Directive 2008/50/EC) and does not fall under the national ambient air quality network, which is managed by the EPA. Consequently, there are significant uncertainties and gaps in knowledge regarding NH_3 fluxes and secondary particulate matter levels in Ireland.

1.2 Legislative Framework and Policy Relevance

This project aims to contribute to the established knowledgebase of the levels of NH_3 gas and particulate matter (PM) concentrations at emission hot-spots. This project is also conducted in order to aid in the development of Irish environmental policy and strategic initiatives designed to combat and mitigate pollution. Recent EU-wide initiatives have been directed at bringing about a reduction in nitrogen (N) emissions through legislative measures, such as the Gothenburg Protocol and the establishment of National Emission Ceilings (NEC). The primary aim of these legislative measures has been to lessen acidification and eutrophication in natural and semi-natural ecosystems. The NEC (Directive 2001/81/EC) established emission ceilings for pollutants such as NH_3 , which is classified as an eutrophying pollutant. Signatories to the convention (including Ireland), are under obligation to mitigate, limit and negate NH_3 pollution. To achieve the goals for air quality as set out by the EU, the development of strategies and policies regarding NH_3 production is required, based on monitoring, consultation, and a greater understanding on the processes and dynamics involved. In addition to the NEC directive, NH_3 emission abatement is also required under the Directive on Industrial emissions (Directive 2010/75/EU), the Nitrates and Water Framework Directives (Directive

91/676/EEC, Directive 2000/60/EC) and the National Clean Air Strategy (Directive 2001/81/EC).

PM has been acknowledged as an important atmospheric pollutant with no safe threshold currently established. Both the recent Gothenburg Protocol 2020 and the NEC Directive 2030 have listed ceilings for PM emissions in recognition of their associated health impacts and the transboundary nature of the pollutant.

In Ireland, the nationwide emissions of NH_3 continues to exceed the levels set by the NEC (EPA, 2018), and hence breach the national emissions ceiling limit of 116 kilotons per annum. NH_3 trends differ from other transboundary trace gas pollutant emissions such as SO_2 and NO_x which have seen a steady decrease. Indeed, NH_3 emissions remained static for nearly a decade before rising again in 2016 and continued to breach the NEC limit. This is partially due to agricultural intensification resulting from policies such as Food Harvest 2020 (Department of Agriculture, Fisheries and Food, 2015) and Food Wise 2025 (Department of Agriculture, 2015). The data collected and compiled in this research will contribute to the knowledge base for Ireland. This will greatly assist measures designed to implement relevant directives controlling emissions as well as other strategies set forth by the EU on atmospheric pollution mitigation.

While measurement is a critical aspect of environmental monitoring, on its own it remains insufficient to provide the intrinsic interpretation of data with other aspects affecting emissions for a given site. This gap in knowledge and understanding can be targeted by the use of models. The effective use of models in agriculture and land-use management requires ongoing innovation in simulation design and greater understanding of system processes. (Tonitto, Woodbury, & McLellan, 2018; Vardoulakis, Fisher, Gonzalez-Flesca, & Pericleous, 2002).

The need for pollution and environment models has been highlighted by the demands of the Convention on Long-range Transboundary Air Pollution (CLRTAP) and the European Commission, with little guidance on the choice of model. Consequently, a high degree of variability can be seen among models, as individual countries and organizations have adopted certain approaches to modelling air and water quality depending on local policy objectives, resources, and the availability of historical data.

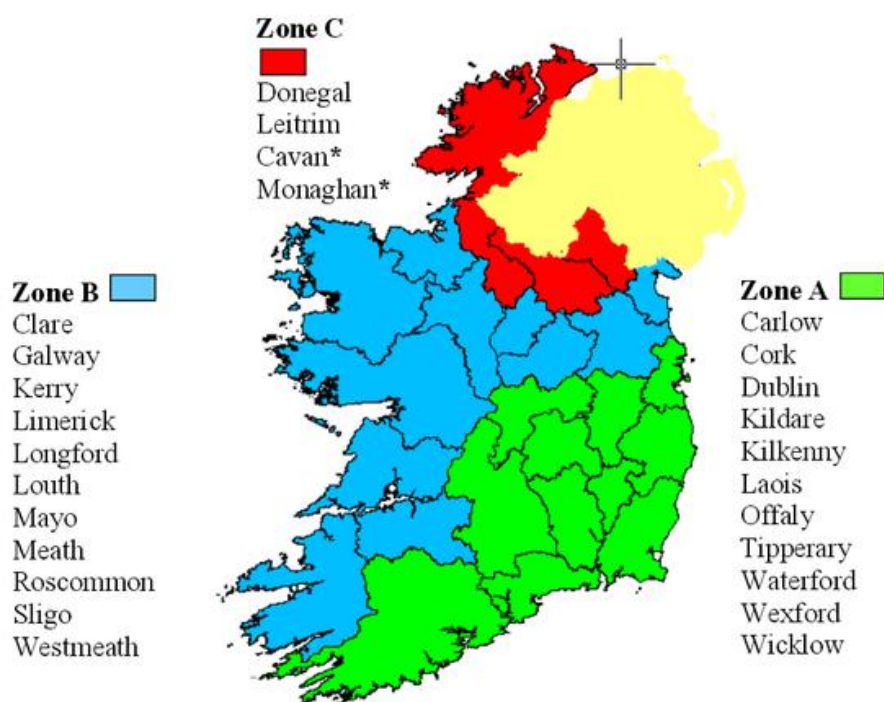
1.3 Rationale

The chosen economic activity for this study was agriculture, more specifically, arable agriculture. Ireland's land-use is primarily invested in agriculture, with a leading 66.1 %, of which arable agriculture account for 15.4% with the remainder being permanent pasture. 10.9% of land use is forestry, and 23% is classified as 'other', of which 1.8% was settlement (CSO, 2020). In Ireland, agriculture is responsible for 99% of NH_3 emissions to the atmosphere (Teagasc, 2020).

From an emission-intensity standpoint, grassland would be a more likely candidate for study as it accounts for a larger portion of the landmass, however, the emissions arising from arable agriculture in Ireland are much less explored, and indeed reported, while grasslands are studied with a much higher frequency. Additionally, while greenhouse gas emissions are higher in areas where the main landcover type is grassland, the atmospheric component of interest (NH_3) is not classified as a greenhouse gas by definition, therefore emissions of NH_3 gas are not included when greenhouse gases are reviewed and discussed (Teagasc, 2020). Therefore, the selection of study sites were chosen where the main economic activity was arable agriculture as it is an area which has not been studied as intensively as pasture landcover emissions, with the potential to be a considerable

contributor (due to fertilizer use) to atmospheric NH_3 concentrations and secondary PM formation.

As mentioned in Section 1.1, one main source of NH_3 gas in the atmosphere is fertilizer application. Management and application of fertilizer, whether it is organic, or inorganic is vital for emission reduction and mitigation. Thus, depending on landcover type, fertilizer application has set timelines. For pastureland, slurry and N-based fertilizers are applied in spring, and N-based fertilizers are applied in autumn (Teagasc, 2011). Similarly, for arable agriculture, the main application times are spring and autumn, with either slurry or N-based fertilizers being applied during spring, with a second application of N-based fertilizers in autumn. If synthetic fertilizers are used, a phosphate-rich fertilizer is also applied during autumn. Ireland also has prohibited times during the year when no fertilizer may be applied regardless of landcover or fertilizer type (Figure 1.1).



Prohibited periods of fertilization			
Fertilizer type	Zone A	Zone B	Zone C
Chemical	15 th September- 12 th January	15 th September-15 th January	15 th September- 31 st January
Organic	15 th October- 12 th January	15 th October- 15 th January	15 th October- 31 st January
Farmyard Manure	1 st November- 12 th January	1 st November- 15 th January	1 st November- 31 st January

Figure 1.1 Prohibited periods of fertilization in Ireland

1.4 Aims and Objectives

The aim of this research is to combat the issues and gaps introduced above by proposing that understanding ecosystem production and nutrient pollution requires an elucidation of NH_3 dynamics (pathways of transport and interactions), for the control and mitigation NH_3 throughout the biosphere as well as emerging secondary pollutants, namely PM. This will allow compliance with national and EU air, soil, and water quality directives. This study will supply data for the development of a conceptual model directed at exploring the nature and dynamics of NH_3 flux secondary PM production from a spatial

and temporal perspective, on a localised basis. This modelling approach is systems based and strives to develop a holistic conceptualisation of the processes at work.

To achieve this, the following objectives were set forth:

1. Establish a monitoring network, with a focus on atmospheric sampling of NH_3 and PM
2. Identify and characterise sources and precursor species contributing to NH_3 -PM formation
3. Identify and map biophysical and biochemical pathways of interactions and transport of NH_3 and PM, as well as potential variability of concentrations
4. Identify the driving parameters, variables, and constants of NH_3 on a site basis
5. To develop a conceptual model based on field data obtained.

There is limited understanding of the mechanics and drivers of NH_3 production, transport and conversion to PM, yet this area remains of critical importance from both an environmental quality and human health perspective. Fundamentally, this project aims to address this deficit in understanding and to advance the knowledge base on which a new conceptual framework for model development processes can be proposed. Achieving these objectives will also enable this project to serve as a basis for future multi-disciplinary projects incorporating socio-economic elements.

This thesis is structured into a total of 6 chapters. As the project is multi-disciplinary, with various components, each of these was assigned a chapter. Chapters 1 and 2 establish the current state-of-the-art, present the current gaps in knowledge. Chapters 3-5 describes the techniques and methodologies employed, the results and discussion of the monitoring schemes set up for atmospheric, water and soil monitoring, and the conceptual model

devised based on the data collected. Chapter 6 contains the general conclusions of the project.

Chapter 2: Literature Review

2.1 Introduction

This part of the study was undertaken as a systematic literature review in order to address the following research questions:

1. Identification and characterization of sources and precursor species contributing to NH_3 -PM formation
2. Identification and mapping (including sampling and modelling) of biophysical and biochemical pathways of interactions and transport of NH_3 and PM, as well as variability of concentrations
3. Identification of the driving parameters, variables, and constants of NH_3 on a site basis

The goal of the review was to assess journal articles and papers published, including other systematic literature reviews, making this a tertiary study. The steps involved in this part of the study are documented below.

2.1.1 Search process

The search process was a manual search of literature containing the following key words:

Ammonia; atmospheric ammonia; ammonia emissions; ammonia deposition; nitrogen; nitrogen cycling; nitrogen cycle; biospheric nitrogen; atmospheric nitrogen sources; atmospheric nitrogen sinks; nitrogen emission; nitrogen deposition; atmospheric emissions; reactive nitrogen; atmospheric pollution; particulate matter; PM_{10} ; $\text{PM}_{2.5}$; secondary particulate matter; agriculture; arable agriculture; agricultural emissions; agricultural ecosystems; ecosystem dynamics; fertilizer use; synthetic fertilizer; organic

fertilizer; slurry; land use; land cover types; peatland; grassland; crop production; cereal crop; pasture; permanent pasture; dairy production; animal husbandry; source pollution; pollution dynamics; groundwater dynamics; leaching; soil leaching; surface water; hydrology; hydrological dynamics; hydrological cycle; soil dynamics; soil chemistry; aerated soil; anaerobic soil; nitrogen fertilizer response; nitrogen mineralization; organic turnover; nutrient enrichment; nutrients; nutrient leaching; lithology; food security; sustainability; biodiversity; environmental effects; human health; Ireland; modelling; special mapping; temporal variation; model; simulation model; spectrometry.

Each published paper and journal article was reviewed, and literature reviews and literature surveys addressing the research questions of interest were given primary importance due to the size of the topic, in order to gain an overview of the research questions being addressed. An inclusion and exclusion criteria was applied to determine relevance of papers collected using the key words detailed above (Section 2.1.2.).

To gain greater understanding of the topic undertaken, geographical information system tools were also utilised to assess and review data collected during the review. In order to assess sites of potential importance and further understand pollution dynamics (including identification and mapping of precursor gases and pathways of interactions), spatial, attribute and metadata were used. Maps developed by Teagasc were used, such as county soil maps, as well as the maps developed during the Irish Soil Information System project, a collaboration between the EPA and Teagasc (Creamer et al., 2014). These maps were developed using a unique technique, where digital soil mapping techniques were combined with ordnance survey mapping, providing highly detailed information on soil depths, soil textures, carbon content, carbon exchange capacity, and pH. Additionally, geological survey maps and ordnance survey maps were also utilised in order to gain

better understanding of lithology and soil chemistry, as well as provide a basis for site selection, with a specialized focus on County Dublin.

2.1.2 Inclusion and exclusion criteria

Peer-reviewed articles on the following topics were included:

1. Systematic literature reviews
2. Meta-analyses
3. Papers addressing key components of this review (i.e.: addressing the research questions listed in Section 2.1)
4. Papers and reviews where only one element of the article was relevant to this review were also included

Papers on the following topics were excluded:

1. Informal literature reviews
2. Conference proceedings
3. Duplicate reports

2.2 Introduction of Nitrogen

Nitrogen (N₂) is a vital element for life on Earth and constitutes approximately 79% of the atmosphere. It can be found in major and minor pools throughout the biosphere in various forms. However, excessive anthropogenic contributions of various nitrogen (N) compounds have made it one of the four primary pollutants resulting in significant damage to both environmental and human health (Behera et al., 2013; Morán et al., 2016).

A pollutant or novel entity is a substance or energy introduced into the environment resulting in the deterioration or diminution in the environmental state or otherwise adversely affecting the usefulness of a resource.

Pollutants can be both naturally occurring and anthropogenic in origin. It is significant to note that the definition of a substance or entity as a pollutant may depend on a variety of system factors including spatial and temporal aspects. Hence, a substance in one situation may be regarded as a nutrient whilst in another, the same substance might be regarded as a pollutant. A common example of this occurs in water system where substances originally classified as nutrients rise in concentration to such an extent that they become deleterious to the system and represent hazardous agents (pollutants). Such occurrences then create situations where the former nutrients now pose a threat to the wider environment and human health via their presence and concentrations.

Species of N can be present as gases and particles (solid or liquid) in the atmosphere or alternatively as part of water vapor (Behera et al., 2013; Krupa, 2003). Various forms of N are present in the atmosphere, including oxides (nitrogen dioxide (NO_2) and nitric oxide (NO) collectively known as NO_x), nitric acid (HNO_3), nitrate (NO_3^-), ammonia (NH_3) and ammonium (NH_4^+) (Fowler et al., 2013; Galloway, 2005; Galloway et al., 2004; Galloway et al., 2008). Among all the forms of N present in the atmosphere, NH_3 plays a key role in atmospheric reactions resulting in the formation of inorganic secondary particulate matter (Gong et al., 2013; Petetin et al., 2016).

NH_3 gas is emitted to the atmosphere from both natural and anthropogenic sources. Natural sources include emissions from both aquatic and terrestrial ecosystems (volatilization from oceans and soils), and biomass and woodland burning. The principal anthropogenic sources of NH_3 emitted to the atmosphere are agricultural, with

contributions from industrial processes (mineral fertilizer production) and vehicle emissions (Hyde, Carton, O'Toole, & Misselbrook, 2003; Sapek, 2013). Agricultural contributions of atmospheric NH_3 are attributed to animal husbandry, volatilization from livestock waste and losses from agricultural crops (growth practices and management) (Faria et al., 2013; Leip et al., 2015; Sapek, 2013). Concentrations of NH_3 in the air in Europe are consequently spatially correlated with areas containing intensive agricultural activity (Skj  th et al., 2011).

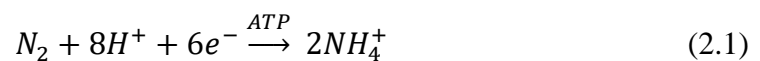
For example, when urea is used as a fertilizer, it is hydrolysed by the enzyme urease (a naturally occurring enzyme in soil microbes yielding ammonium carbonate) and converted to NH_4^+ and hydroxyl ions (OH^-). In alkali conditions, OH^- and NH_4^+ react to form volatile NH_3 gas which escapes to the atmosphere (Doyle et al., 2017). Fertilizers can also be dissolved in soil water, resulting in chemical components such as NH_4^+ being leached into water courses, or form part of the run-off from land. The amount of NH_3 volatilised from fertilizer usage on arable soils is largely dependent on soil properties (organic matter content, microbiological activity, pH, the acid buffering capacity and cation exchange capacity) as well as general weather conditions (Doyle et al., 2017).

2.3 Biogeochemical Cycling of Nitrogen

Nitrogen is a highly stable atmospheric constituent in the form of N_2 , due to its chemistry. Molecular N is chemically inert, partly due to the N-N bond energy (945 kJ mol^{-1}), meaning a large activation energy is required to break this bond, posing a kinetic limitation, as well as making most reactions endothermic (Wayne, 2000). There are natural processes which are capable of bringing N_2 into combination with other elements to make them biologically and chemically viable. These processes are referred to as

‘nitrogen fixation’ processes and are energy dependent. Lightning is a natural phenomenon capable of nitrogen fixation by producing NO_x, which is consequently converted to respective acidic forms and subsequently removed by wet deposition from the atmosphere, or alternatively, through a range of atmospheric reactions(Johnson et al., 2010).

Although N is the most abundant gas in the atmosphere, plants cannot use it in this form. Biological fixation is a process by which independent microbes fix N₂ into soils. This process is important for terrestrial environments, as it provides one of the major sources of biologically and chemically available nitrogen to terrestrial flora (Fowler et al., 2013). The other major source of N for terrestrial ecosystems is N fixation through symbiotic organisms. These symbiotic organisms are found in the root nodules of legumes (peas, beans, etc.) (Shober & Taylor, 2015). These N-fixing microorganisms are collectively known as diazotrophs and include rhizobia, azotobacter, azospirillum, Frankia alni and cyanobacteria. Assimilation of N is catalysed by an enzyme known as *nitrogenase* (Wayne, 2000). This enzyme reduces N₂ to NH₄⁺ ions, by use of the energy-rich phosphate, Adenosine Triphosphate (ATP) (Hertel et al., 2011):



The symbiotic micro-organisms derive the ATP used for the assimilation of N from the host plant, which in turn obtains ~90% of the of the fixed N (Butterbach-Bahl et al., 2011; Cabello et al., 2009). Other elements of the soil microbiological processes involve *nitrifying* bacteria oxidizing NH₄⁺ to NO₃⁻ *denitrifying* bacteria reducing NO₃⁻ to N₂; and *ammonifying* bacteria reconvert organic matter to NH₃ (Figure 2.1)(Wayne, 2000).

The terrestrial N cycle consist of soil, flora and fauna pools containing low quantities of N (in comparison to atmospheric and lithospheric reservoirs) yet it still exerts a substantial impact on the natural dynamics of the biogeochemical N cycle. Generally, plants and vegetation acquire N from the soil in much greater quantity than any other element. However, most plants are only able to take up N in two of its forms: NH_4^+ and NO_3^- (Kern & Simon, 2011; Widdison & Burt, 2008). The microbiological processes maintain the disequilibrium and imbalances present between atmospheric concentrations of N_2 and terrestrial and marine N ions.

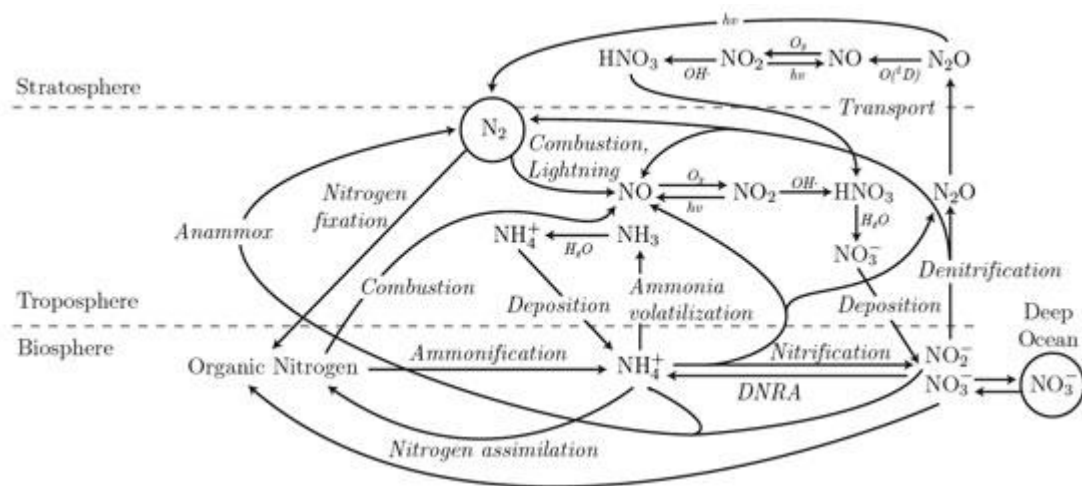


Figure 2.1 The nitrogen cycle-reactions over the arrows indicate the chemical reaction taking place, transforming one form of N to another and the chemical species over the arrows are the reactants species involved in the reaction. (Darrouzet-Nardi, 2005)

Global budget estimates of N_2 are imprecise, more so than those made for C. However, the major reservoir pools of N are still indicative of how it is cycled through the biogeochemical process of the Earth (Figure 2.1). Although most of the N is recycled within both the marine and terrestrial ecosystems these systems are not fully closed. Thus N is able to transfer between the biosphere and atmosphere. Increasing emissions of reactive N species such as NH_3 affect the overall biogeochemical cycling of N. This

distorts the N balances maintained by microbiological processes (Galloway et al., 2014; Pan et al., 2016). NH_3 is responsible for a large number of reactions at the core of the biogeochemical cycle. Thus, even partial overloading of reactants within the system can affect the entire biogeochemical cycling of any given element.

It is significant to note that more than 40% of the N in applied fertilizer is lost as NH_3 . Additionally, under specific environmental and edaphic conditions, an average of 10-14% of synthetic fertilizer applied has been reported as lost through volatilization (Basosi et al., 2014; Behera et al., 2013; Bouwman, Boumans, & Batjes, 2002; De Klein et al., 2006). Recent estimates suggest, approximately 100 million metric tonnes of N fertilizer is produced per annum, in comparison to 1 million metric tonnes 40 years ago (circa 1970's) (Viney P. Aneja et al., 2001; Behera et al., 2013).

Agricultural systems are inclined to concentrate N, by the use of either organic or synthetic fertilizers, creating an enriched reservoir of NH_3 which can transfer to the atmosphere (Figure 2.2). The annual average concentration of NH_3 , measured across 40 sites in Ireland in 1999 was $1.45 \mu\text{g}/\text{m}^3$ (Farrell, 2000). Annual averages obtained for each site ranged between 0.14 and $7.24 \mu\text{g}/\text{m}^3$. In 2013, another study performed by Doyle et al., (2017), found the annual average concentration of NH_3 to be $1.72 \mu\text{g}/\text{m}^3$ across 25 sites in Ireland. The minimum detectable concentration was $0.20 \mu\text{g}/\text{m}^3$ and the maximum concentration detected during the study was $10.51 \mu\text{g}/\text{m}^3$. These studies also demonstrated a strong correlation between atmospheric concentrations and regions with high NH_3 emissions. The difference between minimum and maximum concentrations observed between the two studies show that atmospheric emissions of NH_3 are on an increasing trajectory.

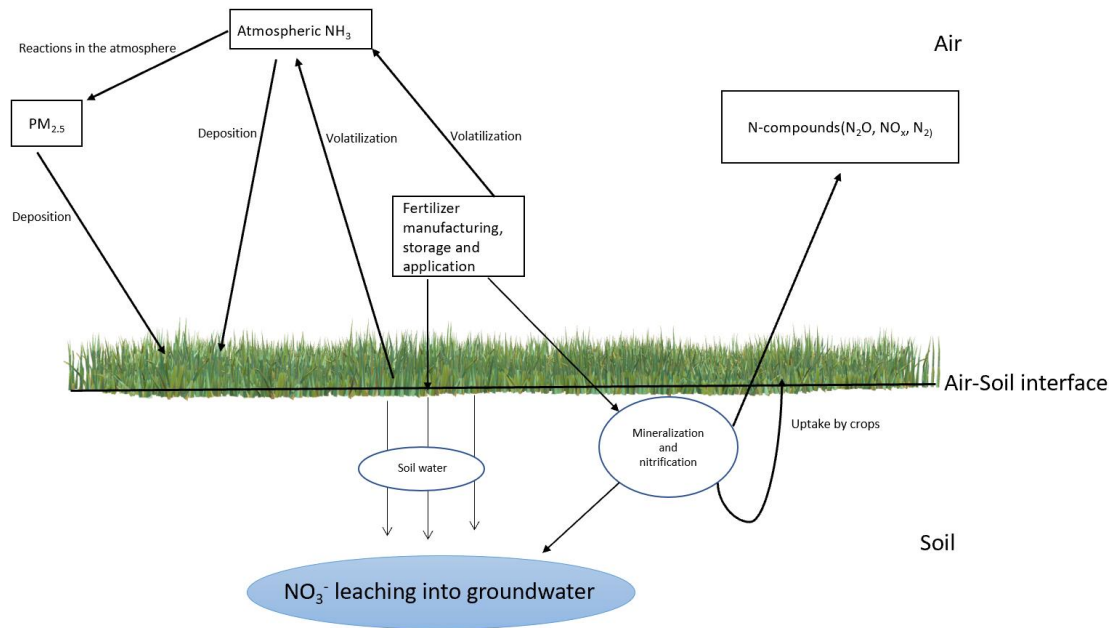


Figure 2.2 Abbreviated nitrogen cycle, showing the role of ammonia (adapted from Doyle et al., (2017))

2.4 Atmospheric Chemistry of Ammonia and Secondary Particulate Matter Formation

Atmospheric NH₃ emissions from agriculture can be broken down into two categories: animal husbandry and arable agriculture. Within these, there are many facets which contribute various amounts of NH₃ to the atmosphere, however, the four major components are synthetic fertilizer application (10%), grazing (12%), manure management housing and storage (48%), and manure land spreading (30%) (Hennessy, Buckley, & Cushion, 2011). While fertilizer application accounts for the least of the atmospheric NH₃ emitted, it is also the least researched area in Ireland in terms of emissions.

NH₃ emission from fertilizer application arises through the process of volatilization, a physical process highly dependent on temperature and pH (Bouwman et al., 2002b). As

NH₃ enters the atmosphere, it generally moves laterally with a relatively short half-life, and can be deposited within a small radius (few hundred meters) of the source clinging to nearby surfaces. However, the atmospheric residence time of NH₃ is dependent on various factors, such as conversion rate of NH₃ to NH₄⁺ and the rate of deposition of each species. A residence time of between 0.8 and 4 days for NH₃ and between 5 and 19 days for NH₄⁺ is generally accepted (Doyle et al., 2017).

In the atmosphere, NH₃ gas can react with sulfur dioxide (SO₂) and NO_x to form secondary PM. Additionally, since NH₃ is a highly alkaline gas, it can also undergo neutralization reactions with acids present in the atmosphere (sulfuric acid (H₂SO₄), HNO₃ and in certain cases hydrochloric acid (HCl)) (Fuzzi et al., 2015; Martins et al., 2015; Pathak, Wu, & Wang, 2009; Snider et al., 2016; Tucker, 2000; Vayenas et al., 2005). NH₃ aerosols comprise a significant portion of particulate matter (PM) present in the atmosphere, making up approximately 30- 50% of aerosol mass of PM (Anderson, Strader, & Davidson, 2003; Behera et al., 2013a; Skjøth & Geels, 2013). In addition to NH₃ there are a number of other precursor species (e.g.: NO_x, SO_x and HCl) which can lead to PM formation in the atmosphere. This is attributed to NH₃ being one of the few alkaline components in the atmosphere, which can undergo neutralization reactions with acidic species present.

NO_x is a general term used to describe nitrogen oxides which can play a role in air pollution, particularly nitrous oxide (NO) and nitrogen dioxide (NO₂). Sources of NO_x emissions include power plant boilers, incinerators, gas turbines, engine spark ignition systems and diesel engines, glass manufacturing, petroleum refineries, agriculture, cement manufacture, etc. NO_x production is also associated with the nitrogen cycle (Almaraz et al., 2018; Darrouzet-Nardi, 2005; Jaeglé, Steinberger, Martin, & Chance,

2005; Stavrakou et al., 2013). When NO and NO₂ are dissolved by water, as can occur in clouds or fog, it forms HNO₃ and nitrous acid (HNO₂).

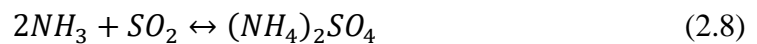
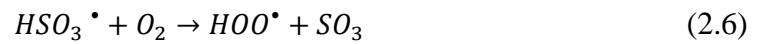
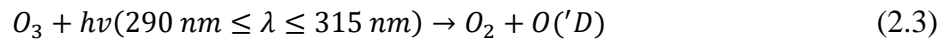
HNO₃ can also be formed through a series of photochemical reactions. These reactions involve the NO_x system and the production of ozone (O₃) (Wayne, 2000). The formation of ammonium nitrate (NH₄NO₃) aerosols (equation 2.2) depends on environmental conditions such as relative humidity and temperature due to the reaction equilibrium (Saylor, Myles, Sibble, Caldwell, & Xing, 2015). For instance, low temperatures result in the equilibrium of the system deviating towards the aerosol phase (Bauer et al., 2007; Nowak et al., 2010; Petetin et al., 2016; Schiferl et al., 2014).



SO_x is another generic term referring to sulfur oxides, of which the most common form is sulfur dioxide (SO₂). In the lower atmosphere, SO₂ is present as a dense, colourless gas, which occurs naturally as a decay product of organic matter (Wayne, 2000). Volcanic eruption can also produce SO_x, as part of volcanic plumes. Anthropogenic sources of SO_x include coal burning by electric power companies, as well as the outputs from metal smelting (Dean, 2001; Fioletov et al., 2016; Jain et al., 2016; B. G. Miller, 2017; Miller, 2015). SO₂ is a precursor for sulfuric acid (H₂SO₄), which plays a key role in ammonium sulfate ((NH₄)₂SO₄) aerosol formation, which has a low vapour pressure (equation 2.3).

H₂SO₄ is formed through photochemical reactions involving hydroxyl radicals. Hydroxyl radicals oxidise SO₂ to sulfuric trioxide (SO₃), which then reacts with oxygen to form H₂SO₄. Additionally, H₂SO₄ is also emitted from the paper industry, namely pulp and paper mills, and as a by-product of fertilizer application (Brimblecombe, 2003; Speight,

2017). While H_2SO_4 does occur in the atmosphere, due to chemical stability, $(NH_4)_2SO_4$ is the preferred form. By reacting with acidic aerosols containing H_2SO_4 , every 2 moles of NH_3 removes a mole of H_2SO_4 (reaction ration of 2:1).



The third precursor gas recently recognized as a contributor PM formation is HCl (equation 2.4). However this gas is not abundant in the atmosphere and only makes a minor contribution to the total PM mass globally, the extent of which remains still unquantified (Sanhueza, 2001).



Anthropogenic HCl is mainly emitted through biomass burning and waste and coal combustion, with coal combustion being the biggest contributor (Sanhueza, 2001). The

co-combustion of solid fuels (e.g.: peat) with coal in power stations with state-of-the-art efficiency is regarded as one of the most profitable and cost-effective options for the reduction of coal usage in the energy sector (Wolf, Stephan, Fendt, & Spliethoff, 2017). Naturally emitted HCl arises from volcanos and the degassing of sea-salt (Sanhueza, 2001).

As with any chemical species, NH_3 gas in the atmosphere reacts with each component (SO_x , NO_x , H_2SO_4 , etc.) depending on their affinity to NH_3 (Bauer et al., 2007; Gong et al., 2013). H_2SO_4 is a highly acidic element of the atmosphere, having a much greater affinity for NH_3 than HCl and HNO_3 . As a result, atmospheric NH_3 will neutralize H_2SO_4 primarily on the grounds of its higher affinity, leaving the excess available to react with HNO_3 and HCl (Balasubramanian et al., 2013; Fine et al., 2008; Squizzato et al., 2013; Walke et al., 2006). The respective importance of each compound in this aerosol system is also dependent on atmospheric concentrations of each of the gases present at one time. Each precursor gas reacts with NH_3 individually. This, in terms of reaction dynamics in the atmosphere, makes NH_3 the limiting reagent, meaning the thermodynamic state and atmospheric concentration of NH_3 gas in the atmosphere can actually dictate secondary aerosol formation dynamics (Walker et al., 2006).

Primary sources of PM (emissions which do not undergo reactions in the atmosphere, but are directly emitted) include wildfires, geogenic and biogenic sources (Okubo & Kuwahara, 2020). Anthropogenic sources of primary PM comprise industrial processes (e.g.: smelters, smokestacks of thermal powerplants, etc.), combustion sources (biomass burning), electric power industry (from the use of fuels containing sulfur, coal and oil), residential emissions (burning of coal and peat), construction (dust and particles emitted from preparation of an area for a building or structure, to actual completion), and

vehicular emissions (Acharya, 2018; Geddes & Murphy, 2012; Miller, 2015; Tucker, 2000).

2.5 Deposition Processes Ammonia and Secondary Particulate Matter

As with all species (e.g.: PM, gases, etc.) transferred to the atmosphere, deposition processes eventually bring these materials back to the surface. Atmospheric NH_3 can undergo deposition in three major forms: NH_3 gas is returned to the surface by dry deposition, it is deposited as an aerosol in submicron atmospheric water droplets forming a salt in association with other atmospheric components (this is not to be confused with PM formation, where NH_3 undergoes a neutralization reaction with oxides of sulfur and nitrogen), and as NH_4^+ in the form of wet deposition (Hanson & Lindberg, 1991).

Dry deposition refers to atmospheric NH_3 gas being directly deposited back to ground level surfaces. Gaseous elements in the atmosphere are not deposited back onto planetary surfaces under the influence of gravitational attraction (Lovett, 1994). This is owed to the translational kinetic energy of particles competing with sedimentary forces (drafting, tumbling, etc.). Consequently, as with all atmospheric gases, the density of NH_3 decreases with increasing altitude in the atmosphere (Wayne, 2000). The main driving force for dry deposition of NH_3 gas from the atmosphere is turbulent diffusion. Turbulent diffusion is one of various dominant transfer processes in the free atmosphere, referring to the transport of mass, heat and momentum within the atmosphere (e.g.: gases) (Hemond, Fechner, Hemond, & Fechner, 2015; Venkatram & Du, 2003, 2015). This may be affected by near surface winds, turbulence, atmospheric stability of NH_3 (conversions between NH_3 gas and NH_4^+), surface roughness and spatial distribution of sources of NH_3 (Phillips et al., 2004).

High levels of dry deposition are predicated for locations where the highest emission rates are measured such as western Europe (England, Belgium and the Netherlands) and eastern U.S. (Pennsylvania and New York) (Behera et al., 2013; Vet et al., 2014). Low levels of deposition are predicted for low emission and/or low precipitation areas (e.g.: Sahara, Taklimakan, and Great Victoria deserts) of the continents with values ranging between 0.1 and 0.5 kg N ha⁻¹ a⁻¹. Dry deposition to oceans is generally less than 0.5 kg N ha⁻¹ a⁻¹ with the exception of near-coastal regions (Vet et al., 2014; L. Zhang, Brook, & Vet, 2003).

The Arctic and Southern Ocean, and the continent of Antarctica had dry deposition levels lower than 0.1 kg N ha⁻¹ a⁻¹ (Vet et al., 2014). A global-scale study of modelled patterns of oxidized and reduced forms of N dry deposition for the year of 2001 (Figure 2.3 and 2.4 respectively) (Shaw et al., 2014), provides a historical baseline for emissions. The differences arise in relation to the reduced forms (NH₃ and NH₄⁺), while oxidized forms refer to all other species of N emitted to the atmosphere.

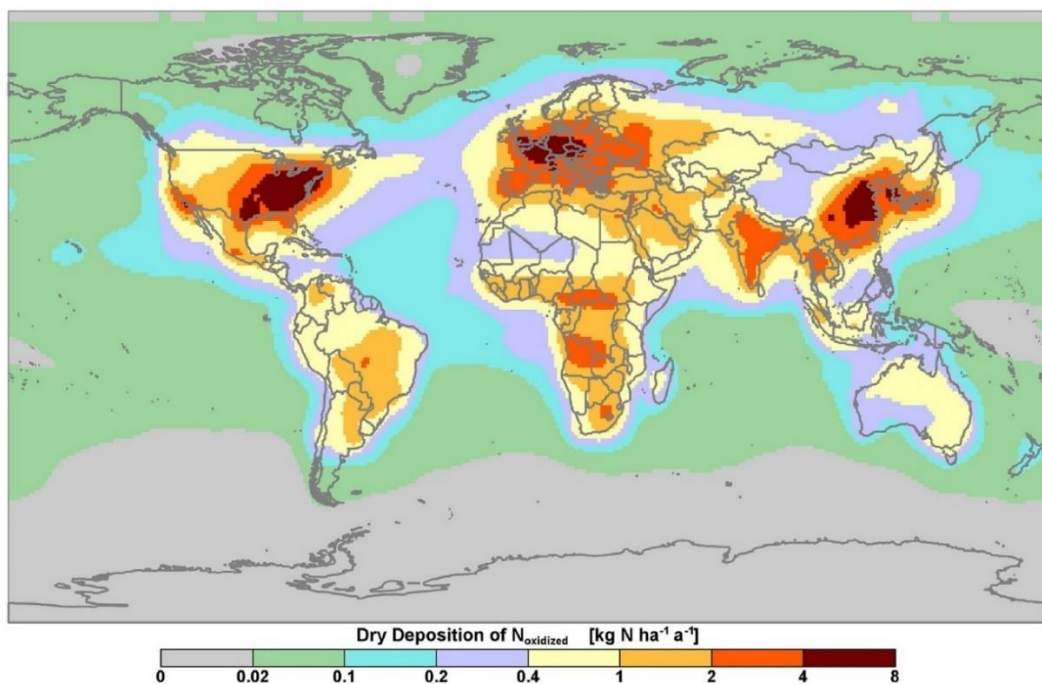


Figure 2.3 Ensemble-mean pattern of dry deposition of oxidized forms of N in kg N ha⁻¹ a⁻¹ for the year of 2001 (Shaw et al., 2014)

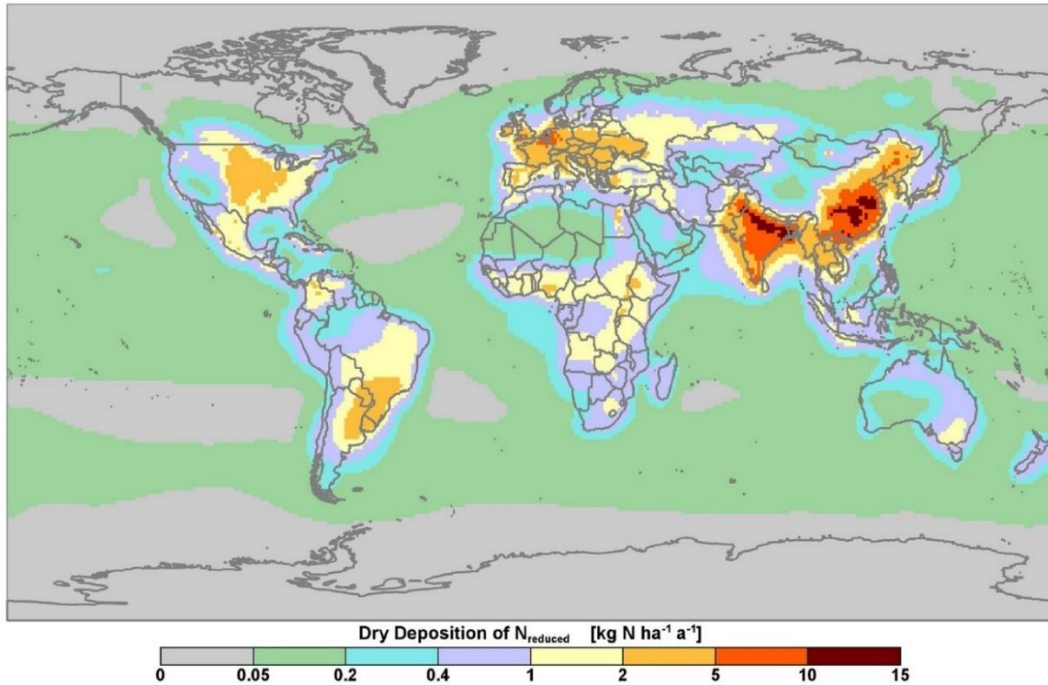
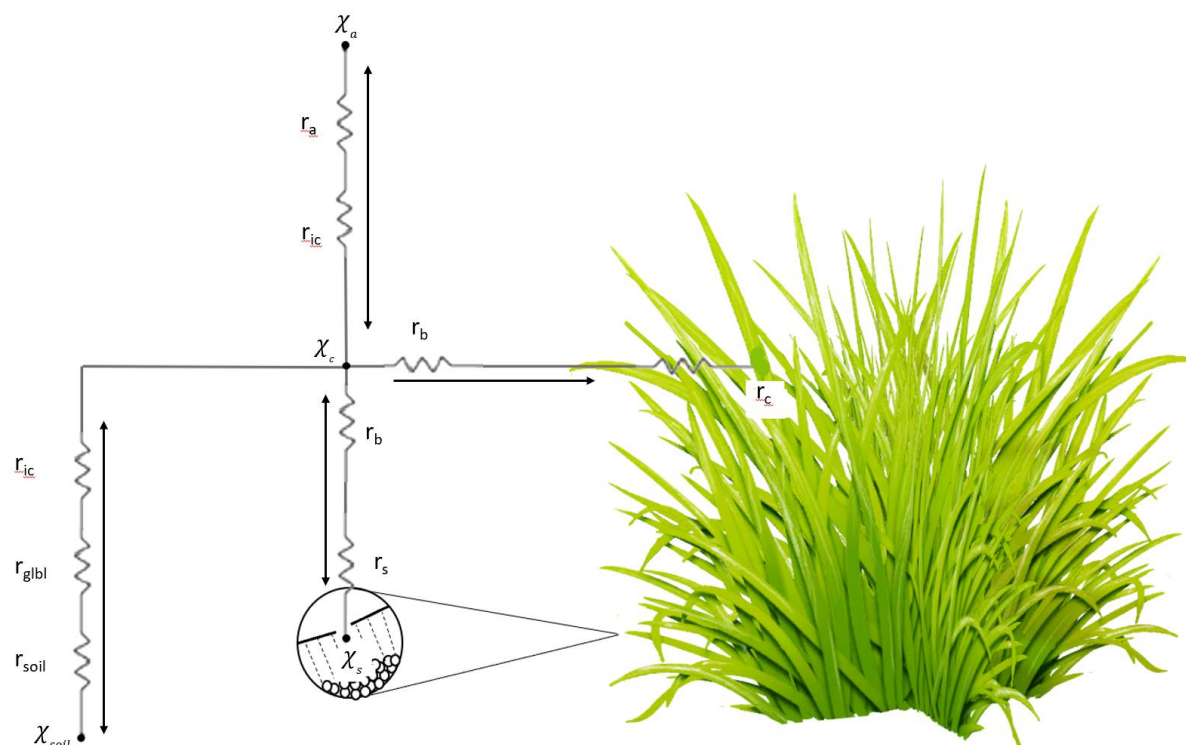


Figure 2.4 Ensemble-mean pattern of dry deposition of reduced forms of N in kg N ha⁻¹ a⁻¹ for the year of 2001 (Shaw et al., 2014)

Notably, unlike many other atmospheric components, NH₃ flow is bidirectional, meaning it can flux between the atmosphere, and vegetation and soils (Delon et al., 2017; Dennis et al., 2010; Pearson & Stewart, 1993). This is due to plants and soils having their own concentrations of NH₃, resulting in a potential flux between the atmosphere and planetary surfaces.




	Resistance to deposition	r_a	Aerodynamic resistance
χ_s	Stomatal compensation point	r_b	Laminar boundary layer resistance
χ_c	Canopy compensation point	r_{ic}	In-canopy resistance
χ_a	Atmospheric compensation point	r_s	Stomatal resistance
χ_{soil}	Soil compensation point	r_{soil}	Soil resistance
		r_c	Cuticular resistance
		r_{glbl}	Ground laminar boundary layer resistance

Figure 2.5 Resistance model schematic for bidirectional ammonia flux adapted from Pleim et al., (2013)

There are compensation points in the leaf stomata and the soil which have their own concentration (Figure 2.5). Thus, the fluxes through these pathways are bidirectional; the flux is depositing if the air concentration exceeds the surface compensation concentration and emitting if the surface concentration is in exceedance (Loubet et al., 2001; Pleim et al., 2013; Pleim et al., 2019).

The surface compensation concentration in soil and leaves are the NH_3 concentration in the soil pore (air space) or the stomatal cavity, in equilibrium with aqueous NH_4^+ ion and hydrogen (H^+) ions in solution in soil water or the apoplast leaf tissue respectively (Pleim et al., 2013, 2019; M. A. Sutton, Schjorring, & Wyers, 1995). Sutton et al., (1992) found NH_3 emission to be favoured during warm, dry conditions and deposition to be favoured during cool, wet conditions. This is due to the relationship between NH_3 on leaf surfaces and the presence of water on the cuticle (Behera et al., 2013).

As mentioned before, when transferred to the atmosphere, NH_3 can also rapidly transform into NH_4^+ due to reactions with water present in the atmosphere. Normally, there is less NH_3 present in the atmosphere at one time than NH_4^+ , except at localised hot-spots, where large quantities are volatilised (Warneck, 1988). Wet deposition removes NH_3 and NH_4^+ (ionised form of NH_3 in the atmosphere) from the atmosphere through two main processes, namely nucleation scavenging and impact scavenging. Nucleation scavenging occurs when particles act as cloud condensation nuclei (Kane, Rendell, & Jickells, 1994). As water accumulates on the particle, the aerosol may increase in size until the plume (fog) droplets deposit on planetary surfaces or fall from the air as precipitation. When the plume is combined with clouds, NH_4^+ is relocated into cloud droplets (Pacyna, 2008). These aggregate by various microphysical processes to raindrops or even snowflakes and are deposited from the atmosphere (Behera et al., 2013). While this process acts over both NH_4^+ and NH_3 , it is a more efficient deposition pathway for NH_3 , however this process

is different from the in-cloud scavenging of NH_4^+ aerosols (namely PM), as aerosols provide cloud condensation nuclei (Bouwman et al., 1997).

Impact scavenging occurs by physical contact with the much larger droplets of precipitation, or in the case of NH_3 , through absorption (on contact with droplets of precipitation) due to its high solubility (Kane et al., 1994). Impact scavenging is one of the atmosphere's cleansing processes and this removal process determines the chemical composition of precipitation (Lovett, 1994). While many studies have focused on the relationship between concentrations of gas and/or particle in the atmosphere measured at the surface and the corresponding concentration of ions in precipitation collected (Duce et al., 2008; Misra et al., 1985; Scott, 1981) few studies have investigated the changes which occur in gas and particle concentrations during precipitation events.

Precipitation as well as cloud water tend to be slightly acidic (Hontoria et al., 2003), so that most of the NH_3 scavenged by drops reacts with a hydrogen ion (H^+) to form NH_4^+ (Behera et al., 2013). It can, henceforth be considered as a potential component of 'acid rain', using the term in its broadest sense (Bouwman et al., 1997).

Tørseth et al. 2012 has found an average decrease in both oxidized and reduced forms of N concentrations in precipitation from 1990 to 2009 in Europe, with minor reductions occurring from the late 1990s, amounting to an estimated 25% of total N concentrations in precipitation. On a global scale, total NH_3 emissions in 2001 were estimated at 58.5 (± 9.5) Tg, of which 70.1% were continental (landlocked), while 16.2% were coastal. In general, trends in wet deposition can be compared with the trends of emission of precursor gases. However, when analysing wet deposition of precursor gases such as NH_4^+ , NO_3^- and S, emissions from abroad (outside of Europe) must also be considered.

For that reason, trends can only be accurately determined if transboundary transport is taken into account (Van der Swaluw et al., 2011).

These findings are also supported by the study conducted by Vet et al. 2014, reporting most of the NH_3 emitted being deposited near the source of emission. However, patterns suggest that a significant portion is transported off the continents where it's subsequently deposited in the off-shore zone of major oceans. Transport of N emissions from continental non-coastal and coastal areas to deep ocean zones represents an important source of oceanic N input within oceanic systems (Behera et al., 2013a, 2013b; Leip et al., 2011).

Patterns suggest that nitrogen oxide-nitrogen ($\text{NO}_x\text{-N}$) and ammonia-nitrogen ($\text{NH}_3\text{-N}$) emissions are transported off the continents where they subsequently undergo wet deposition in off-shore regions of major oceans such as the North Atlantic Ocean and North Pacific Ocean, most notably off the west coast of Europe, east coast of southern Asia and the east coasts of North America (Billen et al., 2011; Vet et al., 2014). Figure 2.6 shows the modelled estimated N deposition during the year of 2000 (Dentener et al., 2006). Due to the difficulty of establishing a global model given difficulties such as inconsistencies in reporting of emission levels, etc., overarching studies such as the one depicted by Figure 2.6 is the most recent global estimate of N deposition.

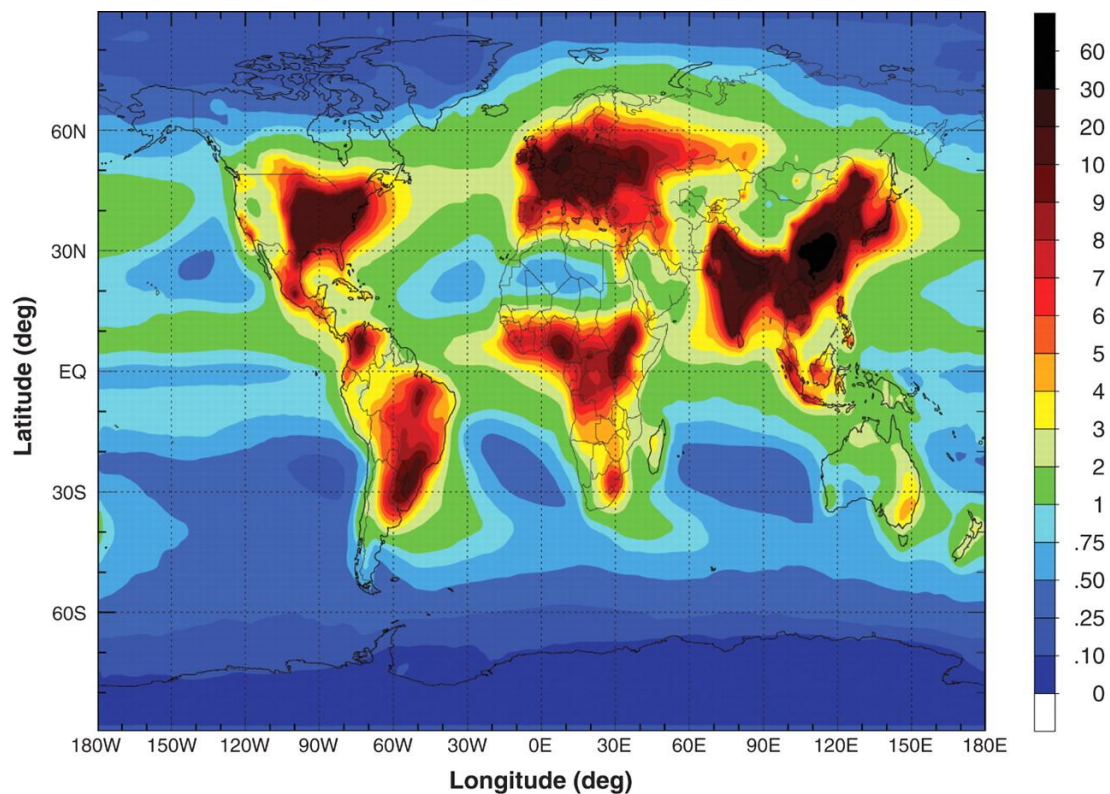


Figure 2.6 Model estimated N deposition from global total N emissions, with an estimated total of 105 Tg N yr⁻¹ (unit scale in kg N ha⁻¹ yr⁻¹) for the year 2000 (Dentener et al., 2006)

Ambient PM, like NH₃ gas, can be removed from the atmosphere through wet and dry deposition (Yanan Wu et al., 2018). The dry deposition of aerosol NH₄⁺ (PM) is somewhat different to that of gaseous NH₃. They share the aspect of atmospheric turbulence dominating the transport from the atmospheric to planetary surfaces, however, mechanisms such as Brownian motion, inertial impaction, interception, phoretic forces, etc. play key roles in the deposition of PM. However, these forces act differently depending on the size of PM (i.e.: whether it is PM₁₀ or PM_{2.5}) (Loosmore & Cederwall, 2004). (Kulshrestha, 2017; Pacyna, 2008). The size of PM also ensures that re-emission into the atmosphere does not occur easily, hence PM flux (including secondary inorganic aerosols (SIA)), unlike NH₃ flux, is unidirectional (Giardina & Buffa, 2018).

Ambient PM wet deposition process are collectively known as wet scavenging. Wet scavenging is an essential process for the maintenance of balance between sources and sinks of atmospheric PM (Yang et al., 2015). Wet scavenging of atmospheric PM occurs through two notable processes: below-cloud scavenging (washout) and in-cloud scavenging (rainout) (Roy et al., 2019). In the process of wet deposition, particles are incorporated into hydrometeors before being brought back to the surface in aqueous form (Santachiara, Prodi, & Belosi, 2013).

Similarly to dry deposition, both in-cloud and below-scavenging is highly dependent on the size of PM, with rates of removal differing for each size fraction (Behera et al., 2013; Tobias & Neubauer, 2019). Consequently, coarse particles are deposited near source areas while fine and ultrafine fractions are transported away from sources prior to deposition (Baker, 2010; Censi, Darrah, & Erel, 2012; Santachiara et al., 2013). Monitoring at both national and EMEP scale has indicated Ireland having a number of important transboundary pollution pathways, namely from the United Kingdom, Europe and North America, through pollution sources also arise from Africa, especially during springtime when elevated levels of Saharan dust are detected in Ireland (Environmental Protection Agency, 2016).

Atmospheric PM can also serve as cloud condensation nuclei (CCN) (Deshler, 2015; Dickinson, 2012; Herckes & Collett, 2015; Lohmann, 2015; Rosenfeld, 2018; Tao & Matsui, 2015; Wang, 2002). Condensation of nitric acid on aerosols may enhance aerosol activation to cloud droplets by providing additional soluble material to the particle surface, as well as elevating the water uptake and growth of aerosol particles (Cai et al., 2019; Forbes & Garland, 2016; Goodman et al., 2000; Hämeri et al., 2000; Silvern et al., 2017; Squizzato et al., 2013; Yi et al., 2018).

Under favourable meteorological conditions, hygroscopic particles are attracted to PM present in the atmosphere, leading to a rapid increase in PM mass fractions (namely PM₁₀ and PM_{2.5}) (Andreae, 2009). The process of hygroscopic growth can be described by Köhler's theory of water vapour condensation, forming liquid cloud drops based on equilibrium thermodynamics (Lohmann et al., 2016). This process plays a key role in cloud physics, making atmospheric PM a vital element in understanding cloud formation, as well as the role it plays in the Earth's climate systems.

Additionally, as a result of its role in cloud physics, long range transport of PM (mainly referring to the fine size fraction here, as the coarse size fraction tends to be deposited near its source) is also facilitated in this way. Ireland's climate is typified by high humidity, therefore NH₄NO₃ would be present as aqueous state particles, serving as cloud condensation nuclei and allows for long range transport as well as immediate local deposition. This makes identification of the sources of secondary PM hard to pinpoint and characterise, as emissions can travel from country to country or even from a source country to a different continent. Additionally, source and receptor relationships are poorly understood as secondary emissions may originate from different source regions to the receptor surfaces where they are deposited.

2.5 Controlling factors of emission, transport, and deposition processes of ammonia and secondary particulate matter

Emissions of pollutants are controlled by various factors. Biotic factors represent all living things which affect emissions, such as the flora and fauna of a given environment. Abiotic factors refer to all the non-living factors which can affect emissions, for example meteorology and climate. Anthropogenic activities also affect and can control the

emission of pollutants. It must be acknowledged that, while biotic and abiotic factors play major roles in the control of emission of secondary PM, the biggest control factor for the formation of secondary PM will be the availability of precursor gases. Therefore, it can be suggested that anything which may control and/or affect NH_3 emissions, will have an indirect effect on secondary PM formation.

The stores of N can be broken down into three major reservoirs: atmosphere, lithosphere, and hydrosphere. The exchanges of N in its various forms results in what is known as the N cycle (Cabello et al., 2009). As demonstrated in the previous section, anthropogenic activities such as agriculture have the ability to influence and even alter the N cycle between these three major pools by additional N loading through the use of synthetic fertilizers to soils and vegetation. The N cycling of anthropogenic loads is affected by climate, soil properties, vegetation type and land-use management particularly in the agricultural sector (Butterbach-Bahl et al., 2011). Soil texture, pH, C: N ratio, soil organic matter content (SOM) and moisture content all exhibit significant control effects on the soil's ability to cycle various forms of N (Cabello et al., 2009).

Physical properties such as soil texture and clay content can also affect N cycling of soils (Breuer, Kiese, & Butterbach-Bahl, 2002; Palmer et al., 2017). Fine textured soils (soils composed of fine particles with a high content of silt and clay) exhibit greater water holding capacity and higher concentrations of SOM than soils with coarse textures (high proportions of sand and loam present) (Butterbach-Bahl et al., 2011; Butterbach-Bahl et al., 2013; McLauchlan, 2006). As a result, anaerobic processes associated with N losses in gaseous forms such as N_2O and NO occur more frequently in fine texture soils due to their greater tendency to exhibit anaerobic conditions (Butterbach-Bahl et al., 2013; Skiba et al., 2009).

Coarse textured soils have a higher ion exchange capacity than fine textured soils, which enables NO_3^- to leach at higher rates. Overall cation exchange capacity (CEC) of soils also affects ammoniacal N ($\text{NH}_3\text{-N}$) concentrations through the reaction of positively charged NH_4^+ with the negatively charged cation exchange sites. This means that soils which have a low CEC, will be more likely to lose large amounts of NH_3 through volatilization, compared to soils with high CEC (Bouwman et al., 2002). SOM content of soils plays a significant role in determining the pace of N cycling in soils (Li, Frolking, & Butterbach-Bahl, 2005), while C:N ratio can control gaseous emissions of N to the atmosphere as well as the leaching of N components (e.g.: $\text{NO}_3\text{-N}$) into groundwater sources (Klemedtsson et al., 2005).

Soil pH impacts various processes in the cycling of N, affecting the equilibrium between NH_4^+ and NH_3 (Hamaoui-Laguel et al., 2014; Rochette et al., 2013; Smith et al., 2009). NH_3 (pK_a of 9.3 at 25°C) increases from 0.1 to 50% as pH increases from 6 to approximately 9 (Bouwman et al., 2002). This is due to soil pH influencing the three main processes by which reactive N (N_r) is emitted to the atmosphere: nitrification and denitrification. Both volatilization and nitrification processes may reduce NH_3 concentration by decreasing the availability of NH_4^+ and by increasing acidity (pH imbalances) (Bouwman et al., 2002; Kesik et al., 2006).

Temperature and moisture content of soils also play key roles in the control of microbial activity of soils. Both factors can contribute to high-capacity N cycling where neither temperature nor the moisture content are acting as limiting factors, creating anaerobic conditions, without full saturation of soils (Breuer et al., 2002; Corre, Beese, & Brumme, 2003). Temperature and mineralization of N_r exhibit a linear relationship up to approximately 30°C (Gutiñas et al., 2012; Schindlbacher et al., 2004). However, this relationship can become nutrient limited at temperature higher than 30°C , as temperature

response of nitrification is dependent on the availability of NH_4^+ . Additionally, NH_4^+ assimilation by plants is also a temperature dependent reaction, and works at a faster rate than nitrification, resulting in the nutrient limiting effect (Gutiñas et al., 2012).

N mineralization is also affected by the type of vegetation present through litter quality, as well as the overall N cycling of a given ecosystem (Butterbach-Bahl et al., 2011). Competing vegetation can limit growth resources within soils such as moisture content (Roberts, Harrington, & Terry, 2005). The parameters of the vegetation (type of vegetation, root depth, etc.) itself also have a distinct influence on the N cycling of soils. The types of canopy present affect N trace gas exchange such as NH_3 , through leaf geometry and canopy structure; while root distribution affects leaching N from soils and N turnover rates by microbiota present (Rothe, Huber, Kreutzer, & Weis, 2002; Teepe, Brumme, & Beese, 2000). Due to Ireland's climate, grasslands can provide a year-round surface for reactions, as well as trees which do not lose their leaves for the winter season. During growing seasons (spring and summer) foliage (leaves) would be the dominant surfaces for reactions (Hill, 1971).

Anthropogenic activities affect N cycling on both spatial and temporal scales of various magnitudes. Human management of ecosystems has a crucial role in regulating the N load and its efflux to and from the atmosphere. This management interaction of the N cycle has been mediated through the role of fertilization, irrigation, drainage management of soils, tillage practices, liming, grazing, soil compaction, and crop-rotation. These activities have ecosystem-scale effects and are mediated by substrate availability of soil microbes, aeration, soil microbial composition and soil moisture (Erisman et al., 2013; Guiry et al., 2018; Jenkinson, 2001).

Climate (on both local and global scales) and pollutant emissions have a cyclic effect on one another. Natural global climate changes have been aggravated by anthropogenic disruptions such as increasing emission of pollutants such as NH_3 and PM. The terrestrial N cycle has been drastically modified by global climate change as a result of increasing demand for land use changes (e.g.: deforestation to make way for agricultural land-use) and fossil fuels (Galloway et al., 2004). Additionally, climate affects the microbiota present in terrestrial ecosystems including soils and is a significant determinant of type and species present.

Microbial processes involved in denitrification and nitrification are greatly affected by these components of a global climate change, resulting in serious environmental issues, such as elevated NO_3^- leaching and NO_x emissions (Davidson et al., 2007). The impacts of multiple components of climate change on microbial communities and the associated processes mediated by microorganisms are variable and microbial functions respond differently to different climate factors which have an influence over activity (Classen et al., 2015; Rinnan et al., 2007). Microbial communities lead nutrient cycling, and their management of nutrient availability plays a central role in controlling plant biomass. Furthermore, nitrification and denitrification are two essential processes in the global N cycle controlled by microbiota, contributing greatly to global N turnover, particularly NO_x emissions (Zhang et al., 2017). Climate change can directly affect microbial communities, which in turn impact net primary production through the alteration of nutrient availability (Delgado-Baquerizo et al., 2014).

Similarly, to NH_3 , formation and transport of PM are also affected by local meteorological conditions and climate change. Ambient relative humidity (RH) and temperature are key meteorological factors for the determination of the state of PM. For example, reactions of NH_3 with HNO_3 at low temperatures will show a shift in the

equilibrium of the system towards the aerosol phase. Low RH results in NH_4NO_3 forming as a solid particle (Bauer et al., 2007; Seigneur, 2019). These dynamics are closely related to the close relationship between temperature and RH. As temperature increases, the air's capacity to hold moisture also increases, resulting in the RH decreasing (Hernandez et al., 2017; Wayne, 2000). Changes in temperature as an onset of global climate change therefore will affect local RH, as well as global meteorological dynamics. These changes can affect PM dynamics including transport pathways, and PM formation on a localized basis (McMurry & Wilson, 1983; Zang et al., 2019).

The optical effects of PM are also strongly influenced by RH, as hygroscopic components absorb water, changing both the diameter of particles and the wavelength-dependent refractive indices and the extent of scattering (mie scattering) of PM (Martin et al., 2003). This bears a significant influence on regional and global climate, as it effects the radiative forcing, also known as climate forcing both regionally and globally (Chang & Park, 2004; Kim, Kim, & Kang, 2011; Zhang et al., 2000). Radiative forcing is the difference between insolation absorption by the Earth and the energy which is radiated back to space. Changes in the refractive index of PM can alter the radiative balance of the Earth's climate systems, and forcing temperatures to increase or decrease, a process collectively known as climate forcing (Ban-Weiss & Collins, 2015; Bellouin, 2015; Haywood, 2016; Isaksen et al., 2012; J. Kim et al., 2015; Pulselli, 2008; Pulselli & Marchi, 2015; Vallero & Letcher, 2013).

The specifics of the sources and causes of local high levels of PM are unique to each location. Generally, a thermal inversion layer and/or high surface pressure can lead to increased PM concentrations (Hawkins & Holland, 2010). Although thermal inversions are transient atmospheric effects, they can trap pollutants such as aerosols and result in smog close to the ground. Thermal inversions are temporarily stable because of the

temperature-pressure gradient where low temperatures and high pressures are close to the ground and as such disrupt and/or suppress convections, resulting in a “cap” effect. Cheng et al. (1992) found that high pressure associated with maritime tropical and non-polar continental air masses generated the highest total particulate matter concentrations. These air masses were defined by high pressure and temperature values, high dew points, percent of clear sky and stability (Wayne, 2000). Lower PM concentrations are generally correlated with polar air masses (such as polar maritime, returning polar maritime and polar continental air masses). Depending on weather conditions (precipitation, wind direction, wind speed, etc.), these air masses occur ahead of a low pressure system (Hawkins & Holland, 2010). These air masses are generally advected from the Atlantic Ocean in Ireland.

Terrain also affects with specific weather patterns and can influence air masses which influence PM levels. Augmented stability in valleys form geomorphological traps associated with cold air drainage and is most prevalent under synoptic high pressure conditions (Beaver et al., 2010). During unstable conditions, the opposite may be true, as mountains act to increase upward vertical motions in the atmosphere and hence decrease surface PM levels. Mountains can also heighten PM concentrations by trapping pollution that may alternatively be dispersed (Chuang et al., 2008).

2.6 Modelling the Soil-Water-Atmosphere Nexus in Ammonia and Particulate Matter dynamics

The development, parameterisation and validation of NH_3 models over the years, to a great extent, have been based on a steadily emerging availability of data on NH_3 concentrations in a broad range of ecosystems and the atmosphere and/or flux datasets

across all scales (Flechard et al., 2013). At sub-ecosystem scales (chamber, plot, field), this has stemmed from technological advances in NH_3 measurement and analysis, both quantitatively and qualitatively.

The use of flux measurement instrumentation capable of lower detection limits than was available before, while also selectively quantifying gaseous NH_3 from aerosol NH_4^+ allows for higher accuracy measurements (Aneja et al., 2001; Butler et al., 2015; Dammers et al., 2017; Mount et al., 2002; Norman et al., 2009; Schwab et al., 2007; Singh et al., 2001; Sutton et al., 2001; Von Bobritzki et al., 2010). On a field scale, Bowen ratio techniques at remote background locations (i.e.: for sub-parts per billion levels of NH_3 are present) and at over-fertilised agricultural ecosystems aided in the generation of many exchange datasets (Milford, Theobald, Nemitz, & Sutton, 2001; Nemitz et al., 2000).

The key mechanisms and controls of NH_3 exchange have been determined at a substrate, plant, and ecosystem level, though a substantial gap in knowledge still remains regarding the complete process of NH_3 dynamics. This can partially be attributed to the lack of regulation of NH_3 as a gaseous atmospheric pollutant. Compared to other atmospheric gaseous pollutants such as SO_2 , NO_x and volatile organic compounds (VOCs), no extensive control measures have been put in place for the control and mitigation of NH_3 emissions (Behera et al., 2013).

Despite the contribution NH_3 makes to the overall atmospheric PM mass loading, there are currently very few regulations in place and incentive programmes to reduce emissions are lacking in many countries, including Ireland. In fact, Ireland has been implementing policies which are counteractive to the reduction and mitigation strategies which should be in place, through schemes such as the Food Harvest 2020 (Department of Agriculture, Fisheries and Food, 2015) and Food Wise 2025 (Department of Agriculture, 2015) which

boast agricultural intensification. This has resulted in atmospheric NH_3 concentrations exceeding the permitted levels for six years in a row (2016 to present).

2.6.1 Direct source measurement: state-of-the-art techniques

Measurement techniques of atmospheric NH_3 have improved over the last two decades. One major difficulty when developing measurement techniques for atmospheric NH_3 arises from simultaneous presence of NH_3 gas and NH_4^+ in the form of PM (liquid and solid state) (Norman et al., 2009). Additionally, variations in atmospheric concentrations and the ability of NH_3 gas to interact with surfaces (Norman et al., 2009; Bobruzki et al., 2010) presents further difficulties when developing techniques for the measurement of atmospheric NH_3 . These difficulties have resulted in development of measurement techniques being slower than for many other substances that can present as atmospheric pollutants.

The most widely used techniques for NH_3 measurement are denuder sampling techniques (active sampling) and diffusive samplers (passive sampling). Doyle et al., (2017) defines diffusive samplers as: “A diffusive sampler is a device which is capable of taking samples of gas or vapor pollutants from the atmosphere at a rate controlled by a physical process, such as diffusion through a static air layer or permeation through a membrane.” Diffusive sampling relies on the mass flux of substances from regions of high concentration to regions of low concentration.

Denuder sampling techniques such as the Annual Denuder Method (ADM) has proven to be a successful method for NH_3 gas sampling. Denuders work based on a laminar airstream passing through a suitably long tubular enclosure whose walls are coated in the appropriate sorbent for a given acidic or basic gas present in the atmosphere. The sampler

also has a capacity to differentiate between NH_3 as part of PM and NH_3 gas (Tang et al., 2018; Tang et al., 2018). Despite widespread use, both denuder techniques and diffusive sampling methods come with limitations such as relatively low time resolution, highly labor-intensive sampling procedure and post-sampling wet-chemistry analysis, which can introduce contaminants to the samples during storage or analysis (Norman et al., 2009). Despite these limitations, denuders and diffusive samplers remain the most cost-efficient sampling techniques for atmospheric sampling of NH_3 and PM.

Other methods for measuring ambient atmospheric NH_3 are spectroscopic techniques such as Photoacoustic Spectroscopy (PAS, Besson et al., 2006; Huszár et al., 2008; Schmohl, Miklos, & Hess, 2020), Differential Optical Absorption Spectroscopy (DOAS, Dammers et al., 2017; Mount et al., 2002), Tunable Diode Laser Absorption Spectroscopy (TD-LAS, Yao et al., 2015) and Chemical Ionization Mass Spectroscopy (CMIS, Schwab et al., 2007). These techniques rely on infra-red (IR) or laser-based systems such as laser diodes detectors which can single out NH_3 gas. This results in high accuracy and precision when measuring NH_3 in the atmosphere. Differences in accuracy and precision of the instrumentation used for the measurement of atmospheric NH_3 arise from differences in inlet length, calibration frequency of each instrument and the frequency of changes of collection vessels such as filters or diffusion tubes (Sutton et al., 2001).

With modifications, the precision of passive diffusion tubes could be improved. They also found the optimized method for sampling using the denuder technique with a time resolution of two weeks and ambient atmospheric concentrations of $>2\mu\text{g m}^{-3}$ NH_3 . While differences were found in the concentrations measured using the techniques mentioned in the text above, there still was an overall high correlation of $R^2>0.84$ reported.

Correlations deviated from this figure when concentrations were below 10 ppb NH_3 , due to differences in inlet length of samplers and time-response.

Bobrutski et al., (2010) looked at an array of techniques (highlighted above) from spectroscopic to wet chemistry methods comparing the techniques listed above. This is an extremely complex process which will be briefly discussed here. A full review can be found in Bobrutski et al., (2010). All of the spectroscopic techniques mentioned above tend to be quite expensive and require specific installation and training, therefore may not necessarily be readily available. Facilities which use these types of analysis and offer services to carry them out for third parties can be quite expensive also. Thus, at university level, these techniques, while providing good accuracy and precision, are not necessarily an option many can avail of. In contrast, wet chemistry methods are inexpensive (when compared to the price of instrumentation and software) and come with an extensive range and multiple options of measurement for any single component. Wet chemistry techniques also can offer reduced preparation times (some methods, for example CMIS require an extensive number of steps before samples are ready for analysis), which can make wet chemistry methods less labor-intensive.

2.6.2 Modelling of Ammonia and Particulate Matter

Various numerical models have been generated for the implementation of modified gradient techniques to infer the surface flux of NH_3 (and chemically reactive species) from field measurements, while also accounting for gas-to-particle interconversion (GPIC) and its effects on vertical flux divergence (Bajwa, Arya, & Aneja, 2008; Kruit et al., 2010; Pleim et al., 2013, 2019; Schrader et al., 2016; Skiba et al., 2009; Wichink Kruit et al., 2017; Zöll et al., 2016). Modelling results presented in the literature suggested that

atmospheric reactions could theoretically change NH_3 fluxes by as much as 40% (Flechard et al., 2013) or even cause flux reversal.

While most emission model studies focus on the influence of precursor species concentrations (e.g.: NH_3) on aerosol concentrations; Zöll et al., (2016) has shown a novel approach to NH_3 emission modelling, with an overall aim of creating a better understanding of the geological and temporal aspects of emissions. Models focusing on results prior to this study resulted in the models being too simplistic, with inaccuracies in estimating emissions, by not accounting for environmental factors affecting emissions overall. This model qualitatively compares two semi-empirical parameterizations of a quasi-bidirectional non-stomatal compensation point, and a unidirectional non-stomatal resistance model. This improved understanding has allowed for a more complicated model construct having higher accuracy and precision than other models of this type.

Many localized field experiments based around NH_3 deposition measure concentration decreasing over distance from the source. Dry deposition processes control the transfer of pollutants from the atmosphere to the surface (Wayne, 2000). However, its exact mechanisms are poorly understood. Studies conducted in Denmark have made critical improvements of atmospheric models of NH_3 , specifically regional N deposition assessments. The model was built by replacing static seasonal variations with dynamic applications accounting for physical processes (e.g.: volatilization) and agricultural management practices such as seasonal timing of fertilization (Geels et al., 2012). However, the data required for such a model to be constructed is insufficient in most European countries, as many inventories are poorly managed or do not exist on a nation-wide scale.

The state-of-the-art of NH_3 surface-atmosphere exchange mechanisms, in terms of measurement and modelling, has been investigated in a number of reviews (Sutton et al., 2007; Zhang, Wright, & Asman, 2010). Existing models of surface exchange are reviewed at different scales from leaf to the global level, with a focus on the development of canopy-scale models and their application at larger scales (regional). A large number of models have been generated to simulate NH_3 exchange fluxes for various ecosystem components (soil, leaf, plant, plant canopy, litter) or processes (heterogeneous phase chemical reactions) (Asaadi et al., 2018; Flechard et al., 2013; Hansen et al., 2013; Pleim et al., 2013). These components have been modelled either individually or at a canopy scale 1-dimensional (1-D) soil-vegetation-atmosphere basis. Larger scale models (landscape, regional or global) models are 2-D or even 3-D, usually including simplified versions of canopy-scale models simulating 1-D surface exchange, as part of the wider context including chemistry, emissions, dispersion and deposition (Figure 2.7) (Flechard et al., 2013; Pleim et al., 2019; Wu et al., 2009).

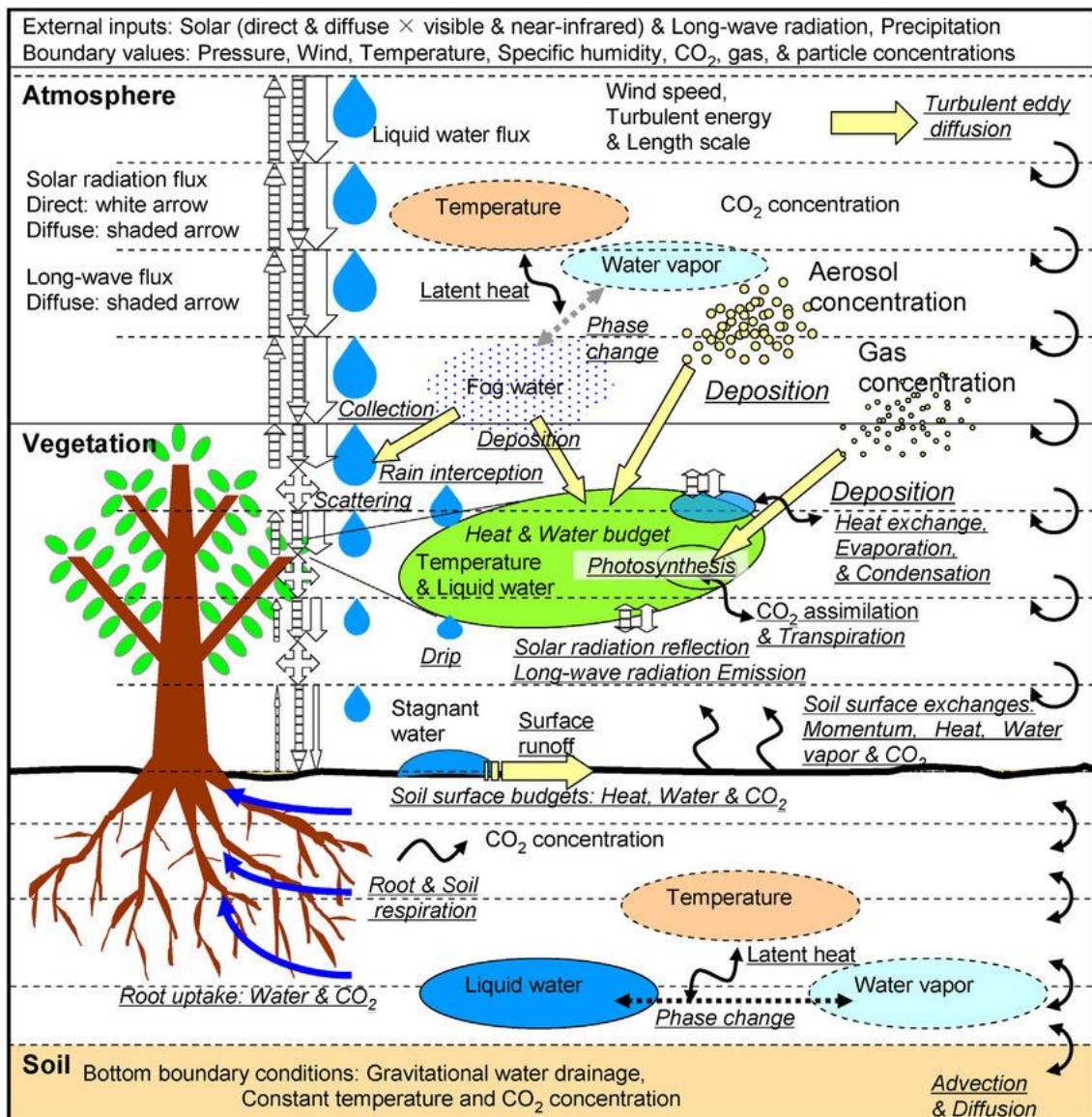


Figure 2.7 An example of a multi-layer 2-D model schematic: the SOiL-VEgetation model by Katata et al.,(2013)

Canopy-scale models incorporate individual component processes and the interactions they undergo within the soil-vegetation-atmosphere framework (Flechard et al., 2013; Massad et al., 2008; Sutton et al., 2013; Walker et al., 2008; Wu et al., 2009; Zhang, Wright, & Asman, 2010). The objective of this type of modelling is to determine the net ecosystem NH_3 flux from the following inputs: (i) atmospheric NH_3 levels; (ii)

meteorology, or alternatively micrometeorological factors; (iii) ecosystem characteristics such as canopy height, depth and leaf area index (LAI) (Flechard et al., 2013) (generally, defined as “the one-sided area of green foliage projected onto a unit area of ground” (Nikolov & Zeller, 2006)). Most models are based on the resistance analogy, in which the flux (F_x) between two potentials, A and B, is equal to the potential difference divided by the resistance, with the canopy-atmosphere-soil being represented as a network of potentials connected by resistances in series for different layers and in parallel for different pathways (Giardina & Buffa, 2018).

Several experimental campaigns have been carried in order to supply data for the dry deposition velocities for different types of pollutants (e.g.: PM) and deposition surfaces (Giardina & Buffa, 2018; Giardina et al., 2019; Hansen et al., 2013; Janhäll, 2015; Kouznetsov & Sofiev, 2012; Le Roux, Hansson, & Claustres, 2016; Mohan, 2016). However, due to the issues associated with influencing factors which play a part in deposition velocity, differences between the data lead to a difficulty in generalizing this phenomenon (Giardina & Buffa, 2018).

Due to this controversy, the dry deposition process cannot be studied using a single modelling approach. Indeed, the models proposed in literature are incapable of representing dry deposition phenomena as a whole for several categories of pollutants such as PM and its deposition surfaces (plant canopy, water surfaces, etc.) as their applications are only valid for a definitive set of conditions (certain types of climate, meteorology, topography, etc.) (Giardina & Buffa, 2018; Giardina et al., 2019). Kinetics for the chemical source and/or sink associated with the $\text{NH}_3\text{-HNO}_3\text{-NH}_4\text{NO}_3$ triad are described either using chemical timescales, reaction rate coefficients or as a full model of size-resolved chemistry with the addition of microphysics (Massad & Loubet, 2013).

Atmospheric forecasting of pollution events is a recent development with a large research focus involving research institutes globally in model development (Menut & Bessagnet, 2010). While these types of models are still in the development stage, some of the first systems have appeared as “operational” systems. However, due to large disagreements in the area of parameterization, these models are largely experimental and until a unified set of parameters are established on an EU-wide scale, these models will remain contested.

The difficulties of unified parameters for modelling in the EU mainly arise from the differences of environmental factors between countries such as the temperature effects of local meteorology, climate, and geographical features which all affect emission and deposition processes. Thus, generally, temperature effects are not taken into account in current European models including Chemistry Transport Models (CTMs) (Menut & Bessagnet, 2010). Skjøth & Geels (2013) found that this is also the case for Chemistry Climate Models (CCMs). These findings are in agreement with the proposed theory of Zöll et al., (2016) which seeks to improve models by applying the dynamic processes (national meteorological effects, transport and geographical variations) which results in spatio-temporal variations of emissions of pollutants such as NH_3 .

Most EU models (such as CTMs for example) receive data from the EMEP system which is known as a gridded emission inventory. These inventories are constructed based on national emission factors integrated with gridded activity data such as number of animals on a national basis (Skjøth & Geels, 2013). However, the data represented by the EMEP campaign is too generalized for accurate and precise model constructs to be achieved, especially for models with a forecasting element. This can be seen currently, as it applies to the 27 air pollution prediction models in use in the EU with a temporal profile element. These models are used for the forecasting of NH_3 pollution, do not have sufficient

accuracy or precision, as most either over or under-estimate ambient atmospheric concentrations (Geels et al., 2012).

As there is currently no continuous monitoring of ambient atmospheric NH_3 concentrations in Ireland, most European-scale models exclude Ireland as there is insufficient data supplied for inclusion. In order for Ireland to be included in modelling campaigns, high detail data is required. A monitoring campaign based on the dynamics of NH_3 emission and deposition processes can provide such data, as well as provide clarification of PM dynamics and transportation.

2.7 Concluding Remarks

Ambient atmospheric NH_3 is an important substance that can act as a pollutant contributing significantly to secondary PM generation, a contribution which is often under-estimated due to the short-range transport of NH_3 from hot-spots and its short half-life in the atmosphere. Studies focusing on NH_3 measurement are often based on distance, meaning the distance NH_3 is transported from an area of interest, especially in deposition study models. The dynamics of NH_3 through the biosphere are poorly defined, thus source and receptor interactions and effects are crudely understood at best. While a cause-and-effect relationship has been established between NH_3 and secondary PM and mitigation strategies have started to recognize that reduction of precursor gases inevitably serve the reduction of secondary PM, the lack of understanding of system dynamics and the precise nature of how to efficiently mitigate both species of pollutants is still not clearly understood.

Accurate models of the spatial and temporal distribution of NH_3 and PM emissions are crucial input to models of atmospheric transport and deposition. This is particularly

important when the resulting deposition maps are utilized to establish suitable mitigation strategies and ecosystem decline as a result of pollution. The accuracy and precision of prediction models is dependent on the quality of the input data, and an understanding of system mechanics. Hence, there is a need to establish high-quality emission and deposition inventories for both species of NH_3 and PM. This task requires an analysis and monitoring of the dynamics of both NH_3 and PM rather than investigating only precursor gases from which concentrations of secondary pollutants are extrapolated. However, long-term campaigns of direct measurements on which these inventories and models are based still remain difficult to conduct.

All techniques of measurement are affected by the built-in bias of the design chosen whether spectroscopic or techniques based on wet-chemistry methods. To these potential errors, additional ones arise from geographical features of the terrain (presence of hills and valleys, presence of water sources, groundwater dynamics, etc.) where measurements are carried out as well as local meteorological effects which can affect measurement. Choosing the most suitable method of measurement can minimise these errors, improving data quality by precise and accurate measurements, making it a crucial step in any research study. Therefore, any and all studies based around NH_3 pollution and secondary PM arising from NH_3 should take the above-mentioned factors into consideration. Furthermore, studies with the aim of contributing towards a continuous monitoring system for Ireland have to consider the quality of data that the monitoring network would provide, as it would have to be sufficient to contribute not only at a national, but at a European-wide scale.

Chapter 3: Methodology

3.1 Introduction

This chapter outlines the experimental techniques employed throughout the project in order to address the research aims and associated objectives given in Chapter 1.

The chapter has been divided into five separate sections:

3.1 Network Operation

3.2 Atmospheric Sampling and Analysis

3.3 Water Sampling and Analysis

3.4 Soil Sampling and Analysis

Atmospheric monitoring and analysis was carried out on a continuous basis, while the monitoring of water and soil nutrient levels were carried out as background monitoring to obtain a baseline for the concept of the model being proposed. It also allowed further understanding of NH_3 and PM dynamics arising from nutrient enrichment in managed ecosystems. The sites under observation were denoted as “Site 1” and “Site 2”, corresponding to an “active” (site under arable agricultural management) site (Figure 3.1). Additionally, a third site was chosen as a control for atmospheric monitoring purposes. This site was entitled “Site 3”, based in a remote area in the peatlands of the Wicklow Mountains, Co. Wicklow (Figure 3.1).

The site selection for this project was a novel approach and was a key component for this study. Sites were chosen to meet a predefined set of criteria. The criteria used for the site selection were as follows:

1. Location(s) of maximum concentration which would be affected by any modification occurring at the location(s).
2. Location(s) of maximum atmospheric NH_3 concentration (a source for NH_3).
3. Location(s) where synthetic fertilizer is used, as opposed to organic.

Two sites under arable agricultural management were chosen. These sites were also dubbed “active” site (this is due to the anthropogenic activity of interest taking place directly at the sites). This allowed for direct monitoring of source emissions and source concentrations. In keeping with the criteria used to select the active sites, the control site also had a set criterion which had to be met, including the following:

1. Location of minimum concentration which would be affected by any modification occurring at the location(s).
2. Location of minimum atmospheric NH_3 concentration (away from source of NH_3 emissions).
3. Location, which is under no management, a natural site without anthropogenic interference.

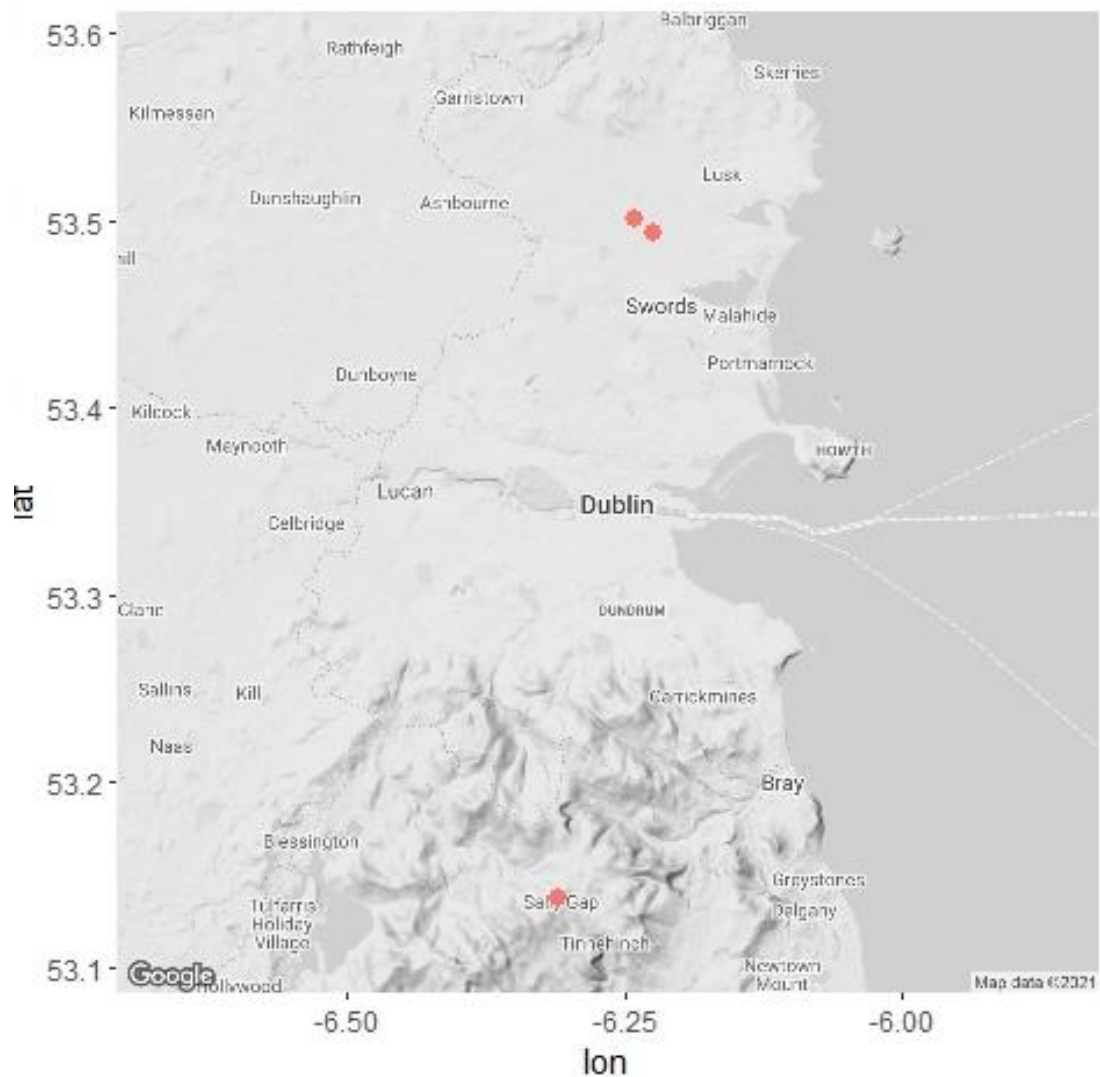


Figure 3.1 Map of chosen locations for monitoring in Ireland

3.2 Site 1

Site 1 (County Fingal, 53.491268, -6.226477, Figure 3.2) is 11.2 ha and contains arable agriculture, with winter wheat (*Triticum aestivum*), winter barley and field beans (commonly known as fava beans, *Fabaceae*). Prior to field beans, rapeseed (*Brassica napus subsp. napus*) was cultivated on the farm (the change was made circa 2019). The three different crop types being grown are in agreement with the environmental regulations in place for arable agriculture. The change in plant type

occurred as beans are a species of plants which are classified as legumes. As discussed in Chapter 2, legumes are capable of generating biologically and chemically available forms of N (such as NH_3), reducing the need for fertilization. A phosphate-based fertilizer is regularly applied in autumn, while a nitrogen-based fertilizer is applied throughout the entire growing season.

In the case of Site 1 (Figure 3.2) the nitrogen-based fertilizer applied throughout the growing season is Calcium Ammonium Nitrate (CAN). This is a widely used fertilizer and is of approx. 4% of synthetic fertilizer utilized globally. Additionally, sulphate of ammonia is also applied as fertilizer. However, due to its tendency to increase soil acidification, this fertilizer is used sparingly (21 units= 21 kg per annum). In terms of the wheat grown, 110 units of fertilizer were used per annum and for barely, 190 units were used per annum. Teagasc carries out the yearly monitoring of soil pH for this site, and lime is applied when pH is out of balance. The rest of the practices and management are carried out locally, with no external party involvement.

As mentioned, fertilization is carried out as standard practice, with the addition of all activities generally associated with arable agriculture. This includes ploughing, harvesting, tilling, sowing, irrigation, and cultivation. These activities affect soil and water quality by generating run-off, facilitating soil erosion, soil compaction, degradation of microbiomes present, loss of soil structure and potential increases in soil salinity.

Site 1 also contains a water source, a pond (as per the requirement of the set criteria described in Section 3.1). The pond at Site 1 is aquifer-fed, therefore leaching and run-off are the major exposure routes for water nutrient loading. The bedrock at the site is

a shale-type sedimentary rock known as slate, a metamorphic rock. This type of bedrock is typical of this area (Creamer et al., 2014).

While the basic information given in this section was obtained throughout the study, further collection of background information could not be carried out due to COVID-19. The farmers in question, who own the property are elderly, and due to restrictions in place initially, as well as ethical considerations, further collection of information was not facilitative. Thus, the knowledge regarding fertilization dates, amounts of fertilizer applied are made via inferences from the data obtained throughout the study, as well as information readily available (such as fertilization bans, types of fertilizers generally used during certain times during the year in Ireland, etc.).

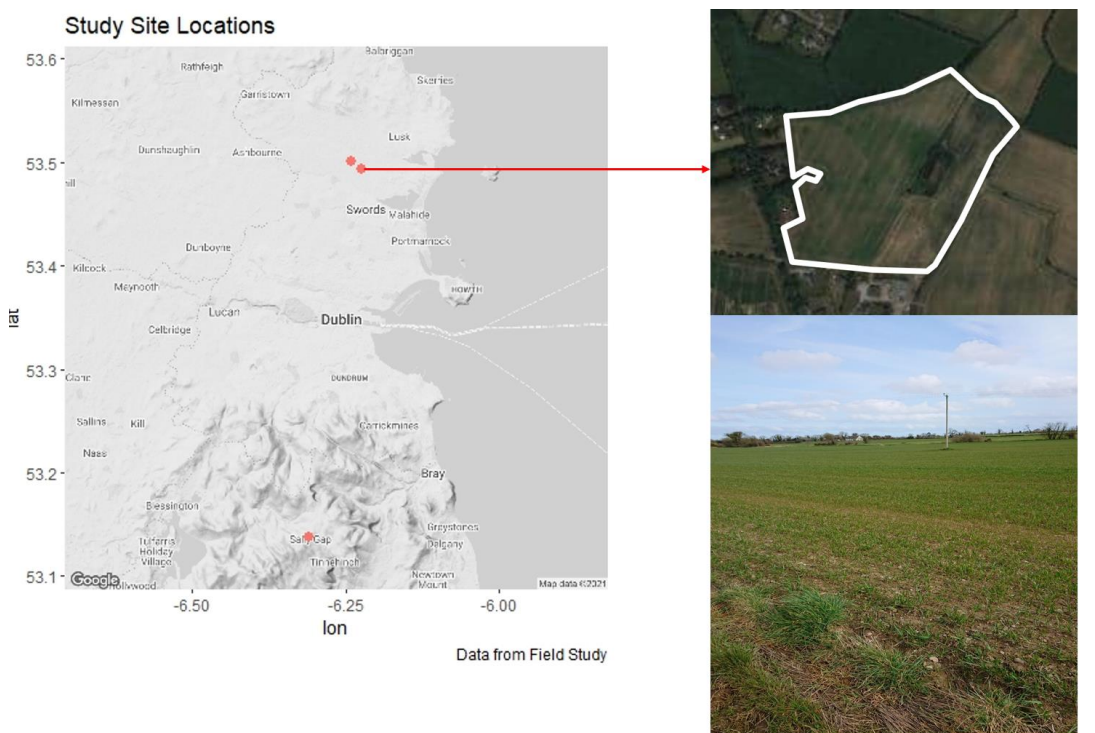


Figure 3.2 Map of Site 1

3.3 Site 2

Site 2 (County Fingal, 53.501679, -6.241714) is an arable agricultural site which is rented out to a company known as Country Crest. As standard practice, fertilizer is used to augment nutrient deficiencies and maximise production on Site 2. In addition, activities generally associated with arable agriculture are also carried out, including ploughing, harvesting, tilling, sowing, irrigation, and cultivation. These activities affect soil and water quality by generating run-off, facilitating soil erosion, soil compaction, degradation of microbiomes present, loss of soil structure and potential increases in soil salinity. The main crops being grown are wheat and barley.

Site 2 also has a water source on-site, an in-stream pond (as per the set criteria for site selection given in Section 3.1). This means that the pond has a stream running through it, creating an influx and an efflux point. The stream runs along the borders of six farms, which means the pond is not only affected by the direct run-off from Site 2, but also from the six other farms. This creates a potential for higher levels of nutrient loading at Site 2, than at Site 1. Similarly to site 1, the bedrock at the site is a shale-type sedimentary rock known as slate, a metamorphic rock. This type of bedrock is typical of this area (Creamer et al., 2014).

While the basic information given in this section was obtained throughout the study, further collection of background information could not be carried out due to COVID-19. The farmers in question, who own the property are elderly, and due to restrictions in place initially, as well as ethical considerations, further collection of information was not facilitative. Thus, the knowledge regarding fertilization dates, amounts of fertilizer applied are made via inferences from the data obtained throughout the study, as well as information readily available (such as fertilization bans, types of fertilizers generally used during certain times during the year in Ireland, etc.).

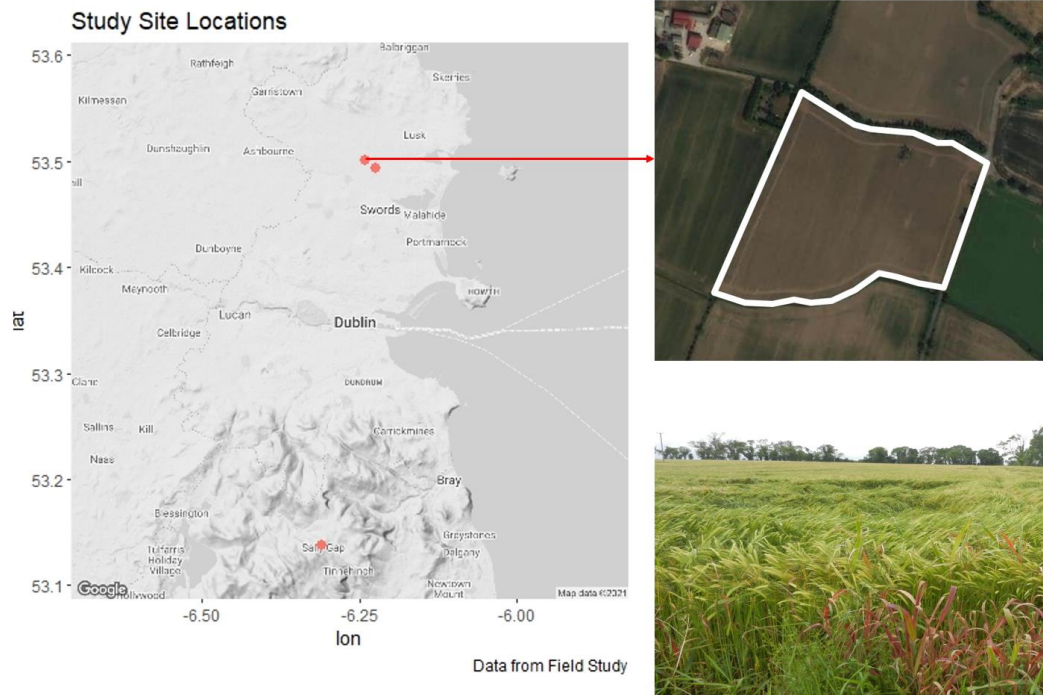


Figure 3.3 Map of Site 2

3.4 Site 3

Site 3 (53.1497842, -6.3057120) was chosen as a control site for air quality monitoring purposes. While background spot-checks were carried out for this site for water quality, the measurements generally were below the limit of detections for nutrients, therefore no continuous background monitoring for water quality was carried out. As the soil at this site was peat, which is carbon-rich (due to it being decomposed vegetation and organic matter accumulated over time), it would not have provided a basis of comparison to agricultural soils, therefore soil monitoring was not carried out. This site had no anthropogenic activity directly at the site, however, fauna such as red deer, hare, and a variety of birds were prevalent. As the site was in a protected habitat, interference was kept to a minimum. The fauna present provided a potential source of

interference with the samplers and the levels of atmospheric NH_3 concentrations measured. This is due to animal excreta containing NH_3 , as discussed in Section 2.

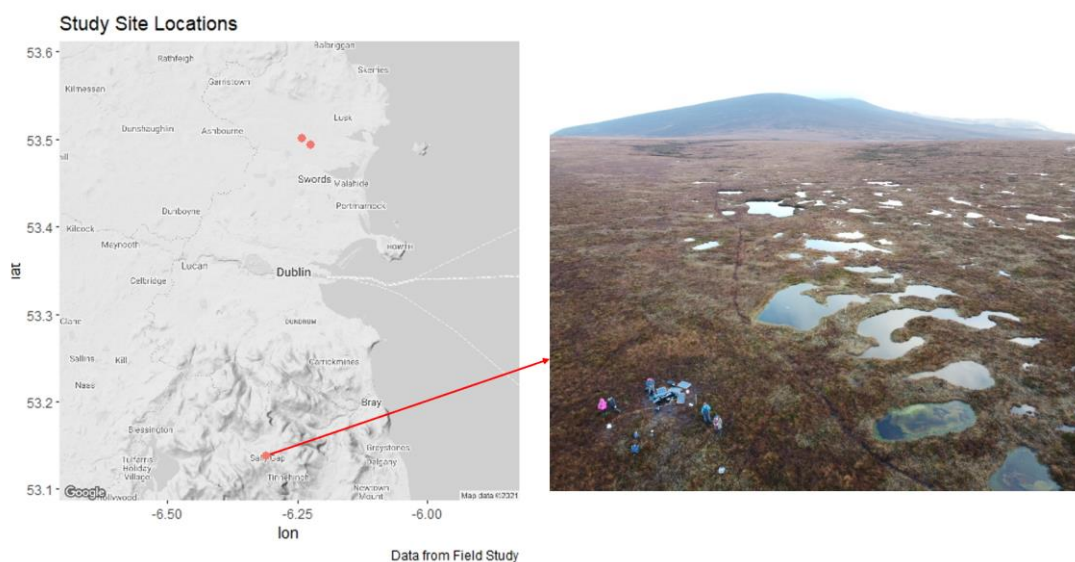


Figure 3.4 Map of Site 3

3.5 Overview of Research Methods

For the purposes of this project, a large number of techniques were considered and tested before the final decision was made on which ones to employ. The same set of techniques and sampling procedures were applied to all study sites, if sampling took place at a given site (Table 3.1).

Table 3. 1 Sampling carried out for each site during the monitoring period

Sampling	Site 1	Site 2	Site 3
Water Sampling	Yes	Yes	No
Soil Sampling	Yes	Yes	No
Atmospheric Sampling	Yes	Yes	Yes
Meteorological measurement	Yes	Yes	No

The research framework employed was an empirical framework, involving the collection of empirical evidence to either prove or disprove the hypothesis, and to meet the aims of the project (Chapter 1). Sampling was carried as using systematic sampling, with set time intervals for all sample collections. If sample collection occurred outside the specified timeframes, it was flagged in order to indicate any deviations from the general framework. Systematic sampling allowed for the minimisation of deviations in data, as well as under- and over-sampling. For atmospheric sampling, as sampling was carried out at an emission source, it was important to ensure sample collection dates are dispersed enough that the data is representative of the site in question, however, not so dispersed as to lead to overloading of samplers and bleeding on the filters and denuders used. To establish these parameters, the literature was reviewed extensively (Chapter 2). In addition, the manufacturer was also consulted regarding the sampler's capacities, as well as trainings were undertaken to ensure samples will not be compromised and will permit for maximal return.

Once the time intervals were established, the next consideration was the number of sampling units present at each site. One housing unit for a passive sampler hosted two exposed samplers (duplicate sampling, as required by the calculations) and a field-

control. To avoid any loss of data, auxiliary housing units were deployed. The original research design ideologically would have analysed all returned samplers (samplers from both the primary and auxiliary housing units), however, COVID-19 restrictions put the project behind by a year, which has reduced analysis times considerably. Thus, auxiliary samplers from the auxiliary housing unit set up at each of the sites were not analysed, unless the primary samplers were compromised. Sites 1 and 2 had a total of 3 sampling housing units on-site each (1 primary, and 2 auxiliary housing units), as these sites were under continuous anthropogenic management which put the housing units at potential risk of data loss. Site 3 had 1 primary and 1 auxiliary sampler. While anthropogenic disturbance was extremely minimal at Site 3, weather conditions and disruptions from local fauna were a potential risk, thus the deployment of an auxiliary unit.

The placement of the samplers were determined with considerations to geographical features (hills and valleys present), as well as the amount of disturbance samplers were to receive in a given location (reduction of data loss). The samplers were placed on flat ground and dispersed so that if a given area was disturbed, the auxiliary samplers would still remain viable. The instrumentation measuring meteorological factors (temperature, humidity, precipitation, etc.) were set up alongside the primary samplers, which resulted in the formation of monitoring stations being created at each site.

With regards to the background sampling, as this was spot analysis, the timing of sampling was aligned with the atmospheric sampling, to ensure unified conditions. Water sampling was carried out throughout the monitoring period. Soil sampling was carried out for the leaching study conducted as part of this project. The sampling was carried out in triplicate, collecting composite samples from the 0.-20 cm (topsoil) layer

of the soil (further discussed in Section 3.9.3). The samples collected were composite soil samples.

The analytical techniques chosen were based on extensive research, with special regard toward the type and amount of data required. The main focus of the project was to generate quantitative data via analysis of samples collected on site, which in turn was to be combined with qualitative data. The literature gave an extensive account of the current state-of-the-art currently in use (Section 2.6.1) for studies such as the one devised here, with a lot of potential choices for methodological design. Techniques which rely on high-performance instrumentation can be expensive, and depending on the sensitivity of the instrument, highly labour intensive to prepare (Section 2.6.1). Therefore, with special consideration given to the fact that the samples which were to be analysed were environmental samples coming in from live sites (meaning samples which would have complicated matrices, living biomes present, etc.) a mixture of wet chemistry methods (detailed in Sections 3.7, 3.8, 3.9) were chosen with some readily available state-of-the-art techniques such as Ion Chromatography (IC), Ion-Coupled Plasma Mass Spectroscopy (ICP-MS) and X-Ray Fluorescence (XRF) (Figures 3.6, 3.7 and 3.8). All statistical analysis carried out on the data obtained depending on the number of samples analysed. Generally, all data was analysed by either using ANOVA or using a t-test (Figure 3.5).

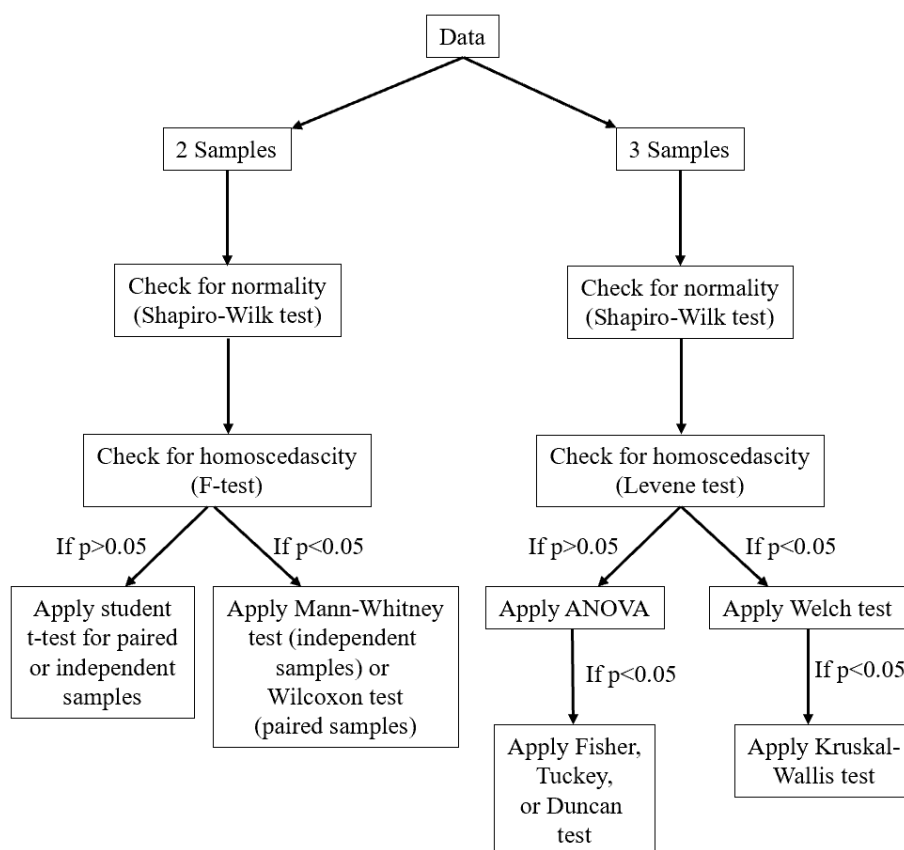


Figure 3.5 Statistical analysis

Samples collected during atmospheric sampling were analysed using a novel technique developed for this project, using IC. The method was optimised and developed for the analysis of atmospheric NH_3 and aerosol NH_4^+ , using a column known as a CS16 column. This column is specialized for the separation of sodium and ammonium ions, which was a vital consideration due to the location where the sampling is occurring. Ireland is an island, which means sea salt spray and thus the amount of the sodium ion in the atmosphere can pose significant interference when analysing samples by IC. The development of this technique allowed for accurate and reproducible results. It also had the added benefit for being non-labour intensive, with minimal sample cleaning of sample matrices required in the process. This reduced the risk of sample loss and potential for compromising samples.

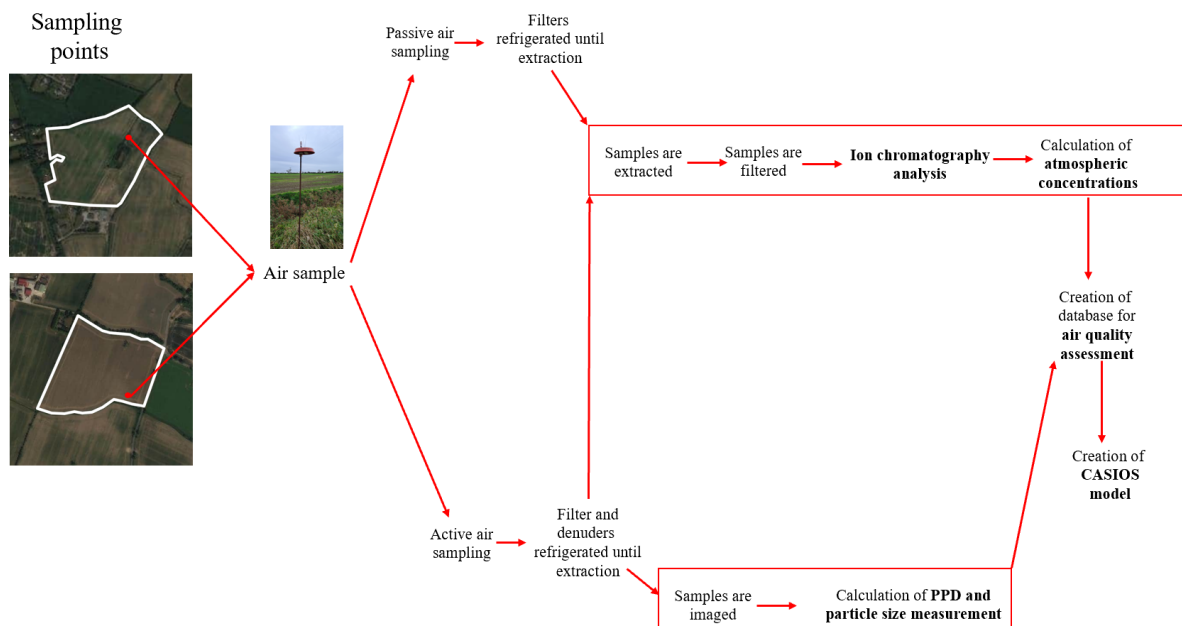


Figure 3.6 Atmospheric workflow from sampling to modelling

Background water monitoring revolved around nutrient monitoring in the samples collected. To aid in the decision as to which nutrients to analyse for, the literature, as well as nutrients measured for by the EPA and the EEA were reviewed. The wet chemistry methods were optimised and tested prior to use on actual samples. Each method (Section 3.8) was chosen as it could be performed quickly (each method took less than 3 hours) and efficiently, with reproducible results.

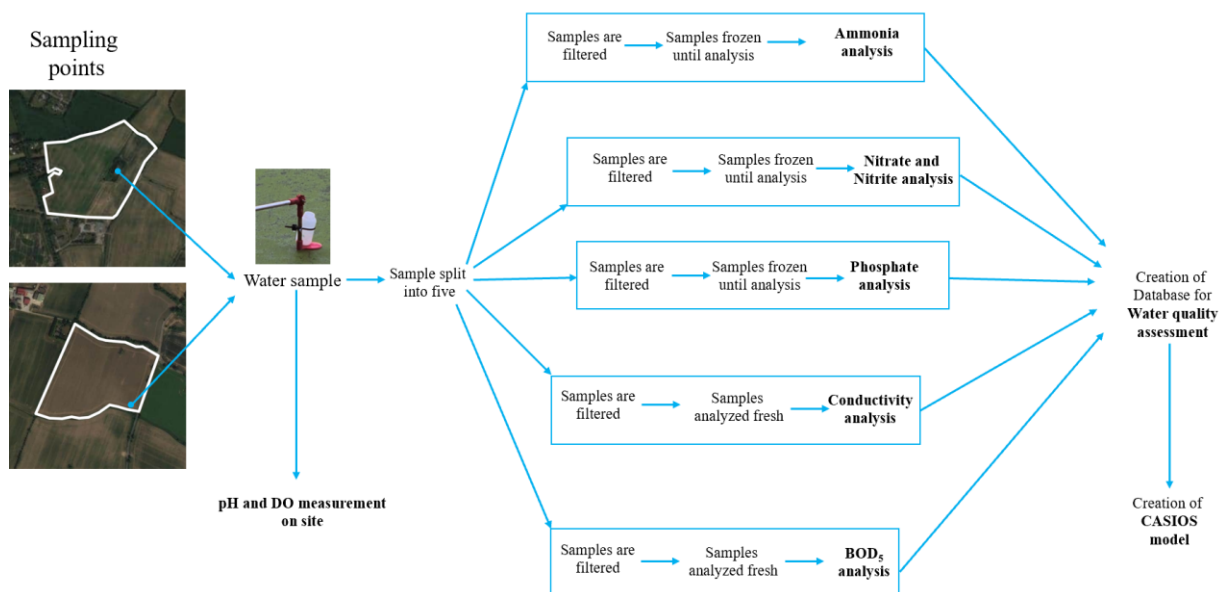


Figure 3.7 Water workflow from sampling to modelling

Soil monitoring and analysis was designed with a unique approach, due to the development of a leaching study to further understand nutrient movement and enrichment in agricultural environments. Therefore, the analytical techniques were chosen in order to facilitate the study of changes in soil quality, when an external pressure (in this case, precipitation, and temperature) is applied.

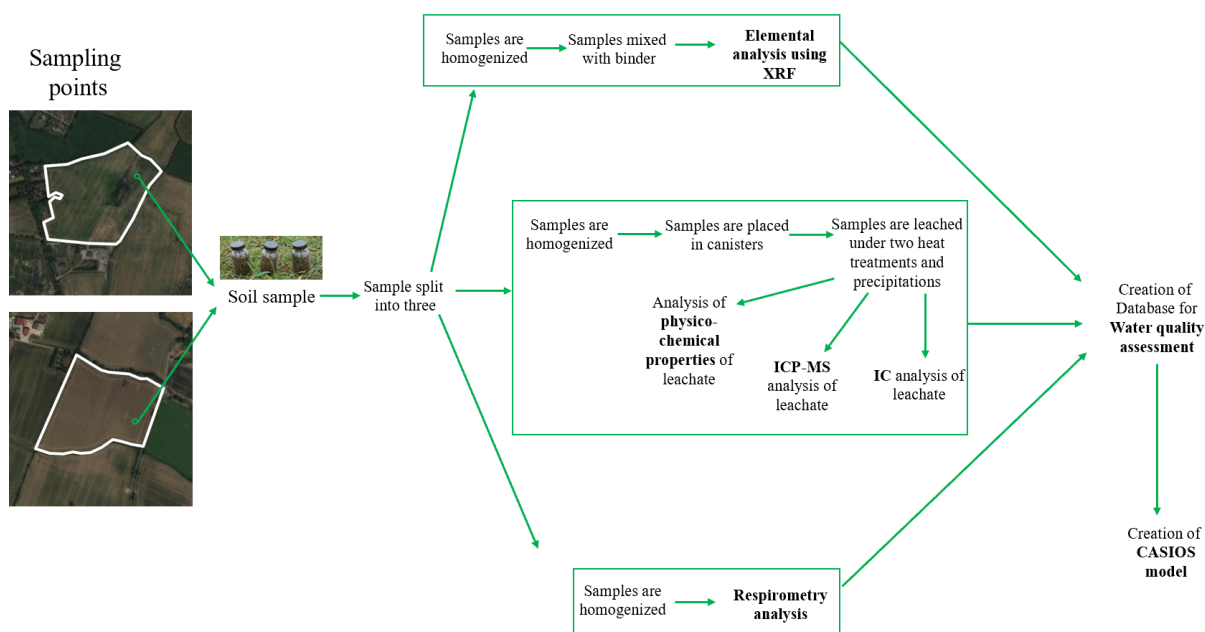


Figure 3.8 Soil workflow from sampling to modelling

3.6 Network Operation

The passive samplers chosen for atmospheric sampling were the CEH ALPHA[®] (UK Centre for Ecology and Hydrology supplied Adapted Low-cost Passive High Absorption) samplers. The sampling unit was designed for the measurement of atmospheric NH₃ and did not require electricity. These samplers used citric acid coated filters, with the system consisting of replicate ALPHA samplers attached to a shelter on a pole or post, at approx. 1.5 m from the ground. Replicate samplers were used in order to attain a more reliable measurement of atmospheric concentrations of NH₃.

Similarly, for active sampling of NH₃ and the sampling of PM, CEH DELTA[®] II (Centre for Ecology and Hydrology supplied DEnuder for Long-Term Atmospheric) samplers were chosen. This system is a low-volume denuder air sampling system,

designed for sampling acidic (NH_4^+ , HNO_3 , HCl , SO_2) and basic (NH_3 , NO_3^- , NO_2^- , SO_4^{2-}) atmospheric components. The DELTA samplers were based on the concept of a single bore glass denuder sampling for gases while a laminar air stream passes through the coated denuder. Aerosols passing through the denuder are collected by coated filters while NH_3 is captured by the acid walls of the denuder system. The DELTA sampling systems can be adjusted for any given sampling period for up to a month, by adjusting the flow rate of the air pumps (0.2-0.4 L/min). Stable air sampling is achieved via the small air pumps, with air volumes being measured by a high sensitivity dry gas meter. The system has low voltage (10-36 V) and can be powered by alternative energy sources such as solar panels or wind turbines. The passive sampling systems are referred to as ALPHA sampling units, while the active sampling systems are referred to as DELTA sampling units.

All sites contained ALPHA passive samplers, while the Site 1 was also set up with a DELTA active sampler. The first set of ALPHA passive samplers were deployed between 5th March 2021 for Site 3 and 13th November 2021 for Sites 1 and 2. The first co-ordinated swap occurred on the 9th of April 2021 for Site 3 and 21st of December 2020 for Site 1 and 2. The extended exposure at Sites 1 and 2 were to be done to test the capacity of the samplers. However, it was established that only one-month sampling periods were necessary for the passive samplers, and a collection frequency of every 3 weeks for the active sampler.

Thirty-one ALPHA passive samplers (Figure 3.9) were required for each one-month exposure period (3 sites \times 8 sampling units- 3 sampling units on Site 1 and 2; and 2 sampling units on Site 3, each containing 3 samplers per sampling unit; + 2 travel blanks + 1 laboratory blank= 28). Batches of 60 samplers were prepared at a time. Of the DELTA II Denuder active sampling system, one was set up at Site 1. Site 2 was

exposed to a public road, and therefore to minimise interference, the active sampler as was only set-up at Site 1. The DELTA II active samplers were set up to run with 12V wet cell batteries and solar panels, so that no external energy source was required to run the samplers for the duration of the project (Figure 3.10).



Figure 3.9 ALPHA passive sampler units



Figure 3.10 DELTA II Denuder active sampler unit

Agriculture in Ireland has uses permits that limit periods of fertilization, with a ban on fertilization for the winter months, depending on area (Figure 1.1). This creates not only a seasonal trend, but also a trend dependant on fertilization periods.

To further understand NH_3 and PM dynamic controls, micrometeorological measuring stations were set up at each site (Figure 3.11). These contained measuring devices that determined air temperature and precipitation events. The weather monitoring system used elevated micrometeorological stations. Air temperature was measured continuously using HOBOWare© temperature probes at both sites. Precipitation volume and occurrence was measured using a HOBOWare© rain gauge. A weather monitoring station from Met One Instruments was also deployed to Site 1 where the DELTA II Denuder system was deployed. This allowed for the on-site measurement

of wind speed, wind direction, relative humidity, barometric pressure and air temperature.



Figure 3.11 Elevated set-up for micrometeorological stations at Site 1 (RHS) and Site 2 (LHS)

3.7 Atmospheric Sampling and Analysis

3.7.1 Initial inspection and handling of filters for samplers

The following procedures outlined below were followed for filter preparation, handling, storage for ALPHA passive samplers. The filter cases were labelled with the date of their receipt upon arrival and used in the order of receipt. The filter cases were opened one at a time and used fully before the next filter case was opened. All filters were visually inspected for defects (Table 3.2). If defects were detected during the preliminary inspection, the filter was discarded. Filters were coated for sampling and

placed in fresh petri dishes labelled accordingly, sealed using parafilm, placed inside grip-seal bags, and refrigerated (approx. 4°C) in an air-tight box until use.

Table 3. 2 Defect criteria and description (State of Alaska Department of Environmental Conservation, 2017)

Defect	Description
Pinhole	A small hole appearing as a distinct and obvious bright point of light when examined over a light source
Separation of ring	Any separation or lack of seal between the filter and the filter border reinforcing the ring
Chaff or flashing	Any extra material on the filter surface, particularly along the edge that would prevent an airtight seal during sampling
Loose material	Any extra loose material or dirt particles on the filter
Discoloration	Any obvious discoloration that might be evidence of contamination
Filter nonconformity	Any obvious visible nonconformity in appearance of the filter when viewed over a light source that might indicate gradation in density of porosity or porosity across the face of the filter
Other	A filter with any imperfection not described above, such as irregular surfaces

3.7.2 Quality Control and Validation

Three types of filter blanks were utilised for the filter processing procedures of both ammonia and particulate matter. All blanks were coated with the appropriate coating (citric acid) solution. Laboratory blanks are unexposed filters utilised to determine

contamination during the storage of the filters. Coated filters ready for use had a maximum shelf life of six months, after which any unused filters from a particular coated stock were discarded and a fresh set of coated filters were prepared for use.

Field blanks are coated, unexposed filters which are used to determine whether contamination occurs during sample transport, setup and recovery. Field blanks were transported on site in the assigned sampling body with protective caps in place, installed into sampler and consequently removed and transported back to the laboratory during collection of samples (Figure 3.2). Field blanks occurred at a frequency of 10-15% of routine operating frequency.

Travel blanks are coated, unexposed filters which are used to determine if any contamination occurs during the transport of samplers. The travel banks are stored with the main batch of samplers until deployment. The travel blanks were brought back once deployment occurred and stored in a grip-seal bag in air-tight containers refrigerated (at 4°C) until the end of the exposure period.

3.7.3 ALPHA passive sampler preparation

The sampling system used for the atmospheric sampling of ammonia was the CEH ALPHA Sampler system (Figure 3.12). This system is a diffusive sampler system, which operates with the use of filters. The criteria for choice of filter coating solution is highly climate dependant (Table 3.3). Thus, for the coating of the filters to be used in an Irish climate, citric acid was chosen. All glassware was washed and dried in an oven (at 45 °C) for 24 hours prior to use. A 50 ml volumetric flask was removed from the oven and cooled to room temperature. Citric acid (6 g, 0.031 moles) was weighed out and transferred to the volumetric flask. To this, 50 ml of methanol was added. This

solution is hereafter referred to as “coating solution”. The coating solution was transferred to a 100 ml Duran bottle. To a petri dish, 6 filters were added using tweezers. An aliquot of 55 µl of coating solution was dispensed at the centre of each filter paper. The petri dish containing the filters were placed inside a desiccator and dried for 30 minutes, under vacuum. The coated filters were removed from the desiccator and stacked into a clean petri dish using anti-static tweezers. The petri dishes were labelled accordingly and sealed using parafilm and refrigerated (approx. 4°C) in an air-tight box until use. For deployment, the filters were placed inside the sampling body of the ALPHA Sampler, with the PTFE membrane and solid sampling cap. For every 3 sampler deployed, 1 was used as a blank.

Table 3. 3 Criteria for coating solution

Coating Solution	Climatic conditions
Citric acid	Temperate climates
Phosphoric acid	Hot, dry climates-to be avoided in high humidity conditions (>70%)
Oxalic acid	Not recommended

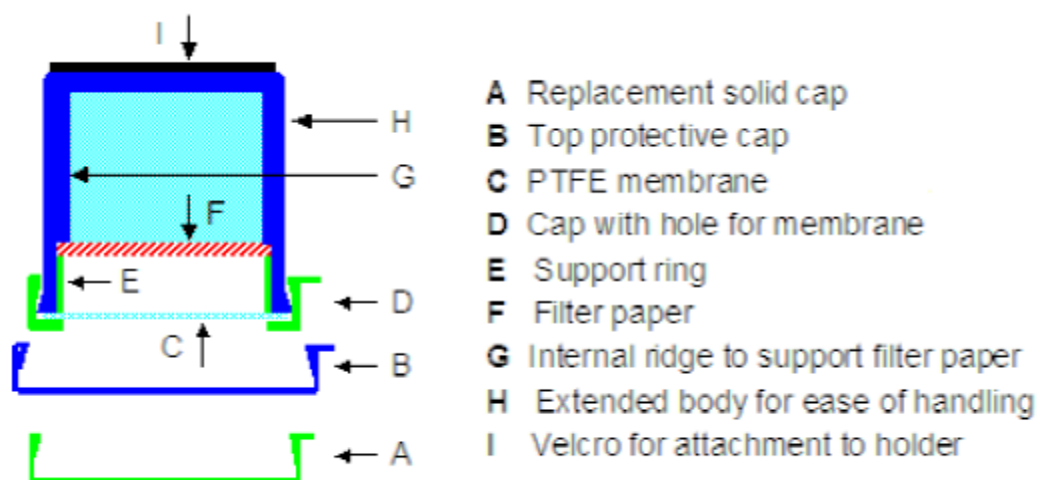


Figure 3.12 Detailed outline of CEH ALPHA Sampler body adapted from Poskitt, (2017)

3.7.4 Extraction of ammonia from ALPHA passive sampler filters

All glassware was washed and dried in an oven (approx. 45 °C) for 24 hours prior to use. A filter was extracted from the sampling body collected from field and transferred to the sampler tube using tweezers. The sampler tube containing the filter was treated with 3 ml of deionised water added as part of the extraction of NH_3 from the filter and the cap was replaced on the sampler tube and sonicated for 15 minutes. The extracted solution was allowed to stand for a further 15 minutes. Once the filters were extracted for a total of 30 minutes, the filters were removed, and the extracts were capped and sealed. This procedure was followed for all filter extractions. The filter extracts were stored refrigerated (approx. 4°C) until analysis (Martin et al., 2019). If analysis was not possible straight away, samples were stored in a freezer (approx. -18 °C).

The accuracy and precision of passive (diffusion) sampling methods have uncertainties due to the limitations of the sampler. A detailed uncertainty budget was investigated by Martin et al., (2019), where they found that measurements at a critical

level of $1 \mu\text{g}/\text{m}^3$, sampling rate had a relative uncertainty of 3.28×10^{-2} , and a variance of 1.07×10^{-3} .

3.7.5 DELTA II active sampler preparation

The sampling system used for the collection of atmospheric particulate matter was the CEH DELTA II Sampler system (Figure 3.13, 3.14, 3.15 and 3.16). This system is an active sampler system, which operates with the use of filters. The criteria for choice of filter coating solution was the same as detailed in Section 3.3.4 (Table 3.3). Prior to coating, the denuders were degreased to ensure an even coating.

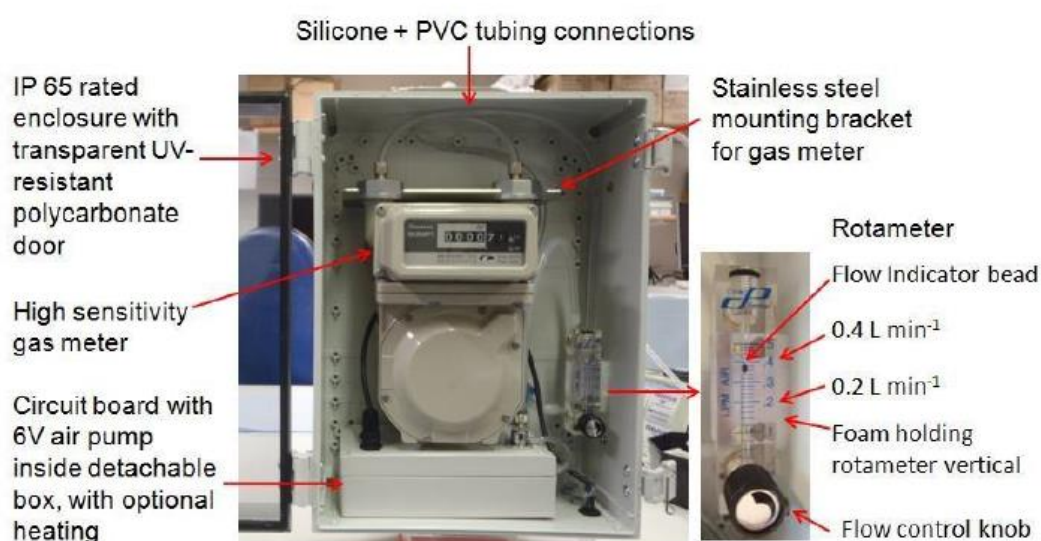


Figure 3.13 Components of monitoring enclosure of low voltage DELTA II Sampler System adapted from Tang et al., 2017

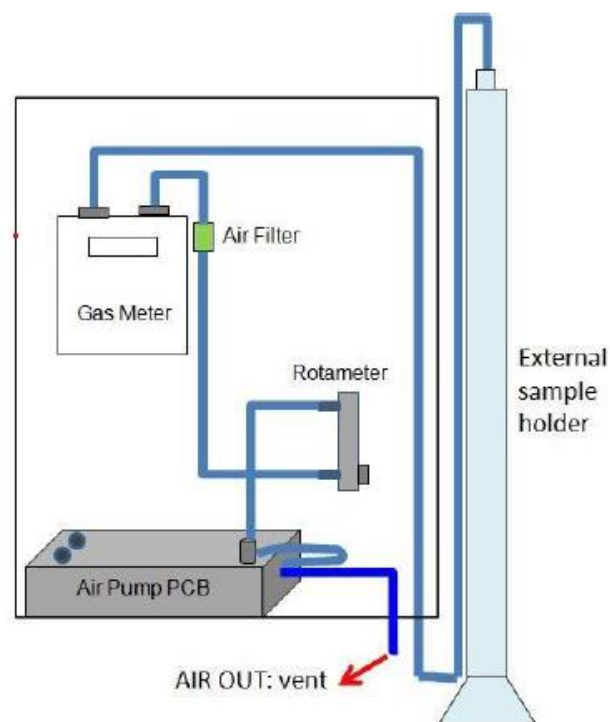


Figure 3.14 Details of connection to the gas meter (Tang et al., 2017)

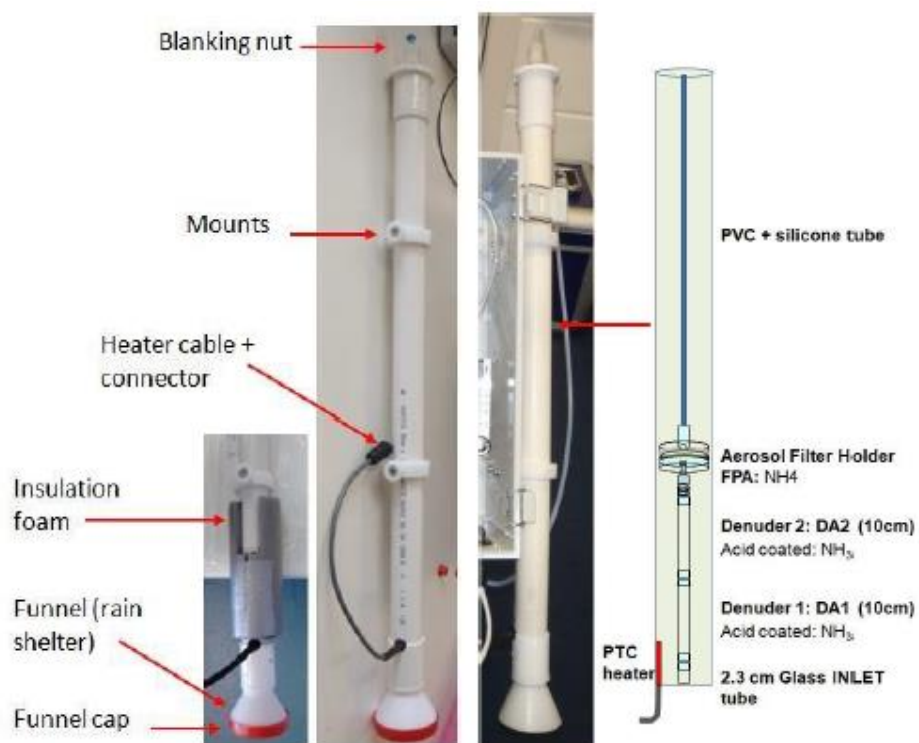


Figure 3.15 Details of external sample holder for speciated collection of ammonia gas and particulate ammonium

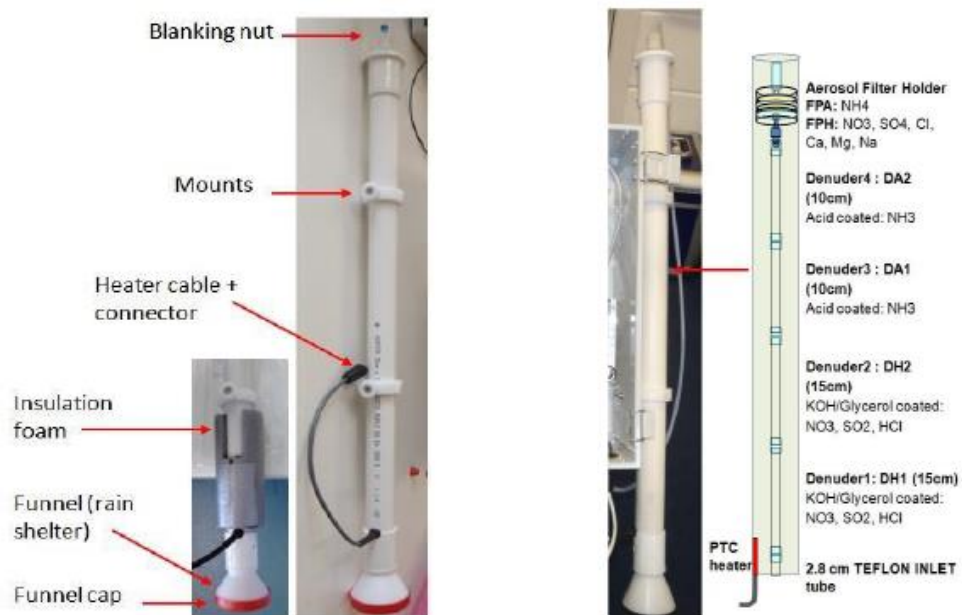


Figure 3.16 Details of external sample holder for speciated collection of reactive gases (nitric acid, sulfur dioxide, hydrochloric acid and ammonia) and particulates (nitrate, sulfate, chloride, ammonium, sodium, calcium and magnesium)

3.7.6 Degreasing of DELTA II denuders for sampling atmospheric gases

Using a 1 L volumetric flask, sodium hydroxide (1 g, 0.025 M) was added, and the solution was made to mark with deionised water (0.1% (w/v) sodium hydroxide solution). A set of clean, dry denuders were immersed in the 0.1% (w/v) sodium hydroxide solution for 24 hours. The glass denuders were rinsed post-immersion, firstly with tap water, then with deionised water, three times respectively. The degreased denuders were dried in the oven (approx. 100 °C) (Martin et al., 2019).

3.7.7 Coating solution for DELTA II denuders sampling atmospheric ammonia

All glassware was washed and dried in an oven (at 45 °C) for 24 hours prior to use. A 100 ml volumetric flask was removed from the oven and cooled to room temperature. Citric acid (5 g, 5% w/v) was weighed out and transferred to the volumetric flask. To this, 50 ml of methanol was added, and the solution was stirred until the citric acid fully dissolved. The citric acid solution was made up to mark with methanol.

3.7.8 Acid coating solution for filters sampling ammonium aerosols

Using a 10 ml volumetric flask, citric acid (1.3 g, 12% w/v) and methanol (approx. 5 ml) were added and the solution was stirred until the citric acid fully dissolved. The solution was made to mark with methanol.

3.7.9 Coating procedure for DELTA II filters

The 5% w/v citric acid coating solution was transferred from the 100 ml volumetric flask to a 100 ml Duran bottle. The denuder was attached to a pipette filler, acting as a “pipette”. Coating solution was drawn up through the denuder until approx. 1 cm from the top and allowed to stand for 10 seconds. The coating solution was dispelled from the denuder and excess coating solution was wiped from the outside casing of the denuder. The denuders were dried for 24 hours. The coated denuders were placed in zip-lock bags, labelled, and dated. The denuders were inspected for even coating (the coating is not visible immediately; it develops over time) and any denuders with an imperfect coating were rejected. The coated denuders were stored refrigerated

(approx. 4 °C) in sealed bags, in air-tight containers until deployment (Tang et al., 2018).

3.7.10 Coating procedure for DELTA II filters

On a clean petri-dish, 6 filters were arranged using tweezers and 60 µL aliquots of 12% w/v citric acid coating solution were dispensed at the centre of each filter. The petri dish containing the filters were placed inside a desiccator and dried for 1 hour, under vacuum. The coated filters are removed from the desiccator and stacked into a clean petri dish using tweezers. The petri dishes were labelled accordingly and sealed using parafilm, placed inside zip-lock bags and refrigerated (approx. 4°C) in an air-tight box until use (Tang et al., 2018).

3.7.11 Assembly of DELTA II active sampler sampling unit containing filters

The tweezers and the benchtop were cleaned using isopropyl wipes. Using tweezers, a 25 mm diameter silicone O-ring was positioned on the base of the Millipore aerosol filter holder, onto which a 24 mm acid coated filter paper was placed, followed by another 25 mm O-ring. The stack of O-ring, filter paper, O-ring was compressed into the base, ensuring a tight fit. The top section of the was inserted halfway down the base, compressing the O-ring with the rest of acid coated filter and O-ring further, forming a gas-tight fit (Figure 3.17). Both ends of the aerosol sampler were sealed using end caps (Tang et al., 2018).

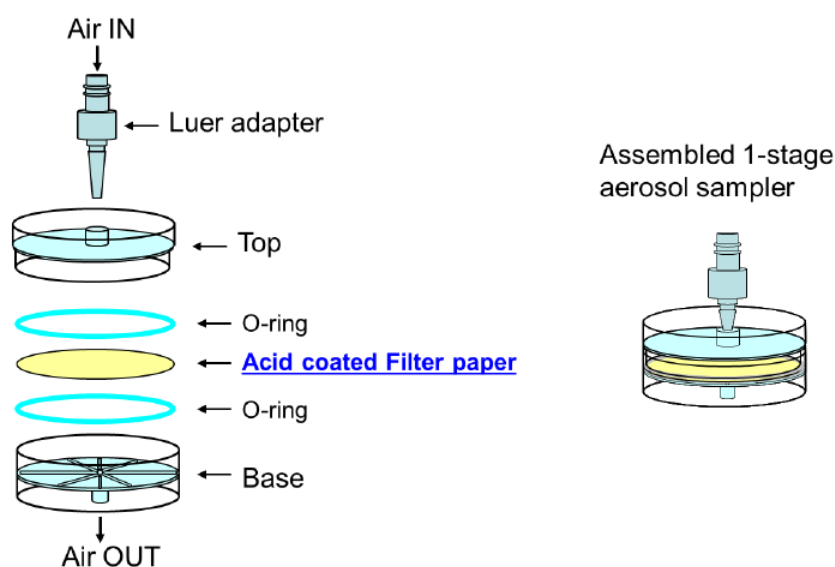


Figure 3.17 Detailed diagram of aerosol sampler components (LHS) and the assembled aerosol sampler (RHS) adapted from Tang et al., 2017

3.7.12 Assembly of DELTA II active sampler train

The sampling trains used for the collection of NH_3 and PM consisted of a short Teflon denuder inlet, and two short denuders coated in 5% w/v citric acid solution (10 cm, Denuders 1 and 2, denoted DA1 and DA 2 respectively) (Figure 3.18). The denuders were assembled in series (Tang et al., 2018).

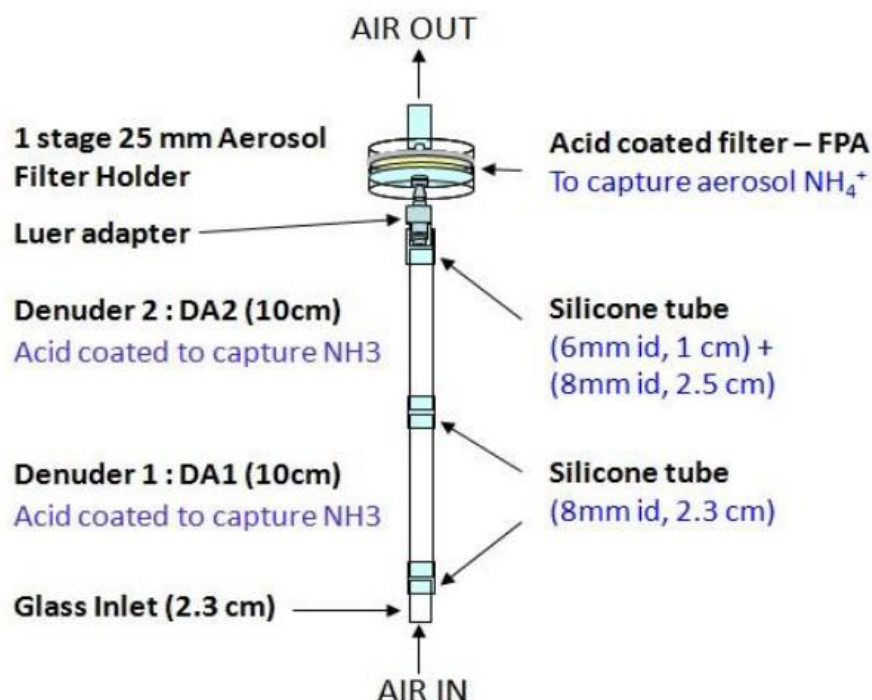


Figure 3.18 Assembly of full sampling train, connected in series for the sampling of NH_3 and PM

3.7.13 Setting up DELTA II active samplers on site

Nitrile gloves were worn for the assembly of the components while on site. The red blanking nut and red funnel cap were removed and stored in a labelled zip-lock bag. The tubing connected to the base of the samplers was connected to the gland fitting at the top of the sampler. The mounts for the sampler were lined up with the slots on the sampler's main body (housing the gas meter and electrical box) and were connected by sliding down the notches on the sampler. The funnelled face of the sampler was facing downwards. The holder was secured by replacing the metal slide pins through the holes of the lower notches. The plug of the heater cable was connected to the sample holder (into the corresponding socket on the base of the sampler enclosure).

The cable was fixed with a locking nut (Figure 3.3). The pump was set up to work at 0.2 L/minute.

3.7.14 Collection of exposed samples from each DELTA II active sampling unit

The heating cable was disconnected by unscrewing the locking nut. The metal slide pin securing the sample holder was removed and the sample holder was pushed upwards, disconnecting the sample holder from the plastic inlet. The sample holder was sealed with the funnel cap and blanking nut. The denuders were transported back to the laboratory, where they were stored refrigerated (approx. 4 °C).

3.7.15 Extraction of 5% w/v citric acid coated DELTA II denuders

The aerosol sampler was removed, and the denuders were separated. The top outlet and bottom inlet pieces were removed from the ammonia/ammonium sampling train and 3ml deionised water was added to the denuder. The caps were replaced, and the denuder was inverted for 5 minutes. The denuder was allowed to extract for 30 minutes, then inverted for an additional 5 minutes. The solution was decanted into auto-sampler tubes (Tang et al., 2018).

3.7.16 Extraction of 12% w/v citric acid coated DELTA II filters

Using a clean 25 ml Duran bottle, 4 ml of deionised water and a filter was added. The container was capped and left to extract for one and a half hours. Using a pair of tweezers, the filter was soaked and lifted three times to ensure all chemical species of

interest were extracted. The extracted solution was decanted into auto-sampler tubes (Tang et al., 2018). The accuracy and precision of this method of sampling was determined by the manufacturer, using inter-comparison studies. The sampler is capable of providing robust estimates of atmospheric NH_3 concentrations with bi-weekly sampling periods for concentrations $<0.1 \mu\text{g}/\text{m}^3$ or, conversely concentrations of $>20 \mu\text{g}/\text{m}^3$ (Sutton, et al., 2001).

3.7.17 Ion chromatography analysis of extracts

The method developed for the ion chromatography analysis was a novel approach and was a key component for this study. For this purpose, several eluents were prepared of varying strength (Tables 3.4). The eluent used was Dionex™ Methanesulfonic acid (MSA) (the original solution was 0.4 M, which was diluted to the desired eluent strength for analysis). The eluent was filtered using a filtration apparatus followed by sonication for 30 minutes. The ion chromatography system purged for 1 hour using the respective eluent for each method development trial.

Table 3.4 Dilution of Dionex™ Methanesulfonic acid cation eluent concentrate working standard solution (0.4 M)

Concentration	Dilution
38 mM	To a 100 ml volumetric flask, 9.5 ml of MSA was added and diluted to mark. This eluent was used in a trial for method development with a C12 column.
35 mM	To a 100 ml volumetric flask, 8.75 ml of MSA was added and diluted to mark. This eluent was used in a trial for method development with a C16 column.
30 mM	To a 100 ml volumetric flask, 7.5 ml of MSA was added and diluted to mark. This eluent was used in a trial for method development with a C16 column.
20 mM	To a 100 ml volumetric flask, 5 ml of MSA was added and diluted to mark. This eluent was used in a trial for method development with a C12 column.
15 mM	To a 100 ml volumetric flask, 3.75 ml of MSA was added and diluted to mark. This eluent was used in a trial for method development with a C12 column.

For the method development, two different columns were tested. One column was a Dionex IonPac™ CS12A, and the other column as a Dionex IonPac™ CS16, with respective guard columns (Tables 3.5 and 3.6).

Table 3.5 Column specifications of Dionex IonPac™ CS12A

Parameters	Description
Diameter	2 mm
Length	250 mm
Packing material	Carboxylic/Phosphonic acid
Particle size	8.5 µm
Guard Column	Dionex IonPac™ CG12A Guard Column

Table 3.6 Column specifications of Dionex IonPac™ CS16

Parameters	Description
Diameter	3 mm
Length	250 mm
Packing material	Carboxylic acid
Particle size	5.5 µm
Guard Column	Dionex IonPac™ CG16 Guard Column

The system was optimised by varying the concentration of the eluent for a given column used until an ideal chromatogram was obtained, with good baseline separation between peaks (Tables 3.7-3.11). The method was optimised using a Dionex™ Combined six cation standard (Table 3.12). Using ammonium as a reference point, the stock standard solution was diluted (1:10 dilution) to establish a working standard solution (25 ppm, 25 ml). Using the working standard solution, a set of calibration standards were established. For the CS12A column, after running each calibration standard, the 5 ppm calibration standard was analysed as a sample, to confirm the method and calibration standards used. For the CS16 column, the 2 ppm calibration standard was analysed as a sample to confirm the calibration standards and the method used. The method chosen was Method 5 (Table 3.11), using the 35 mM eluent and the CS16 column and CG16 guard column, as this method provided baseline separation between peaks. All peaks were resolved, and the runtime could be reduced to 25 minutes per run. The samples were analysed using ion chromatography with an injection of ultra-pure water in-between runs to ensure minimal column bleed (Tang et al., 2009). As the system did not have a temperature control chamber, the analysis was carried out at air temperature. All samples and corresponding blanks were analysed using the method described above.

Table 3.7 Ion Chromatography method 1

Parameter	Description
Flow rate	0.25 ml/ minute
Detector	Conductivity detector
Eluent composition	15 mM Dionex™ MSA
Run time	28 minutes
Injection volume	0.2 ml
Rinse volume	1.8 ml
Column	Dionex IonPac™ CS12A Analytical Column
Guard Column	Dionex IonPac™ CG12A Guard Column
Suppressor	Dionex CERS™ 500
Suppression	11 mA

Table 3.8 Ion Chromatography method 2

Parameter	Description
Flow rate	0.25 ml/ minute
Detector	Conductivity detector
Eluent composition	10 mM Dionex™ MSA
Run time	45 minutes
Injection volume	0.2 ml
Rinse volume	1.8 ml
Column	Dionex IonPac™ CS12A Analytical Column
Guard Column	Dionex IonPac™ CG12A Guard Column
Suppressor	Dionex CERS™ 500
Suppression	8 mA

Table 3.9 Ion Chromatography method 3

Parameter	Description
Flow rate	0.25 ml/ minute
Detector	Conductivity detector
Eluent composition	5 mM Dionex™ MSA
Run time	80 minutes
Injection volume	0.2 ml
Rinse volume	1.8 ml
Column	Dionex IonPac™ CS12A Analytical Column
Guard Column	Dionex IonPac™ CG12A Guard Column
Suppressor	Dionex CERS™ 500
Suppression	4 mA

Table 3.10 Ion Chromatography method 4

Parameter	Description
Flow rate	0.36 ml/ minute
Detector	Conductivity detector
Eluent composition	30 mM Dionex™ Methanesulfonic acid cation eluent concentrate
Run time	35 minutes
Rinse volume	1.8 ml
Injection volume	0.2 ml
Column	Dionex IonPac™ CS16 Analytical Column
Guard Column	Dionex IonPac™ CG16 Guard Column
Suppressor	Dionex CERS™ 500
Suppression	37 mA

Table 3.11 Ion Chromatography method 5

Parameter	Description
Flow rate	0.36 ml/ minute
Detector	Conductivity detector
Eluent composition	35 mM Dionex™ Methanesulfonic acid cation eluent concentrate
Run time	25 minutes
Rinse volume	1.8 ml
Injection volume	0.2 ml
Column	Dionex IonPac™ CS16 Analytical Column
Guard Column	Dionex IonPac™ CG16 Guard Column
Suppressor	Dionex CERS™ 500
Suppression	37 mA

Table 3.12 Dionex™ Combined six cation standard

Cation	Concentration (ppm)
Lithium	50
Sodium	200
Ammonium	250
Potassium	500
Magnesium	250
Calcium	500

3.7.18 Calculation of air concentration of ammonia and particulate matter

The quantity of NH_3 collected on the filter of the ALPHA passive sampler is given as:

$$Q = (c_e - c_b)v \quad (3.1)$$

where Q is the quantity of NH_3 , c_e is the concentration of filter extract of exposed filter ($\mu\text{g/ml}$), c_b is the concentration of filter extract of field blank filter ($\mu\text{g/ml}$) and v is the total volume of extract (ml). The ambient atmospheric concentration of NH_3 in $\mu\text{g/m}^3$ is given as:

$$\chi_a = \frac{Q}{V} \quad (3.2)$$

where V is the effective volume of air sampled- for a passive sampler, this is calculated using the following equation:

$$V = \frac{DA t}{L} \quad (3.3)$$

Where D is the diffusion coefficient of NH_3 in air, A is the cross-sectional area of the sampler, t is the sampling duration and L is the length of the sampler. The value of D at 10°C was taken as $2.09 \times 10^{-5} \text{ m}^2 \text{ s}^{-1}$ (Sutton et al., 2001).

In the case of the DELTA II denuder system, the amount of trace gas (in this case NH_3) collected on a denuder is given by:

$$Q = (c_e - c_b)v \quad (3.4)$$

where Q is the quantity of NH_3 , c_e is the concentration of filter extract of exposed filter ($\mu\text{g/ml}$), c_b is the concentration of filter extract of field blank filter ($\mu\text{g/ml}$) and v is the total volume of extract (ml). The ambient atmospheric concentration of NH_3 is determined as:

$$C_a = \frac{Q}{V} \quad (3.5)$$

where V is the effective volume of air sampled. For active samplers, this is taken as a direct reading from the gas meter fitted to the sampler.

Using two glass denuders connected in series also allows for the determination of the system's capture efficiency, by allowing for a comparison of the amount of NH_3 captured by both denuders (Sutton et al., 2001). An infinite series correction factor is then applied to account for any NH_3 not adsorbed by the glass denuders, based on this capture efficiency. The corrected air concentration ($C_{a(\text{corrected NH}_3)}$) is determined by:

$$C_{a(\text{corrected NH}_3)} = C_{a(\text{Denuder 1})} \times \left[\frac{1}{1 - \left(\frac{C_{a(\text{Denuder 2})}}{C_{a(\text{Denuder 1})}} \right)} \right] \quad (3.6)$$

At a typical capture efficiency of 90% in the first denuder, the correction corresponds to 1% of the corrected air concentration. At 80%, 75% and 70%, the correction corresponds to 6%, 11% and 17% of the corrected air concentration respectively. This correction equation does not work for a capture efficiency of <60%, as the correction

accounts for more than 50% of the air concentration obtained using this method, and therefore in those cases, should not be used. In those instances, NH₃ concentration is determined as:

$$C_{a \text{ (corrected NH}_3\text{)}} = C_{a \text{ (Denuder 1)}} + C_{a \text{ (Denuder 2)}} \quad (3.7)$$

The capture efficiency was calculated for all samples collected. In all but one instance, the capture efficiency was 100%. The only time capture efficiency was not 100% percent (capture efficiency was >60%, therefore still accepted), the atmospheric concentration was adjusted using equation 3.6.

3.7.19 Imaging of particulate matter (DELTA II sampler)

A filter from each season was imaged using an Olympus CX23 binocular brightfield microscope, with an ISH500 camera attachment. The images were analysed using ImageJ. The diameter of the particles was calculated using their surface area measurement.

3.8 Water Sampling and Analysis

As mentioned in Section 3.2, Ireland has permitted fertilization periods, with a ban on fertilization for the winter months, depending on area (Figure 3.3). This creates not only a seasonal trend, but also a trend dependant on fertilization periods. As there are water sources (ponds) at each of the active sites, background monitoring of nutrient loading has been carried out in order to further understand the dynamics of pollutants through the managed ecosystems. A similar approach was taken to the background monitoring of water at each site, to that of atmospheric sampling. The temperature of the water was measured continuously using HOBOWare© temperature probes (Figure 3.19). In the pond, the temperature probe was attached to a floatation device and deployed to roughly the middle of the pond, where it was held in place using an anchor. The physical properties such as pH, conductivity, etc., were also monitored for ponds at each site via spot analysis.



Figure 3.19 Continuous monitoring of water temperature at Site 1 (LHS) and Site 2 (RHS). The probe attached to the floatation devices are depicted inside the red squares.

3.8.1 Ammonia analysis in water using the phenate method

Reagents used:

Phenol solution: 11.1 ml of liquified phenol ($\geq 89\%$) was mixed with 60 ml of 95% v/v ethyl alcohol in a 100 ml volumetric flask and was made to mark using of 95% v/v ethyl alcohol.

Sodium nitroprusside, 0.5% w/v reagent: sodium nitroprusside (0.5 g) was added to a 100 ml volumetric flask and dissolved in 80 ml of ultra-pure water (UPW). Once dissolved, the solution was diluted to mark, mixed thoroughly, and transferred and stored in an amber bottle.

Alkaline citrate reagent: to a 1 L volumetric flask containing 800 ml of UPW, trisodium citrate (200 g) and sodium hydroxide (10 g) were added. The slurry was dissolved by continuous stirring using a stir rod and stir plate and the solution was diluted to mark using UPW.

Oxidizing solution: 100 ml of alkaline citrate was mixed with 25 ml of 5% sodium hypochlorite. This solution was prepared fresh for each analysis.

To a 100 ml Erlenmeyer flask containing 25 ml of sample, phenol solution (1 ml), sodium nitroprusside reagent (1 ml), and oxidizing solution (2.5 ml) were added; with thorough mixing after each addition. The samples were covered with parafilm, and the colour was left to develop in subdued light for at least one and a half hours (indophenol is stable for 24 hours). The absorbance was measured at 640 nm using a UV-Vis Spectrometer. A standard calibration curve was also established using a set of NH_3

standards between 0.05 and 5 mg/L NH_3 (Parsons, Maita, & Lalli, 1984; Solórzano, 1968).

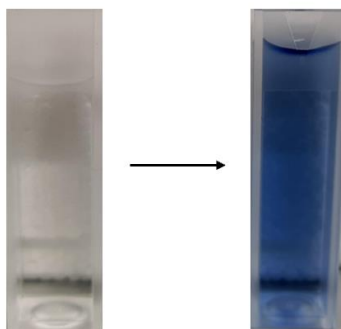


Figure 3.20 Colour change of sample when indophenol blue is formed by a reaction of ammonia, hypochlorite and phenol catalysed by sodium nitroprusside

3.8.2 Nitrate and Nitrite analysis using the vanadium chloride method

Reagents used:

Sulphanilamide reagent: To a 500 ml volumetric flask containing 300 ml of UPW, sulphanilamide (5.0 g) and 50 ml of HCl (12 N) were added. Once the solution cooled to room temperature, the solution was made to mark using UPW.

N-(1-naphthyl)-ethylenediamine dihydrochloride (NED) reagent: To a 500 ml volumetric flask containing 400 ml UPW, NED (0.5 g) was added and dissolved. The solution was made to mark using UPW.

Griess-reagent: NED and sulphanilamide were mixed in equal proportions prior to performing the analysis. This reagent was made fresh for every analysis.

Vanadium (III) chloride (VCl_3), 2% w/v reagent: To an amber bottle containing 50 ml of HCl (6 N), 1 g of VCl_3 was added and dissolved fully. Generally, complete

dissolution of VCl_3 would be achieved in approx. 1 hour, indicated by a shift from a turbid slurry-like solution to a transparent solution. The solution was filtered through a $0.45\ \mu\text{m}$ filter and stored at $4\ ^\circ\text{C}$.

3.8.2.1 Determination of Nitrite

To a 1.5 ml Eppendorf vial, 1 ml of sample was added followed by the addition of Griess-reagent ($50\ \mu\text{L}$) and mixed gently. The vials were incubated at $25\ ^\circ\text{C}$ for 20 minutes. From this mixture, $350\ \mu\text{L}$ of was transferred to a 96-well microplate and the absorbance was measured at $540\ \text{nm}$ using a ThermoFisher Multiskan Go microplate absorbance reader.

3.8.2.2 Determination of Nitrate

To the remaining mixture in the Eppendorf vial, VCl_3 ($70\ \mu\text{L}$) was added. The vials were closed and gently mixed, then incubated in a water bath ($60\ ^\circ\text{C}$) for 25 minutes. Then the vials were removed from the water bath and cooled to room temperature. An aliquot of $350\ \mu\text{L}$ was transferred to a 96-well microplate and the absorbance was measured at $540\ \text{nm}$ using a ThermoFisher Multiskan Go microplate absorbance reader. However, in order to determine the concentration of NO_3^- in the sample, a parallel analysis of $\text{NO}_2\text{-N}$ and $\text{NO}_3\text{-N}$ is performed simultaneously.

In these samples, a distinction is necessary between the contributions of the two compounds. The measured absorbance in the $\text{NO}_3\text{-N}$ step actually refers to a combination of both $\text{NO}_2\text{-N}$ and $\text{NO}_3\text{-N}$, denoted as ABS_{NOX}^V :

$$ABS_{NOX}^V = ABS_{NO2}^V + ABS_{NO3}^V + ABS_{reagents}^V \quad (3.8)$$

The use of both NO₂-N and NO₃-N standards allows for a calibration curve of the complete reaction in the presence of VCl₃ to be procured, shown by equations 3.9 and 3.10:

$$ABS_{NO2}^V = S_{NO2}^V[NO_2] + ABS_{reagents}^V \quad (3.9)$$

$$ABS_{NO3}^V = S_{NO3}^V[NO_3] + ABS_{reagents}^V \quad (3.10)$$

Where ABS_{NO2}^V and ABS_{NO3}^V are the absorbance of the sample, S_{NO2}^V and S_{NO3}^V are the slope of the respective calibration curves, $[NO_2]$ and $[NO_3]$ are the respective concentrations of NO₂-N and NO₃-N, and $ABS_{reagents}^V$ is the absorbance of the sample blank (i.e.: the intercept of the calibration curve). As mentioned above, the measured absorbance is a combination of each nitrogen species, therefore can be determined from a combination of equations 3.9 and 3.10 as follows:

$$ABS_{NO2}^V = S_{NO2}^V[NO_2] + S_{NO3}^V[NO_3] + ABS_{reagents}^V \quad (3.11)$$

Therefore, the concentration of NO₃-N in a given sample can be calculated as:

$$[NO_3] = \frac{(ABS_{NOX}^V - ABS_{reagents}^V - (s_{NO_2}^V [NO_2]))}{s_{NO_3}^V} \quad (3.11)$$

Where $[NO_2]$ is the concentration of NO_2 -N determined for a given sample and $[NO_3]$ is the concentration of NO_3 -N in the sample (García-Robledo, Corzo, & Papaspyrou, 2014).

3.8.3 Ortho-Phosphate analysis

Reagents used:

Ammonium molybdate-antimony potassium tartrate reagent: to a 1 L volumetric flask containing 800 ml of UPW, ammonium molybdate (8 g) and antimony potassium tartrate (0.2 g) were added and dissolved. The solution was made to mark using UPW.

Ascorbic acid reagent: to a 1 L volumetric flask containing 800 ml UPW, acetone (2 ml) and ascorbic acid (60 g) was added and dissolved. The solution was made to mark using UPW.

Sulfuric acid (11 N) reagent: to a 1 L volumetric flask containing approx. 600 ml of UPW, concentrated sulfuric acid (18 M, 310 ml) was added slowly. The solution was allowed to cool to room temperature then was made to mark using UPW.

Stock phosphorous solution: to a 1 L volumetric flask containing 800 ml of UPW, monopotassium phosphate (KH_2PO_4 , 0.4393 g, pre-dried in an oven at 105 °C for one hour) was added and dissolved. The solution was diluted to mark using UPW (1 ml stock phosphorous solution= 0.1 mg P).

Standard phosphorous solution: to a 1 L volumetric flask containing approx. 800 ml of UPW, stock phosphorous solution (100 ml) was added and diluted to mark using UPW (1 ml of standard phosphorous solution= 0.01 mg P)

To a 250 ml Erlenmeyer flask containing 50 ml of sample, sulfuric acid reagent (11 N, 1 ml) and ammonium molybdate-antimony potassium tartrate (4 ml) were added and mixed. To this solution, ascorbic acid reagent (2 ml) was added and mixed. After 5 minutes, the absorbance was measured at 650 nm, using a UV-Vis Spectrometer. A standard calibration curve was also established using the method above for a set of PO₄-P standards between 0.05 and 1 mg/L (Habibah et al., 2018).

3.8.4 Five-day biological oxygen demand

Reagents used:

Calcium chloride solution: To a 1 L volumetric flask, calcium chloride (27.5 g) was added and diluted to mark with deionised water.

Ferric chloride solution: Solution supplied by HACH™ Instrument company.

Magnesium sulfate solution: Solution supplied by HACH™ Instrument company.

Phosphate buffer solution: Buffer solution supplied by HACH™ Instrument company.

Sample aliquot was determined based on the value of BOD₅ < 7 mg/L. If the value obtained exceeded 7mg/L of BOD₅, dilutions were performed as shown in Table 3.13. The dilution water (1 L) was aerated before addition of nutrient solutions. Post-aeration, 1 ml of each of phosphate buffer solution, magnesium sulfate solution, ferric chloride solution were added. The container of dilution water was shaken for 5 minutes

to saturate the solution with oxygen. The dilution water was placed in water bath at 20 °C to establish constant temperature for analysis. The samples were brought to temperature using the water bath and aerated for 15 minutes. Where required, dilutions were performed. Dilution of BOD₅ water was also performed to obtain an uptake range. Each subsample was mixed by inversion. For each sub-sample, a large bore pipette was used for volumes less than 50 ml, and a graduated cylinder for volumes exceeding 50 ml. The sample was transferred into a BOD₅ bottle.

If dilution was required, the BOD₅ bottle was made to mark using dilution water. Three samples were prepared using dilution water alone (sample blanks). The initial dissolved oxygen (DO) concentration was measured using a DO meter of each sample and sample blank. Where necessary, glass beads were added to the BOD₅ bottles to displace the sample up to the neck of the bottle, displacing any air, leaving no bubbles. The BOD₅ bottle was capped with a glass stopper and inverted to see if there are any air bubbles present. The BOD bottle was sealed using deionised water. An over cap was placed on top of the stopper. The BOD₅ bottle were placed in the water bath (20 °C) and incubated for 5 days. After the 5-day incubation period, the over cap was removed, the water seal was poured off and the glass stopper was removed. Final concentration of DO was measured using the same DO meter with which the initial measurement was taken (Hocking & Hocking, 2005; Muralikrishna & Manickam, 2017; Scholz & Scholz, 2006)

Table 3. 13 Dilution criteria of BOD₅ samples adapted from Delzer & Mckenzie, 1999

Anticipated range value of BOD ₅	Aliquot of sample (ml)	Aliquot of dilution water (ml)
0-7	300	0
6-21	100	200
12-42	50	250
30-105	20	280
60-210	10	290
120-420	5	295
300-1050	2	298
600-2100	1	299

3.9 Soil Sampling and Analysis

Soil sampling, as with water sampling, was carried out on a spot sampling basis to establish background monitoring at each site. The temperature was measured at a continuous basis, using HOBOWare© temperature probes. The probe was inserted in the topsoil (0-10 cm deep), near the meteorological monitoring station platforms at both sites (Figure 3.21).



Figure 3.21 Soil temperature probes at Site 1 (LHS) and Site 2 (RHS)

3.9.1 Moisture content analysis of soil by gravimetric method

The weight of each container was taken by placing them on an analytical balance. The weight was noted down, and the sample containers were placed in the oven for 1 hour (105 °C). The containers were placed in a desiccator and allowed to cool for 30 minutes, then reweighed. This procedure was continued until constant weight was reached (weight difference between two consecutive measurements <0.2 mg). This was noted as “tare weight”. When the container reached constant weight, 5 g of soil sample was weighed into each container. This was noted as “weight of wet soil”. The soil was placed in the oven for 3 hours and cooled in a desiccator for 30 minutes, then reweighed. The samples were placed back in the oven for a period of 1 hour followed by a 30-minute cooling period in the desiccator and reweighed. This was continued until constant weight was achieved. This was noted down as the “weight of dry soil”. The % moisture content was calculated as follows:

$$\% \text{ moisture content} = \frac{\text{weight of wet soil (g)} - \text{weight of dry soil (g)}}{\text{weight of dry soil (g)}} \times 100\% \quad (3.12)$$

3.9.2 Elemental analysis of soil

The soil was air-dried for 48 hours prior to analysis. The soil was sieved using a 3.15 mm sieve and ground with a pestle and mortar. An aliquot of 4.0 g of ground soil was weighed out and a binder (0.8 g) was added. The binding agent and the soil was homogenised by shaking for 10 minutes. The sample was loaded into a 30 tonne press and put under 15 tonnes of pressure for 5 minutes. The height and diameter of the samples of the pressed pellets were taken for calculating the density of the samples. The composition of the sample was analysed using X-ray Fluorescence (XRF). This analysis was carried out in the laboratories of the Faculty of Chemistry at the University of Belgrade, Belgrade, Serbia, as part of a Short Term Scientific Mission funded by the EU COSTAction CLIMO (CLimate-Smart forestry in MOuntain regions).

3.9.3 Leaching study of soils

This section outlines a leaching study undertaken in conjunction with this project. The following methods and techniques were developed uniquely for this project and provided a novel approach forming a principal component of this study. As there are water sources at each site (ponds), nutrient leaching from the soil during period of intense rain is a major transport pathway leading to heightened nutrient loads in arable agricultural ecosystems. This can occur through components leaching directly into the ponds on site, or by leaching into groundwater. Thus, as a component of this project,

this portion of the work was conducted in collaboration with, and in the laboratories of the Faculty of Chemistry at the University of Belgrade, Belgrade, Serbia, as part of a Short Term Scientific Mission funded by the EU COSTAction CLIMO (CLimate-Smart forestry in MOuntain regions). The effects of intense rainfall are difficult to measure and thus far, little research has been carried out in this area in Ireland.

Soil health is a vital component of arable agricultural ecosystems and the management practices (e.g.: tilling) can result in a fast-paced degradation of this aspect of the soil. This results in increasing amount of fertilizer being required for the soil to be of an adequate quality in order to be used for crop production. Therefore, the intrinsic relationship of intense rainfall (based on measured field values), leaching and general soil health was explored. This broadens the soil analysis, therefore broadening the proposed concept model.

As all the effects could not be investigated as a whole, due to the sheer number of known effects and complexity of the issue, a focus was decided upon. The focus of the study was to analyse the soil for changes in elemental composition, as well as ion composition pre-and post-precipitation events. Ireland has seen an increase in the frequency of extreme wind and precipitation storms in the last decade, which has been unprecedented according to records kept by Met Éireann (Met Éireann). Current records show that the winter with the highest number of storms to date has been the winter of 2013-2014.

The experimental techniques introduced in the following sections were used throughout this portion of the project. All soil samples underwent the same pre-treatment. The samples were air-dried for 48 hours prior to the beginning of the experiments. The soil samples for the simulation were sieved using a 3.15 mm sieve.

Larger silt blocks were broken to smaller fractions along natural fault lines formed in the air-dried soil. The samples were divided based on site; hence the soils were labelled as Site 1 (S1) and Site 2 (S2). From the sieved soil, 250 g were weighed and placed in each canister. All analysis was carried out in triplicate.

3.9.4 Design of precipitation simulations

For the purposes of the rain simulation, a chamber serving as a housing unit for the operation was designed (Figure 3.22). The chamber was designed with a minimum capacity of 2 canisters containing samples, however, it actually was able to house 3 canisters in total. The housing unit was connected to a tank containing the precipitation mixtures being used and the pump which acted as the precipitation source.



Figure 3.22 Design of rain simulation chamber

The precipitation simulation chamber set-up was tested for uniformity, to ensure no bias was introduced into the experiment by the placement of canisters containing the samples. The time of precipitation initiation, volume of precipitation and the number of trials carried out to achieve uniformity in the testing apparatus were used to determine a homogenous placement of canisters, by calculating the coefficient of variation (CV) between results obtained for each of the canisters (Kibet et al., 2014). Each trial had a duration of 10 minutes and with a precipitation intensity of 20%. Precipitation depth (R_D) was calculated using the following equation:

$$R_D = V_R \div A_C \quad (3.13)$$

Where V_R was volume obtained and A_C was the area of the bottom of the canister. The CV was calculated using the following formula:

$$CV = STD_R \div \bar{X}_R \quad (3.14)$$

Where STD_R denoted the standard deviation of rainfall depth and \bar{X}_R denoted average precipitation depth. If $CV < 0.05$, the experimental set up was accepted as uniform and used throughout the experiments. When the acceptable criteria were met, the canister placement was noted down (Figure 3.23), and this placement was used for the entirety of the simulations.



Figure 3.23 Canister placement inside the rain simulation chamber for the duration of the project

Soils were brought from two active sites (County Fingal, Dublin). Both samples underwent analysis for changes under precipitation trials. Additionally, three drying scenarios were applied based on soil temperature values observed during field monitoring (between -5°C and 35 °C):

Scenario 1: Freeze-Thaw:

Post-precipitation, soil samples were placed in the freezer overnight between -2 and -5 °C. Prior to the consecutive simulation (next cycle) the soil samples were removed from the freezer and left to thaw for 3 hours.

Scenario 2: Oven Drying:

Post-precipitation simulation, soil samples were placed in the oven (drying) for 3 hours at 35°C. Then the samples were removed from the oven and left at room temperature (between 18 and 25 °C) overnight.

Scenario 3: Air drying

Post-precipitation simulation, the soils were air dried at room temperature (between 18 and 25 °C) overnight. By simulating these scenarios, a gradient was created to cover the spectrum of temperatures seen at field-level monitoring.

3.9.4.1 Precipitation simulation using an artificial precipitation mixture

The differences in drying procedures are to simulate seasonal variations. This way soil response and environmental stressors were studied for two of the seasonal extremes (summer and winter conditions). In each simulation, the leachate from the soil was collected and the pH, electronic conductivity (EC), temperature, and total volume of

leachate were measured. Rainfall parameters were set up using values found in the archives of Met Éireann (Met Éireann). Intense heavy rainfall values typical of winter are commonly between 10 and 30 mm per hour. The experimental set up was set for 10 mm of rain per hour for a 3-hour period. The rainwater was synthetically produced in the laboratory and the pH was fixed using acids commonly found in rainwater such as sulfuric and nitric acid (Table 3.14). The samples undergoing rainfall simulations were dried by two methods: freeze-drying and oven drying.

Table 3.14 Rainfall simulation conditions

Rate of precipitation	10 mm/hr
Pump intensity	7%
pH of rainwater	Between 6 and 6.5
Temperature	Between 16 and 20°C

3.9.4.2 Precipitation simulation using natural precipitation (melted snow)

The second set of simulations were carried out with melted snow dubbed ‘snow’ from here on, to compare the treatment of synthetically prepared precipitation to naturally occurring precipitation, as well as soil response and the environmental stresses. Similarly, to the first set of simulations described above, simulation conditions were based on field data as well as historical data for Ireland (November 2018-present). As precipitation is not classified by the type, but merely as precipitation by meteorological services, snowfall was taken as a baseline for the conditions of the simulation, counting it as sleet. Commonly, moderate snowfall is classified as 1 cm of snow per hour. The experimental set up was set for 1 cm of snow (sleet) per hour for a 1-hour period. The sleet solution used was collected from field and stored in a cool room (at 4°C) in order to melt the snow to be able to pass it through the pump system (Table

3.15). The samples undergoing sleet-snow simulations were dried by two methods: freeze-drying and air drying at room temperature.

Table 3.15 Sleet snow simulation parameters

Rate of precipitation	10 mm/hr
Pump intensity	4%
Temperature	Between 16 and 20°C

3.9.5 Soil leachate analysis

The leachate collected during the precipitation simulations was analyzed by two techniques, namely ion chromatography and inductively couple plasma mass spectrometry.

3.9.5.1 Ion Chromatography

The working standard solution was prepared from the Thermo Scientific supplied Combined Seven Anion Standard II (Table 3.16).

Table 3.16 Concentration of anions in Thermo Scientific supplied Combined Seven Anion Standard II

Anion	Concentration (mg/L)
Fluoride	20
Chloride	30
Nitrite	100
Bromide	100
Nitrate	100
Phosphate	150
Sulfate	150

Reagents used- calibration standards (chloride was used as a reference point for all dilutions):

1 µg/ml: To a 10 ml volumetric flask, Combined Seven Anion Standard II (0.333 ml) was added and diluted to mark with UPW.

2.5 µg/ml: To a 10 ml volumetric flask, Combined Seven Anion Standard II (0.833 ml) was added and diluted to mark with UPW.

5 µg/ml: To a 10 ml volumetric flask, Combined Seven Anion Standard II (0.167 ml) was added and diluted to mark with UPW.

7.5 µg/ml: To a 1 ml volumetric flask, Combined Seven Anion Standard II (0.250 ml) was added and diluted to mark with UPW.

10 µg/ml: To a 1 ml volumetric flask, Combined Seven Anion Standard II (0.333 ml) was added and diluted to mark with UPW.

20 µg/ml: To a 1 ml volumetric flask, Combined Seven Anion Standard II (0.670 ml) was added and diluted to mark with UPW.

To establish a baseline prior to any treatment, representative soil sample (0.3 g, homogenised sample) from each site was analysed in triplicate. The soil was extracted using UPW. Extraction of ions was performed using a sonicator (30 minutes sonication, 30 minutes left to settle followed by 30 minutes of sonication). The soil solution was centrifuged (20 minutes, 900 RPM) in order for the extract to be decanted and filtered using a 0.22 micron filter prior to injection. All leachate samples to be analysed were also filtered using a 0.22 micron filter prior to injection. No additional work was done on the leachate samples prior to analysis.

Table 3.17 Ion chromatography method

Parameter	Value for soil solution
Guard-Column	Dionex AG12 4x50 mm
Column	Dionex AS12 4x250 mm
Eluent	10-45 mM KOH in 15 mins (gradient used)
Temperature	30 °C
Flow-rate	1 ml/min
Injection Volume	1 ml
Rinse Volume	1 ml
Detector	Suppressed Conductivity, ASRS ULTRA II, 4mm
Run time	30 minutes

3.9.5.2 Inductively coupled plasma mass spectrometry (ICP-MS) analysis

The leachate obtained during the simulation was submitted to ion chromatography analysis prior to ICP-MS analysis, as ICP-MS analysis required the acidification of the samples. Once the samples have been analysed by ion chromatography, the remaining sample was acidified using concentrated nitric acid (1 ml, 16 M).

3.10 Development of the CASIOS model

The Conceptual Ammonia-aeroSol bIOspheric Simulation (CASIOS) model is a novel conceptual model developed to simulate system dynamics in an arable agricultural setting. It introduces the ideology of a holistic biospheric approach, allowing for an overview of dynamics in the air-water-soil nexus. The goal of the model was to identify sources, link various components (also known as sub-systems namely soil,

water, air) of the system, assess the risk and state of components, and provide a description of a hazardous agents' harmful effects, including inner comparisons with other agents present in the system with related structure or exposure. In the case of CASIOS, hazardous agents in an agricultural setting included NH_3 and PM in the atmosphere, nutrients such as $\text{NH}_3\text{-N}$, $\text{NO}_3\text{-N}$, $\text{NO}_2\text{-N}$ and $\text{PO}_4\text{-P}$ at elevated concentrations in water and $\text{NO}_3\text{-N}$ in soils.

To achieve this, summary measures were utilised, which allowed for the potency assessment of the agents' stimulus on the arable agricultural system under study. When no significant response was evident post-exposure to the agent, the potency was set to a boundary value under which no indicated potent response occurs (e.g.: eutrophication of water sources). The potency boundaries (limits) used were provided by previous studies carried out using the parameters measured during the monitoring period (Section 3.2-3.4) (Bozorg-Haddad et al., 2021; Doyle et al., 2017; EPA, 2017; Fanning et al., 2017; Rusydi, 2018; Saalidong et al., 2022; U.S.EPA, 2017). Exceeding this potency boundary, the agent was assessed as having a potential to affect the system overall as well as one or more sub-systems, leading to impacts on system functioning. For example, fertilizer applied to the soil under wetter weather conditions has a potential to become run-off from the land and enter the water column, increasing nutrient concentrations for $\text{NH}_3\text{-N}$ above the potency boundary (limit) value (these values are given in Section 4.2). This can potentially result in algal blooms and eutrophication, increased concentrations of $\text{NO}_3\text{-N}$, and in severe cases, toxic effects to aquatic flora and fauna.

The biggest concern for the model was how to measure and define cause-effect links from a biospheric perspective, without over-simplification or exaggeration of the parameters and variables used. If the sub-systems (air, water, soil) were viewed

individually, each has a complex break-down of a substances, from the moment of entry through to its exit from said sub-system and over-simplifying these intricate pathways could lead to significant contributions being over-looked. However, from a biospheric viewpoint, sub-system dynamics with minute-detail are also not possible, as it could potentially exaggerate the importance of certain pathways. Additionally, if the concept model becomes over-complicated, it proves an impracticality from a field-measurement perspective (e.g.: field-measurements being too labour intensive for the potential outputs of the model), as well as becoming too complex to allow for a simulation to be facilitated through programming software. This creates a requirement for a very refined balance of complexity. To meet this requirement, CASIOS was also analysed and reviewed using complexity theory contexts.

The premise of complexity theory is that a system which appears chaotic, has a hidden order to its behaviour and evolution, with the ideology that specific traits are shared by most complex systems (Sammut-Bonnici, 2008). The generic matrix of these systems involves the combination of independent variables behaving and forming a singular cohesive unit. These variables have the potential to respond to their environment, forming “networks” (links between sub-systems such as transport pathways).

The sub-systems under study, while appearing to be stand-alone systems in their own right, form a singular unit known as the biosphere. With all sub-systems having a potential relationship with one another, viewing them separately could lead to simplified simulations and assessments. This is due to possible interactions interfaces being excluded on the basis that a given agent is ‘exiting’ the sub-system (e.g.: NH_3 volatilized from the soil post-fertilization). Therefore, viewing the biosphere as the

system, with sub-systems such as water soil and air allows for not only transport pathways but the recognition of exchange interfaces.

The specific traits shared by all these sub-systems are potential stimuli which result in changes in the system (drivers), the pressures these potential stimuli place on system functioning and the impacts which the system will incur as a result. Therefore a network between sub-systems is formed primarily based on drivers, pressures, and impacts (independent variables), which allows for the mapping of the biosphere system.

Following this assessment, each sub-system is linked, and potential interactions are explored at exchange interfaces. For example, water nutrient levels (e.g.:NO₃-N) could potentially increase from leaching of soil following heavy precipitation events. Building on these variables and assessing the CASIOS model's requirements, a Drivers, Pressures, State, Impacts, Responses (DPSIR) framework was chosen as the basis of the CASIOS model. This also allowed for the addition of the assessment of the state of the sub-systems present and a potential for responses which could improve the system. The DPSIR framework is widely used in order to aid environmental policy decisions and policy formation as a whole (Kelble et al., 2013; Wang et al., 2022). However, the framework itself, while allowing for links and relationships to be formed on a biospheric level, required an addition of another category, under the label 'Context', modifying the framework to accommodate for potential temporal and spatial changes between sites (Section 5.2).

Chapter 4: Results and Discussion

4.1 Introduction

The previous chapter (Chapter 3) introduced and described the experimental techniques used to obtain and process the samples from all sites under consideration in this project. These techniques were chosen to explore the dynamics of NH_3 and PM formation in the atmosphere, relying on the state-of-the-art techniques described in the literature review. The experimental techniques developed and implemented a continuous monitoring network for atmospheric sampling. The approach also employed background monitoring of the water/soil nutrient loading taking place. This chapter outlines the results obtained from sampling for the monitoring period of the study. These results are reviewed and analysed within four separate sections:

4.2 Atmospheric Monitoring

4.3 Water Background Monitoring

4.4 Soil Background Monitoring

4.5 Micro-meteorological Monitoring

4.2 Atmospheric Monitoring

4.2.1 Ion Chromatography method development and optimization

In order to develop an optimised method for the analysis of samples obtained from both ALPHA and DELTA II denuder samplers, two columns and a range of eluent concentrations were used. Based on established protocols, two columns were selected from a range of available columns currently used for NH_4^+ detection in environmental

samples: CS12A and CS16 (Klein, 2006; Michalski, Pecyna-Utylska, & Kernert, 2021; Thomas, Rey, & Jackson, 2002).

4.2.1.1 Method development and optimization using a CS12A column

The first column used to attempt the development of an optimised method for the detection of NH_4^+ was a CS12A analytical column with the corresponding guard column described in Section 3.3.17. The eluent concentrations were varied in order to optimize the baseline separation of peaks using a $2.5 \mu\text{g/ml}$ NH_4^+ concentration standard. However, no baseline separation was achieved between the sodium (Na^+) and NH_4^+ peaks (Figure 4.1). The eluent strength was lowered to 5 mM, with no baseline separation and an increased run time of 80 minutes for one sample. Since an UPW injection had to be made after each sample and standard injection, this meant that the run time of a single sample would have been 160 minutes. Therefore, the column was found inefficient for NH_4^+ detection, due to co-elution with Na^+ .

4.2.1.2 Method development and optimization using a CS16 column

The second column tested was a CS16 analytical column with the corresponding guard column (Section 3.3.17). The initial eluent strength used was 30 mM with a $2.5 \mu\text{g/ml}$ NH_4^+ concentration standard, which produced baseline separation between Na^+ and NH_4^+ and an optimal run time of 30 minutes. However, at this eluent strength there was no baseline separation between the magnesium (Mg^+) and potassium (K^+) peaks. As both Mg^+ and K^+ are abundantly present in environmental samples (e.g.: naturally from rainwater in the atmosphere) and may form part of the PM samples collected, the eluent strength was increased to 35 mM. This resulted in a more optimized run time

(25 minutes per injection), with all peaks reaching baseline separation and were fully resolved (Figure 4.1 D).

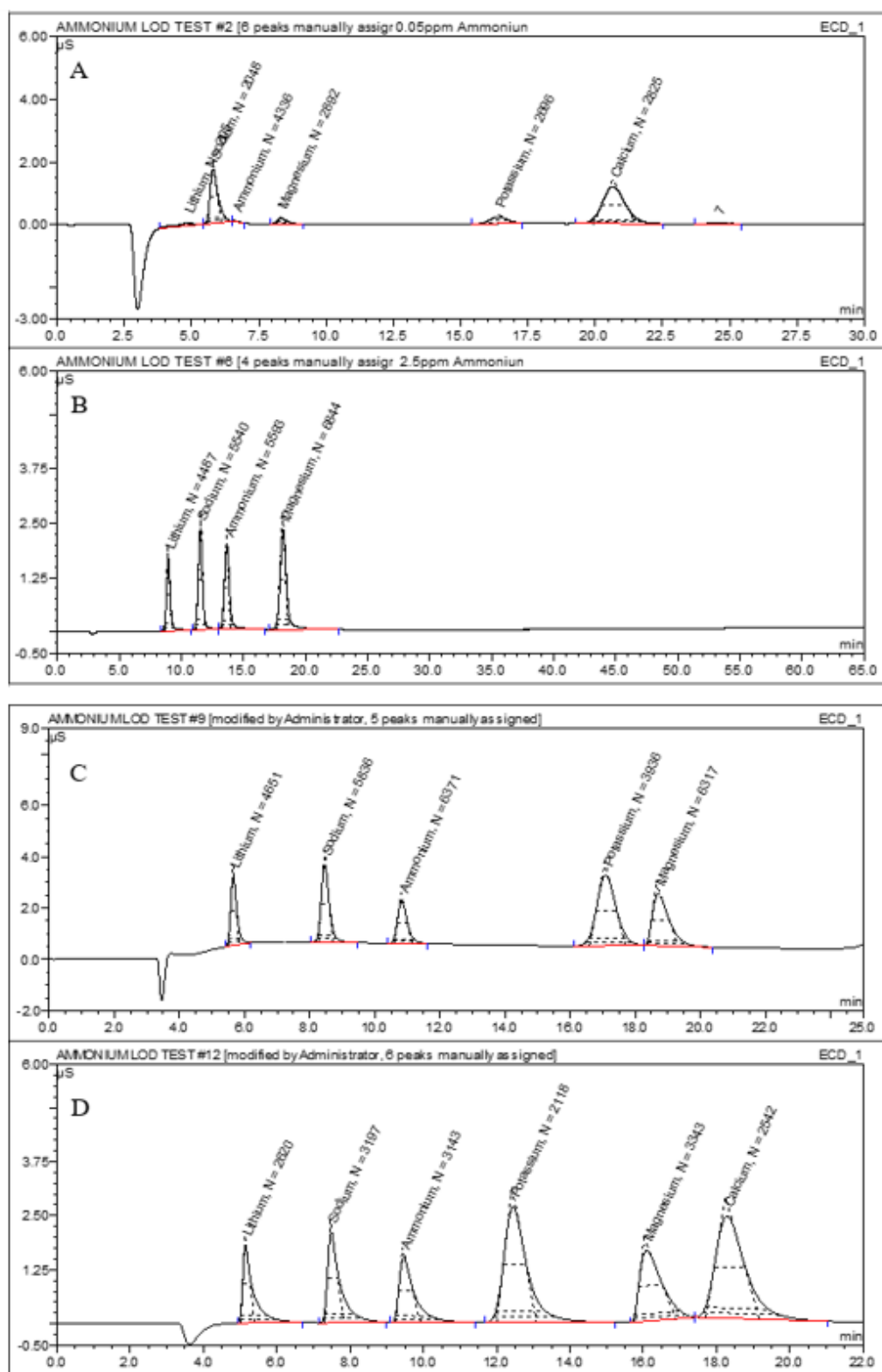


Figure 4.1 Comparison of chromatograms during method optimization: A) Chromatogram of 2.5 µg/ml NH₄⁺ standard with CS12 column and 15 mM eluent; B) Chromatogram of 2.5 µg/ml NH₄⁺ standard with CS12 column and 5 mM eluent; C) Chromatogram of 2.5 µg/ml NH₄⁺ standard with CS16 column and 30 mM eluent; D) Chromatogram of 2.5 µg/ml NH₄⁺ standard with CS16 column and 35 mM eluent

4.2.1.3 Limit of detection

Once the optimum column and eluent strength has been established, the limit of detection (LOD) of the column was tested with respect to NH_4^+ . LOD is defined as the concentration of a given analyte in a test sample which can be reliably distinguished from zero. Establishing the LOD for NH_4^+ allows for the determination of a detection limit for the atmospheric samples using this analytical technique. The limit of detection is defined as the signal showing a standard deviation which is 1/3 of the relative signals (Bruno et al., 2000). A range of standards were prepared in the concentration range of 0.2 – 0.002 $\mu\text{g}/\text{ml}$ NH_4^+ . The lowest quantifiable concentration where NH_4^+ was detected was found to be 0.02 $\mu\text{g}/\text{ml}$ NH_4^+ (Figure 4.2).

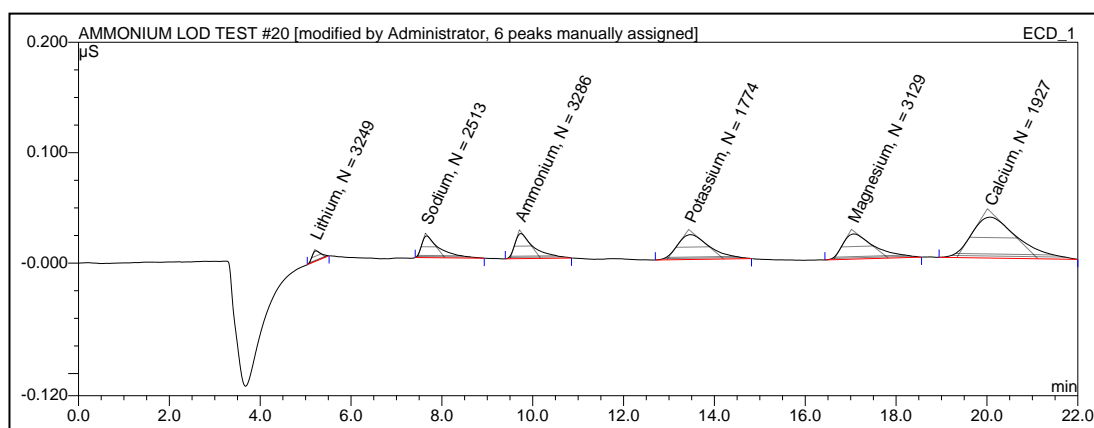


Figure 4.2 Chromatogram of 0.02 $\mu\text{g}/\text{ml}$ NH_4^+

4.2.2 Atmospheric NH_3 Concentrations (ALPHA samplers)

The average concentration measured during the monitoring period was 1.49 ± 0.96 $\mu\text{g}/\text{m}^3$ (Table 4.1, Figure 4.4). This is in approximate agreement with the previous two sampling campaigns carried out in Ireland, where the average concentrations detected

were 1.45 $\mu\text{g}/\text{m}^3$ during the Ammonia1 study (Kluizenaar & Farrell, 2000) and 1.72 $\mu\text{g}/\text{m}^3$ during the Ammonia2 study (Doyle et al., 2017).

Table 4.1 Mean NH_3 concentration ($\mu\text{g}/\text{m}^3$) and summary of statistics for each site

	n	Sampling start	Sampling Finish	Mean ($\mu\text{g}/\text{m}^3$)	Min ($\mu\text{g}/\text{m}^3$)	Max ($\mu\text{g}/\text{m}^3$)	Median ($\mu\text{g}/\text{m}^3$)	Range ($\mu\text{g}/\text{m}^3$)
Site 1	13	13.11.2020.	18.01.2022.	1.27	0.44	2.42	1.05	1.98
Site 2	13	13.11.2020.	18.01.2022.	1.70	0.30	5.04	1.40	4.74
Site 3	7	05.03.2021.	01.03.2022.	0.52	0.05	1.76	0.193	1.71

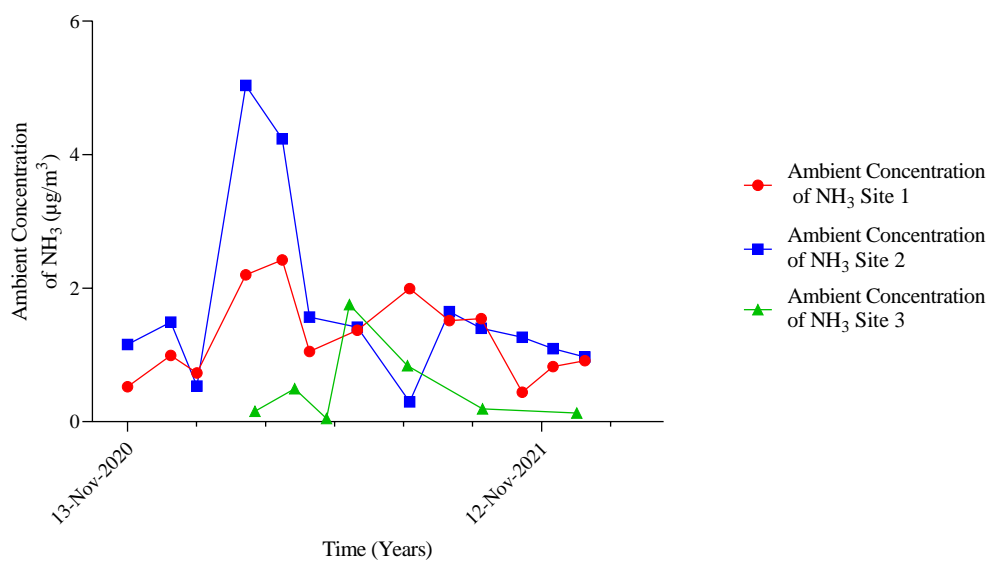
4.2.2.1 Site variation of NH_3 concentrations

The average values over the monitoring period for individual sites ranged from 0.52 $\mu\text{g}/\text{m}^3$ at Site 3 to 1.70 $\mu\text{g}/\text{m}^3$ at Site 2, with an average concentration of 1.45 $\mu\text{g}/\text{m}^3$ for the two active sites between November 2020 and January 2022. The maximum concentration measured 5.04 $\mu\text{g}/\text{m}^3$, was recorded at Site 2 during the period of February-March 2021. None of the measurements taken during the monitoring period were below the LOD (0.02 mg/L NH_4^+), while the minimum concentration detected (above LOD and distinguishable from the corresponding blank measurements) was 0.30 $\mu\text{g}/\text{m}^3$ for the active sites at Site 2 and 0.05 $\mu\text{g}/\text{m}^3$ for the control site (Site 3). Concentrations were highly variable between sites, with the greatest 4-week exposure range obtained in the February-March period of 2021 at Site 2 with 4.50 $\mu\text{g}/\text{m}^3$. A 2-sample t-test was also carried out in order to determine if there is a site-specific concentration difference between the active sites. The test showed that there was no significant effect of location on atmospheric NH_3 concentrations at $p < 0.05$ level [$t=1.026$, $df=24$].

4.2.2.2 Temporal variation of NH₃ concentrations

Temporal variation was observed in the concentration of NH₃ during the monitoring period of November 2020-January 2022. The greatest relative variance for an individual site was obtained for Site 2. However, the variations were not significant according to the 2-sample t-test. Factors such as agricultural activities and weather patterns during the year are the two main drivers for variation in-between sites, as well as concentrations observed. The temporal graphs (Figure 4.4 A and B) show two peak concentrations during the year, one in early spring and one in early autumn. The concentrations are lowered in the consecutive months.

A



B

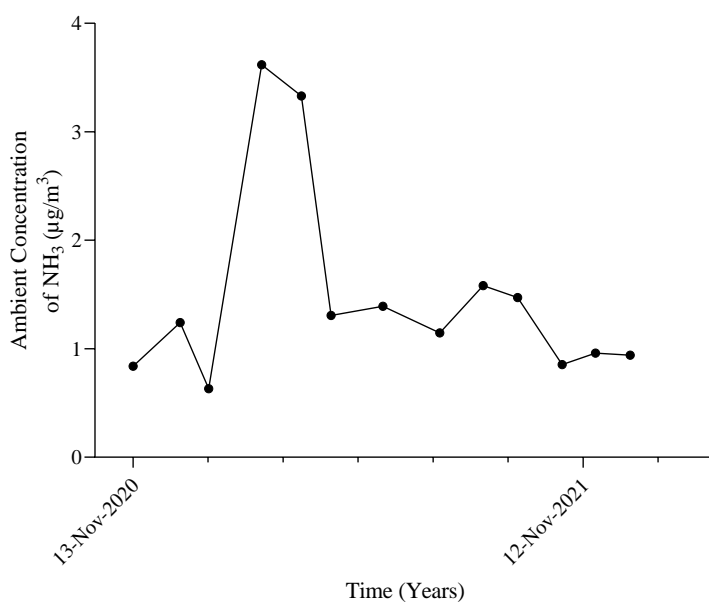


Figure 4.3 Time-series of ambient atmospheric NH_3 concentrations measured at individual site (A) and the average concentrations measured at active sites (B)

The highest recorded concentrations observed in early spring would be indicative of the first fertilizer application, while the secondary highest concentration occurred in late autumn would indicate a second application of fertilizer, one with potentially lower N content based on the size difference of the peaks observed. Environmental factors such as air and soil temperature, and precipitation, which affect these emissions were also investigated to determine the capacity of effect (Figure 4.5).

From the data, temperature shows a potential effect on atmospheric NH_3 concentrations. When temperature begins to rise, atmospheric NH_3 concentrations also increase (Figure 4.4 A). The loss of NH_3 from fertilizer applied to the soil surface increases with temperature, as soil moisture is reduced, and the soil's surface dries (Pedersen, Nyord, Feilberg, & Labouriau, 2021). As air temperature increases, soil surface temperature increases. Similarly to air temperature, soil temperature and ambient atmospheric NH_3 concentrations have a potential effect (Figure 4.5 A). This is due to increased emission rates occurring when soil temperature increases due to increased rates of NH_3 volatilization.

As expected, precipitation tends to reduce NH_3 emissions, as it reduces the influence and absolute values of the drivers listed above, hence increasing precipitation is associated atmospheric NH_3 concentrations. This suggests a relationship which is inversely proportional (Figure 4.4 B). This is due to precipitation being a deposition pathway, reducing atmospheric concentrations of NH_3 . Combining these environmental factors and knowledge of agricultural practices allow for a more complete understanding of the fluctuations reported for atmospheric NH_3 concentrations at Sites 1 and 2.

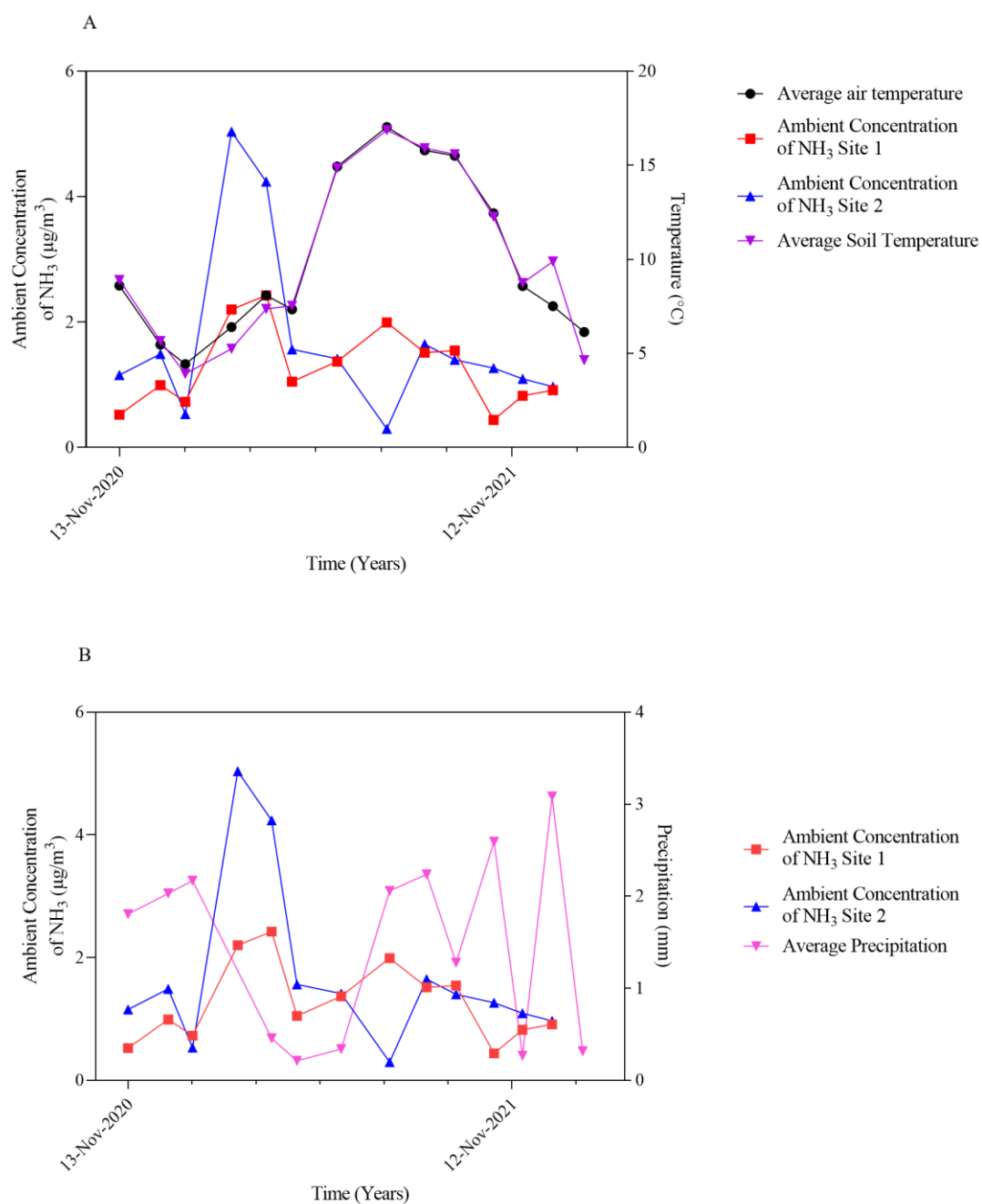


Figure 4.4 Relationship between environmental factors and atmospheric NH_3 concentrations. A) Air and soil temperature; B) Precipitation

4.2.3 Atmospheric NH₃ and Aerosol NH₄⁺ concentrations (DELTA II samplers)

The average concentrations measured during the monitoring period were 0.39 µg/m³ and 0.27 µg/m³ gaseous ambient atmospheric NH₃ and aerosol NH₄⁺ respectively (Figure 4.6, Table 4.2)

Table 4.2 Mean gaseous NH₃ and aerosol NH₄⁺ concentrations (µgm⁻³) and summary of statistics for each component

	n	Mean (µg/m ³)	Min (µg/m ³)	Max (µg/m ³)	Median (µg/m ³)	Range (µg/m ³)
NH ₃ (g)	9	0.39	0	1.25	0.26	1.25
NH ₄ ⁺ (s)	10	0.27	0.03	1.05	0.14	1.02

The average values over the monitoring period for gaseous NH₃ and aerosol NH₄⁺ were 0.39 µg/m³ and 0.27 µg/m³ respectively. The maximum concentrations measured for gaseous NH₃ and aerosol NH₄⁺ were 1.25 µg/m³ recorded during the period of April-May 2021, and 1.05 µg/m³ recorded during the period of June-July 2021. No measurements taken during the monitoring period were under the LOD (0.02 mg/L NH₄⁺), while the minimum concentration detected (above LOD and distinguishable from the corresponding blank measurements) were 0.136 µg/m³ for gaseous NH₃ and 0.03 µg/m³ for aerosol NH₄⁺.

The concentrations for gaseous NH₃ reported using the ALPHA samplers were generally higher compared to those of the DELTA II sampler. One potential cause for differences in the obtained NH₃ concentrations could be the difference in the exposure periods of the two samplers. While the ALPHA samplers were generally collected on

a 4-weekly basis, the DELTA II samplers were only exposed for a maximum of 3-weeks at a time.

4.2.3.1 Temporal variation of gaseous NH_3 and aerosol NH_4^+ concentrations

Gaseous NH_3 concentrations show greater relative variance compared to that of aerosol NH_4^+ . There is a weak temporal variation observed in the concentration of NH_3 during the monitoring period. However, as discussed earlier (Section 4.2.2.2), this could be indicative of effects exerted by agricultural activities and environmental factors affecting NH_3 concentrations, with the addition of RH and wind speed (WS) to account for variations in atmospheric aerosol NH_4^+ concentrations (Figure 4.4). This provides a possible explanation for the trend observed in aerosol NH_4^+ concentration variations during the monitoring period, assuming atmospheric aerosol NH_4^+ concentrations are directly affected by NH_3 dynamics.

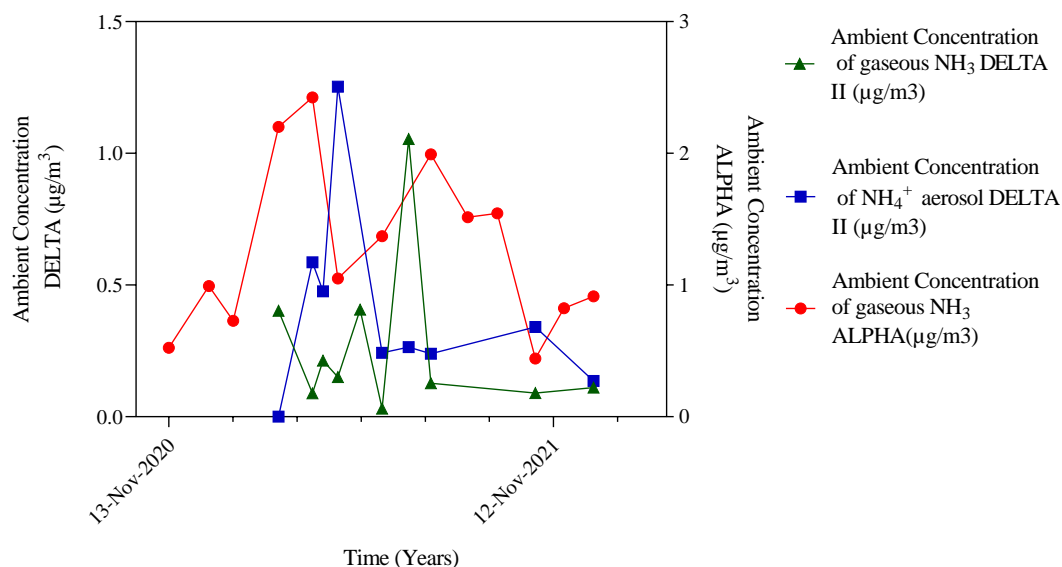


Figure 4.5 Time-series of ambient atmospheric (gaseous) NH₃ and aerosol NH₄⁺ concentrations measured during the monitoring period using ALPHA and DELTA II samplers

When the ALPHA passive and DELTA II active sampling methods were compared, an R^2 value of 0.3 was obtained, which shows that the correlation between the two sampling methods is moderate. The differences in the data obtained for the in-field measurement of gaseous NH₃ collected by the DELTA II and ALPHA samplers could be attributed to the difference in sampling times. The ALPHA samplers were exposed for a duration of 4 weeks per collection period, while the DELTA II samplers were exposed for only 3 weeks per collection period. Another possible factor which may cause the differences observed could potentially be due to the uptake rate of the DELTA II sampler. The DELTA II sampler was set up with a flow rate of 0.2 L/minute (Section 3.3.13) as the sampler was directly at an emission source. This could have potentially affected the sample loading onto the denuders, and result in the variations observed in the data.

As discussed earlier (Section 4.2.2.2), atmospheric NH_3 concentrations show a positive relationship with air and soil temperature (Figure 4.6 A), and an inversely proportional relationship with precipitation (Figure 4.6 B). Aerosol NH_4^+ concentrations increase when air temperature remains stable, and concentrations decrease when temperatures increase. This indicates that air temperature instability (meaning increases) can potentially result in reduced atmospheric NH_4^+ aerosol concentrations. One possible explanation for this is the relationship between RH and air temperature being inversely proportional (when air temperature increases, RH decreases).

Similarly to atmospheric NH_3 concentrations, aerosol NH_4^+ concentrations decrease when wet deposition (precipitation) increases (from August 2021 until January 2022), therefore the relationship is potentially inversely proportional (Figure 4.6 B). During the monitoring period windspeed and RH were also measured. Windspeed had an inversely proportional relationship with both atmospheric NH_3 and aerosol NH_4^+ concentrations (Figure 4.6 C). This is due to increased off-site transport effects of both atmospheric NH_3 and aerosol NH_4^+ resulting in a decrease in their respective concentrations at site level. RH increases aerosol NH_4^+ concentration, indicating a link between aerosol concentrations and RH (Figure 4.6 D). Generally, PM mass concentrations and numbers increase significantly for RH values of 75% (Jayaratne et al., 2018). Peaks in concentrations of atmospheric aerosol NH_4^+ measured are

concurrent with increases in RH and high atmospheric concentrations (compared to baseline) of gaseous NH_3 at Site 1.

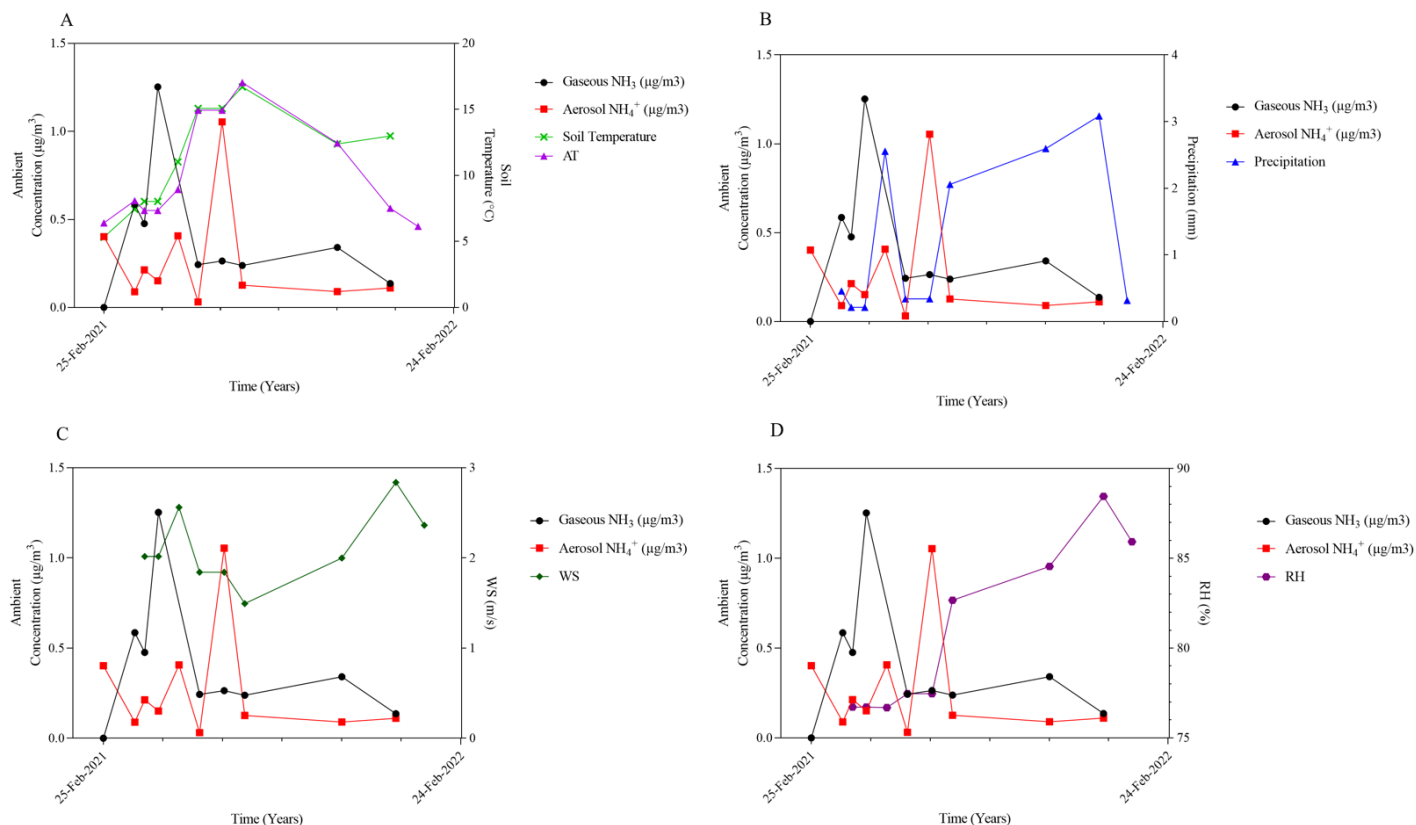


Figure 4.6 Relationship between environmental factors and ambient atmospheric NH_3 (gaseous) and aerosol NH_4^+ concentrations. A) Air and Soil temperature; B) Precipitation; C) WS; D) RH

4.2.3.2 Imaging and size distribution of aerosols

A filter from each season (winter, spring, summer, autumn) during the monitoring period of November 2020-January 2022 was imaged (Figure 4.7) using a brightfield microscope (Section 3.3.19). Size distribution analysis was performed to determine the size distribution of aerosols representative of each season (Figure 4.8). The particle

population density (PPD) and average particle size for each season were also determined (Table 4.3).

The particles collected by the filters were predominantly in the total suspended particulate matter (TSP) size fractions. This refers to particles having an aerodynamic diameter between 0.1 and 50 μm (European Environment Agency, 2020). Generally, particles were observed to fall within the 2.5-10 μm size fraction (PM_{10}), with the exception of summer, where particles were predominantly in the 10-50 μm size fraction. PM_{10} accounted for 68%, 56%, 17% and 58% of total particles sampled in winter, spring, summer, and autumn respectively.

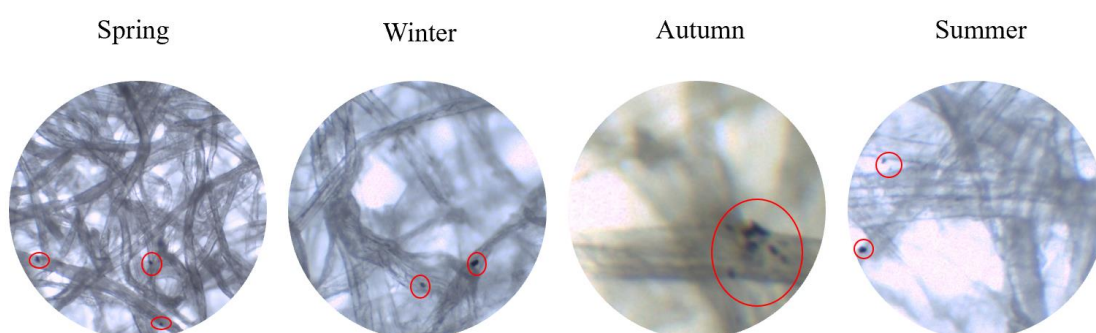


Figure 4.7 Particulate matter samples from each season

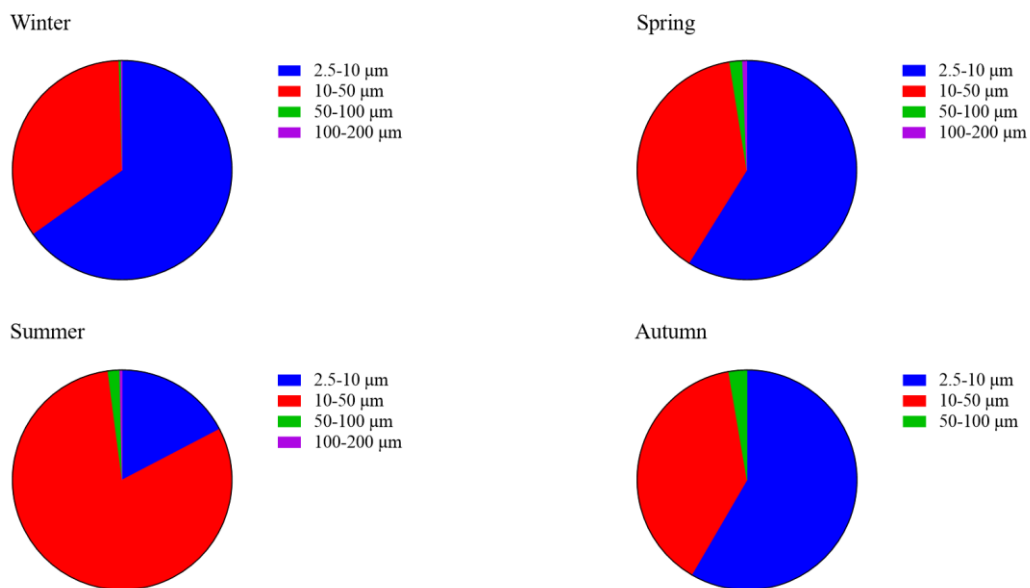


Figure 4.8 Size distribution of aerosols representative of each season during the monitoring period

Table 4.3 PPD and average particle size representative of each season during the monitoring period

	Winter	Spring	Summer	Autumn
PPD (particle/mm)	1.351	0.678	0.587	0.605
Average diameter (µm)	13.089	23.672	22.319	17.617

The highest PPD was obtained during winter with 1.351 particle/mm, while the lowest PPD was obtained during summer with 0.587 particles/mm. PPD therefore was approximately twice as high for samples collected during winter, as opposed to those collected during the summer season for these filters. This could be indicative of seasonal weather effects (Figure 4.6). During winter, cold air masses move slower than those during the summer, due to an increased density (Meng et al., 2019; Nawrot et al., 2007). This enables PM to remain static in a given location for longer periods.

4.3 Water Analysis

As Section 3.1, Site 1 and 2 both contained a water source which allowed for the background analysis of nutrient loading in arable agricultural ecosystems. Nutrient loading and the arising pollution thereof, is a key environmental concern, resulting in degrading impacts on the state of surface water in Ireland. While Ireland has maintained a higher-than-average European standard for water quality in terms of groundwater and lake water quality, monitoring at emission hot-spots is detrimental to the upkeep of these standards as these sites have the capacity to decrease water quality throughout a catchment (EPA, 2017). Therefore, a focus was applied to the background monitoring whereby nutrient-based indicators were used to assess the water quality of each site. Nutrients such as $\text{PO}_4\text{-P}$, $\text{NH}_3\text{-N}$, and $\text{NO}_3\text{-N}$ are responsible for eutrophication and algal blooms (Francis-loyd et al., 2009).

The main sources for these nutrients in water at Sites 1 and 2 are agricultural activities, such as the application of fertilizer. Site 3 also contains pools of water on site where monitoring took place. A preliminary spot analysis was carried out at Site 3 to determine if any nutrient loading effects from the surrounding ecosystem could be detected. However, given the environmental setting of Site 3 (remote site in the Wicklow mountains in a blanket peat ecosystem), the results of the analysis showed low-to-no detectable levels of nutrients present with respect to nutrient loading. No further analysis was carried out at this site.

The parameters chosen for the assessment of water quality was based on a review of the parameters commonly used by environmental agencies such as the EPA and the European Environmental Agency (EEA). These parameters include physico-chemical properties which aid in the establishment of the overall water quality at each site, such as pH, conductivity, total dissolved solids (TDS), and dissolved oxygen (DO).

Physico-chemical properties of water are viewed in the broadest sense, referring to physical properties, and relating to certain chemical attributes of water. This term is viewed in a sense of water quality and monitoring thereof. Water is a polar substance, with a relatively high boiling point, high specific heat, cohesion, adhesion, and density. Additionally, water is a universal solvent, capable of dissolving chemical substances used in activities such as fertilization. An increase of substances such as these nutrients can result in damages to a given water body's ecology. Additionally, commonly assessed nutrients were also measured, including $\text{NH}_3\text{-N}$, $\text{NO}_3\text{-N}$, $\text{NO}_2\text{-N}$ and $\text{PO}_4\text{-P}$.

4.3.1 Background monitoring of water pH

Anthropogenic interferences such as increases and decreases in pH, can have degrading effects on the structure and function of aquatic ecosystems. Variations in pH have a myriad of effects on ecosystems. Acidification of water sources reduce the neutralizing capabilities of water, leading to reduced resilience to future changes in the water body's pH.

Accepted values for freshwater pH in ponds and lakes are generally between 6.5 and 8.5 (Saalidong et al., 2022). Values of pH outside this range affect solubility and biological availability of chemical constituents and nutrients present in aquatic systems and can affect aquatic fauna by impacting individual performance (reproduction and predatory avoidance), species interactions and community structure. A pH below 5.5 indicates poor buffering capacity at a given water source and can be indicative of an acidic system. The average pH for the monitoring period at Sites 1

and 2 were 7.73 and 7.71 respectively (Figure 4.10). These values are within the limits which classify a healthy ecosystem.

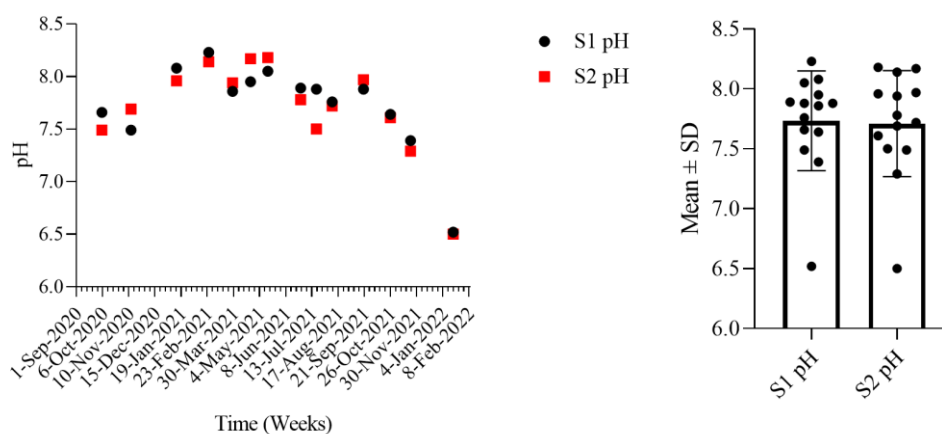


Figure 4.9 pH measured at Site 1 (denoted S1) and Site 2 (denoted S2)

The variation in pH values has not exceeded the range of 6.5-8.5, therefore the pH of the water at both Site 1 and Site 2 are within healthy, good quality water parameters (EPA, 2011). The majority of data points obtained are between 7.5 and 8.5, with fluctuations seen during times of fertilizer application. The trends for Site 1 and Site 2 are very similar, with only minor differences observed (Figure 4.9). An analysis of seasonal variation was also carried out for both Site 1 and Site 2 using a Shapiro-Wilks normality test coupled with a Welch's ANOVA analysis. The analysis showed no significant seasonal variation at either site at $p < 0.05$ level.

In agricultural systems, alkaline pH values can be indicative of lime (a basic, calcium-based compound, oxocalcium) and $\text{NH}_3\text{-N}$ based fertilizer applied to agricultural land entering the water system via run-off post-application. Acidic conditions can potentially arise from acidifying components such as $\text{NO}_3\text{-N}$ entering the water

sources at each site as run-off after fertilization has occurred or as part of precipitation (Figures 4.10 and 4.11).

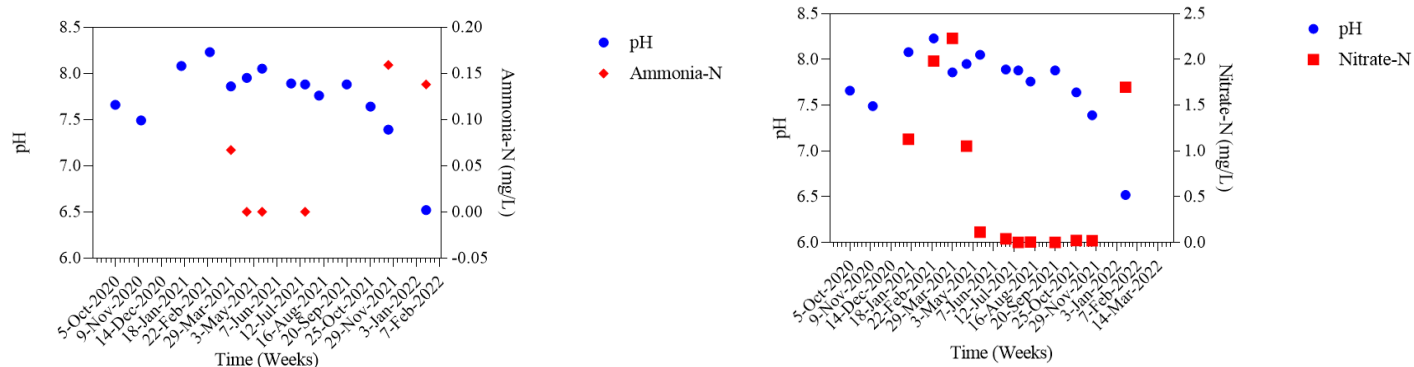


Figure 4.10 Relationship between $\text{NH}_3\text{-N}$ and pH, and $\text{NO}_3\text{-N}$ and pH at Site 1

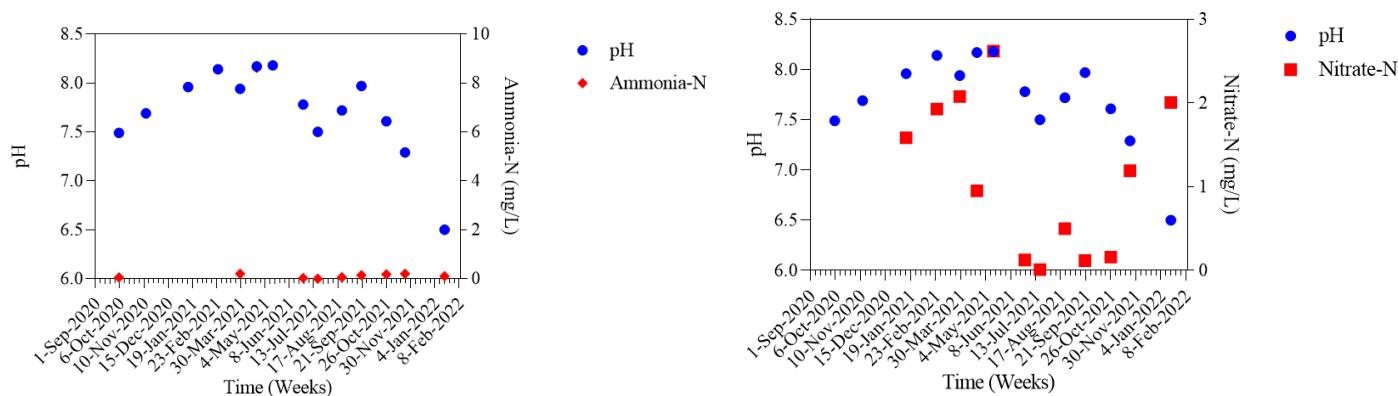


Figure 4.11 Relationship between $\text{NH}_3\text{-N}$ and pH, and $\text{NO}_3\text{-N}$ and pH at Site 2

The water's temperature also has a potential effect on its pH, linked through a positive correlation. This means that when temperatures increase, so does the pH- this does not mean that the water itself becomes more acidic (Figure 4.12). The trends observed

throughout the monitoring period show the potential for chemical enrichment arising from agricultural activity (the main economic activity) at both Sites 1 and 2. These have a potential effect on the pH of the water sources at each site, and therefore the water quality at each site.

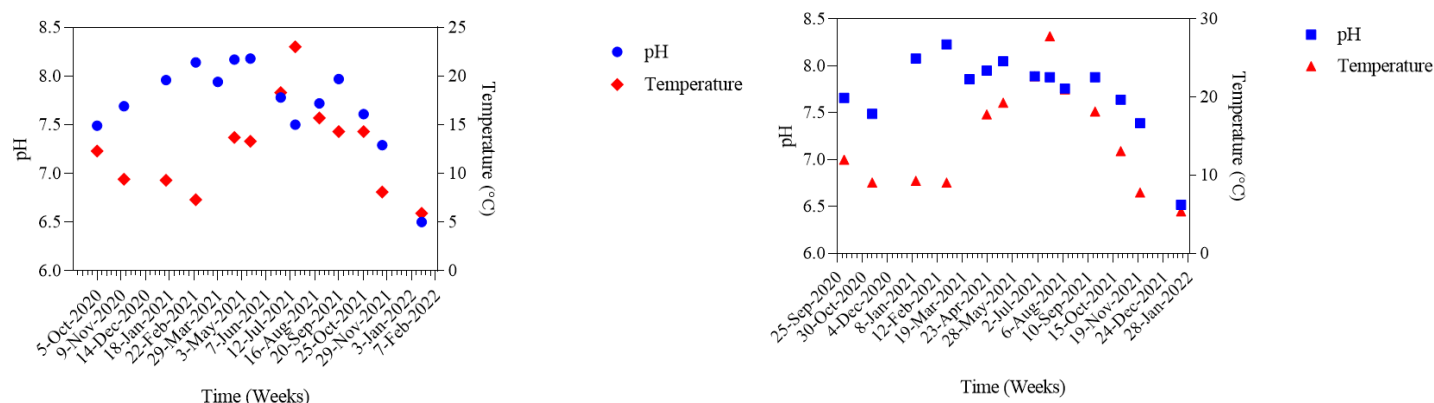


Figure 4.12 Relationship between pH and temperature at Site 1 (LHS) and Site 2 (RHS)

4.3.2 Background monitoring of water electrical conductivity and total dissolved solids

Similarly to pH, variations in electrical conductivity (EC) can be used as an indicator of materials entering the water column which normally would not be present. The EC of freshwater is generally stable, with little variation when the water column does not receive any additions which do not naturally occur, therefore providing a baseline in terms of water quality. However, regarding the current scale, this is slightly arbitrary,

and is viewed in conjunction with the agricultural management practices and activities taking place.

The influx of nutrients in water result in an increased presence of ions. EC is the measure of water's ability to pass electrical flow, and this ability is directly related to the concentration of ions in water at a given time. The higher the concentration of ions in water, the higher its conductivity will be. Sudden increases seen in the data, therefore could be attributed to agricultural nutrient loading of the water column. Another source of ions arise from the naturally occurring inorganic salts present in the water column.

EC was measured at a standardized temperature of 25°C (specific conductance value), in order to facilitate comparability of samples. Site 2 shows a greater variability than Site 1 (Figure 4.13). This could be indicative of additional influx of nutrients from the stream connected to the pond, which is absent at Site 1, leading to greater loads may be seen at Site 2. The average conductivity measured for Sites 1 and 2 during the monitoring period were 616 ± 125 and 913 ± 325 $\mu\text{S}/\text{cm}^1$ respectively.

This was corroborated by the data obtained for nutrient levels observed for Site 1 and Site 2 during the study period. Further analysis of the data obtained also highlights the potential significance of the geographical variation between the ponds is the level of EC measured at Site 1 compared to that at Site 2. The difference in scale of measurement shown reveals that at Site 2 EC levels are approx. 1.5 times those seen at Site 1 (Figure 4.13). The data was also analysed for seasonal variation, using a Shapiro-Wilks normality test coupled with a Welch's ANOVA analysis. The analysis showed no significant seasonal variation at either site at $p < 0.05$ level.

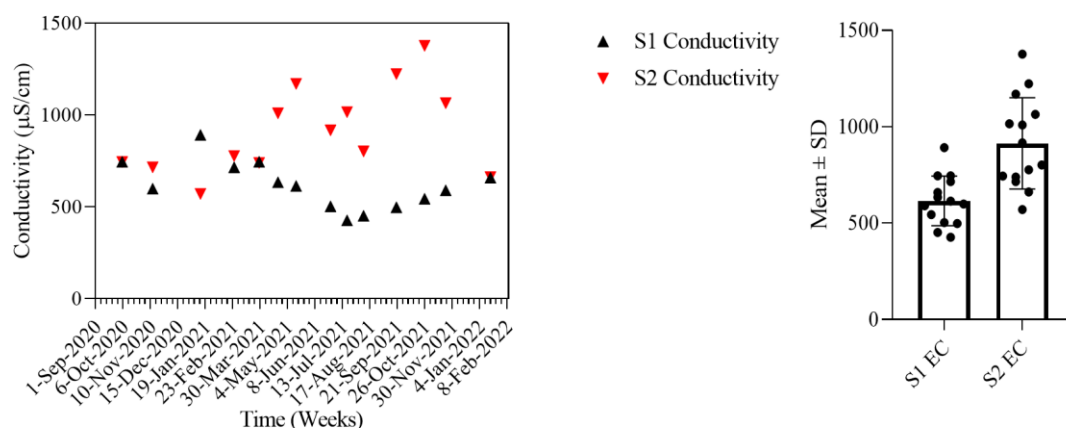


Figure 4.13 Electronic Conductivity measured at Site 1 (denoted S1) and Site 2 (denoted S2)

Total Dissolved Solids (TDS) measures the concentration of dissolved materials in a given water column, including inorganic salts and organic matter, with no distinction between ions (Moujabber et al., 2006). Freshwater concentrations of TDS generally remain below 1000 mg/L, and anything above this concentration is classified as “brackish” (Gray et al., 2011). TDS concentration fluctuations often result from changes to the water balance (increased precipitation, increased water use for irrigation, etc.), salt-water intrusion or by anthropogenic activity (in this case arable agriculture). As with the measurement of EC, fluctuations are attributed to agricultural activities at both sites. The average TDS during the monitoring period was determined as 337.472 ± 91.167 and 516.441 ± 156.104 mg/L respectively (Figure 4.14).

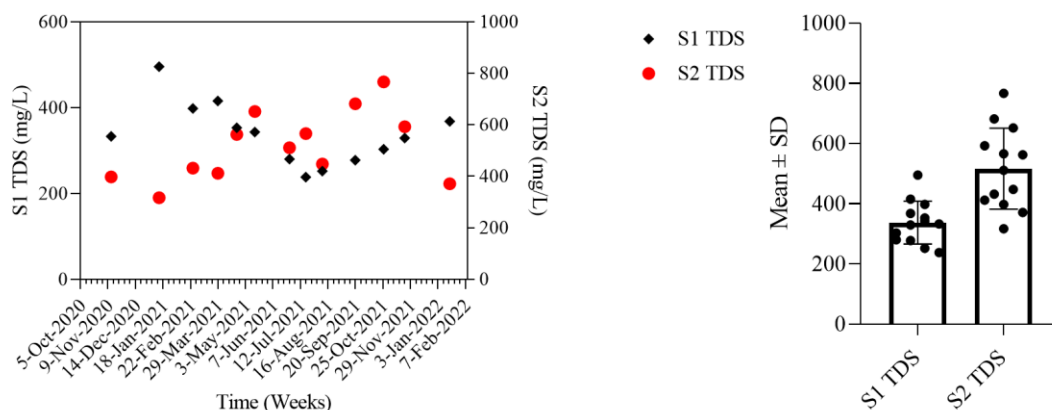


Figure 4.14 TDS measured at Site 1 (denoted S1) and Site 2 (denoted S2)

The results obtained from the background monitoring are in agreement with the EC results seen for both sites. Site 2 shows a greater variability than Site 1, which potentially could be a result of additional influx of materials from the stream which is absent at Site 1 (Figure 4.14). With regards to water quality, both TDS and EC are relatively normal when compared to values obtained for freshwater systems. However, as a result of the high variability of the data, water quality at both sites is evaluated as moderate (Bhateria & Jain, 2016).

The difference in the scale of results indicates that at Site 2 TDS levels were approx. twice as those measured at Site 1 (Figure 4.14). The data here too was analysed for seasonal variation, using a Shapiro-Wilks normality test coupled with a Welch's ANOVA analysis. The analysis showed no significant seasonal variation at either site at $p < 0.05$ level. The high variability observed for both EC and TDS throughout the monitoring period shows potential for both ponds receiving a continuous addition of materials capable of dissolving in the water column, which are independent of seasonal variation.

Due to the relationship of the EC of water with the presence of inorganic salts, the relationship between TDS and EC was also analysed for both Site 1 and Site 2 (Figure 4.15). The main difference between the two locations is the EC measured (values of less than 1000 $\mu\text{S}/\text{cm}$ measured at Site 1, while EC values of more 1000 $\mu\text{S}/\text{cm}$ were measured at Site 2).

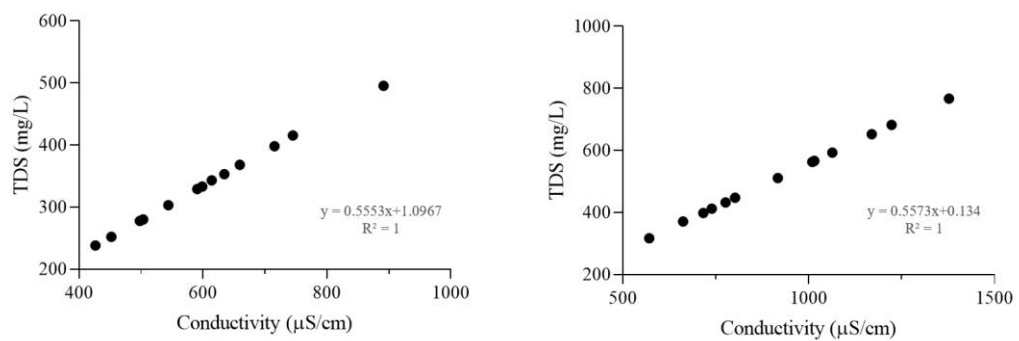


Figure 4.15 TDS-EC correlation at Site 1 (LHS) and Site 2 (RHS)

The TDS/EC ratio for both sites was found to be 0.55 ($R^2=1$), and therefore can be expressed using the equation 4.3 (Rusydi, 2018):

$$\text{TDS} = 0.55 \times \text{EC} \quad (4.3)$$

The findings obtained for the study period are in agreement with values reported elsewhere (McNeil & Cox, 2000), where the variation of TDS/EC ratio for freshwater was established as 0.5-1.00.

4.3.3 Background monitoring of water biological oxygen demand

Biological Oxygen Demand (BOD) is an important component of water quality, as it is the measurement of oxygen required to oxidize soluble organic matter into water. Without an appreciable level of oxygen, aquatic organisms cannot exist in water. The BOD values in ponds can increase during periods of fertilizer application as chemical components enter the aquatic systems, some of which are organic in nature.

BOD is measured as five-day BOD (BOD_5), meaning the measure of molecular oxygen consumed by micro-organisms during a 5 day period under optimum conditions (constant temperature set at 20 °C, in a chamber with no light). The average concentrations being 3.0 ± 2.3 and 3.0 ± 2.5 mg/L for Sites 1 and 2 respectively (Figure 4.16). Higher BOD_5 results indicate an increased requirement of oxygen, decreasing the general oxygen levels for higher forms of aquatic life and is indicative of the aquatic system's capacity for rapid depletion of oxygen.

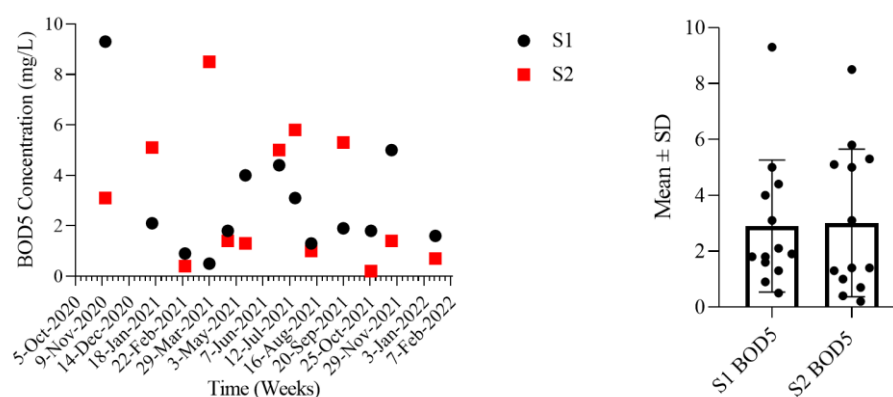


Figure 4.16 BOD_5 values measured at Site 1 (denoted S1) and Site 2 (denoted S2)

The concentrations of BOD₅, (Figure 4.16), indicate highly varying trends for both Site 1 and 2. The high variation observed during the study period, especially when BOD₅ concentrations were high could potentially indicate eutrophication (resulting in algal blooms) occurring at both ponds. When the algal blooms start to die off, the bacteria responsible for the breakdown of the dead material (decomposers) consumes oxygen in the water column, which can often lead to low and in some cases even hypoxic conditions. This is potentially indicated by the data obtained during the August 2021-January 2022 months (Figure 4.16).

During the summer, the photosynthetic activity of the algal blooms encourages the growth of decomposers also, which in turn has a potential to increase the BOD₅ values for the months of May, June, and July. From the results, it can therefore be concluded that the ponds at both sites have the capacity for rapid depletion of oxygen from the water column, which reduces biodiversity in these aquatic ecosystems.

4.3.4 Background monitoring of water dissolved oxygen concentrations

Dissolved Oxygen (DO) refers to the amount of oxygen available for aquatic flora and fauna in the water column (Bhateria & Jain, 2016). Low levels of dissolved oxygen (generally levels below 5 mg/L DO, a concentration determined by DO requirement for larger aquatic fauna such as fish) is considered to be an indicator of degradation of water quality and an unhealthy system due to substances entering the water column (Bozorg-Haddad et al., 2021). The average DO concentrations for Sites 1 and 2 were 8.3 ± 1.4 and 6.9 ± 2.4 mg/L respectively (Figure 4.17).

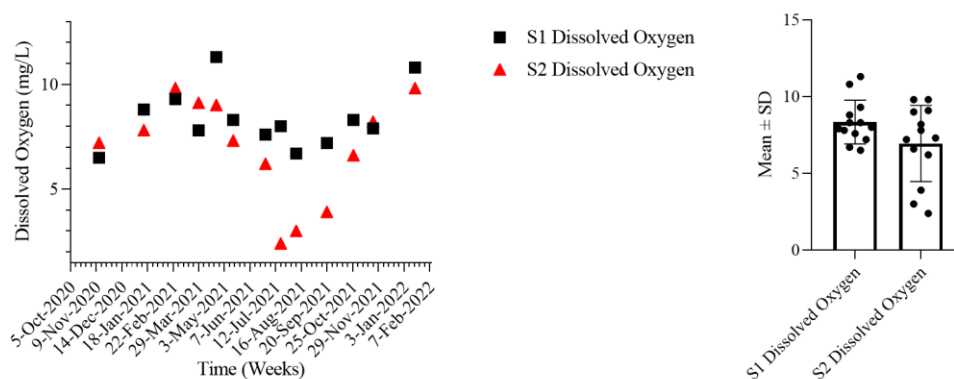


Figure 4.17 DO values measured at Site 1 (denoted S1) and Site 2 (denoted S2)

Site 2 shows a greater variability when compared to Site 1 (Figure 4.17). This variation can potentially be due to the geographical differences between the two sites (the presence of the stream at Site 2 leading to greater nutrient loading), and greater eutrophication occurring at Site 2. From a water quality perspective, Site 1 has moderate water quality, while Site 2 is classified as unhealthy, due to the low DO concentrations obtained during the months of May-September 2021. This could indicate the water systems' inability to support larger life forms as DO levels are too low.

However, temperature and the presence of certain nutrients, such as $\text{NH}_3\text{-N}$ could also potentially affect DO levels in freshwater systems. Temperature has an inversely proportional link with the amount of oxygen which can dissolve in water (or any gas) (Bozorg-Haddad et al., 2021). This means that when water temperature is low, it is capable of holding more dissolved oxygen, than at higher temperatures (Figure 4.18).

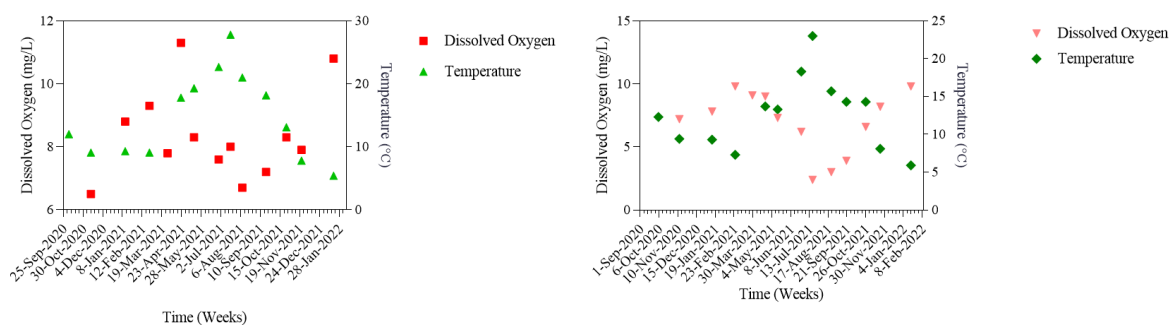


Figure 4.18 Relationship between DO and temperature at Sites 1 (LHS) and 2 (RHS)

Nutrient loading, likewise, to temperature, could possibly affect the amount of oxygen which can be dissolved in the water column. As mentioned before, when aquatic systems receive excessive nutrient loading (eutrophication), algal blooms can occur. This excess algal growth can block sunlight, required for photosynthesis by aquatic fauna, which in turn leads to reduced levels of DO in the water column (Figure 4.19). It must be noted that $\text{PO}_4\text{-P}$ addition at Site 1 only occurred once, due to liming, while there was a steady loading seen at Site 2 ($\text{PO}_4\text{-P}$ loading occurring at both sites is further analysed in Section 4.3.7).

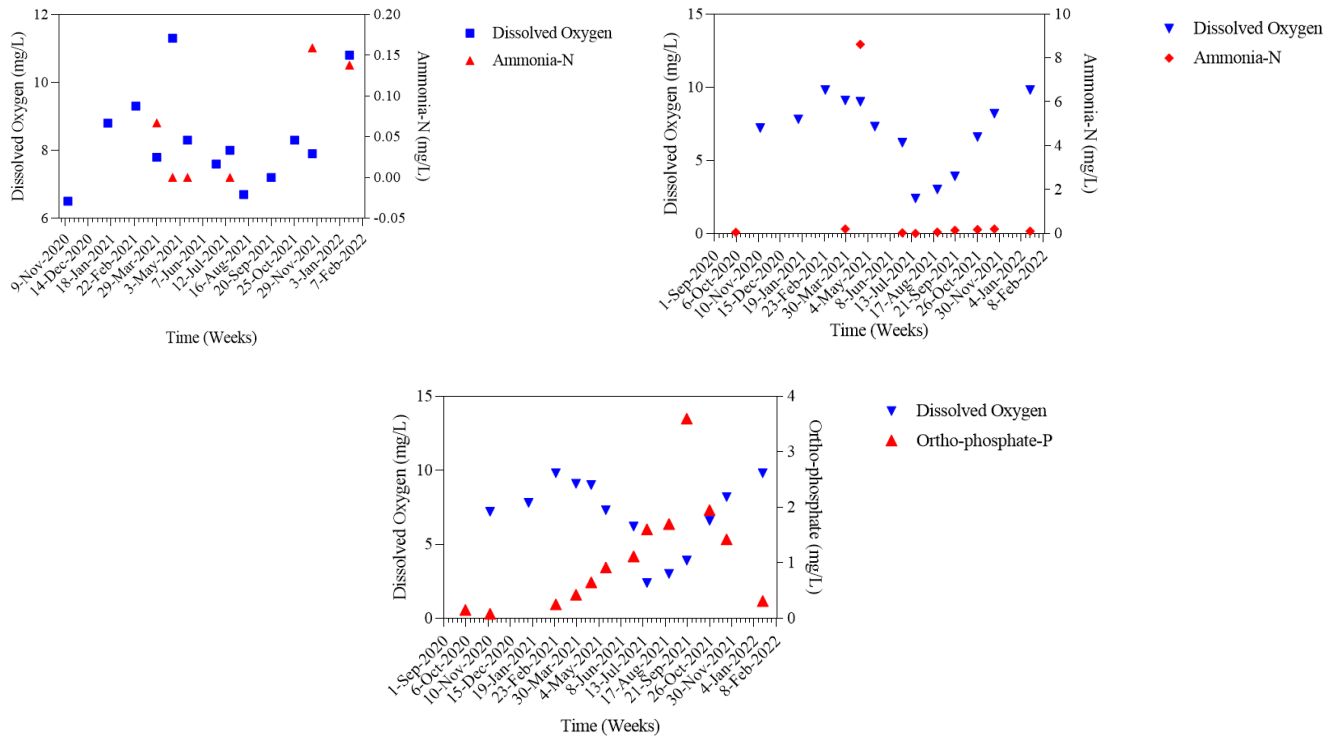


Figure 4.19 Relationship between DO and nutrient loading: $\text{NH}_3\text{-N}$ loading and DO at Site 1 (top LHS); $\text{NH}_3\text{-N}$ loading and DO at Site 2 (top RHS); and $\text{PO}_4\text{-P}$ loading and DO at Site 2 (bottom middle)

A potentially inversely proportional link between $\text{NH}_3\text{-N}$ and DO, as well as $\text{PO}_4\text{-P}$ and DO (Figure 4.19) highlights the importance of nutrient loading in retrospect to water quality and aquatic system health. By conceivably reducing the oxygen levels, life becomes unsustainable in these ecosystems, leading to biodiversity loss and eventual habitat reduction and loss.

The data was also analysed for seasonal variation, using a Shapiro-Wilks normality test coupled with a Welch's ANOVA analysis. The analysis showed no significant seasonal variation for the data obtained at Site 1, however, at Site 2, the seasonal variation was more pronounced, and therefore determined to be significant at $p < 0.05$

level. Thus, seasonal variation has a precedent effect on DO concentrations at Site 2 and can be said to have seasonal variation.

4.3.5 Background monitoring of ammonia concentrations in water

One of the main components of nutrient loading occurring in an arable agricultural setting is NH_3 . NH_3 has been extensively discussed in Chapter 2, including its effects as an eutrophying agent, leading to algal blooms (Figures 4.22 and 4.23). The concentration of $\text{NH}_3\text{-N}$ (mg/L) is a key indicator because of the biological quality of freshwater, due to excessive concentrations leading to biodiversity reduction and loss due to the toxicity of $\text{NH}_3\text{-N}$. While there are no national standards for $\text{NH}_3\text{-N}$ in ponds, a concentration of >0.02 mg/l set forth by the EPA (EPA, 2017) is considered high for freshwater sources, based on toxicological effects of NH_3 on aquatic flora and fauna and eutrophication potential of standing bodies of water. From the data obtained during the study period, both sites are in breach of this limit during the months when $\text{NH}_3\text{-N}$ was detected (Figure 4.20). The average concentration of $\text{NH}_3\text{-N}$ for both Sites 1 and 2 were 0.1 ± 0.0 and 1.0 ± 2.7 mg/L respectively, further demonstrating the issue of nutrient loading (Figure 4.20).

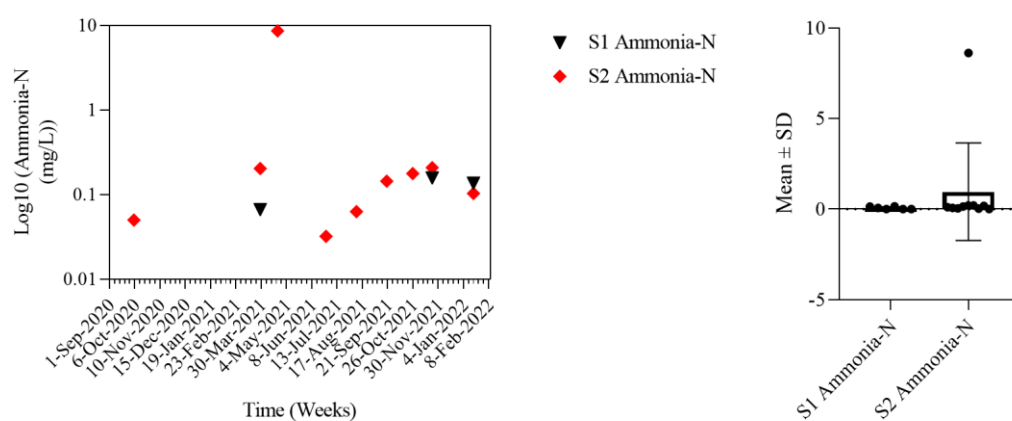


Figure 4.20 Concentration of $\text{NH}_3\text{-N}$ (mg/L) at Sites 1 and 2#



Figure 4.21 Algal bloom at Site 2, July 2020 (RHS), and October 2020 (LHS)

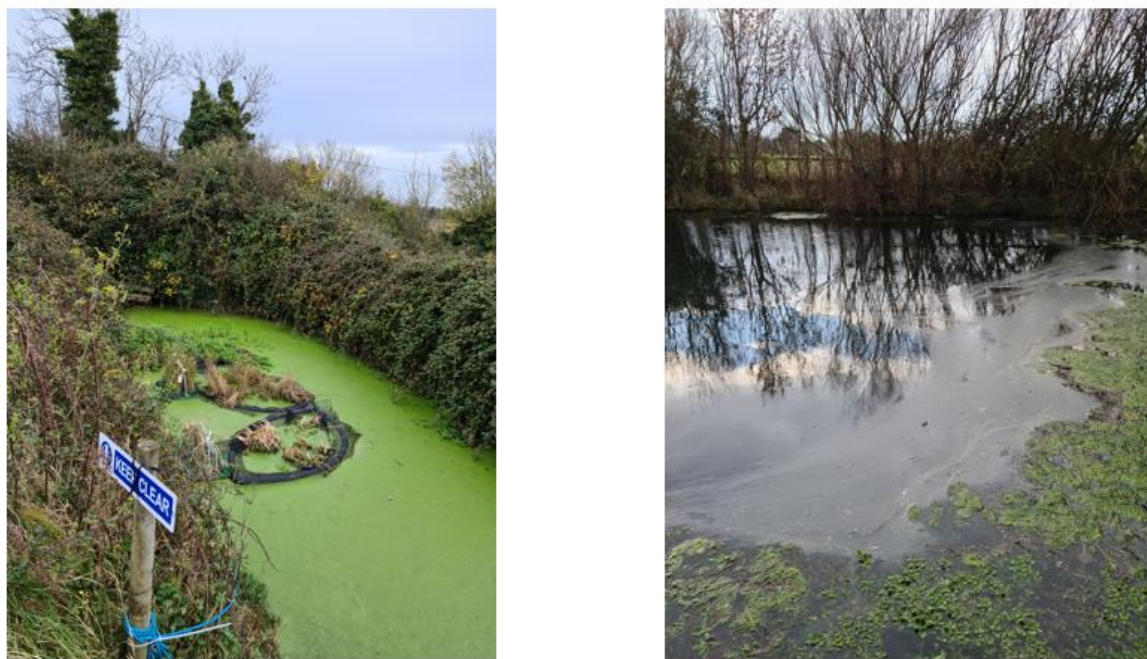


Figure 4.22 Algal blooms at Sites 1 (RHS) and 2 (LHS)

Site 1 has exceeded the permitted limit a total of three times during the study period, while Site 2 exceeded it nine times in total. Site 2 also shows concentrations 50 times the magnitude detected at Site 1. It could potentially be due to the stream which runs along the ridge of six other farms prior to reaching the pond, and therefore collecting run-off and/or leaching. This further supports the idea that geographical features such as the stream present at Site 2 potentially increases nutrient loading when influenced by anthropogenic activities (in this case agriculture). Due to the lack of variation in the data obtained (Figure 4.20), there was no seasonal variation analysis carried out for $\text{NH}_3\text{-N}$.

From a water quality perspective, Sites 1 and 2 can be classified as moderate and unhealthy, respectively (EPA, 2018). This classification is further corroborated when $\text{NH}_3\text{-N}$ concentrations are analysed in parallel with physico-chemical factors which

affect $\text{NH}_3\text{-N}$ concentrations in water, such as temperature and DO (Figure 4.23). Temperature has a potentially direct proportionality with $\text{NH}_3\text{-N}$ toxicity in water. Therefore, if $\text{NH}_3\text{-N}$ is present at high concentration, an increase in water temperature could increase its toxicity to aquatic flora and fauna.

Unlike temperature, DO could have an inversely proportional relationship with $\text{NH}_3\text{-N}$. As $\text{NH}_3\text{-N}$ is oxidized to $\text{NO}_3\text{-N}$ by the process of nitrification carried out by nitrifying bacteria, oxygen levels can decrease in the water column, which in turn can lead to the inhibition of nitrification (Quirós, 2003). This can potentially increase $\text{NO}_3\text{-N}$ concentration in water, while simultaneously reducing $\text{NH}_3\text{-N}$ concentrations (the relationship between $\text{NH}_3\text{-N}$ and $\text{NO}_3\text{-N}$ will be explored in further detail in Section 4.3.6).

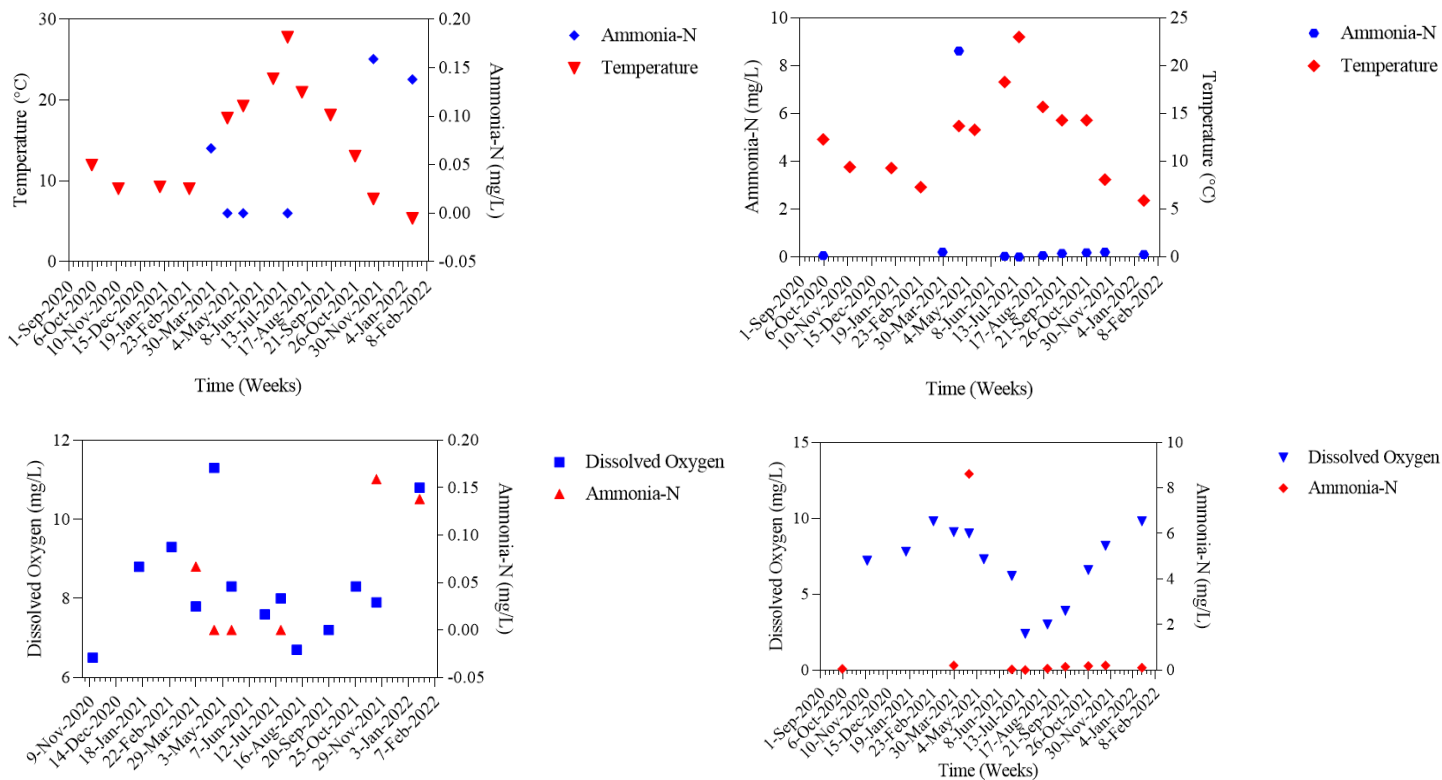


Figure 4.23 Relationships between $\text{NH}_3\text{-N}$ concentration and temperature at Sites 1 (top LHS) and 2 (top RHS); and $\text{NH}_3\text{-N}$ concentration and DO at Sites 1 (bottom LHS) and 2 (bottom RHS)

4.3.6 Background monitoring of nitrite and nitrate concentrations in water

Another major potential component of fertilizer used in agriculture is $\text{NO}_3\text{-N}$. Alike to $\text{NH}_3\text{-N}$, when $\text{NO}_3\text{-N}$ enters aquatic ecosystems, it is a eutrophying agent (especially when coupled with $\text{NH}_3\text{-N}$ and $\text{PO}_4\text{-P}$) and is considered as nutrient loading. $\text{NO}_3\text{-N}$ can also occur from the addition of $\text{NH}_3\text{-N}$ to the water column. As mentioned in the previous section, NH_3 and NO_3^- are linked through the nitrification/denitrification process in water. When nitrification occurs in water, $\text{NH}_3\text{-N}$ is converted to $\text{NO}_3\text{-N}$ through the formation of a transitional compound known as NO_2^- . These processes occur regardless of anthropogenic activity, however, nutrient loading can potentially

cause the cycles to be skewed towards either process, depending on which nutrient is more prevalent in the water column.

NO_2^- is highly unstable form of N in water (hence the demarcation of it being a transitional compound). In unpolluted aquatic system, the concentration therefore should not exceed 0.05 mg/L, as set forth by the EPA. In contrast, the EPA has set a limit of 4 mg/l N for NO_3^- (0.9 mg/l $\text{NO}_3\text{-N}$) for high quality waters; 4-8 mg/l N for NO_3^- (0.9-1.8 mg/l $\text{NO}_3\text{-N}$) for good quality water; 8-12 mg/l N for NO_3^- (1.8-2.6 mg/l $\text{NO}_3\text{-N}$) for moderate quality water; 12-25 mg/l N for NO_3^- (2.6-5.5 mg/l $\text{NO}_3\text{-N}$) for poor quality water; and >25 mg/l N for NO_3^- (>5.5 mg/l $\text{NO}_3\text{-N}$) for very poor quality water (EPA, 2019). The average concentrations were 0.652 ± 0.818 and 1.069 ± 0.859 mg/L $\text{NO}_3\text{-N}$, and 0.023 ± 0.039 and 0.211 ± 0.443 mg/L $\text{NO}_2\text{-N}$, for Sites 1 and 2 respectively (Figure 4.24 and 4.25).

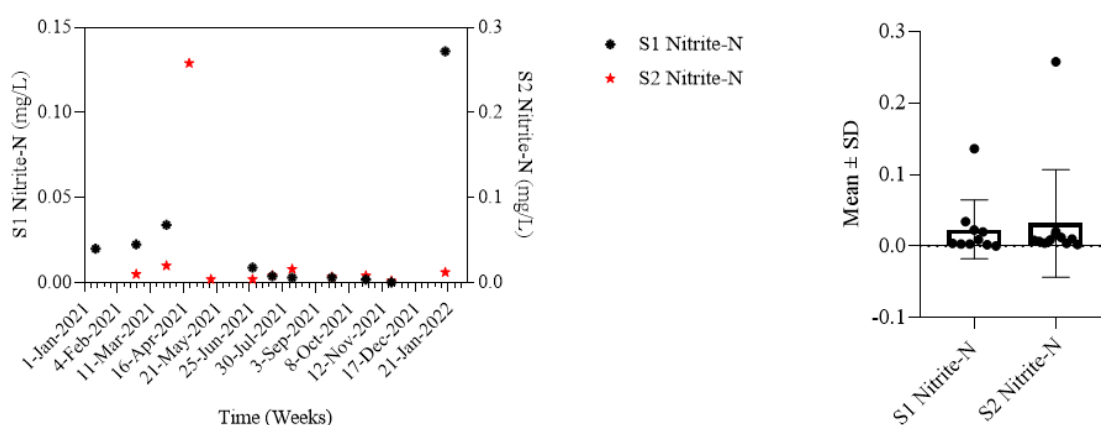


Figure 4.24 Concentration of $\text{NO}_2\text{-N}$ (mg/L) at Sites 1 and 2

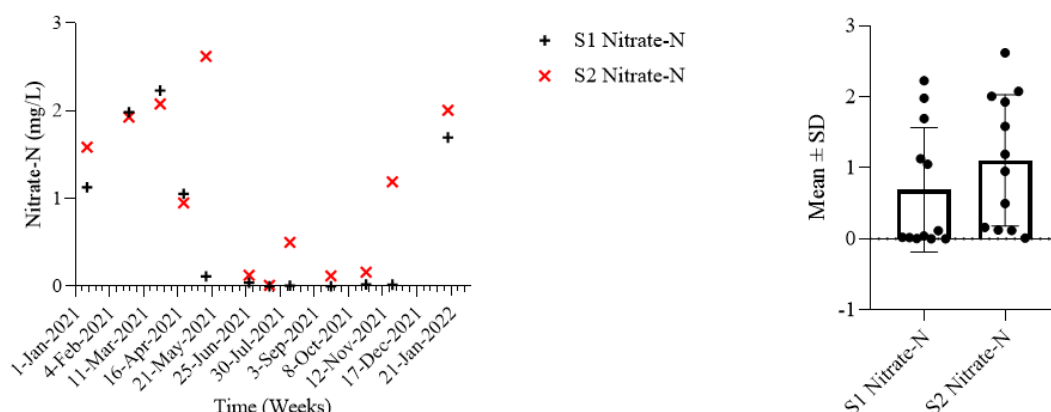


Figure 4.25 Concentration of NO₃-N (mg/L) at Sites 1 and 2

The NO₂-N levels, when comparing Sites 1 and 2, are highly dissimilar and are measurable on a different scale, with Site 2 showing double the concentration in certain cases compared to Site 1. In terms of water quality, it was assessed as moderate, as the exceedance of the 0.05 mg/L limit set forth by the EPA only seen twice during the study period. Likewise, NO₃-N levels remain moderate throughout the study period, not exceeding the moderate rating according to the EPA guidelines at both Sites 1 and 2.

Both sites under observation have similar levels of NO₃-N with major deviations occurring only twice during the study period, where Site 2 had higher concentrations. This can lead to the assumption that NO₃-N-based fertilizers are not used at either site, leaving only moderately elevated levels due to high levels of NH₃-N present in the water as a result of agricultural activities at both sites, as well as naturally available NO₃-N. To further explore the potential process of nitrification taking place at both sites, NO₃-N and NH₃-N levels were compared for both sites given by Figure 4.26.

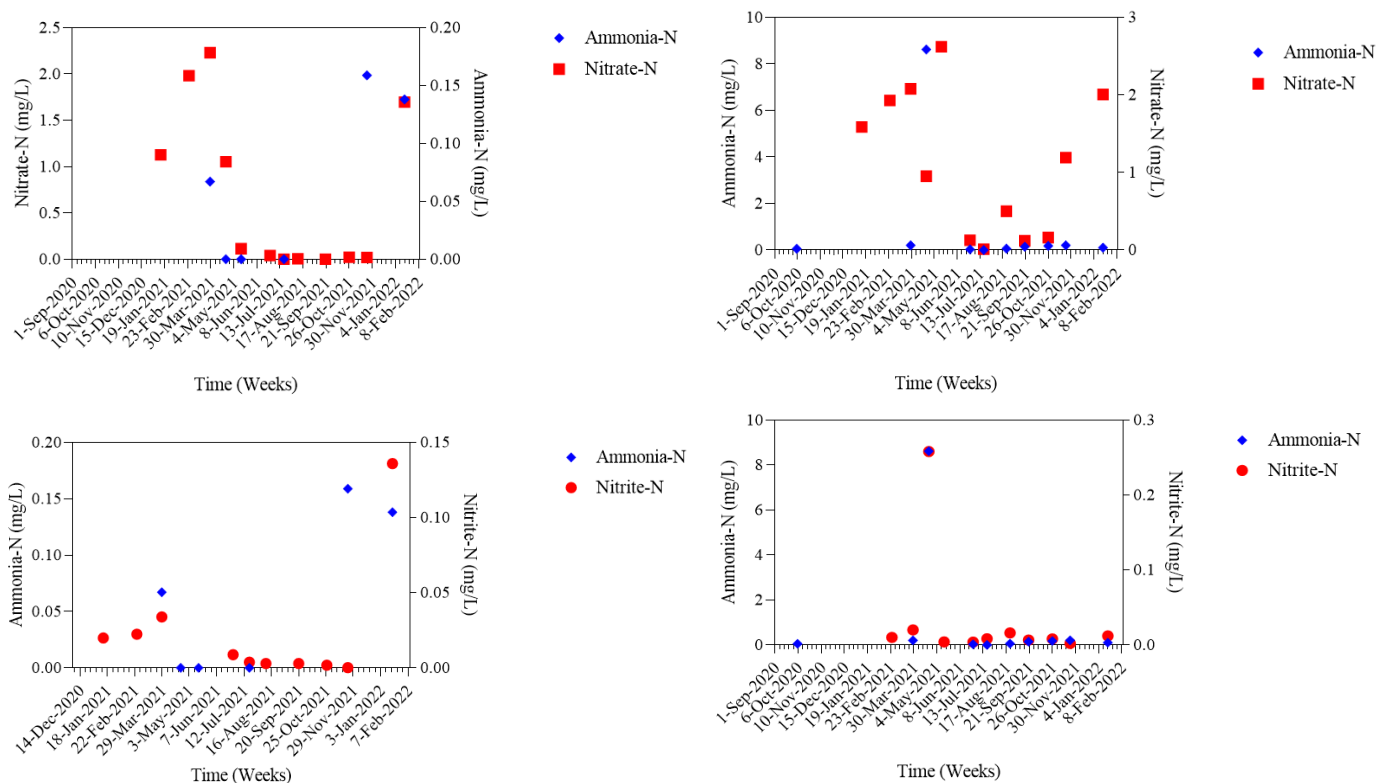


Figure 4.26 Relationships between the concentration of $\text{NO}_3\text{-N}$ (mg/L) and $\text{NH}_3\text{-N}$ at Sites 1 (top LHS) and 2 (top RHS); and the concentration of $\text{NO}_2\text{-N}$ (mg/L) and $\text{NH}_3\text{-N}$ at Sites 1 (bottom LHS) and 2 (bottom RHS)

There is a potentially inverse proportionality between $\text{NO}_3\text{-N}$ and $\text{NH}_3\text{-N}$ (Figure 4.26). When $\text{NH}_3\text{-N}$ concentrations were detected at elevated levels, $\text{NO}_3\text{-N}$ concentrations were reduced, and vice versa at both sites. The water samples were also analysed for the effects of $\text{NH}_3\text{-N}$ concentrations in relations to the levels of $\text{NO}_2\text{-N}$ detected. During the study period, $\text{NO}_2\text{-N}$ levels potentially increase and decrease along with the amount of $\text{NH}_3\text{-N}$ present in the water column at a given time. This indicates that $\text{NH}_3\text{-N}$ and $\text{NO}_2\text{-N}$ are closely linked, and $\text{NH}_3\text{-N}$ loading to both water systems results in heightened $\text{NO}_2\text{-N}$ levels. The data was also analysed for seasonal variation, using a Shapiro-Wilks normality test coupled with a Welch's ANOVA

analysis. The analysis showed no significant seasonal variation at either site at $p < 0.05$ level.

4.3.7 Background monitoring of ortho-phosphate concentrations in water

In order to gain full understanding of nutrient loading dynamics in an agricultural setting, an additional nutrient, which is not directly related to the N cycle but plays a role in nutrient loading dynamics in agricultural systems has been analysed for during the study period. $\text{PO}_4\text{-P}$ is a naturally occurring compound, much like $\text{NH}_3\text{-N}$, predominantly from living and decaying aquatic flora and fauna.

Anthropogenic additions of $\text{PO}_4\text{-P}$ from agricultural activities such as liming (the addition of materials such as burnt lime to rebalance the soil pH to ensure no acidification occurs) and the application of fertilizer ($\text{PO}_4\text{-P}$ forms a large component of organic fertilizers, however, can also be applied as a synthetic fertilizer). Additionally, $\text{PO}_4\text{-P}$, when coupled with compounds such as $\text{NH}_3\text{-N}$ and $\text{NO}_3\text{-N}$, is an integral eutrophying agent, contributing to algal blooms. On account of $\text{PO}_4\text{-P}$ being a eutrophying agent, the EPA has set a national limit of $<0.03 \text{ mg/L}$ $\text{PO}_4\text{-P}$ for water quality to be considered good and for an aquatic ecosystem to be considered healthy (EPA, 2017).

Site 1 had no detectable concentrations of $\text{PO}_4\text{-P}$ bar one occasion, where a concentration of $0.156 \pm 0.946 \text{ mg/L}$ $\text{PO}_4\text{-P}$ was obtained in October 2021. This singular occasion was could potentially be attributed to the liming of the soil during that period. No $\text{PO}_4\text{-P}$ was detected after October, and from historical records

available, the only other time PO₄-P was detected at this site was in October 2018, when liming was carried out on the soil.

In contrast, Site 2 continuously produced high levels of PO₄-P, with a continuous exceedance of the cited EPA limit (Figure 4.27). The average concentration of PO₄-P was 3.007 mg/L for the monitoring period. The continuous loading of PO₄-P indicated that the farms connected to the stream leading to the pond, used organic rather than synthetic fertilizer, potentially in the form of slurry and manure. This is collaborated by the peak observed in PO₄-P concentrations in the water column. The highest PO₄-P concentration observed between 2020-2022 was in the month of October, at which time synthetic fertilizer is already banned from use in County Dublin (Figure 3.4). However, organics fertilizers are still in use during this period.

In terms of water quality, Site 1 meets the EPA guidelines, however Site 2 fails to meet the limit set forth for healthy ecosystems and good water quality. The data was also analysed for seasonal variation, using a Shapiro-Wilks normality test coupled with a Welch's ANOVA analysis. The analysis showed no significant seasonal variation at $p < 0.05$ level at Site 2.

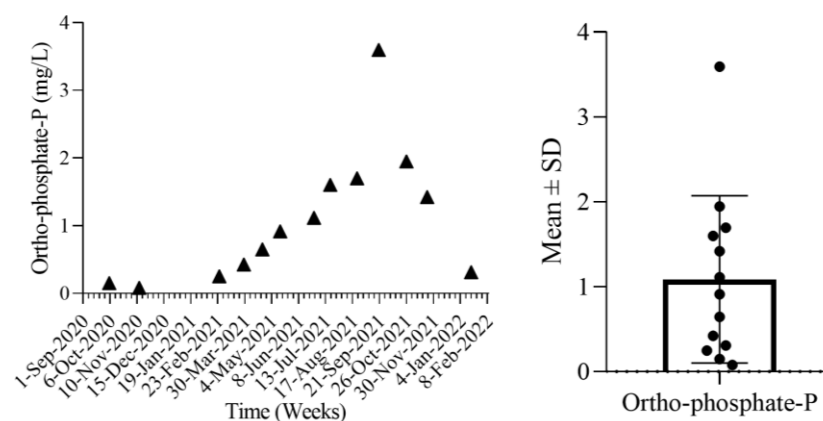


Figure 4.27 Concentration of PO₄-P (mg/L) at Site 2

4.4 Soil Analysis

4.4.1 Elemental analysis of soil by X-Ray Fluorescence

The elemental analysis of the soil was carried out using X-Ray Fluorescence (XRF). The analysis was carried out by Dr Jovana Orlić at the Faculty of Chemistry, University of Belgrade, Belgrade, Serbia (Figure 4.28, Table 4.4).

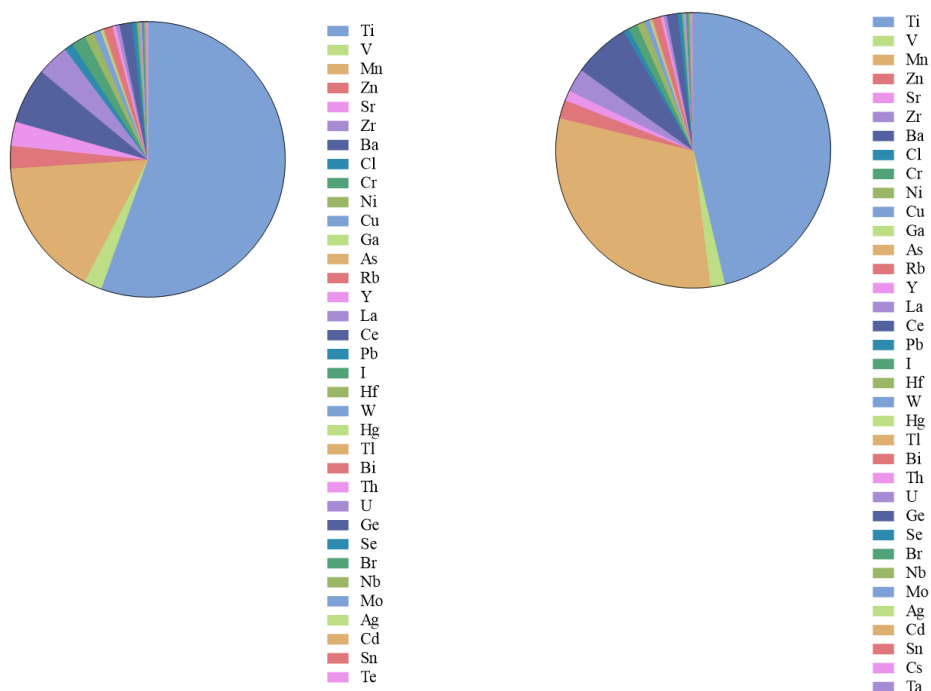


Figure 4.28 Elemental analysis of soils from Site 1 (LHS) and Site 2 (RHS)

Table 4.4 Elemental analysis of soil from Sites 1 and 2

Element	Concentration Site 1 (%)	Concentration Site 2 (%)
Na ₂ O	0.77	0.66
MgO	1.76	1.51
Al ₂ O ₂	9.04	10.66
SiO ₂	53.74	63.93
P ₄ O ₁₀	0.20	0.26
SO ₃	0.13	0.18
K ₂ O	1.35	1.47
CaO	5.50	1.53
Fe ₂ O ₃	3.21	4.08

Elemental analysis was performed in order to gain an elemental make-up of the soil at both Sites 1 and 2. The principal major elements present in the samples from both Sites 1 and 2 are silicone oxide (Al₂O₂) and silicone dioxide (SiO₂) (Table 4.4). The main minor elements detected in soil samples from both sites were titanium (Ti), vanadium (V), manganese (Mn), strontium (Sr), zirconium (Zr) and barium (Ba)

(Figure 4.28). These elements are naturally occurring in the Earth's crust and their presence in the soil are a result of weathering and erosion. There is a variation in the concentrations of the major elements detected when comparing the two sites, this can be a result of differences in the bedrock at each site. Variations in individual elements when comparing the samples from Sites 1 and 2 can also be attributed to variations in physiochemical (electrical conductivity, microbial populations, etc.) and mineralogical characteristics for each site respectively.

The total elemental composition of the soils (determined as % w/w) further elucidate the soil make-up (Table 4.5). The % moisture content of the soils was also carried out in conjunction with the elemental analysis, as moisture content can affect the type, concentration, and chemical structure of elements present (Table 4.5). The total composition of the soil based on elemental and moisture content analysis was determined to be 84.09% w/w and 95.59% w/w for Site 1 and Site 2 respectively.

Table 4.5 Composition of soil

Parameter	Site 1	Site 2
Total elemental composition	76.29% w/w	84.98% w/w
Moisture Content	7.89 % w/w	10.61 % w/w
Final composition	84.09% w/w	95.59 % w/w

4.4.2 Ion Chromatography analysis of soil

Soil samples were collected in triplicate in 2020 and analysed for major anions with a specific interest in NO_3^- , NO_2^- and phosphate (PO_4^{3-}). Other anions included sulphate (SO_4^{2-}), chloride (Cl^-), bromide (Br^-) and fluoride (F^-). While $\text{NH}_3\text{-N}$ forms the core of this study in all aspects of agricultural ecosystems (throughout the biosphere), $\text{NH}_3\text{-N}$ application (fertilizer) in these environments rarely leads to accumulations in the

soil. Instead, $\text{NH}_3\text{-N}$ applied to the soil is volatilised to the atmosphere, is taken up by flora and is readily converted to $\text{NO}_3\text{-N}$. Therefore, tracking $\text{NO}_3\text{-N}$ concentrations in the soil, as well as $\text{NO}_3\text{-N}$ changes due to leaching elucidates how the application of fertilizer affects and alters soil nutrients, nutrient retention, leaching rate (Table 4.6 and Figure 4.29).

Table 4.6 Composition of soil pre-treatment

Soil Sample	F^- ($\mu\text{g/g}$)	Cl^- ($\mu\text{g/g}$)	NO_2^- ($\mu\text{g/g}$)	SO_4^{2-} ($\mu\text{g/g}$)	Br^- ($\mu\text{g/g}$)	NO_3^- ($\mu\text{g/g}$)	PO_4^{3-} ($\mu\text{g/g}$)
Site 1 Sample 1	2.10	83.96	3.15	223.71	0.72	71.39	5.16
Site 1 Sample 2	1.33	189.41	5.10	245.35	0.04	98.84	9.82
Site 1 Sample 3	0.89	61.20	4.37	151.27	0.50	44.54	1.66
Site 2 Sample 1	2.32	53.17	3.47	129.78	0.40	50.34	2.28
Site 2 Sample 2	1.03	56.27	3.56	120.10	0.68	36.29	1.09
Site 2 Sample 3	5.41	80.92	6.97	191.98	0.04	46.39	1.93

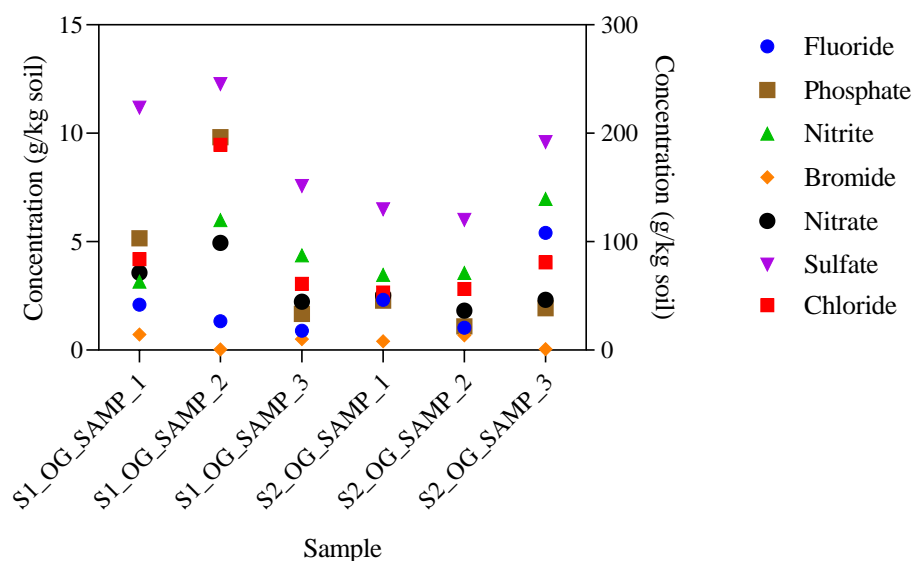


Figure 4.29 Ion analysis of soils from Site 1 (denoted as S1) and Site 2 (denoted S2) pre-treatment

4.4.3 Soil fertility analysis

Soil fertility plays a key role in arable agriculture, as it is a key factor in growing healthy crops. Soil fertility refers to the soil's ability to sustain and accommodate agricultural plant growth, bearing an optimum plant habitat for maximised and consistent plant yield and quality. This umbrella term refers to a myriad of aspects of the soil itself, from biological to chemical, therefore a focus was applied, in order to gain better understanding of soil fertility as a whole. In order to obtain an overall picture, rather than analysing every aspect of the soil itself, a respiration study was set-up to determine the general fertility and capacity of the soil.

Respiration is a fundamental process in the partitioning of energy in soil. Respiration consumes oxygen (O_2) and extricates carbon dioxide (CO_2), resulting in a loss of carbon (C) from the ecosystem (Dilly, 2003). Aerobic conditions allows for the

glycolysis of pyruvate, followed by oxidative decarboxylation, linking into the citric acid cycle associated with a respiratory chain. Under these reactions, when alternative electron acceptors (e.g.: NO_3^-) are minimally used, the respiratory quotient (RQ) for substrates such as glucose is 1. When these conditions are met, the degradation of substrates is understood to be ‘balanced’, meaning the number of moles of CO_2 consumed equals the moles of O_2 evolved. However, soils are complex matrices, with a wide spectrum of substrates present, which are affected by other processes such as immobilisation, as well as environmental and nutritional factors which in turn affect oxidation processes (Stevenson & Cole, 1999). Thus, soil management practices play a role in RQ, with an ability to modify and ‘unbalance’ it.

The analysis was carried out by Dr Vladimir Beškoski at the Faculty of Chemistry, University of Belgrade, Belgrade, Serbia. The analysis was performed using a Micro-Oxymax[®] Respirometer (Figure 4.30).



Figure 4.30 Micro-Oxymax[®] Respirometer

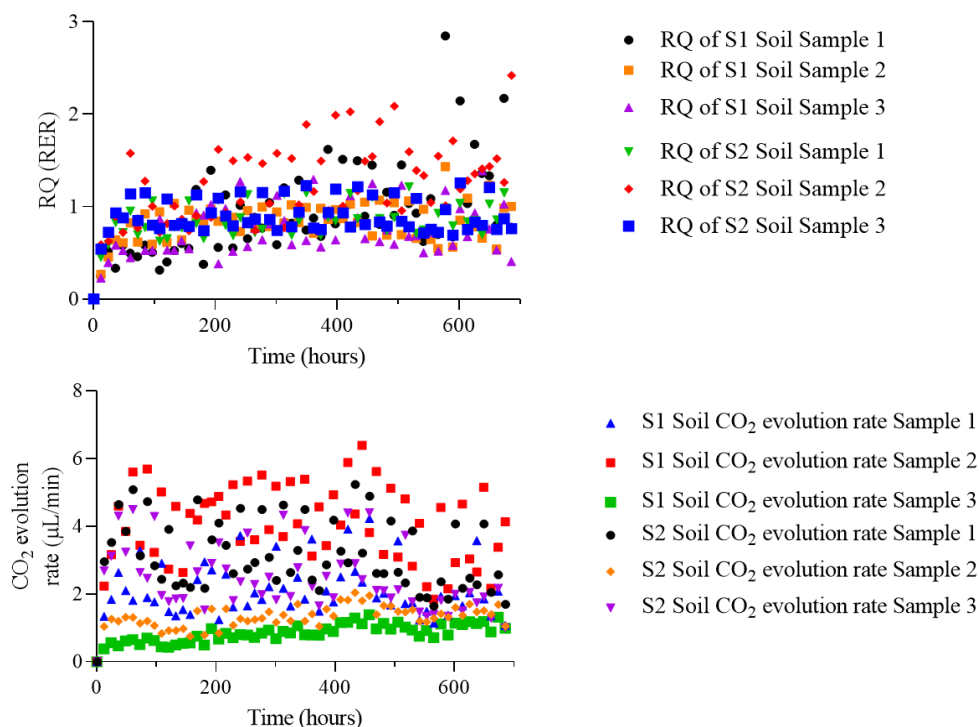


Figure 4.31 RQ (top) and CO₂ evolution rate (bottom) for soils analysed in triplicate from both Sites 1 and 2

The average RQ for Sites 1 and 2 were 0.834 and 0.987 respectively (Figure 4.31). This indicates that the amino acids, refractory compounds or aliphatic organic compounds with relatively low levels of O were mineralised primarily (Chaabane, Josens, & Loreau, 1999). At both sites, RQ values do not equal 1, showing an imbalance, even though O₂ uptake and CO₂ evolution rates were overall highly correlated.

The respiratory analysis was accompanied by a microbiological analysis to determine the overall composition and population of microbial communities (Figure 4.32). Coupled with the respiratory analysis, this provides insight into the health and fertility

of the soil. As expected, chemoorganoheterotrophs are the most abundant population. These include bacteria, actinomycetes and protozoa (Bhattarai, 2015). These microorganisms generally are more adaptable to soil disturbance, such as tilling, and therefore are abundant in agricultural soils. The results are shown in Figure 4.32.

Sample	TC*	TAC*	YM*
Site 1	4,88x10 ⁶	3,43x10 ⁵	2,50x10 ⁴
Site 2	3,50x10 ⁵	1,73x10 ⁵	3,70x10 ³

* unit (cfu**/mL)

** colony forming units

Nutrient agar for total chemoorganoheterotrophs (TC):

Nutrient agar with 0.5 % glucose for total anaerobic chemoorganoheterotrophs (TAC):

Malt agar for yeast and molds (YM).

Figure 4.32 Microbiological analysis of composite soils from Sites 1 and 2

4.4.4 Soil leaching study

As introduced in Section 3.5.4, a soil leaching study was carried out as part of the project, to gain a more holistic understanding of N dynamics in agricultural ecosystems. Precipitation affects soil water dynamics, which have the ability to regulate N cycling in terrestrial ecosystems through physical transport and soil microbial activity responsible for key activities such as nitrification and denitrification (Aranibar et al., 2004). General circulation models currently in use forecast higher frequencies of extreme precipitation events, longer dry intervals between precipitation periods and lower occurrences of rainfall days (Easterling et al., 2000). Therefore, incorporating a study based on these factors to understand and evaluate how

independent and interactive effects of precipitation intensity and amount affect soil leaching and elemental composition facilitates for a more complete picture of ecosystem dynamics.

4.4.4.1 Soil physico-chemical response

The soil leachate was analysed for various physico-chemical factors in order to evaluate the effects of the simulated conditions, namely the pH, EC, and volume of leachate obtained, (Figure 4.33). The results obtained were also analyzed to determine if the variation observed due to precipitation and drying scenarios had a significant effect using ANOVA.

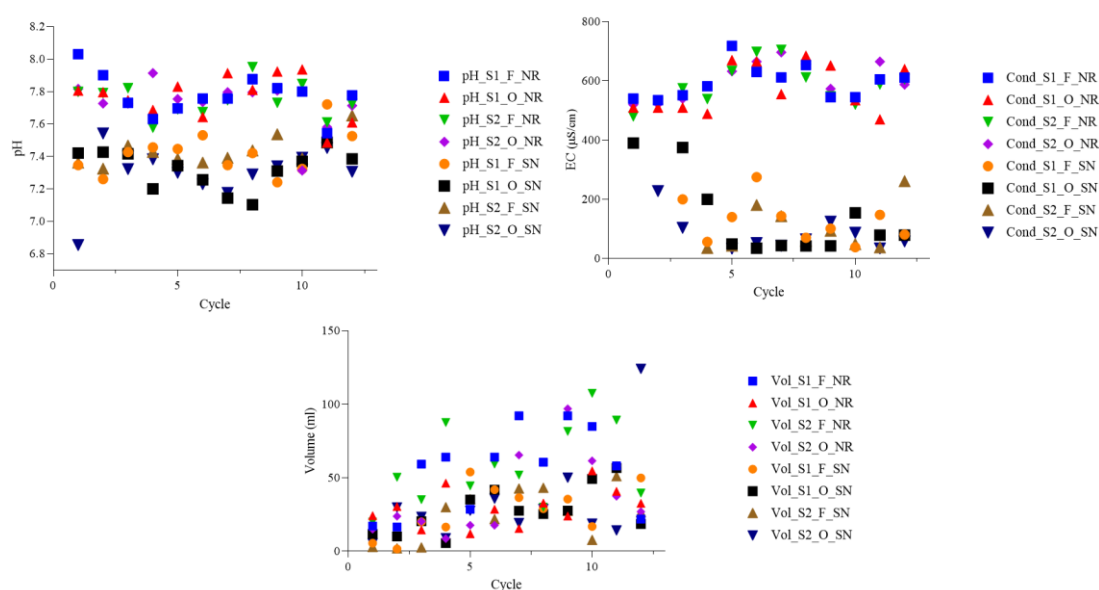


Figure 4.33 Changes in soil leachate pH (top LHS), EC (top RHS) and volume (bottom). S1 and 2 refer to Sites 1 and 2 respectively; ‘F’, ‘A’ and ‘O’ refer to freeze-, air-, and over-drying; and ‘NR’ and ‘SN’ refer to ‘normal rain’ and ‘snow’ respectively.

Variation in pH and EC were influenced by the drying scenario as well as precipitation being applied to the soils, with a significant difference between natural and synthetic precipitation simulations. Oven-dried soils exhibit a larger variability than freeze-thawed soils. This may be due to dissolved nutrients being retained during freezing as the water retained by the soil is frozen and therefore ‘locked’ into the soil; while during oven-drying, a fraction of soil moisture evaporates, removing various ions in this process.

Due to the nature of the simulations, EC was not taken at a standard temperature of 25 °C. Thus, to allow for a standardized measurement, the variability of EC as a function of temperature was analysed (Figure 4.34).

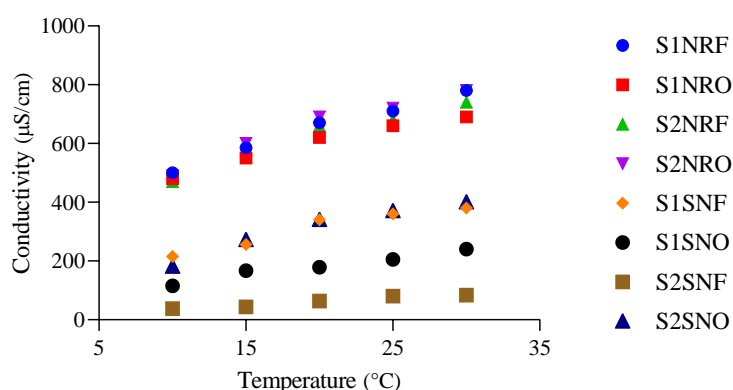


Figure 4.34 Changes leachate EC as a function of temperature. S1 and 2 refer to Sites 1 and 2 respectively; ‘F’, ‘A’ and ‘O’ refer to freeze-, air-, and over-drying; and ‘NR’ and ‘SN’ refer to ‘normal rain’ and ‘snow’ respectively.

During the experiments, the volume of leachate collected from each soil canister was also monitored (Figure 4.33). As expected, soils freeze-thaw produced more leachate

than soils under oven- and air-drying, however, there was no overall significant difference between natural and synthetic precipitation simulations for the volume of leachate obtained. Soils which were under freeze-thaw treatment retained a lot more water, which resulted in samples becoming fully saturated after cycle 2, all the way until the end of the simulations, independent of precipitation type applied.

4.4.4.2 Ionic composition of soil leachate

The soil leachate was analyzed for fluxes of seven major anions, namely fluoride (F^-), chloride (Cl^-), NO_3^- , NO_2^- , phosphate (PO_4^{3-}), sulfate (SO_4^{2-}) and bromide (Br^-).

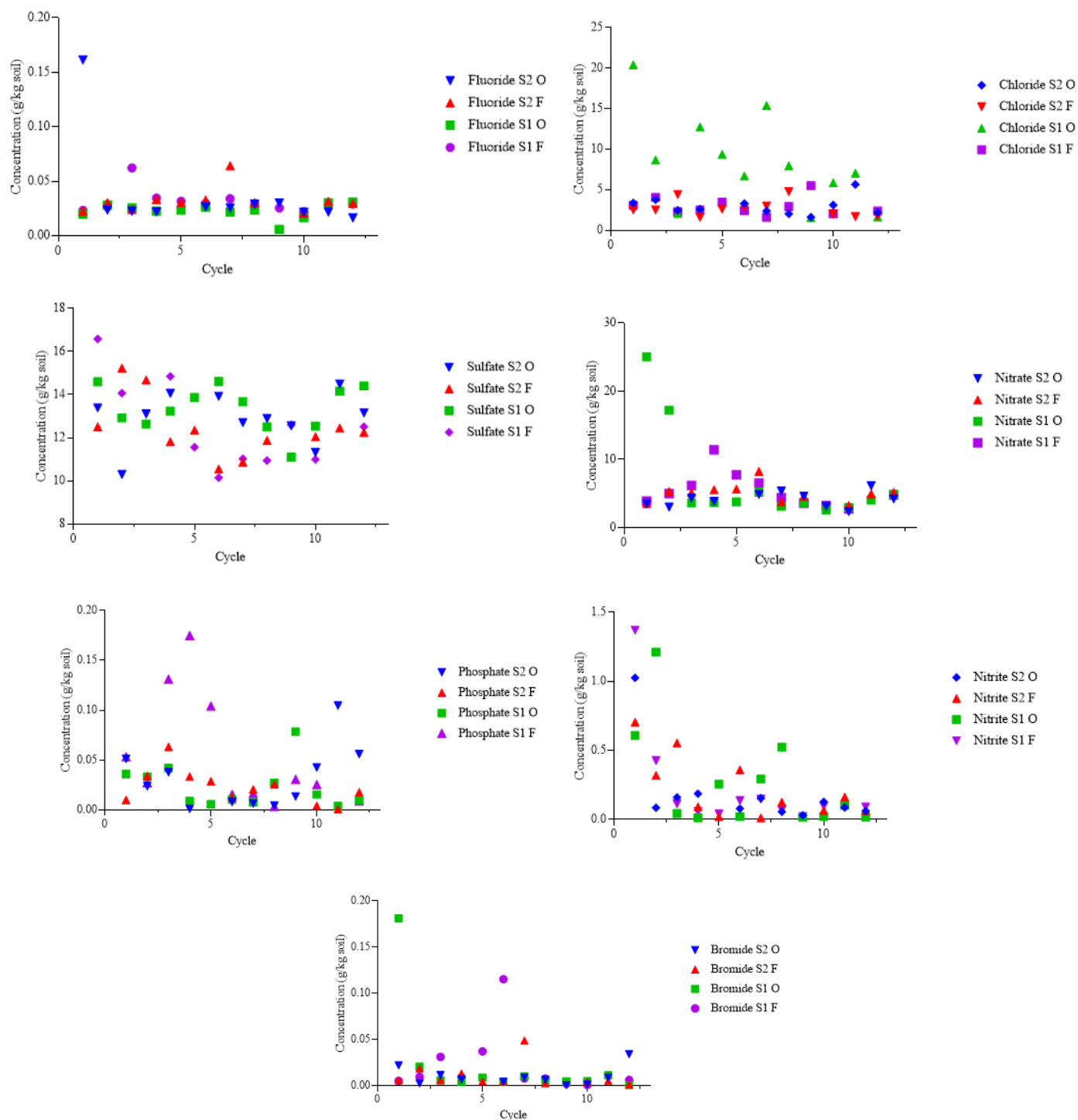


Figure 4.35 Ionic fluxes in soil leachate under synthetic precipitation simulation. S1 and 2 refer to Sites 1 and 2; and ‘F’ and ‘O’ refer to freeze- and over-drying respectively.

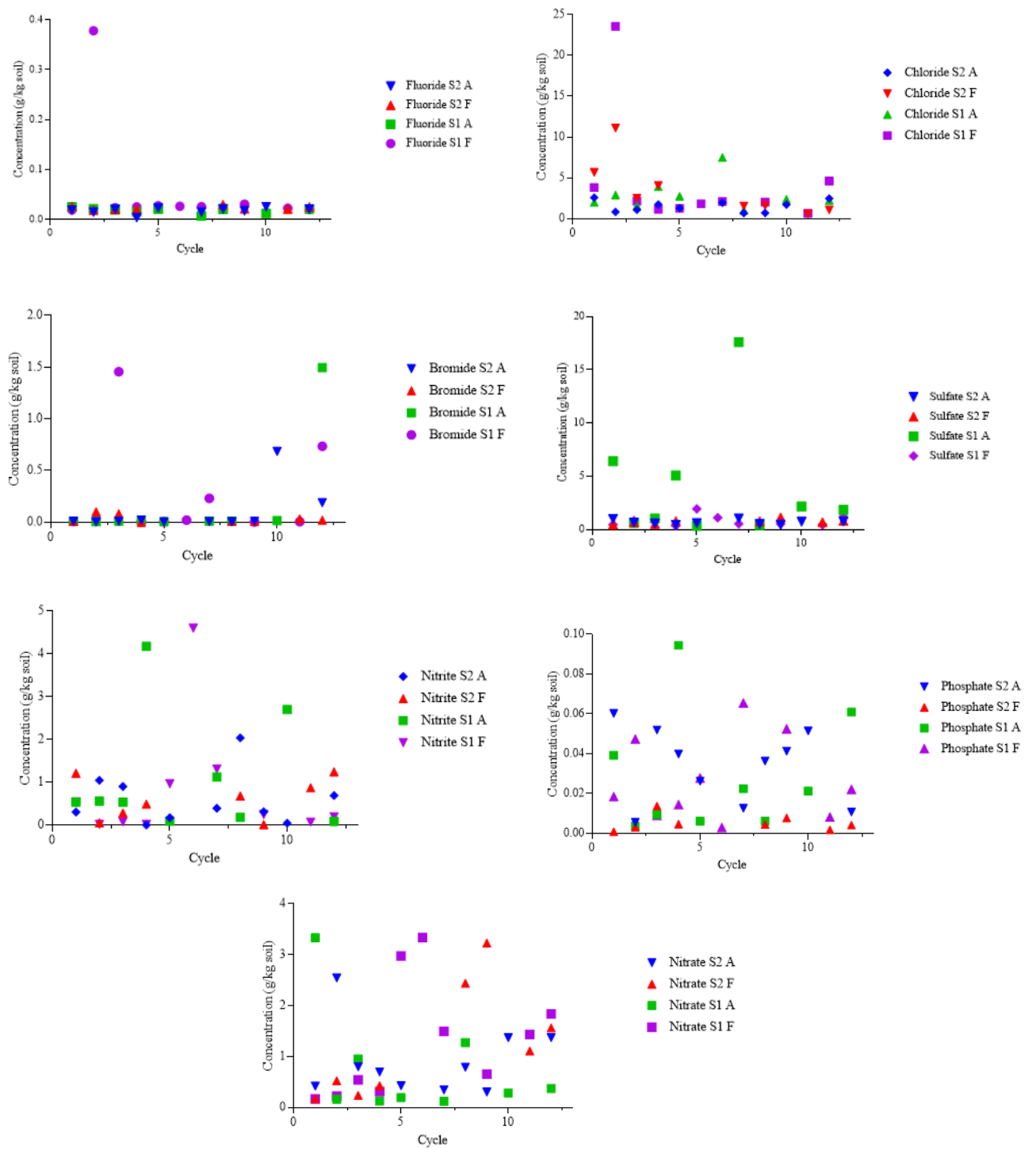


Figure 4.36 Ionic fluxes in soil leachate under natural precipitation simulation.

S1 and 2 refer to Sites 1 and 2; and ‘F’ and ‘A’ refer to freeze- and air-drying respectively.

4.4.4.3 Trace elemental composition of soil leachate

Trace elemental flux analysis of the soil leachate was performed using ICP-MS. The analysis was performed by Dr. Svetlana Djogo-Mračević at the Faculty of Pharmacy, University of Belgrade. The main analytes detected were aluminum (Al), calcium (Ca), magnesium (Mg), sodium (Na), potassium (K), manganese (Mn), iron (Fe), and zinc (Zn). It must be noted that leachate analysis was not possible for every single cycle of the simulations, especially for samples under oven- and air-drying scenarios, as the volume of leachate obtained would not facilitate both IC and ICP-MS analysis.

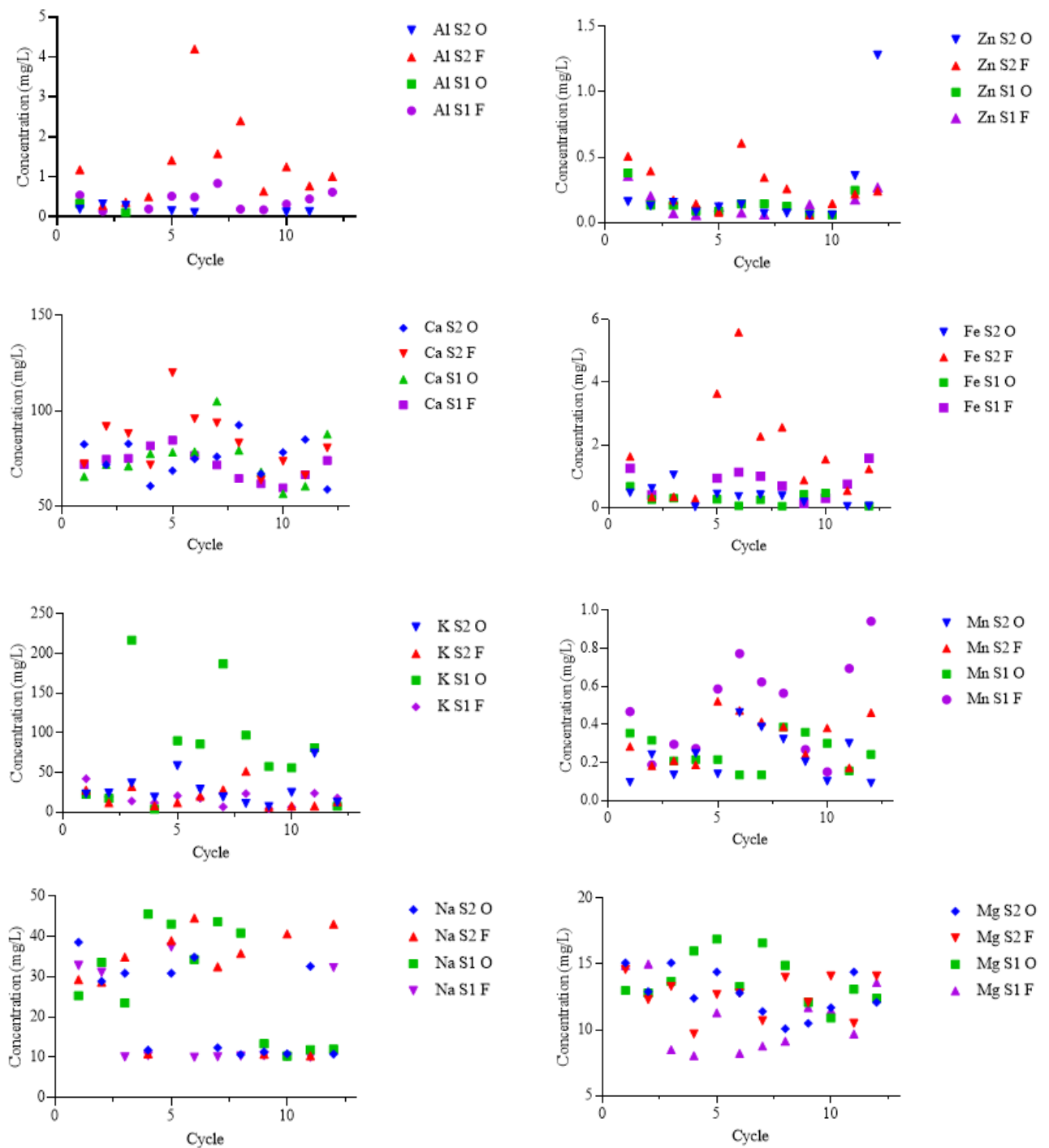


Figure 4.37 Trace element fluxes in soil leachate under synthetic precipitation simulation. S1 and 2 refer to Sites 1 and 2; and ‘F’ and ‘O’ refer to freeze- and over-drying respectively.

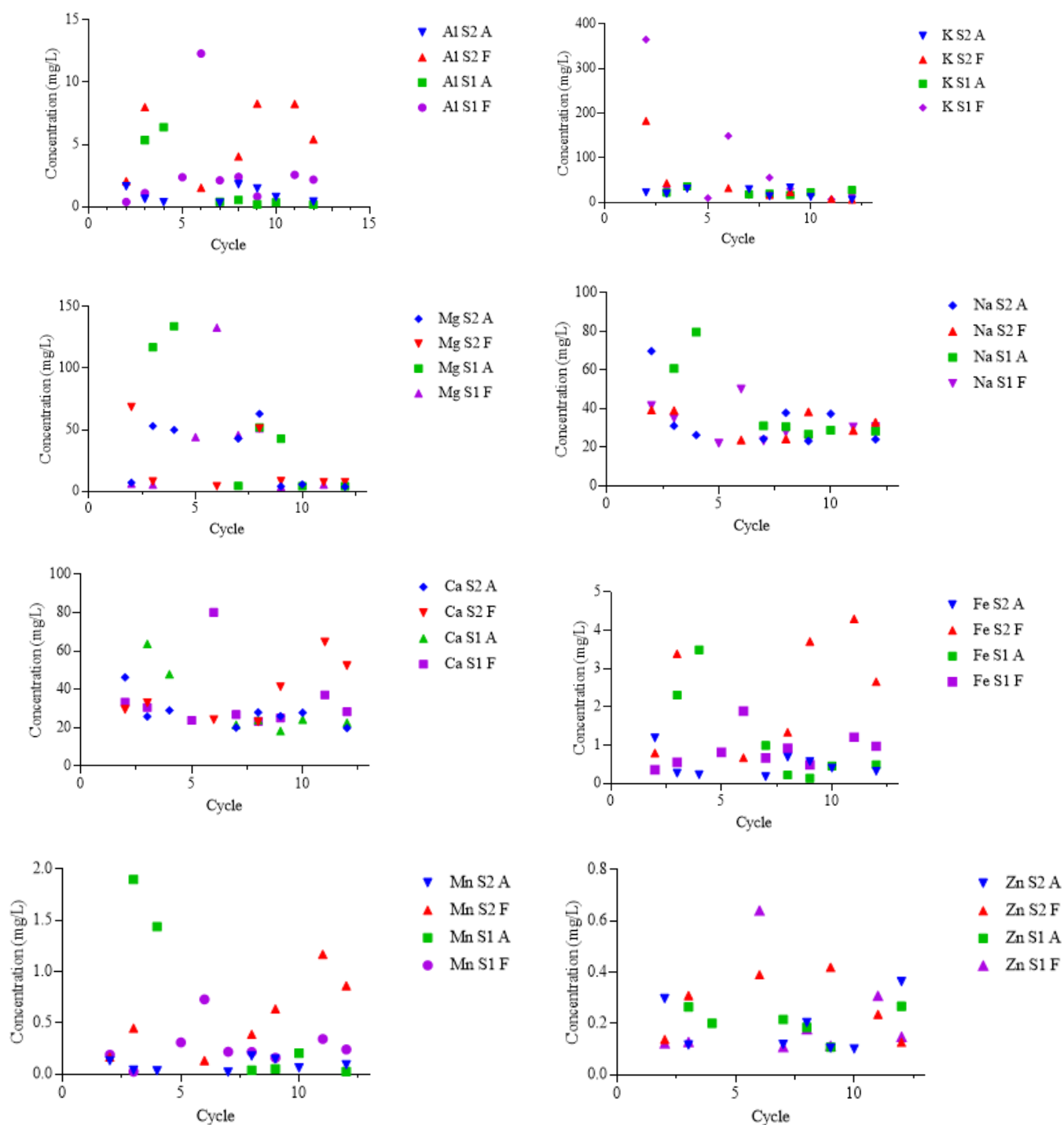


Figure 4.38 Trace element fluxes in soil leachate under natural precipitation simulation. S1 and 2 refer to Sites 1 and 2; and ‘F’ and ‘A’ refer to freeze- and air-drying respectively.

4.5 Micro-meteorological monitoring

Meteorological conditions affect pollutants being released into the atmosphere, such as the state of the pollutant, rate of release and temporal variations in pollutant concentration. Thus, monitoring local micrometeorological conditions allows for more accurate and precise measurement, as well as improving the ideological forecasts of NH_3 and PM events when given a set of conditions. For example, exchange of NH_3 between soil/water and the air is affected by wind speed (Bouwman et al., 2002a). It also controls how far PM will be dispersed in a region. At low wind speeds, trans-boundary pollution is at a minimal risk, however when wind speeds are high, PM may be carried far from its source of origin. Wind direction also affects as to how far and along which trajectories PM may travel. It also controls the amount of pollutant that is transported by the wind (Wang & Ogawa, 2015). The wind speeds and wind direction for the monitoring period were measured at Site 1 using a MetOne weather monitoring station (Figure 4.39). The dominant wind direction was West-South-West, and the most frequent wind class was $0.5\text{-}2.1 \text{ ms}^{-1}$.

Air temperature was monitored for the sampling period using HOBOware continuous temperature probes. The probes were placed at weather monitoring stations established on site. The state of PM is dependent on relative humidity (RH) and air temperature. When PM is in the aerosol phase, it is highly affected by temperature. Lower temperatures cause the system to deviate towards the aerosol phase. Comparative study of the air temperature data collected by independent temperature probes and rain gauges at each site show high correlation between sites. RH was monitored using the MetOne weather station.

Maximum AT measured throughout the monitoring period was 33.43°C and 31.37°C measured at Sites 1 and 2 respectively in July 2019. Minimum AT measured during

the monitoring period was -7.27°C and -7.01°C for Sites 1 and 2 respectively in January 2019 (Figure 4.40, Table 4.6). RH was measured for the year of 2021 at Site 1, with highest and lowest measured values in August 2021 at 96.7 % and April 2021 at 34.8% respectively (Figure 4.40). The annual average RH was measured as 83.1 %.

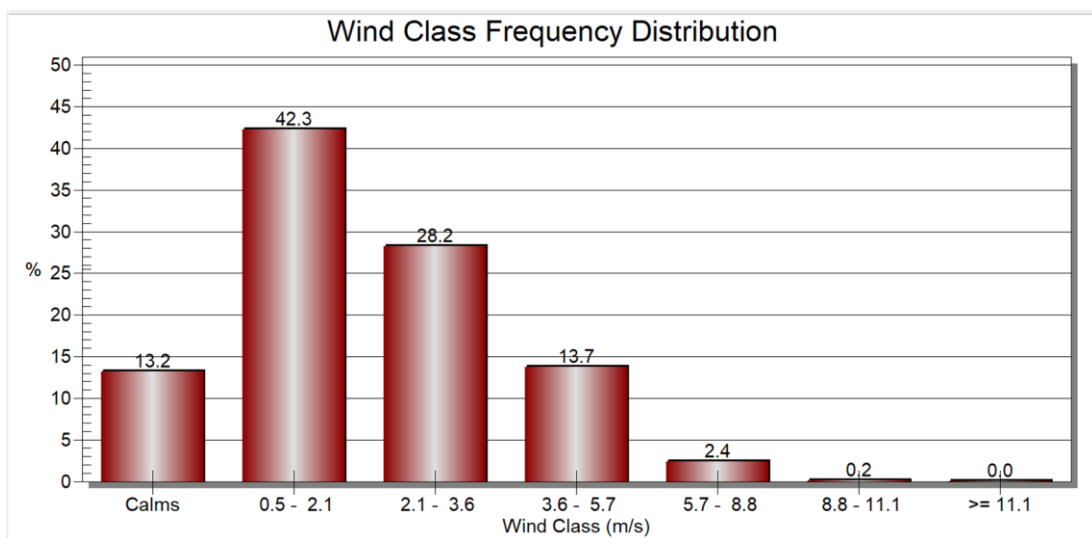
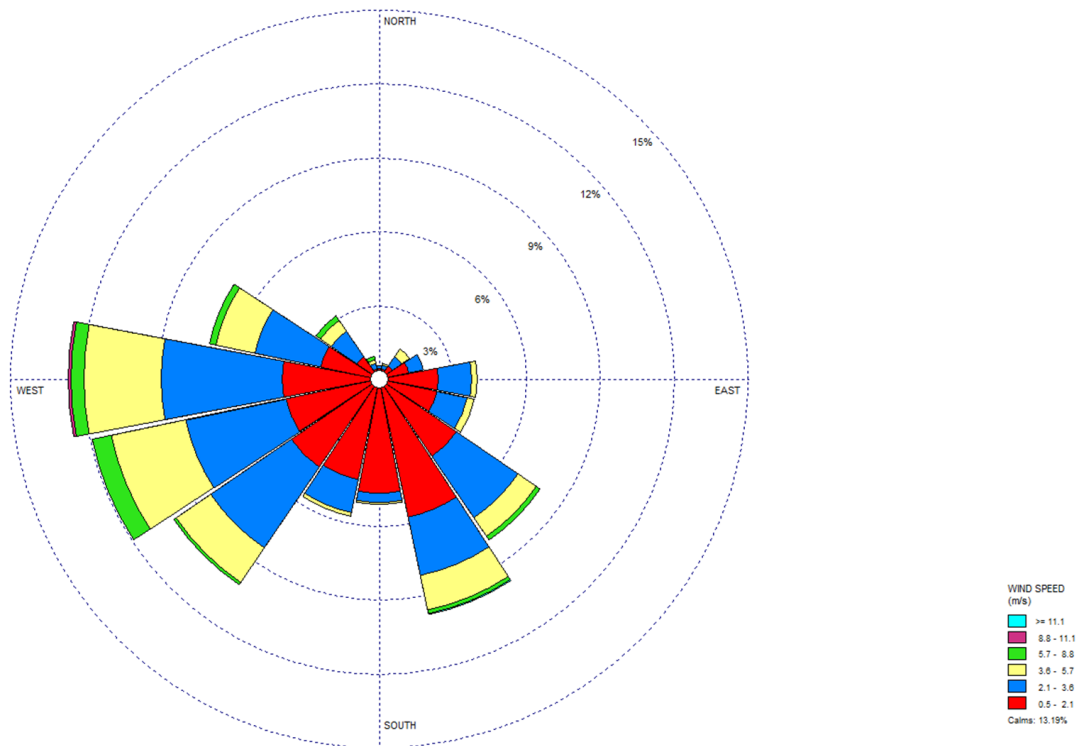


Figure 4.39 Wind rose for Site 1 wind speeds and wind class frequency distributions measured during the monitoring period. Radial bars represent percentages of wind measurements from each directions, each subdivided into six speed categories: $0.5\text{--}2.1\text{ ms}^{-1}$, $2.1\text{--}3.6\text{ ms}^{-1}$, $3.6\text{--}5.7\text{ ms}^{-1}$, $5.7\text{--}8.8\text{ ms}^{-1}$, $8.8\text{--}11.1\text{ ms}^{-1}$, and $>11.1\text{ ms}^{-1}$.

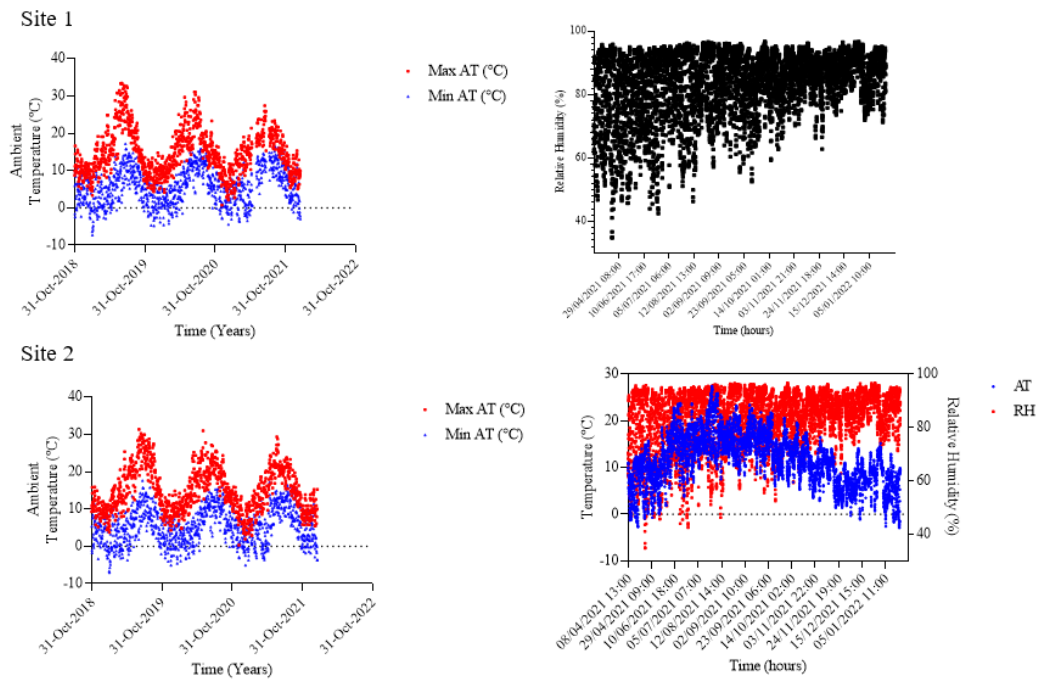


Figure 4.40 AT (LHS) measured at Sites 1 and 2 and RH (RHS top) and a comparison of RH and AT (RHS bottom) during the monitoring period

Table 4.7 Annual average AT measured

Year	Site 1 (°C)	Site 2 (°C)
2019	10.02	10.02
2020	10.21	10.21
2021	10.52	10.52

Precipitation was monitored continuously during the project using a HOBOWare RG3 rain gauge at each site. The rain gauges were installed as part of the on-site weather stations. The rain gauge works with a tipping bucket mechanism. Each tip corresponds to 0.2 mm of rain. The maximum precipitation measured during the monitoring period

was 32.0 and 22.2 mm for Sites 1 and 2 respectively. The minimum precipitation measured was 0.4 and 0.2 for Sites 1 and 2 respectively (Figure 4.41).

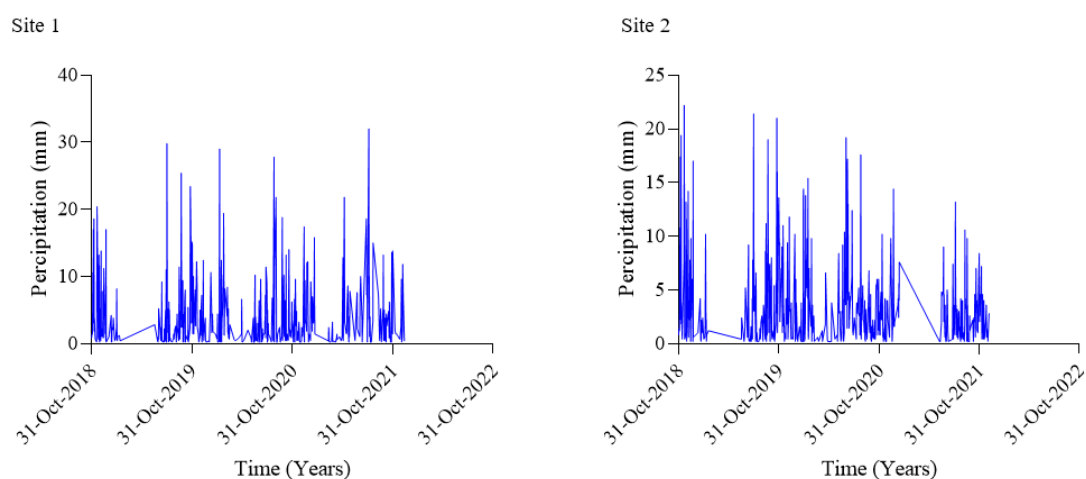


Figure 4.41 Precipitation measured at Sites 1 and 2 during the monitoring period

Table 4.8 Annual average precipitation measured

Year	Site 1 (mm)	Site 2 (mm)
2019	3.827	3.696
2020	3.771	3.332
2021	4.312	2.779

As mentioned in Section 3.4, continuous monitoring of the water and soil temperature was also carried out using temperature probes anchored in the water and soil at both sites. Seasonal increases and decreases of AT cause similar changes in the temperature of water and soil, especially surface-surface interaction points. Increased water temperature outside the regular range of seasonal variations can have damaging effects on water quality, with lower levels of dissolved oxygen, increases in invasive species and pathogens, increasing concentration of NH_3 due to its chemical response to

warmer temperatures, and increasing algal blooms amongst others. Similarly in soils, as the leaching study has demonstrated in Section 4.4, leaching and soil chemical balance of nutrients and trace elements is also affected. Therefore monitoring of seasonal trends is vital in order to establish when unprecedented warm periods occur, resulting in the deterioration of both water and quality.

The annual averages obtained for the soil and water temperature monitoring are given in Table 4.8. The maximum temperatures measured for water and soil at Site 1 were 22.91 °C and 31.27 °C, and the minimum were 2.84 °C and 0.45 °C respectively. At Site 2, the maximum temperature observed for water and soil were 17.48 °C and 35.97 °C, and the minimum were 2.20 °C and -0.10 °C respectively (Figure 4.42).

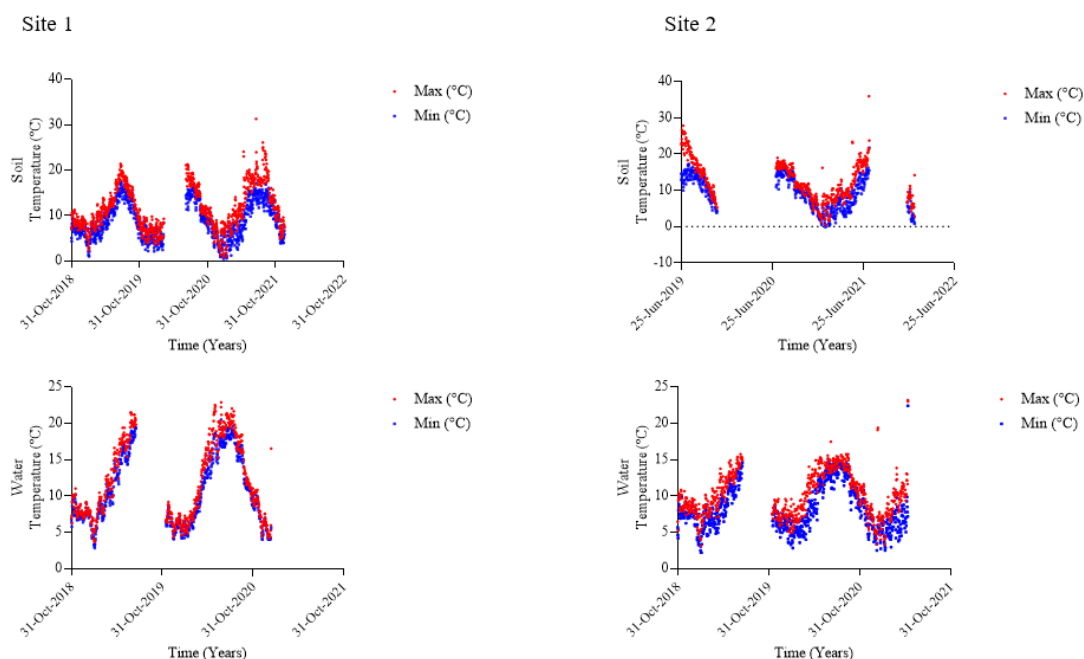


Figure 4.42 Water and soil temperature measured at Sites 1 (LHS) and 2 (RHS)

Table 4.9 Annual average soil and water temperature measured

Year	Site 1		Site 2	
	Soil temperature (°C)	Water temperature (°C)	Soil temperature (°C)	Water temperature (°C)
2019	10.19	10.91	13.69	8.81
2020	9.84	12.16	11.37	10.09
2021	11.19	-	10.35	-

4.6 Discussion of Results

The results presented in this chapter demonstrated NH₃ dynamics and consequent PM formation in an arable agricultural setting. The average values for atmospheric NH₃ over the monitoring period for individual sites ranged from 0.52 µg/m³ at Site 3 to 1.70 µg/m³ at Site 2, with an average concentration of 1.49 µg/m³ for the two active sites between November 2020 and January 2022. The maximum concentration measured 5.04 µg/m³, was recorded at Site 2 during the period of February-March 2021. This is in approximate agreement with the previous two sampling campaigns carried out in Ireland, where the average concentrations detected were 1.45 µg/m³ during the Ammonia1 study (Kluizenaar & Farrell, 2000) and 1.72 µg/m³ during the Ammonia2 study (Doyle et al., 2017). The main emission source for atmospheric NH₃ was identified as agricultural practices, such as application of fertilizer, with minor contributions attributed to emissions from transport.

Atmospheric NH₃ emissions are known to contributed to secondary aerosol NH₄⁺ formation, therefore monitoring and analysis of NH₃ components within atmospheric aerosol NH₄⁺ was also carried out during the monitoring period. The average

atmospheric aerosol concentration was $0.27 \mu\text{g}/\text{m}^3$ during the monitoring period, with the particle size predominantly in the $2.5\text{-}10 \mu\text{m}$ range. The highest PPD filter collected during the monitoring period was collected during winter with 1.351 particle/mm, while the lowest PPD was obtained during summer with 0.587 particles/mm. PPD therefore was approximately twice as high for samples collected during winter, as opposed to those collected during the summer season for these filters. This could be indicative of seasonal weather effects (Figure 4.5). During winter, cold air masses move slower than those during the summer, due to an increased density (Meng et al., 2019; Nawrot et al., 2007). This enables PM to remain static in a given location for longer periods. Another potential cause for this is due to the lack of cover crop during winter giving rise to increased erosion of soil.

Both atmospheric NH_3 and aerosol NH_4^+ were cross analysed with the localized environmental data collected during the monitoring period to determine if there are any meteorological factors which have the ability affect emissions. As discussed earlier (Section 4.2.2.2 and 4.2.2.3), atmospheric NH_3 concentrations show a proportional relationship with air and soil temperature (Figure 4.6 A), and an inversely proportional relationship with precipitation (Figure 4.6 B). Aerosol NH_4^+ and atmospheric NH_3 concentrations increase when air temperature remains stable, and concentrations decrease when temperatures increases. This indicates that air temperature instability can potentially result in reduced atmospheric NH_4^+ aerosol concentrations. One possible explanation for this is the relationship between RH and air temperature being inversely proportional (when air temperature increases, RH decreases).

Both atmospheric NH_3 and aerosol NH_4^+ concentrations decrease when wet deposition (precipitation) increases (from August 2021 until January 2022, Figure 4.6 B). During

the monitoring period windspeed and RH were also measured. Windspeed had an inversely proportional relationship with both atmospheric NH_3 and aerosol NH_4^+ concentrations (Figure 4.6 C). This is potentially due to increased off-site transport effects of both atmospheric NH_3 and aerosol NH_4^+ resulting in a decrease in their respective concentrations at site level. Increasing RH possibly results in increases in aerosol NH_4^+ concentration, indicating a direct link between aerosol concentrations and RH (Figure 4.6 D). Generally, PM mass concentrations and numbers increase significantly for RH values of 75% (Jayaratne et al., 2018). Peaks in concentrations of atmospheric aerosol NH_4^+ measured are concurrent with increases in RH and high atmospheric concentrations (compared to baseline) of gaseous NH_3 at Site 1.

The biggest influence, however, remains agricultural activities and management practices on both sites. Spreading of fertilizer and the timing of spreading, the type of fertilizer used, and the types of crop grown all affect atmospheric NH_3 emissions. One example of this is the difference in atmospheric concentrations measured at the active sites. While both sites use a synthetic inorganic fertilizer, only cereal crops (barley and wheat, as detailed in Section 3.X) are grown at Site 2, while at Site 1 cereal crops and legume (beans) are grown in rotation. Legumes are plants capable of forming symbiotic relationships with nitrogen-fixing bacteria, resulting in a symbiotic relationship between the plant and the bacteria, within which the atmospheric N converted to bioavailable NH_3 is available for the plant to use (Section 2.3) (Shober & Taylor, 2015). Due to this self-sustaining system, less fertilizer is applied, thus reducing emissions, and potentially resulting in the differences seen between the two sites.

Another factor which may affect emissions and therefore potentially influence the atmospheric concentrations of NH_3 is the timing of the fertilizer application. As the

two sites are under different management practices, the timing of fertilizer application are not exactly the same. This is also indicated by the data collected during the study. As mentioned above (Section 4.2.2), during the monitoring period two instances were identified where concentrations rose (“peak” concentrations). The highest was recorded during spring, after the ban on the spreading of fertilizer was lifted for County Fingal (Figure 1.1), followed by another “peak” where concentration levels increased in autumn, just before the ban came back into effect for the county. The second increase in the levels of atmospheric NH_3 detected during the monitoring period is lower than the one observed in spring, however, one potential reason for this is due to the changing of the season bringing increased precipitation levels. This could affect the emission levels measured due to deposition effects. It also increases NH_3 transport throughout the biosphere, by leaching from the soil and run-off into the water sources (ponds) on site, reducing the amount of NH_3 available for volatilization to the atmosphere. Therefore, the timing of fertilizer application could have potential effects on emissions of NH_3 to the atmosphere, and thus, the formation of aerosol NH_4^+ (due to availability of precursor gas).

As mentioned above, NH_3 is not only emitted to the atmosphere, but also is transported throughout the biosphere, affecting various aspects of the ecosystem. In order to further understand the dynamics and potential effects in an agricultural ecosystem, background monitoring of water quality and soil quality were also carried out. Water quality, as discussed above (Section 4.3) was carried out using nutrient-based indicators at each site. Nutrients such as $\text{PO}_4\text{-P}$, $\text{NH}_3\text{-N}$, and $\text{NO}_3\text{-N}$ are responsible for eutrophication and algal blooms (Francis-loyd et al., 2009). Therefore, the nutrients chosen for water quality assessment were $\text{NH}_3\text{-N}$, $\text{NO}_3\text{-N}$, $\text{NO}_2\text{-N}$ and $\text{PO}_4\text{-P}$. These parameters chosen for the assessment of water quality based on a review of

the parameters commonly used by environmental agencies such as the EPA and the European Environmental Agency (EEA). These parameters include physico-chemical properties which aid in the establishment of the overall water quality at each site, such as pH, conductivity, total dissolved solids (TDS), and dissolved oxygen (DO).

Water quality for most indicators were found to be moderate to poor. $\text{NH}_3\text{-N}$ loading at both sites increased during periods of potential fertilizer application. From the data obtained during the study period, both sites were in breach of the EPA limit (<0.02 mg/L) during the months when $\text{NH}_3\text{-N}$ was detected (Figure 4.20). The average concentration of $\text{NH}_3\text{-N}$ for both Sites 1 and 2 were 0.1 ± 0.0 and 1.0 ± 2.7 mg/L respectively, further demonstrating the issue of nutrient loading (Figure 4.20). Similarly, $\text{NO}_2\text{-N}$ levels, when comparing Sites 1 and 2, are highly dissimilar and are measurable on a different scale, with Site 2 showing double the concentration in certain cases compared to Site 1. In terms of water quality, it was assessed as moderate, as the exceedance of the 0.05 mg/L limit set forth by the EPA only seen twice during the study period. Likewise, $\text{NO}_3\text{-N}$ levels remain moderate throughout the study period, not exceeding the moderate rating according to the EPA guidelines at both Sites 1 and 2 (Section 4.3.6).

The final nutrient-based indicator measured was $\text{PO}_4\text{-P}$. Site 1 had no detectable concentrations of $\text{PO}_4\text{-P}$ bar one occasion, where a concentration of 0.156 ± 0.946 mg/L $\text{PO}_4\text{-P}$ was obtained in October 2021. This singular occasion could potentially be attributed to the liming of the soil during that period. No $\text{PO}_4\text{-P}$ was detected after October, and from historical records available, the only other time $\text{PO}_4\text{-P}$ was detected at this site was in October 2018, when liming was carried out on the soil.

In contrast, Site 2 continuously produced heightened levels of $\text{PO}_4\text{-P}$, with a continuous exceedance of the cited EPA limit ($<0.03 \text{ mg/L}$, Figure 4.27). The average concentration of $\text{PO}_4\text{-P}$ was 3.0 mg/L for the monitoring period. The continuous loading of $\text{PO}_4\text{-P}$ indicated that the farms connected to the stream leading to the pond, used organic rather than synthetic fertilizer, potentially in the form of slurry and manure. This resulted in the continuous loading seen during the monitoring period. This is corroborated by the peak observed in $\text{PO}_4\text{-P}$ concentrations in the water column. The highest $\text{PO}_4\text{-P}$ concentration observed between 2020-2022 was in the month of October, at which time synthetic fertilizer is already banned from use in County Dublin (Figure 3.4), however, organic fertilizers (such as slurry) are still in use during this period. This resulted in the water quality at Site 2 to be classified as poor when reviewing this indicator.

The physico-chemical data obtained during the study confirms periods of nutrient loading, with changes in conductivity and TDS when an influx of components enter the aquatic systems at each site. Similarly, pH also varies and changes during periods of nutrient influx. Dissolved oxygen levels are also affected by the influx and efflux of excess nutrients, and with the added variations of seasonal changes (temperature variations), the levels of DO at both sites are moderate to unhealthy, with a potential lack of ability to support larger aquatic lifeforms such as fish (Section 4.3.4).

Soil background monitoring was carried out using laboratory techniques developed specifically for this study. It involved the design of a leaching study, followed by analysis of the leachate to understand the leachability of fertilized, tilled soils. As there are water sources at each site (ponds), nutrient leaching from the soil during periods of intense rain is a major transport pathway leading to heightened nutrient loads in arable agricultural ecosystems. This can occur through components leaching directly

into the ponds on site, or by leaching into groundwater. The study was designed as is detailed above (Section 3.5.3).

An elemental analysis was performed on the untreated soil using XRF, in order to gain an elemental make-up of the soil at both Sites 1 and 2. Additionally, understanding the elemental make-up of soils is essential for studying agricultural contamination and soil fertility, especially when long-term monitoring is being implemented. The chemical make-up of the soil allows for predictions to be made when fertilizer is added, as well as its fertility prior to any additions. Furthermore, elemental analysis can elucidate other issues, which when combined with nutrient enrichment, cause environmental health and soil fertility to decline. An example of this would be the presence of excessive concentrations of heavy metals such as cadmium, lead, etc. The total elemental composition of the soils (determined as %w/w) further elucidate the soil make-up (Table 4.5) and was found to be 76.29% and 84.98% for Sites 1 and 2 respectively. The % moisture content of the soils was also carried out in conjunction with the elemental analysis, as moisture content can affect the type, concentration, and chemical structure of elements present (Table 4.5). The total composition of the soil based on elemental and moisture content analysis was determined to be 84.09% w/w and 95.59% w/w for Site 1 and Site 2 respectively. The remaining composition of the soil can be potentially carbon, however, due to time constraints, this was not further analysed.

As the major elements which are leached from soils are generally in their ionic forms during this process, an anion analysis was also carried out on both the leachate obtained throughout the study, as well as the soil pre-treatment in order to obtain a baseline for comparison. The soil and leachate was analyzed for fluxes of seven major anions, namely fluoride (F^-), chloride (Cl^-), NO_3^- , NO_2^- , phosphate (PO_4^{3-}), sulfate

(SO_4^{2-}) and bromide (Br^-). Anion concentration fluxes were very sensitive to drying scenario and type of precipitation applied. F^- concentrations doubled, NO_2^- concentrations tripled and Br^- concentrations increased by a factor of 10 when natural precipitation was applied to the soil (Figures 4.36 and 4.37). In contrast, PO_4^{3-} concentrations doubled, and NO_2^- concentrations tripled during synthetic rainfall simulations. When compared to the baseline, the concentrations of anions obtained for the soil (Section 4.4.2), anion concentrations were lower by a factor of 10 in soil leachate. The concentration of anions are highly variable overall, however only NO_2^- concentrations show a trend of decreasing concentrations throughout the simulations for all samples. This is due to NO_2^- being a transitional compound formed when NH_3 is converted to NO_3^- .

The high variability seen in anion concentrations overall may be due to the drying scenarios applied. All drying scenarios were designed to put the soil under simulated environmental stress which resulted in water-soluble anions to be released. For example, freeze-thaw scenarios rely on the freeze-thaw action effects on soils, which have the capacity to shatter soil minerals and break up soil aggregates over time, increasing the specific surface area of soil for precipitation (Hinman, 1970). Similarly, during air- and oven-drying scenarios, soil aggregates crack and break, leading to increased specific surface area exposed to precipitation. This can cause increases in anion concentrations, such as seen with Br^- , NO_3^- , PO_4^{3-} and F^- . Leaching of ions leads to decline in soil health and increased potential for weathering effects and an overall loss of ability to support healthy ecosystems, as well as deteriorating nutrient rebalancing and holding capacity.

Similarly, to the IC analysis, trace element analysis using ICP-MS showed fluxes influenced by both the drying scenarios applied as well as the precipitation type

received by the soil (Figures 4.38 and 4.39). Natural precipitation simulations produced greater variability in trace elemental fluxes, generally doubling the concentrations of trace elements detected in the leachate. This is mainly due to the presence of trace elements in natural water sources such as rain and snow. Freeze-thaw scenarios produced higher concentrations and variability of Al, Mn, Fe and Zn. In general, analyte concentrations in leachate were relatively steady, with the exceptions of Na and Mg, where concentrations decreased over prolonged exposure to precipitation and consequent drying. Leaching of trace elements leads to decline in soil health and increased potential for weathering effects and lack of capacity for supporting healthy ecosystems.

As part of the soil quality study, soil leachate was also monitored for physico-chemical properties such as changes in pH, EC and the volume of leachate produced. Variations in pH, EC and volume was influenced by the drying scenario as well as precipitation being applied to the soils, with a significant difference between natural and synthetic precipitation simulations (Section 4.4.4.1). As the soil samples were taken from the first 20 cm of topsoil from an agricultural ecosystem, it must be acknowledged that salt ions in the root distribution layer (0-50 cm) can be highly variable due to plant uptake. This effect was minimized as much as possible at field-level, by timing the sampling during the fallow season at both sites before any arable crop was planted. Therefore, the pH variation seen during the simulation is attributed to the soil only. Additionally, soils at Site 1 are affected by groundwater levels throughout the year, resulting in a seasonal variability of salt ions being present throughout the year. This can affect the soil buffering capacity, however, generally soils are sufficiently self-buffered to accommodate changes in pH (Ng et al., 2022). The soil leachate reflected this self-buffering capacity (Figure 4.33).

Similarly to pH, variation in EC was affected by both drying scenario and precipitation type applied, with a significant difference between natural and synthetic precipitation simulations. Oven- and air-dried cycles release major ions during the initial cycles. Freeze-thaw cycles show more variability with a more gradual release. Freezing and thawing can affect mobile ion transport in soils by influencing nutrient leachability via the forms of nutrients present in the soil, as well as having immediate chemical effects.

Freeze-thaw action can influence nutrients such as phosphorous for example, which become more readily available for water extraction (leachability) through the actions of freezing and thawing in both mineral and organic soils (Bechmann et al., 2005). However, immediate chemical effects of freeze-thaw episodes, for example reactions created by precipitation and alterations in microbial activity often associated with physical alterations in the soil's structural make-up can induce a decrease in nutrient availability in soils (Juan et al., 2018; Liao et al., 2019).

Soil water dynamics and surface flow also played a major role in the volume of leachate produced. Following the initial precipitation simulations (the first cycle where precipitation was applied), the initial flow path for all soils were via macropores or small rocks present. With continuing precipitation, the freeze-dried soils became saturated, wetting became homogenous, and seepage became plug-like. Oven- and air-dried soils did not reach saturation, therefore were also retaining water during every cycle to greater extent.

This provides valuable insight into water flow dynamics at field-level regarding soil water movement in the top-soil where fertilizer is applied. Intense, pro-longed rainfall will lead to run-off on the soil's surface once the soil has reached saturation, as well

as lead to higher magnitudes of nutrient leaching as opposed to intense rainfall occurring after a dry-period.

For a more in-depth understanding, soil fertility analysis was also performed using respirometry (Section 4.4.3). Management practices such as ploughing and tilling have a potential to lead to the destruction of established microbiome and depending on the time of year it is performed, can reduce soil fertility by disrupting natural organic matter cycling. This is supported by the data obtained during the analysis for the soil samples collected. The average RQ for Sites 1 and 2 were 0.834 and 0.987 respectively (Figure 4.31). This indicates that compounds with relatively low levels of O (amino acids, refractory compounds, etc.) were mineralised primarily (Chaabane et al., 1999).

At both sites, RQ values do not equal 1, showing an imbalance, even though O₂ uptake and CO₂ evolution rates were overall highly correlated. This potentially indicates disruptions of microbial activity occur in soils which are under agricultural management. Additionally, it could also lead to excess use of fertilizer on the soil, due to the soil nutrient deficits as a result of disrupted organic matter break-down. Once the soil has been ploughed, a lack of winter-cover lead to increased erosion of the soil and increased soil run-off due to reduced infiltration. Run-off increases nutrient loading in water sources at each site, further facilitated by drainage ditches present at each site.

The respiratory analysis was accompanied by a microbiological analysis to determine the overall composition and population of microbial communities (Figure 4.32). Generally, chemoorganoheterotrophs are the most abundant population in managed ecosystems such as agriculture, which the data has reflected. These include bacteria, actinomycetes and protozoa (Bhattarai, 2015). These microorganisms generally are

more adaptable to soil disturbance, such as tilling, and therefore are abundant in agricultural soils (Figure 4.32).

From this facet of the study, it is demonstrated that soil fertility is potentially affected by the main economic activity at both sites, namely agriculture, both physically and chemically, which in turn leads to the degradation of soil quality over time. To balance this, the use of fertilizers are employed, however, nutrient augmentation still has limitations, unless increased exponentially as the soil degrades. This however is not sustainable and leads to increasing levels of atmospheric emissions and nutrient loading of water sources at a local as well as catchment scale. Additionally, it would also lead to further effects on soil quality, as unbalancing natural levels of nutrients continuously would lead to degrading biomes further. Additionally, increased use of fertilizer would also lead to further disruptions and degradation of biodiversity at catchment scale.

Linking the transport pathways of the dynamics of NH_3 throughout the atmosphere-water-soil nexus in an agricultural ecosystem, with the addition of secondary aerosol NH_4^+ formation demonstrates the importance of mitigation measures and emission reduction required in order to reduce the decline in air, water, and soil quality as whole. During the monitoring period, the effects of agricultural management activities (such as the use of fertilizer, tilling, etc.) and the timing of these activities throughout the year have been observed through a reduction in air, water, and soil quality. Additionally, transport of increased loads of N throughout the biosphere has the potential to increase stress on N cycling. As all major biogeochemical cycles are interlinked, this could also have detrimental effects on other major elemental cycles (e.g.: C cycling, Section 2.3). In order to illustrate this, a conceptual model was developed, known as the CASIOS model. This is discussed in Chapter 5.

The data obtained during the study was assessed and validated using various methods. Water quality parameters such as $\text{NH}_3\text{-N}$, $\text{PO}_4\text{-P}$, $\text{NO}_3\text{-N}$, and $\text{NO}_2\text{-N}$ were measured using absorbance spectroscopy, it required a calibration curve to be performed for each measurement. This allowed for linear regression analysis of the method. Generally, an average R^2 value of 0.99 was attained for all analysis with the exception of $\text{PO}_4\text{-P}$ analysis, where an average R^2 value of 0.98 was obtained. The air quality data obtained through IC analysis was regularly checked using internal standards, and the data was quality controlled and assured using field, travel and laboratory blanks to ensure high quality data. Soil quality data was assured and validated using internal standards for the IC and ICP-MS analysis performed.

4.7 Conclusion

This chapter was concerned with the results obtained for the monitoring period of the study, as well as discussing and demonstrating NH_3 and PM dynamics in arable agricultural ecosystems. It has also suggested pathways of pollutant production, transfer, and propagation processes, as well as site-to-site and temporal variability of pollutants. A source-product relationship was established between ambient atmospheric NH_3 and secondary PM formation at source level. These results demonstrated the dynamics of arable agricultural systems in a novel biospheric perspective. There is limited evidence of this type of biospheric monitoring at an Irish agricultural setting at the nexus of water, soils and land use. Therefore this study presents a novel data set of values for NH_3 , its associated compounds, and related substances, along with an in-depth understanding of N system dynamics and

propagation pathways that collectively regulate NH_3 based pollution events in agriculture.

Chapter 5: Conceptual Model

5.1 CASIOS model premise and framework

Agricultural activities and management practices affect the N cycling of the biosphere in the immediate ecosystem, as well as contribute to atmospheric transport of emitted NH_3 and PM (outlined in Chapters 2 and 4). This could potentially lead to biodiversity loss at a localized, catchment, as well as broader, national, and regional scale. As has been noted (Chapter 1), gaseous NH_3 can lead to biodiversity loss in ecosystems such as peatlands at concentrations of circa $2.2 \mu\text{g}/\text{m}^3$ leading to ecosystem impacts such as loss in moss biodiversity and algal formation (Kelleghan et al., 2019). NH_3 emissions also lead to secondary aerosol formation, which has been shown to affect human and ecosystem health (Mukherjee & Agrawal, 2017; Wu et al., 2018).

Current studies and policies seek to reduce emissions on a single-element basis, meaning air, water and soil quality, health and NH_3 and PM mitigation are all looked at separately (Bash et al., 2010; Coll et al., 2017; Pryor & Klemm, 2004; Van Damme et al., 2015; Wriedt et al., 2007). However, due to the complexity of biospheric reservoirs and interactions between these three major elements, segregation can lead to certain ecological changes and system interactions being overlooked, in order to simplify a given issue. Thus, solving an issue in part, rather than as a whole, can lead to mitigation measures being ineffective in the long-term.

In order to avoid the ‘band-aid’ effect, a higher level of scrutiny is required when assessing NH_3 and consequent secondary PM emissions and mitigation strategies, with a more holistic approach to the system being analysed. The system in the case of this study was an arable agricultural system (Section 3.2). The potential links and relationships in arable agricultural systems still require further clarification to aid

understanding of the complexity of the system and the relationships between the system and the movement of NH₃ and PM, as well as the system's possible responses and the potential signs of NH₃ and PM impacts. Therefore, while keeping the entirety of biospheric interactions in view, key potential variables and indicative responses have been identified in order to help realise the technical requirements of mitigation measures for an arable agricultural system. The construction of a CASIOS model identifying the Drivers, Pressures, State, Impact, and Responses (DPSIR) within which modelling techniques are applied, aims to achieve this (Figure 5.2).

As mentioned earlier (Section 3.6), the DPSIR framework is widely used in order to aid environmental policy decisions and policy formation as a whole. The framework was chosen after careful review of the key concepts of the project (Figure 5.1).

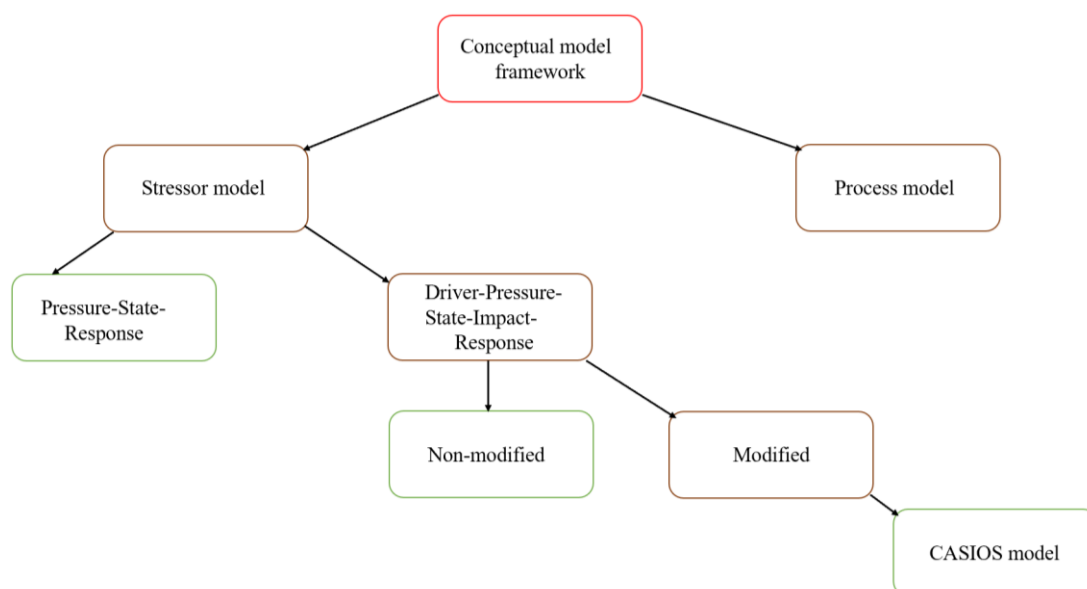


Figure 5.1 Decision tree for the development of the CASIOS model

Firstly, the conceptual model being built was assessed. The two types of conceptual models most often used in environmental assessment are stressor models and process models. Process models are conceptualisations of controls, feedback and interactions accountable for system dynamics, generally represented in a mechanistic way (Carvalho et al., 2014). Stressor models analyse the casual pathways, links and relationships between the pressures, their associated stressors and receptors within a system (Bårdsen, Hanssen, & Bustnes, 2018). These models use weight-of-evidence processes and provide greater insight from a biospheric overview perspective, than a process model, therefore, a stressor model paradigm was chosen.

The framework within a stressor model can be simplified to a Pressure-Stressor-Receptor (PSR) framework, where the receptor is the ecosystem under study (in this case an arable agricultural system), however, as the project progressed, a more in-depth approach was considered, namely a DPSIR framework. While a PSR framework could be used for an overall simplified assessment, it would overlook certain intricacies which have an effect on the system as a whole, and therefore leave a potential gap in the model being developed. The DSPIR framework provides a well-structured assessment of risk coupled with the current state of the system, as well as a forecast of steps which may be taken in order to facilitate abatement of NH₃ emissions and PM formation on a wider scale.

In order to establish a DPSIR model for a system, there is a need to consider nature and the complexity of the cause-effect relationships and the resolution of system dynamics (Sections 4.1 through 4.4). Following this assessment, an adjustment was made to the model framework, adding the idea of 'Context' to the model when reviewing Pressures, State, and Impacts. This resulted in the construction of an adjusted DPSIR framework forming the basis of the CASIOS model.

The next consideration was to evaluate the replicability and transferability of the model. The model is reproducible and can be adapted depending on the focus of the study. For example, the model ideology and framework presented here can be reproduced to be used for grassland systems, with the same evaluation process as described above. The model can also be adapted into a simplified PSR model, which can focus on simply one aspect of the atmosphere-water-soil nexus and follow the same steps to evaluate the responses required to reduce emissions (Figure 5.2).

5.2 CASIOS model for arable agricultural systems

A conceptual model for the purpose of this study is defined as a model consisting of concepts used to represent, understand and simulate a system (J. Johnson, 2008; Parush, 2015). The conceptual model framework chosen to simulate the system dynamics of arable agriculture is a DPSIR framework. However, it has been adjusted to fit a wider scale of scenarios and to further the model's accuracy via the introduction of a sixth concept titled "Context". DSPIR framework models consist of a chain of casual links generally piloting from "driving forces" (encompassing anthropogenic activities which affect a given system) through "pressures" (emissions), leading to "states" (current assessment of the system) and "impacts" (the effect these activities have on the system), eventually arriving at the "responses" required to lessen these effects (United Nations Food and Agriculture Organization). These components form the basis of the model.

This framework analyses all variants of the system, reviewing the relationship between each in order to assign the correct component to each variant. However, when reviewing an environmental biospheric system, some variant would be in danger of

over-simplification if only the five components were used to describe the entire system. Therefore, an additional set of criteria was added known as “context”, which aims to explain any and all deviations not accounted for in the original framework (Figure 5.1). The model was named Conceptual Ammonia-aeroSol bIOspheric Simulation (CASIOS) (Section 3.6).

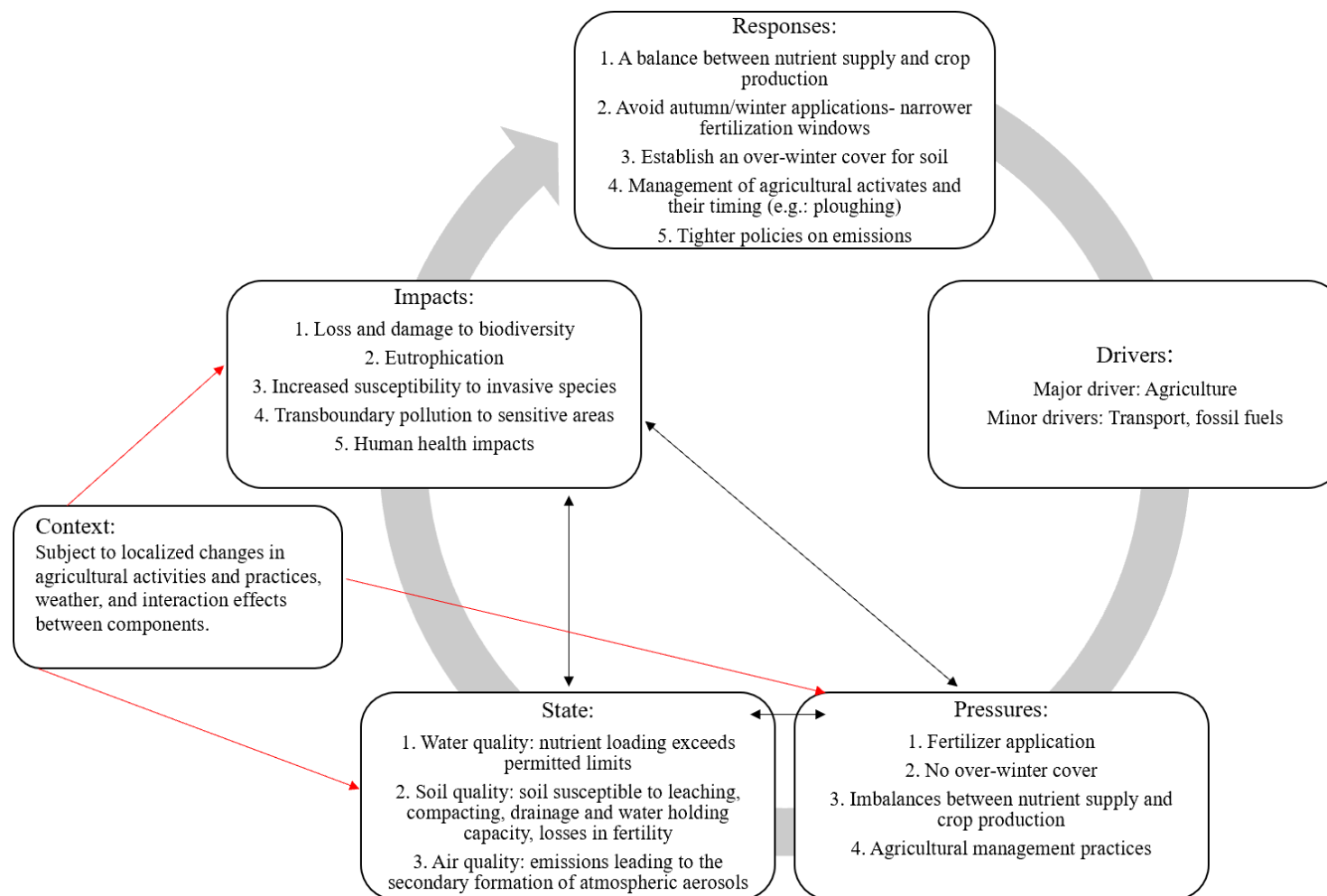


Figure 5.2 Conceptual model developed for arable agricultural system (CASIOS)

5.2.1 Drivers

The main *driving forces* identified at both Sites 1 and 2 were arable agricultural activities. *Driving forces* in this case include socio-economic activities which contribute to changes in the system in the form of instigating or increasing pressures on environmental systems. The major pressure in this case was identified as agriculture, which is the primary socio-economic anthropogenic activity in the northern area of County Fingal, where the sites are located (Haughey, 2021). Minor drivers were identified as fossil fuel use, and transport emissions. Arable agricultural activities include but are not limited to ploughing, tilling, drilling, fertilizer spreading, irrigation, cultivation, planting, and spraying (e.g.: pesticides). All of these activities have the potential to increase emissions of NH_3 to the atmosphere, driving secondary PM formation, increasing the risk of nutrient enrichments, and potentially lowering soil fertility. Additionally, activities such as drilling, ploughing and tilling can potentially loosen the soil over time, resulting in soil becoming loose due to reduced compaction from these activities, indicating an increased risk of erosion (Labiadh et al., 2013).

Connecting this information with arable agriculture being the primary economic activity at each site, the remaining components of the system of the CASIOS model were identified under the assumption that the nutrient enrichment of water sources and the atmospheric NH_3 and subsequent secondary PM measured are originating primarily from the study sites, with some contributions from the surrounding landscape, such as accumulations in water sources for example.

5.2.2 Pressures

Pressures are identified as stressors which arise from the *driving forces* for a given system. The main *pressures* are represented by the nutrients used and NH_3 and PM emissions by the above-mentioned driving forces. As pressures are context dependent, the identified parameters were chosen after a review of their effects on system function. The three main interfaces of interaction are air, water, and soil where NH_3 and PM have a potential pathway to enter natural environments as well as potentially increasing loads of already existing NH_3 and PM within the system, and possibly exit the system. Agricultural practices such as fertilizer application have increase nutrient loading of $\text{NH}_3\text{-N}$ and $\text{PO}_4\text{-P}$ in water at both sites. Additionally, $\text{NO}_2\text{-N}$ and $\text{NO}_3\text{-N}$ levels have could potentially increase (Figures 4.20, 4.24, 4.25, 4.27). This provides a potential link between fertilizer and nutrient enrichment in water sources, with the added consideration of ‘Context’ factors, such as meteorology for example. If fertilizer is applied, followed by precipitation, the fertilizer may become run-off, resulting in $\text{NH}_3\text{-N}$ (and $\text{PO}_4\text{-P}$ if organic fertilizer is used) entering the water column. $\text{PO}_4\text{-P}$ could also follow the same pathway during liming.

Once nutrients have entered the water column, the aquatic system’s processes provide various break-down processes by which nutrients may potentially be displaced to another aspect of the biosphere (e.g.: atmosphere) or accumulate within the aquatic system. $\text{NH}_3\text{-N}$ in the water column will be converted to $\text{NO}_3\text{-N}$ via denitrification. $\text{NO}_3\text{-N}$ can leave the system via the process of nitrification, forming N_2O in the atmosphere, effectively exiting one system component and entering another (Figure 2.1). Alternatively, $\text{NO}_3\text{-N}$ can be converted back to $\text{NH}_3\text{-N}$, in which case it remains within the aquatic system, with a potential for accumulation of nutrient loads (Sections 4.3.5 and 4.3.6).

In particular, fertilizer application during the wetter seasons such as autumn could potentially increase nutrient run-off into water sources, as well as leaching of nutrients from the soil (Sections 4.4.4.2 and 4.4.4.3), which could lead to excessive nutrient augmentation of the soil, misbalancing the nutrient supply of crops. Management practices such as ploughing and tilling have a potential to lead to the destruction of established microbiome and depending on the time of year it is performed, can reduce soil fertility by disrupting natural organic matter cycling. This could also lead to excessive fertilizer application, due to the potential soil deficits of nutrients occurring as a result of disrupted organic matter break-down. Once the soil has been ploughed, a lack of winter-cover lead to increased erosion of the soil and increased soil run-off due to reduced infiltration. Run-off increases nutrient loading in water sources at each site, further facilitated by drainage ditches present at each site (Section 4.6). These provide a direct pathway for nutrients to water sources, increasing nutrient loading.

Emission of gaseous NH_3 increased atmospheric concentrations of both NH_3 and PM. When NH_3 from fertilizer enters the atmosphere, it enters in the gas form. During the monitoring period, increased concentrations observed in the data indicated that fertilizer was applied to the soil, leading to increased atmospheric concentrations of atmospheric NH_3 (Figures 4.4). The increase in atmospheric NH_3 concentration potentially allowed for an increase in secondary PM formation (Figure 4.5). As mentioned earlier (Section 4.2.3), a time lag was observed when comparing peak concentrations throughout the monitoring period between atmospheric NH_3 and PM.

The time lag was approximately one month with the peak in concentration occurring in the period of April-May 2021 for atmospheric NH_3 and June-July 2021 for PM. This could be indicative of the atmospheric timeframe of secondary reactions at source sites with agriculture being the primary socio-economic activity. When atmospheric

NH₃ concentrations increased again in the period of October-November 2021, it occurred more gradually, and the peak produced was less significant than the one seen in April-May. However, the PM concentration started to rise correspondingly in January 2022 as the sampling was finishing, further indicating the possibility of this being the atmospheric reaction time for secondary PM formation.

Another aspect to consider is the potential fallout from the study sites to larger areas and natural habitats. During the monitoring period of 2021-2022, PM and atmospheric NH₃ concentrations indicated a link with weather effects such as wind, RH, air temperature and precipitation (wet deposition) (Figure 4.6). These factors have a potential control over NH₃ concentrations in the atmosphere, reducing the concentration of NH₃ available for the formation of secondary PM, consequently lowering concentrations. Additionally, PM is also affected by these factors, as atmospheric transport is facilitated by wind speed and direction, and wet deposition (scavenging occurring at source, while deposition may occur elsewhere off-site). Hence, the introduction of the concept of “context” as demonstrated by the CASIOS model above is to be considered when reviewing pressures for policy purposes. Local weather patterns can potentially affect the concentrations of both atmospheric NH₃ and PM, facilitating atmospheric transport away from source. This also provides a possible pathway for atmospheric NH₃ and PM to enter natural ecosystems at heightened concentrations away from source, as demonstrated by the study conducted by Kelleghan et al., (2021).

5.2.3 States

States refer to the condition of the system under study. Most often, *states* in a system are described using governmental/protection agency guidelines for evaluation. In terms of the system under study, *states* have several characterizations given the variety of environmental factors under observation (water, soil, and air quality) (Sections 4.1 through to 4.4). From a water quality perspective, nutrient loading exceeds the permitted limits set forth by the EPA at both sites, resulting in both water sources being classified as moderate, however during intensive agricultural activity such as fertilization, this classification changes to poor, due to the increased nutrient loading in the water column (Section 4.2).

Soil quality at both sites has also degraded due to agriculture. Soil drainage and water holding capacity have reduced. The soils' natural ability to restabilize following events such as heavy precipitation or heightened temperatures has also been affected. Soil compaction occurs easily, affecting water infiltration (Section 4.3).

Air quality is affected by emissions directly related to agricultural activities. Increased atmospheric NH_3 concentrations were observed at both sites during potential fertilizer application. Increased concentrations of PM have also been observed during the study period, coinciding with increased atmospheric concentrations of NH_3 . All of these variants are affected by a set of contextualized parameters (Figure 5.1), especially interaction effects between variants and micrometeorology (Section 4.1). For example, when soil health declines, increased emissions to both water sources and the atmosphere can occur, leading to declining air and water quality. Therefore, in order for the system to improve, all components of the system has to be maintained at a healthy status.

Micrometeorology could also potentially affect emissions and the localization of deposition (Section 4.4). Additionally, it could affect reactions occurring throughout the biosphere, such as the potential formation of secondary PM in the atmosphere, and the conversion of $\text{NH}_3\text{-N}$ to $\text{NO}_3\text{-N}$ in water. Therefore, modelling these reactions without the context criteria which can affect these components could lead to biased forecasts of emissions, making the criteria of context vital.

5.2.4 Impacts

Impacts refers to the effects pressures have on a given system. A compromised system (through imbalanced relationships and interaction pathways) could have far-reaching *impacts* to the biota and the environment. Understanding the pathways, interactions, and transport of NH_3 and PM through environmental media is of key importance for accurate and precise predictions for a given system. In the case of agricultural systems, leaching and run-off from soils lead to water quality decline, increased eutrophication potential and algal blooms.

Nutrient loading to the water sources at both sites have potentially increased nutrient loading and algal blooms occurring from early spring to early autumn (Section 4.3). This was indicated by reduced water oxygen levels, affecting the water ability to support flora and fauna. This has a potential to lead to loss of biodiversity over time as well as increased susceptibility to invasive species.

Invasive species are also persistent among the flora present on land. Nettles and spiny sow thistle are widespread throughout the ecosystem, invading areas such as ridges and embankments of water sources. These species commonly occur as a result of high presence of N in soils.

As mentioned earlier, transport of atmospheric NH_3 and PM, could also lead to biodiversity losses occurring away from study sites and sources. This can potentially result in the decline and damage of species in sensitive areas such as peatlands for example (Kelleghan et al., 2019, 2021b).

Another impact to consider is the human health impact, especially due to the production of PM. PM_{10} , due to its size, can penetrate past the bronchi, and enter the lungs where it can lodge into the tissue and result in a number of cardiovascular and pulmonary issues such as aggravation and increasing of asthma, bronchitis, high blood pressure, increased rate of heart attacks, strokes and increasing premature mortality rates (Ghosh, Rabha, Chowdhury, & Padhy, 2018; van Zelm et al., 2008). Higher atmospheric concentrations of PM could potentially increase the number and severity of health impacts.

5.2.5 Responses

In order to mitigate impacts, improve state and reduce pressures, structural and normative-based *responses* are required. As part of the conceptual model, five responses have been suggested to reach these goals. Firstly, a revision of crop production and nutrient supply is suggested, in order to balance the requirements with the application. If the nutrient supply requirements of given crops and soils are assessed appropriately, nutrient augmentation has a potential to be not only more sustainable, but also cost-effective, as unnecessary losses would also be reduced as a result. This would provide increased yields and increased profits, by way of reduction of costs.

A narrowing of fertilization windows during the year would also decrease the potential of NH_3 entering and leaving the system. Applications during wetter seasons such as late August and early September lead to higher volumes of run-off, as well as excessive application in order to reach desired crop yields due to wash-out. If the application window was narrowed, emissions would be reduced and both EU and national directives and emission limits such as the NEC limits could be met.

Management practices such as establishing over-winter crop cover at both sites would improve soil health and fertility, potentially reducing nutrient augmentation requirements and therefore emissions of NH_3 . Timing of practices such as ploughing can also boost soil health, for example if ploughing is done during autumn as opposed to spring. This is due to the soil moisture content of soils. If ploughing is done during initial stages of the rainy season, the soil is more compact, therefore does not raise dust and loose soil.

In terms of policies currently in action such as the Food Wise 2025 (Department of Agriculture, 2015) calling for the intensification of agricultural production, is in complete contrast with environmental policies and agreements such as the Gothenburg Protocol for example which Ireland is a part of. Thus, a unification and common ground has to be reached when policies are devised, so that agricultural intensification is achieved in a sustainable way, which curbs emissions instead of leading to their increase, especially atmospheric NH_3 .

5.3 Conclusion

This chapter aimed to demonstrate the conceptual model developed as part of this project. The key to the development of the CASIOS model demonstrated above, was the cause-effect relationships established for the system using a new, more holistic approach to an agricultural system which looks at more than one component of the ecosystem at one time. One main short-coming of the DSPIR framework generally arises from the lack of heterogeneity of data collected at different temporal scales, however, this was curbed with the addition of the concept of context to the model framework. This introduced some elasticity to the CASIOS model which is often lacked when a DSPIR framework is employed, thus introducing a novel conceptual model.

Chapter 6: General Conclusion and Future Work

The work reported in this thesis aimed to further develop an understanding of NH_3 dynamics and elucidate the mechanism of secondary PM formation from NH_3 sources. From the data obtained, a conceptual model incorporating air quality with soil and water quality for arable agricultural systems was to be developed, that may be implemented to generate short-term forecasts of these pollutants, based on environmental parameters.

In order to achieve this, a set of study sites were located based on the criteria outlined in Chapter 3. Three sites have been selected in total, two active sites (sites where the primary socio-economic activity is arable agriculture) and a control site (remote location in the Wicklow mountains where pollutant effects are assumed to be minimal). Following the selection of sites, the dynamics of each site was evaluated, and the major biophysical and biochemical pathways of interactions and transport of pollutants were established. A set of monitoring networks were built at each of the sites. All sites were monitored for atmospheric NH_3 using passive samplers (ALPHA samplers), and Site 1 had the addition of being monitored for atmospheric NH_3 and aerosol NH_4^+ using an active sampling system (DELTA II sampler). The other two sites were not set up with active samplers due to the samplers being too exposed.

While the study produced a considerable knowledgebase, one limitation which continuously posed a risk to the study was the power supply at remote locations for instruments such as the MetOne and the DELTA II sampler. Power supply could not be relied upon at all times, or due to seasonal effects, was restricted to minimal supply which posed the threat of instruments shutting down mid-sampling. One recommendation for remote sampling therefore would be to experiment with multi-source sustainable power supply options (for example solar panels combined with a

wind turbine). This could be achieved by adding an auxiliary power switch with a sensor which recognizes when one set of power supply source is no longer sufficient, and thus switches to another. This would allow for long-term monitoring campaigns such as these to ensure data collection remained uninterrupted.

Once the major pathways were identified, the driving parameters, variables and constants at each arable agricultural site were established, followed by a collective assessment of parameters which exhibit effects on atmospheric NH_3 and PM entering and exiting the system on a biospheric scale. From this, the pathways of NH_3 production, transfer, and propagation were mapped, as well as the secondary production of PM in an arable agricultural setting. Once established, the background monitoring parameters were established for water and soil quality analysis. This further developed the mapped out pathways of nutrient transfer through the water-soil interface, as well as gave further insight into emissions to the atmosphere.

The precursor species (atmospheric NH_3) relationship to PM formation was determined through monitoring, and a species contribution to secondary PM was determined at source level. These results demonstrated the dynamics of arable agricultural systems in a novel biospheric perspective. There is limited evidence of this type of biospheric monitoring in an Irish agricultural setting at the nexus of water, soils and land use. Therefore, this study presents a novel data set of values for NH_3 , its associated compounds, and related substances, along with an in-depth understanding of N system dynamics and propagation pathways that collectively regulate NH_3 based pollution events in agriculture.

Using the data collected, a novel conceptual model (CASIOS) was developed, forming cause-effect relationships for an arable agricultural system. The key to the development of the CASIOS model was the cause-effect relationships established based on the field data collected for the system. Additionally, the system was observed as a whole (biosphere), rather than segregating it to its major and minor pools (namely lithosphere, hydrosphere, atmosphere), which allowed for the investigation of not only the individual dynamics of each, but also their interactions and transfer at interfaces. One main short-coming of the DSPIR framework generally arises from the lack of heterogeneity of data collected at different temporal scales, however, this was curbed with the addition of the concept of context to the model framework. This introduced some elasticity to the CASIOS model which is often lacked when a DSPIR framework is employed, thus introducing a novel conceptual model.

Although the work reported here has contributed to the fundamental knowledgebase currently being built on environmental pollutants and contaminants, as well as the mapping of source dynamics, there are a number of questions and challenges which would merit further investigation. Further characterization of precursor species could be investigated, with particular emphasis on acidic species which contribute to the formation of PM.

Optimisation of the monitoring network and adjusting sampling trains to adjust for the inclusion of acidic species would allow for further elucidation of PM formation dynamics and would merit further research. This would also mean additional contaminants being monitored at a higher resolution, such as $\text{NO}_3\text{-N}$ dynamics through the biosphere. Finally, the types of PM present at a study site could also be further investigated, as pollen and organic materials form a considerable part of PM in these ecosystems, as was also seen in the data presented during this study. By including

organic components, a more complete picture would be obtained of system dynamics still.

References

- Acharya, B. (2018). Chapter 10 - Cleaning of Product Gas of Gasification. In P. B. T.-B. G. Basu
Pyrolysis and Torrefaction (Third Edition) (Ed.) (pp. 373–391). Academic Press.
<https://doi.org/https://doi.org/10.1016/B978-0-12-812992-0.00010-8>
- Adams, P. J., Seinfeld, J. H., & Koch, D. M. (1999). Global concentrations of tropospheric
sulfate, nitrate, and ammonium aerosol simulated in a general circulation model. *Journal of
Geophysical Research Atmospheres*, 104(D11), 13791–13823.
<https://doi.org/10.1029/1999JD900083>
- Allen, A. G., Harrison, R. M., & Erisman, J.-W. (1989). Field measurements of the dissociation
of ammonium nitrate and ammonium chloride aerosols. *Atmospheric Environment* (1967),
23(7), 1591–1599. [https://doi.org/10.1016/0004-6981\(89\)90418-6](https://doi.org/10.1016/0004-6981(89)90418-6)
- Almaraz, M., Bai, E., Wang, C., Trousdell, J., Conley, S., Faloona, I., & Houlton, B. Z. (2018).
Agriculture is a major source of NO_x pollution in California. *Science Advances*, 4(1), 1–9.
<https://doi.org/10.1126/sciadv.aao3477>
- Anderson, N., Strader, R., & Davidson, C. (2003). Airborne reduced nitrogen: ammonia
emissions from agriculture and other sources. *Environment International*, 29(2–3), 277–
286. [https://doi.org/10.1016/S0160-4120\(02\)00186-1](https://doi.org/10.1016/S0160-4120(02)00186-1)
- Andreae, M. O. (2009). Correlation between cloud condensation nuclei concentration and aerosol
optical thickness in remote and polluted regions. *Atmospheric Chemistry and Physics*, 9(2),
543–556. <https://doi.org/10.5194/acp-9-543-2009>
- Aneja, V P, Bunton, B., Walker, J. T., & Malik, B. P. (2001). Measurement and analysis of
atmospheric ammonia emissions from anaerobic lagoons. *Atmospheric Environment*,
35(11), 1949–1958. [https://doi.org/https://doi.org/10.1016/S1352-2310\(00\)00547-1](https://doi.org/https://doi.org/10.1016/S1352-2310(00)00547-1)
- Aneja, Viney P., Roelle, P. A., Murray, G. C., Southerland, J., Erisman, J. W., Fowler, D., ...

- Patni, N. (2001). Atmospheric nitrogen compounds. II: Emissions, transport, transformation, deposition and assessment. *Atmospheric Environment*, 35(11), 1903–1911. [https://doi.org/10.1016/S1352-2310\(00\)00543-4](https://doi.org/10.1016/S1352-2310(00)00543-4)
- ApSimon, H. M., Kruse, M., & Bell, J. N. B. (1987). Ammonia emissions and their role in acid deposition. *Atmospheric Environment* (1967), 21(9), 1939–1946. [https://doi.org/10.1016/0004-6981\(87\)90154-5](https://doi.org/10.1016/0004-6981(87)90154-5)
- Aranibar, J. N., Otter, L., Macko, S. A., Feral, C. J. W., Epstein, H. E., Dowty, P. R., ... Swap, R. J. (2004). Nitrogen cycling in the soil-plant system along a precipitation gradient in the Kalahari sands. *Global Change Biology*, 10(3), 359–373. <https://doi.org/10.1111/j.1365-2486.2003.00698.x>
- Asaadi, A., Arora, V. K., Melton, J. R., & Bartlett, P. (2018). An improved parameterization of leaf area index (LAI) seasonality in the Canadian Land Surface Scheme (CLASS) and Canadian Terrestrial Ecosystem Model (CTEM) modelling framework. *Biogeosciences*, 15(22), 6885–6907. <https://doi.org/10.5194/bg-15-6885-2018>
- Asman, W. A. H., Sutton, M. A., & Schjørring, J. K. (1998). Ammonia: emission, atmospheric transport and deposition. *New Phytology*, 139_ _ (x), 27–48. Retrieved from c:%5Creference%5C370.pdf
- Baek, B. H., Aneja, V. P., & Tong, Q. (2004). Chemical coupling between ammonia, acid gases, and fine particles. *Environmental Pollution*, 129(1), 89–98. <https://doi.org/10.1016/j.envpol.2003.09.022>
- Bajwa, K. S., Arya, S. P., & Aneja, V. P. (2008). Modeling studies of ammonia dispersion and dry deposition at some hog farms in North Carolina. *Journal of the Air and Waste Management Association*, 58(9), 1198–1207. <https://doi.org/10.3155/1047-3289.58.9.1198>
- Baker, J. (2010). A cluster analysis of long range air transport pathways and associated pollutant concentrations within the UK. *Atmospheric Environment*, 44(4), 563–571.

<https://doi.org/10.1016/j.atmosenv.2009.10.030>

- Balasubramanian, R., Behera, S. N., & Betha, R. (2013). Insights into chemical coupling among acidic gases, ammonia and secondary inorganic aerosols. *Aerosol and Air Quality Research*, 13(4), 1282–1296. <https://doi.org/10.4209/aaqr.2012.11.0328>
- Ban-Weiss, G. A., & Collins, W. D. (2015). AEROSOLS | Role in Radiative Transfer. In G. R. North, J. Pyle, & F. B. T.-E. of A. S. (Second E. Zhang (Eds.) (pp. 66–75). Oxford: Academic Press. <https://doi.org/https://doi.org/10.1016/B978-0-12-382225-3.00053-0>
- Bårdsen, B. J., Hanssen, S. A., & Bustnes, J. O. (2018). Multiple stressors: modeling the effect of pollution, climate, and predation on viability of a sub-arctic marine bird. *Ecosphere*, 9(7). <https://doi.org/10.1002/ecs2.2342>
- Bash, J. O., Walker, J. T., Katul, G. G., Iones, M. R., Nemitz, E., & Robarge, W. P. (2010). Estimation of in-canopy ammonia sources and sinks in a fertilized maize field. *Environmental Science and Technology*, 44(5), 1683–1689. <https://doi.org/10.1021/es9037269>
- Basosi, R., Spinelli, D., Fierro, A., & Jez, S. (2014). Mineral nitrogen fertilizers: Environmental impact of production and use. In *Fertilizers: Components, Uses in Agriculture and Environmental Impacts* (pp. 3–43).
- Bauer, S. E., Koch, D., Unger, N., Metzger, S. M., Shindell, D. T., & Streets, D. G. (2007). Nitrate aerosols today and in 2030: A global simulation including aerosols and tropospheric ozone. *Atmospheric Chemistry and Physics*, 7(19), 5043–5059. <https://doi.org/10.5194/acp-7-5043-2007>
- Beaver, S., Palazoglu, A., Singh, A., Soong, S.-T., & Tanrikulu, S. (2010). Identification of weather patterns impacting 24-h average fine particulate matter pollution. *Atmospheric Environment*, 44(14), 1761–1771. <https://doi.org/10.1016/J.ATMOSENV.2010.02.001>
- Bechmann, M. E., Kleinman, P. J. A., Sharpley, A. N., & Saporito, L. S. (2005). Freeze-Thaw

- Effects on Phosphorus Loss in Runoff from Manured and Catch-Cropped Soils. *Journal of Environmental Quality*, 34(6), 2301–2309. <https://doi.org/10.2134/jeq2004.0415>
- Behera, S. N., Sharma, M., Aneja, V. P., & Balasubramanian, R. (2013a). Ammonia in the atmosphere: A review on emission sources, atmospheric chemistry and deposition on terrestrial bodies. *Environmental Science and Pollution Research*, 20(11), 8092–8131. <https://doi.org/10.1007/s11356-013-2051-9>
- Behera, S. N., Sharma, M., Aneja, V. P., & Balasubramanian, R. (2013b). Ammonia in the atmosphere: A review on emission sources, atmospheric chemistry and deposition on terrestrial bodies. *Environmental Science and Pollution Research*, 20(11), 8092–8131. <https://doi.org/10.1007/s11356-013-2051-9>
- Bellouin, N. (2015). AEROSOLS | Role in Climate Change. In G. R. North, J. Pyle, & F. B. T.-E. of A. S. (Second E. Zhang (Eds.) (pp. 76–85). Oxford: Academic Press. <https://doi.org/https://doi.org/10.1016/B978-0-12-382225-3.00054-2>
- Besson, J. P., Schilt, S., Rochat, E., & Thévenaz, L. (2006). Ammonia trace measurements at ppb level based on near-IR photoacoustic spectroscopy. *Applied Physics B: Lasers and Optics*, 85(2–3), 323–328. <https://doi.org/10.1007/s00340-006-2335-6>
- Bhateria, R., & Jain, D. (2016). Water quality assessment of lake water: a review. *Sustainable Water Resources Management*, 2(2), 161–173. <https://doi.org/10.1007/s40899-015-0014-7>
- Bhattarai, B. (2015). Variation of Soil Microbial Population in Different Soil Horizons. *Journal of Microbiology & Experimentation*, 2(2), 75–78. <https://doi.org/10.15406/jmen.2015.02.00044>
- Billen, G., Silvestre, M., Grizzetti, B., Leip, A., Garnier, J., Voss, M., ... Lancelot, C. (2011). Chapter 13: Nitrogen flows from European regional watershedsto coastal marine waters. *The European Nitrogen Assessment Sources Effects and Policy Perspectives*, 271–297. <https://doi.org/10.1017/CBO9780511976988.016>

- Binkley, D., Stottlemeyer, R., Suarez, F., & Cortina, J. (1994). Soil nitrogen availability in some arctic ecosystems in northwest Alaska: responses to temperature and moisture. *Ecoscience*, 1(1), 64–70. <https://doi.org/10.1080/11956860.1994.11682229>
- Bouwman, A. F., Boumans, L. J. M., & Batjes, N. H. (2002a). Estimation of global NH_3 volatilization loss from synthetic fertilizers and animal manure applied to arable lands and grasslands. *Global Biogeochemical Cycles*, 16(2), 8-1-8-14. <https://doi.org/10.1029/2000GB001389>
- Bouwman, A. F., Boumans, L. J. M., & Batjes, N. H. (2002b). Estimation of global NH_3 volatilization loss from synthetic fertilizers and animal manure applied to arable lands and grasslands. *Global Biogeochemical Cycles*, 16(2), 8-1-8-14. <https://doi.org/10.1029/2000gb001389>
- Bouwman, A. F., Lee, D. S., Asman, W. A. H., Dentener, F. J., Van Der Hoek, K. W., & Olivier, J. G. J. (1997). A global high-resolution emission inventory for ammonia. *Global Biogeochemical Cycles*, 11(4), 561–587. <https://doi.org/10.1029/97GB02266>
- Bozorg-Haddad, O., Delpasand, M., & Loáiciga, H. A. (2021). Water quality, hygiene, and health. *Economical, Political, and Social Issues in Water Resources*, 217–257. <https://doi.org/10.1016/B978-0-323-90567-1.00008-5>
- Breuer, L., Kiese, R., & Butterbach-Bahl, K. (2002). Temperature and Moisture Effects on Nitrification Rates in Tropical Rain-Forest Soils. *Soil Science Society of America Journal*, 66(3), 834. <https://doi.org/10.2136/sssaj2002.0834>
- Brimblecombe, P. (2003). The Global Sulfur Cycle. *Treatise on Geochemistry*, 645–682. <https://doi.org/10.1016/B0-08-043751-6/08134-2>
- Brumme, R., Borken, W., & Finke, S. (1999). Hierarchical control on nitrous oxide emission in forest ecosystem. *Global Biogeochemical Cycles*, 13(4), 1137–1148.
- Bruno, P., Caselli, M., De Gennaro, G., Ielpo, P., & Traini, A. (2000). Analysis of heavy metals

- in atmospheric particulate by ion chromatography. *Journal of Chromatography A*, 888(1–2), 145–150. [https://doi.org/10.1016/S0021-9673\(00\)00503-3](https://doi.org/10.1016/S0021-9673(00)00503-3)
- Buijsman, E., Maas, H. F. M., & Asman, W. A. H. (1987). Anthropogenic NH₃ emissions in europe. *Atmospheric Environment* (1967), 21(5), 1009–1022. [https://doi.org/10.1016/0004-6981\(87\)90230-7](https://doi.org/10.1016/0004-6981(87)90230-7)
- Butler, T., Marino, R., Schwede, D., Howarth, R., Sparks, J., & Sparks, K. (2015). Atmospheric ammonia measurements at low concentration sites in the northeastern USA: implications for total nitrogen deposition and comparison with CMAQ estimates. *Biogeochemistry*, 122(2–3), 191–210. <https://doi.org/10.1007/s10533-014-0036-5>
- Butterbach-Bahl, K., Gundersen, P., Ambus, P., Augustin, J., Beier, C., Boeckx, P., ... Zechmeister-Boltenstern, S. (2011). Nitrogen processes in terrestrial ecosystems. In *The European Nitrogen Assessment* (pp. 99–125). <https://doi.org/10.1017/CBO9780511976988.009>
- Butterbach-Bahl, Klaus, Baggs, E. M., Dannenmann, M., Kiese, R., & Zechmeister-Boltenstern, S. (2013). Nitrous oxide emissions from soils: How well do we understand the processes and their controls? *Philosophical Transactions of the Royal Society B: Biological Sciences*, 368(1621). <https://doi.org/10.1098/rstb.2013.0122>
- Cabello, P., Roldán, M. D., Castillo, F., & Moreno-Vivián, C. (2009). Nitrogen Cycle. In M. B. T.-E. of M. (Third E. Schaechter (Ed.) (pp. 299–321). Oxford: Academic Press. <https://doi.org/https://doi.org/10.1016/B978-012373944-5.00055-9>
- Cai, G. (1997). Ammonia volatilization. *Developments in Plant and Soil Sciences*, 193–213. <https://doi.org/10.1007/BF00378047>
- Cai, Z., Li, F., Rong, M., Lin, L., Yao, Q., & Huang, Y. (2019). Introduction. In *Novel Nanomaterials for Biomedical, Environmental and Energy Applications* (pp. 1–36). Elsevier. <https://doi.org/10.1016/B978-0-12-814497-8.00001-1>

- Carvalho, A., Mimoso, A. F., Mendes, A. N., & Matos, H. A. (2014). From a literature review to a framework for environmental process impact assessment index. *Journal of Cleaner Production*, 64, 36–62. <https://doi.org/10.1016/J.JCLEPRO.2013.08.010>
- Cassman, K. G., & Munns, D. N. (1973). DIVISION S-3 — SOIL MICROBIOLOGY, 1233–1237.
- Censi, P., Darrah, T. H., & Erel, Y. (2012). Medical geochemistry: Geological materials and health. *Medical Geochemistry: Geological Materials and Health*, 9789400743, 1–194. <https://doi.org/10.1007/978-94-007-4372-4>
- Chaabane, K., Josens, G., & Loreau, M. (1999). Respiration of *Abax ater* (Coleoptera, Carabidae): A complex parameter of the energy budget. *Pedobiologia*, 43(4), 305–318.
- Chang, L.-S., & Park, S.-U. (2004). Direct radiative forcing due to anthropogenic aerosols in East Asia during April 2001. *Atmospheric Environment*, 38(27), 4467–4482. <https://doi.org/https://doi.org/10.1016/j.atmosenv.2004.05.006>
- Chuang, M.-T., Chiang, P.-C., Chan, C.-C., Wang, C.-F., Chang, E.-E., & Lee, C.-T. (2008). The effects of synoptical weather pattern and complex terrain on the formation of aerosol events in the Greater Taipei area. *Science of The Total Environment*, 399(1–3), 128–146. <https://doi.org/10.1016/J.SCITOTENV.2008.01.051>
- Classen, A. T., Sundqvist, M. K., Henning, J. A., Newman, G. S., Moore, J. A. M., Cregger, M. A., ... Patterson, C. M. (2015). Direct and indirect effects of climate change on soil microbial and soil microbial-plant interactions: What lies ahead? *Ecosphere*, 6(8). <https://doi.org/10.1890/ES15-00217.1>
- Coll, J., Curley, M., Walsh, S., & Sweeney, J. (2017). *HOMERUN: Relative homogenisation of the Irish precipitation network*. Environmental Protection Agency.
- Corre, M. D., Beese, F. O., & Brumme, R. (2003). Soil nitrogen cycle in high nitrogen deposition forest: Changes under nitrogen saturation and liming. *Ecological Applications*, 13(2), 287–

298. [https://doi.org/10.1890/1051-0761\(2003\)013\[0287:SNCIHN\]2.0.CO;2](https://doi.org/10.1890/1051-0761(2003)013[0287:SNCIHN]2.0.CO;2)
- Creamer, R. E., Simó, I., Reidy, B., Carvalho, J., Fealy, R. M., Hallett, S., ... Schulte, R. P. O. (2014). *Irish Soil Information System Synthesis Report*.
- CSO. (2020). Central Statistics Office- Census of Agriculture 2020. Retrieved from <https://www.cso.ie/en/releasesandpublications/ep/p-coa/censusofagriculture2020-preliminaryresults/landutilisation/>
- Dammers, E., Schaap, M., Haaima, M., Palm, M., Wichink Kruit, R. J., Volten, H., ... Erisman, J. W. (2017a). Measuring atmospheric ammonia with remote sensing campaign: Part 1 – Characterisation of vertical ammonia concentration profile in the centre of The Netherlands. *Atmospheric Environment*. <https://doi.org/10.1016/j.atmosenv.2017.08.067>
- Dammers, E., Schaap, M., Haaima, M., Palm, M., Wichink Kruit, R. J., Volten, H., ... Erisman, J. W. (2017b). Measuring atmospheric ammonia with remote sensing campaign: Part 1 – Characterisation of vertical ammonia concentration profile in the centre of The Netherlands. *Atmospheric Environment*, 169, 97–112. <https://doi.org/10.1016/j.atmosenv.2017.08.067>
- Darrouzet-Nardi, A. (2005). Remote Sensing of Earth's Nitrogen Cycle. Retrieved May 23, 2018, from <http://anthony.darrouzet-nardi.net/works/remotesensingN.html>
- Davidson, E. A., De Carvalho, C. J. R., Figueira, A. M., Ishida, F. Y., Ometto, J. P. H. B., Nardoto, G. B., ... Martinelli, L. A. (2007). Recuperation of nitrogen cycling in Amazonian forests following agricultural abandonment. *Nature*, 447(7147), 995–998. <https://doi.org/10.1038/nature05900>
- De Klein, C., Novoa, R. S., Ogle, S., Smith, K., Rochette, P., Wirth, T., ... Walsh, M. (2006). N₂O emissions from managed soils, and CO₂ emissions from lime and urea application. In *IPCC Guidelines for National Greenhouse Gas Inventories* (Vol. 4, pp. 1–54). Hayama, Japan.

- Dean, S. W. (2001). Natural Atmospheres: Corrosion. *Encyclopedia of Materials: Science and Technology*, 5930–5938. <https://doi.org/10.1016/B0-08-043152-6/01033-0>
- Delgado-Baquerizo, M., Maestre, F. T., Escolar, C., Gallardo, A., Ochoa, V., Gozalo, B., & Prado-Comesaña, A. (2014). Direct and indirect impacts of climate change on microbial and biocrust communities alter the resistance of the N cycle in a semiarid grassland. *Journal of Ecology*, 102(6), 1592–1605. <https://doi.org/10.1111/1365-2745.12303>
- Delon, C., Galy-Lacaux, C., Serça, D., Loubet, B., Camara, N., Gardrat, E., ... Mougin, E. (2017). Soil and vegetation-atmosphere exchange of NO, NH₃, and N₂O from field measurements in a semi arid grazed ecosystem in Senegal. *Atmospheric Environment*, 156, 36–51. <https://doi.org/10.1016/j.atmosenv.2017.02.024>
- Delzer, G. C., & McKenzie, S. W. (1999). Five-day biochemical oxygen demand. In *TWRI Book 9* (Vol. 7, pp. 1–20).
- Dennis, R. L., Mathur, R., Pleim, J. E., & Walker, J. T. (2010). Fate of ammonia emissions at the local to regional scale as simulated by the Community Multiscale Air Quality model. *Atmospheric Pollution Research*, 1(4), 207–214. <https://doi.org/10.5094/APR.2010.027>
- Department of Agriculture, F. and the M. (2015). *Local Roots A vision for growth for the Irish agricultural economy for the next 10 years. Terms of reference for the 2025 Agri-Food Strategy Committee.*
- Deshler, T. (2015). CHEMISTRY OF THE ATMOSPHERE | Observations for Chemistry (In Situ): Particles. In G. R. North, J. Pyle, & F. B. T.-E. of A. S. (Second E. Zhang (Eds.), *Encyclopedia of Atmospheric Sciences Science* (Second Edi, pp. 379–386). Oxford: Academic Press. <https://doi.org/https://doi.org/10.1016/B978-0-12-382225-3.00264-4>
- Dickinson, R. E. (2012). Interaction Between Future Climate and Terrestrial Carbon and Nitrogen. In A. Henderson-Sellers & K. B. T.-T. F. of the W. C. (Second E. McGuffie (Eds.), *The Future of the World's Climate* (Second Edi, pp. 289–308). Boston: Elsevier.

<https://doi.org/https://doi.org/10.1016/B978-0-12-386917-3.00011-7>

Dilly, O. (2003). Regulation of the respiratory quotient of soil microbiota by availability of nutrients. *FEMS Microbiology Ecology*, 43(3), 375–381. [https://doi.org/10.1016/S0168-6496\(02\)00437-3](https://doi.org/10.1016/S0168-6496(02)00437-3)

Directive 2000/60/EC. (n.d.). Retrieved December 28, 2018, from https://eur-lex.europa.eu/resource.html?uri=cellar:5c835afb-2ec6-4577-bdf8-756d3d694eeb.0004.02/DOC_1&format=PDF

Directive 2001/81/EC. (n.d.-a). Retrieved February 5, 2019, from <https://eur-lex.europa.eu/legal-content/EN/TXT/PDF/?uri=CELEX:32001L0081&from=EN>

Directive 2001/81/EC. (n.d.-b). Retrieved November 20, 2018, from <https://eur-lex.europa.eu/legal-content/EN/TXT/PDF/?uri=CELEX:32001L0081&from=EN>

Directive 2008/50/EC. (n.d.). Retrieved February 5, 2019, from <https://eur-lex.europa.eu/legal-content/EN/TXT/PDF/?uri=CELEX:32008L0050&from=en>

Directive 2010/75/EU. (n.d.). Retrieved January 28, 2019, from <https://eur-lex.europa.eu/LexUriServ/LexUriServ.do?uri=OJ:L:2010:334:0017:0119:en:PDF>

Directive 91/676/EEC. (n.d.). Retrieved December 28, 2018, from <https://eur-lex.europa.eu/legal-content/EN/TXT/PDF/?uri=CELEX:31991L0676&from=en>

Doyle, B., Cummins, T., Augustenborg, C., & Aherne, J. (2017). *Ambient Atmospheric Ammonia in Ireland, 2013-2014*. Retrieved from [http://www.epa.ie/pubs/reports/research/air/EPA_RR_193_Essentra_web_\(1\).pdf](http://www.epa.ie/pubs/reports/research/air/EPA_RR_193_Essentra_web_(1).pdf)

Du, H., Kong, L., Cheng, T., Chen, J., Yang, X., Zhang, R., ... Ma, Y. (2010). Insights into ammonium particle-to-gas conversion: Non-sulfate ammonium coupling with nitrate and chloride. *Aerosol and Air Quality Research*, 10(6), 589–595. <https://doi.org/10.4209/aaqr.2010.04.0034>

- Duce, R. A., LaRoche, J., Altieri, K., Arrigo, K. R., Baker, A. R., Capone, D. G., ... Zamora, L. (2008). Impacts of atmospheric anthropogenic nitrogen on the open ocean. *Science*, 320(5878), 893–897. <https://doi.org/10.1126/science.1150369>
- Easterling, D. R., Meehl, G. A., Parmesan, C., Changnon, S. A., Karl, T. R., & Mearns, L. O. (2000). Climate Extremes: Observations, Modeling, and Impacts. *Science*, 289(September), 2068–2075.
- El Moujabber, M., Bou Samra, B., Darwish, T., & Atallah, T. (2006). Comparison of different indicators for groundwater contamination by seawater intrusion on the Lebanese coast. *Water Resources Management*, 20(2), 161–180. <https://doi.org/10.1007/s11269-006-7376-4>
- Elderling, A., Solomon, P. A., Salmon, L. G., Fall, T., & Cass, G. R. (1991). Hydrochloric acid: A regional perspective on concentrations and formation in the atmosphere of Southern California. *Atmospheric Environment. Part A. General Topics*, 25(10), 2091–2102. [https://doi.org/10.1016/0960-1686\(91\)90086-M](https://doi.org/10.1016/0960-1686(91)90086-M)
- Environmental Protection Agency. (2011). *Integrated Water Quality Report 2011*. Kilkenny.
- Environmental Protection Agency. (2018). *Water Quality in 2017-An Indicators Report*. Retrieved from [https://www.epa.ie/pubs/reports/water/waterqua/Water Quality in 2017 - an indicators report.pdf](https://www.epa.ie/pubs/reports/water/waterqua/Water%20Quality%20in%202017%20-%20an%20indicators%20report.pdf)
[http://www.epa.ie/pubs/reports/water/waterqua/Water Quality in 2017 - an indicators report.pdf](http://www.epa.ie/pubs/reports/water/waterqua/Water%20Quality%20in%202017%20-%20an%20indicators%20report.pdf)
- Environmental Protection Agency (EPA). (1999). Nitrogen oxides (NO_x), why and how they are controlled. *Epa-456/F-99-006R*, (November), 48. [https://doi.org/EPA 456/F-99-006R](https://doi.org/EPA%20456/F-99-006R)
- Environmental Protection Agency (EPA). (2016). *Chapter 2-Air. Ireland's Environment- An Assessment*. <https://doi.org/10.5040/9780567672407.0009>
- EPA. (2017). *Water quality in 2017: an indicators report*.
- EPA. (2018). *Ireland's Transboundary Gas Emissions 1990-2016*. Retrieved from

- <https://www.epa.ie/pubs/reports/air/airemissions/Irelands Air Pollutant Emissions 2016.pdf>
- EPA. (2019). Water Quality in 2019: An indicators report. *Environmental Protection Agency*, 48.
- Erismann, J. W., Galloway, J. N., Seitzinger, S., Bleeker, A., Dise, N. B., Roxana Petrescu, A. M., ... de Vries, W. (2013). Consequences of human modification of the global nitrogen cycle. *Philosophical Transactions of the Royal Society B: Biological Sciences*, 368(1621).
<https://doi.org/10.1098/rstb.2013.0116>
- European Environment Agency. (2020). 6.4. Suspended particulates. Retrieved from <https://www.eea.europa.eu/publications/2-9167-057-X/page021.html>
- Fanning, A., Craig, M., Webster, P. Bradley, C., Tierney, D., Wilkes, R., Mannix, A. (2017). *Water Quality in Ireland 2010-2015*. (Vol. 306).
- Faria, L. D., do Nascimento, C. A. C., Vitti, G. C., Luz, P. H. D., & Guedes, E. M. S. (2013). Loss of Ammonia from Nitrogen Fertilizers Applied to Maize and Soybean Straw. *Revista Brasileira De Ciencia Do Solo*, 37(4), 969–975. <https://doi.org/10.1590/S0100-06832013000400014>
- Farrell, E. (n.d.). Ammonia monitoring in Ireland: A full year of ammonia monitoring; set-up and results. Retrieved from <http://erc.epa.ie/safer/resource?id=408a1a9a-2072-102f-a0a4-f81fb11d7d1c>
- Fenn, L. B., & Hossner, L. R. (1985). Ammonia Volatilization from Ammonium or Ammonium-Forming Nitrogen Fertilizers. In *Advances in Soil Science* (Vol. I, pp. 123–169).
https://doi.org/10.1007/978-1-4612-5046-3_4
- Fine, P. M., Sioutas, C., & Solomon, P. A. (2008). Secondary particulate matter in the United states: Insights from the particulate matter supersites program and related studies. *Journal of the Air and Waste Management Association*, 58(2), 234–253.
<https://doi.org/10.3155/1047-3289.58.2.234>
- Fioletov, V. E., McLinden, C. A., Krotkov, N., Li, C., Joiner, J., Theys, N., ... Moran, M. D.

- (2016). A global catalogue of large SO₂ sources and emissions derived from the Ozone Monitoring Instrument. *Atmospheric Chemistry and Physics*, 16(18), 11497–11519. <https://doi.org/10.5194/acp-16-11497-2016>
- Flechar, C., Massad, R. S., Loubet, B., & Personne, E. (2013). Advances in understanding models and parameterisations of biosphere-atmosphere ammonia exchange. *Biogeosciences Discussions*, 10(November 2014), 5385–5497. <https://doi.org/10.5194/bgd-10-5385-2013>
- Forbes, P. B. C., & Garland, R. M. (2016). Outdoor Air Pollution. In *Comprehensive Analytical Chemistry* (Vol. 73, pp. 73–96). Elsevier. <https://doi.org/10.1016/BS.COAC.2016.02.004>
- Fowler, D., Coyle, M., Skiba, U., Sutton, M. A., Cape, J. N., Reis, S., ... Voss, M. (2013). The Global Nitrogen Cycle in the Twentyfirst Century. *Philosophical Transactions of the Royal Society B: Biological Sciences*, 368(1621). <https://doi.org/10.1098/rstb.2013.0164>
- Francis-floyd, R., Watson, C., Petty, D., & Pouder, D. B. (2009). Ammonia in Aquatic Systems 1. *Fisheries Research*, 1–5.
- Fuzzi, S., Baltensperger, U., Carslaw, K., Decesari, S., Gon, H. D. Van Der, Facchini, M. C., ... Nazione, C. (2015). Particulate matter , air quality and climate : lessons learned and future needs. *Atmospheric Chemistry and Physics*, 15, 8217–8299. <https://doi.org/10.5194/acp-15-8217-2015>
- Galloway, J. (2005). The global nitrogen cycle: past, present and future. *Science in China. Series C, Life Sciences / Chinese Academy of Sciences*, 48 Suppl 2(326), 669–678. <https://doi.org/10.1360/062005-261>
- Galloway, J. N., Dentener, F. J., Capone, D. G., Boyer, E. W., Howarth, R. W., Seitzinger, S. P., ... Vörösmarty, C. J. (2004). *Nitrogen cycles: Past, present, and future. Biogeochemistry* (Vol. 70). <https://doi.org/10.1007/s10533-004-0370-0>
- Galloway, James N., Schlesinger, W. H., Clark, C. M., Grimm, N. B., Jackson, R. B., Law, B. E., ... Martin, R. (2014). *Biogeochemical cycles. Change Impacts in the United States: The*

- Third National Climate Assessment*. <https://doi.org/10.7930/J0X63JT0.On>
- Galloway, James N., Townsend, A. R., Erisman, J. W., Bekunda, M., Cai, Z., Freney, J. R., ... Sutton, M. A. (2008). Transformation of the Nitrogen Cycle : *Science*, 320(May), 889–892. <https://doi.org/10.1126/science.1136674>
- García-Robledo, E., Corzo, A., & Papaspyrou, S. (2014). A fast and direct spectrophotometric method for the sequential determination of nitrate and nitrite at low concentrations in small volumes. *Marine Chemistry*, 162, 30–36. <https://doi.org/10.1016/j.marchem.2014.03.002>
- Geddes, J. A., & Murphy, J. G. (2012). 10 - The science of smog: a chemical understanding of ground level ozone and fine particulate matter. In F. B. T.-M. S. Zeman (Ed.), *Woodhead Publishing Series in Energy* (pp. 205–230). Woodhead Publishing. <https://doi.org/https://doi.org/10.1533/9780857096463.3.205>
- Geels, C., Andersen, H. V., Ambelas Skjøth, C., Christensen, J. H., Ellermann, T., Løfstrøm, P., ... Hertel, O. (2012). Improved modelling of atmospheric ammonia over Denmark using the coupled modelling system DAMOS. *Biogeosciences*, 9(7), 2625–2647. <https://doi.org/10.5194/bg-9-2625-2012>
- Ghosh, S., Rabha, R., Chowdhury, M., & Padhy, P. K. (2018). Source and chemical species characterization of PM10 and human health risk assessment of semi-urban, urban and industrial areas of West Bengal, India. *Chemosphere*, 207, 626–636. <https://doi.org/10.1016/J.CHEMOSPHERE.2018.05.133>
- Giardina, M., & Buffa, P. (2018). A new approach for modeling dry deposition velocity of particles. *Atmospheric Environment*, 180, 11–22. <https://doi.org/10.1016/J.ATMOSENV.2018.02.038>
- Giardina, M., Buffa, P., Cervone, A., & Lombardo, C. (2019). Dry deposition of particle on urban areas. *Journal of Physics: Conference Series*, 1224(1). <https://doi.org/10.1088/1742-6596/1224/1/012050>

- Gonçalves, J. L. M., & Carlyle, J. C. (1994). Modelling the influence of moisture and temperature on net nitrogen mineralization in a forested sandy soil. *Soil Biology and Biochemistry*, 26(11), 1557–1564. [https://doi.org/10.1016/0038-0717\(94\)90098-1](https://doi.org/10.1016/0038-0717(94)90098-1)
- Gong, L., Lewicki, R., Griffin, R. J., Tittel, F. K., Lonsdale, C. R., Stevens, R. G., ... Flynn, J. H. (2013). Role of atmospheric ammonia in particulate matter formation in Houston during summertime. *Atmospheric Environment*, 77, 893–900. <https://doi.org/10.1016/j.atmosenv.2013.04.079>
- Goodman, A. L., Underwood, G. M., & Grassian, V. H. (2000). A laboratory study of the heterogeneous reaction of nitric acid on calcium carbonate particles. *Journal of Geophysical Research-Atmospheres*, 105(D23), 29053–29064.
- Goulding, K. W. T., Bailey, N. J., Bradbury, N. J., Hargreaves, P., Howe, M., Murphy, D. V., ... Willison, T. W. (1998). Nitrogen deposition and its contribution to nitrogen cycling and associated soil processes. *New Phytologist*, 139(1), 49–58. <https://doi.org/10.1046/j.1469-8137.1998.00182.x>
- Granat, L. (1972). On the relation between pH and the chemical composition in atmospheric precipitation. *Tellus*, 24(6), 550–560. <https://doi.org/10.1111/j.2153-3490.1972.tb01581.x>
- Gray, S., Semiat, R., Duke, M., Rahardianto, A., & Cohen, Y. (2011). Seawater Use and Desalination Technology. *Treatise on Water Science*, 4, 73–109. <https://doi.org/10.1016/B978-0-444-53199-5.00077-4>
- Guiry, E., Beglane, F., Szpak, P., Schulting, R., McCormick, F., & Richards, M. P. (2018). Anthropogenic changes to the holocene nitrogen cycle in Ireland. *Science Advances*, 4(6), 4–9. <https://doi.org/10.1126/sciadv.aas9383>
- Gundersen, P., Callesen, I., & de Vries, W. (1998). Nitrate leaching in forest ecosystems is related to forest floor CN ratios. *Environmental Pollution*, 102(1, Supplement 1), 403–407. [https://doi.org/10.1016/S0269-7491\(98\)80060-2](https://doi.org/10.1016/S0269-7491(98)80060-2)

- Gutiñas, M. E., Leirós, M. C., Trasar-Cepeda, C., & Gil-Sotres, F. (2012). Effects of moisture and temperature on net soil nitrogen mineralization: A laboratory study. *European Journal of Soil Biology*, 48, 73–80. <https://doi.org/10.1016/j.ejsobi.2011.07.015>
- Habibah, N., Dhyana Putri, I. G. A. S., Karta, I. W., Sundari, C. D. W. H., & Hadi, M. C. (2018). A Simple Spectrophotometric Method for the Quantitative Analysis of Phosphate in the Water Samples. *JST (Jurnal Sains Dan Teknologi)*, 7(2), 198. <https://doi.org/10.23887/jst-undiksha.v7i2.13940>
- Hamaoui-Laguel, L., Meleux, F., Beekmann, M., Bessagnet, B., Générumont, S., Cellier, P., & Létinois, L. (2014). Improving ammonia emissions in air quality modelling for France. *Atmospheric Environment*, 92, 584–595. <https://doi.org/10.1016/j.atmosenv.2012.08.002>
- Hämeri, K., Väkevä, M., Hansson, H. C., & Laaksonen, A. (2000). Hygroscopic growth of ultrafine ammonium sulphate aerosol measured using an ultrafine tandem differential mobility analyzer. *Journal of Geophysical Research Atmospheres*, 105(D17), 22231–22242. <https://doi.org/10.1029/2000JD900220>
- Hansen, K., Sørensen, L. L., Hertel, O., Geels, C., Skjøth, C. A., Jensen, B., & Boegh, E. (2013). Ammonia emissions from deciduous forest after leaf fall. *Biogeosciences*, 10(7), 4577–4589. <https://doi.org/10.5194/bg-10-4577-2013>
- Hansen, Karin, Thimonier, A., Clarke, N., Staelens, J., Žlindra, D., Waldner, P., & Marchetto, A. (2013). Chapter 18 - Atmospheric Deposition to Forest Ecosystems. In M. Ferretti & R. B. T.-D. in E. S. Fischer (Eds.), *Forest Monitoring* (Vol. 12, pp. 337–374). Elsevier. <https://doi.org/10.1016/B978-0-08-098222-9.00018-2>
- Hanson, P. J., & Lindberg, S. E. (1991). Dry deposition of reactive nitrogen compounds: A review of leaf, canopy and non-foliar measurements. *Atmospheric Environment Part A, General Topics*, 25(8), 1615–1634. [https://doi.org/10.1016/0960-1686\(91\)90020-8](https://doi.org/10.1016/0960-1686(91)90020-8)

- Harrison, R. M., & Pio, C. A. (1983). An investigation of the atmospheric HNO_3 , NH_3 , NH_4NO_3 equilibrium relationship in a cool, humid climate. *Tellus B*, 35 B(2), 155–159. <https://doi.org/10.1111/j.1600-0889.1983.tb00019.x>
- Haughey, E. (2021). *Climate Change and Land Use in Ireland*. Retrieved from https://www.epa.ie/publications/research/climate-change/Research_Report_371.pdf
- Hawkins, T. W., & Holland, L. A. (2010). Synoptic and Local Weather Conditions Associated With $\text{PM}_{2.5}$ Concentration in Carlisle, Pennsylvania. *Middle States Geographer*, 43, 72–84.
- Haywood, J. (2016). Atmospheric Aerosols and Their Role in Climate Change. In T. M. B. T.-C. C. (Second E. Letcher (Ed.), *Climate Change* (Second Edi, pp. 449–463). Boston: Elsevier. <https://doi.org/https://doi.org/10.1016/B978-0-444-63524-2.00027-0>
- Hemond, H. F., Fechner, E. J., Hemond, H. F., & Fechner, E. J. (2015). The Atmosphere. *Chemical Fate and Transport in the Environment*, 311–454. <https://doi.org/10.1016/B978-0-12-398256-8.00004-9>
- Hennessy, T., Buckley, C., & Cushion, M. (2011). National Farm Survey of Manure Application and Storage Practices on Irish Farms. *Teagasc*, ..., (June). Retrieved from <http://m.teagasc.ie/agcatchments/publications/2011/NFS.pdf>
- Herbert, R. A. (1999). Nitrogen cycling in coastal marine ecosystems. *FEMS Microbiology Reviews*, 23(5), 563–590. [https://doi.org/10.1016/S0168-6445\(99\)00022-4](https://doi.org/10.1016/S0168-6445(99)00022-4)
- Herckes, P., & Collett, J. L. (2015). TROPOSPHERIC CHEMISTRY & COMPOSITION | Cloud Chemistry. In G. R. North, J. Pyle, & F. B. T.-E. of A. S. (Second E. Zhang (Eds.), *Encyclopedia of Atmospheric Sciences* (Second Edi, pp. 218–225). Oxford: Academic Press. <https://doi.org/https://doi.org/10.1016/B978-0-12-382225-3.00030-X>
- Hernandez, G., Berry, T.-A., Wallis, S., & Poyner, D. (2017). Temperature and Humidity Effects on Particulate Matter Concentrations in a Sub-Tropical Climate During Winter.

- International Proceedings of Chemical, Biological and Environmental Engineering*, 102(8), 41–49. <https://doi.org/10.7763/IPCBE>
- Hertel, O., Reis, S., Skjoth, C. A., Bleeker, A., Harrison, R., Cape, J. N., ... Erisman, J. W. (2011). Chapter 09: Nitrogen processes in the atmosphere. *The European Nitrogen Assessment: Sources, Effects and Policy Perspectives*, 177–208. <https://doi.org/http://dx.doi.org/10.1017/CBO9780511976988.012>
- Hill, A. C. (1971). Vegetation: A Sink for Atmospheric Pollutants. *Journal of the Air Pollution Control Association*, 21(6), 341–346. <https://doi.org/10.1080/00022470.1971.10469535>
- Hinman, W. C. (1970). Effects of freezing and thawing on some chemical properties of three soils. *Canadian Journal of Soil Science*, 182(June), 179–182.
- Hocking, M. B., & Hocking, M. B. (2005). Water Quality Measurement. *Handbook of Chemical Technology and Pollution Control*, 105–138. <https://doi.org/10.1016/B978-012088796-5/50007-7>
- Hontoria, C., Saa, A., Almorox, J., Cuadra, L., Sánchez, A., & Gascó, J. M. (2003). The chemical composition of precipitation in Madrid. *Water, Air, and Soil Pollution*, 146(1–4), 35–54. <https://doi.org/10.1023/A:1023964610330>
- Hunt, A., Ferguson, J., Hurley, F., & Searl, A. (2016). Social Costs of Morbidity Impacts of Air Pollution. *Environment Working Papers-OECD*, (99), 0–77. <https://doi.org/10.1787/5jm55j7cq0lv-en>
- Huszár, H., Pogány, A., Bozóki, Z., Mohácsi, Á., Horváth, L., & Szabó, G. (2008). Ammonia monitoring at ppb level using photoacoustic spectroscopy for environmental application. *Sensors and Actuators B: Chemical*, 134(2), 1027–1033. <https://doi.org/https://doi.org/10.1016/j.snb.2008.05.013>
- Hyde, B. P., Carton, O. T., O'Toole, P., & Misselbrook, T. H. (2003). A new inventory of ammonia emissions from Irish agriculture. *Atmospheric Environment*, 37(1), 55–62.

[https://doi.org/10.1016/S1352-2310\(02\)00692-1](https://doi.org/10.1016/S1352-2310(02)00692-1)

Isaksen, I. S. A., Granier, C., Myhre, G., Berntsen, T., Dalsøren, S. B., Gauss, M., ... Wuebbles, D. J. (2012). Chapter 12 - Atmospheric Composition Change: Climate–Chemistry Interactions. In A. Henderson-Sellers & K. B. T.-T. F. of the W. C. (Second E. McGuffie (Eds.) (pp. 309–365). Boston: Elsevier. <https://doi.org/https://doi.org/10.1016/B978-0-12-386917-3.00012-9>

Jaeglé, L., Steinberger, L., Martin, R. V., & Chance, K. (2005). Global partitioning of NO_x sources using satellite observations: Relative roles of fossil fuel combustion, biomass burning and soil emissions. *Faraday Discussions*, 130(December 2013), 407–423. <https://doi.org/10.1039/b502128f>

Jain, R. K., Cui, Z. “Cindy,” Domen, J. K., Jain, R. K., Cui, Z. “Cindy,” & Domen, J. K. (2016). Environmental Impacts of Mining. *Environmental Impact of Mining and Mineral Processing*, 53–157. <https://doi.org/10.1016/B978-0-12-804040-9.00004-8>

Janhäll, S. (2015). Review on urban vegetation and particle air pollution – Deposition and dispersion. *Atmospheric Environment*, 105, 130–137. <https://doi.org/https://doi.org/10.1016/j.atmosenv.2015.01.052>

Jenkinson, D. S. (2001). The impact of humans on the nitrogen cycle, with focus on temperate arable agriculture. *Plant and Soil*, 228(1), 3–15. <https://doi.org/10.1023/A:1004870606003>

Johnson, J. (2008). First Principles. *GUI Bloopers 2.0*, 7–50. <https://doi.org/10.1016/B978-012370643-0.50001-9>

Johnson, P. T. J., Townsend, A. R., Cleveland, C. C., Glibert, P. M., Howarth, R. W., Mckenzie, V. J., ... Johnson, J. (2010). Linking environmental nutrient enrichment and disease emergence in humans and wildlife Published by : Ecological Society of America Linked references are available on JSTOR for this article : Your use of the JSTOR archive indicates your acceptance of the. *Ecological Applications*, 20(1), 16–29.

- Juan, Y., Jiang, N., Tian, L., Chen, X., Sun, W., & Chen, L. (2018). Effect of Freeze-Thaw on a Midtemperate Soil Bacterial Community and the Correlation Network of Its Members. *BioMed Research International*, 2018. <https://doi.org/10.1155/2018/8412429>
- Kane, M. M., Rendell, A. R., & Jickells, T. D. (1994). Atmospheric scavenging processes over the North Sea. *Atmospheric Environment*, 28(15), 2523–2530. [https://doi.org/10.1016/1352-2310\(94\)90402-2](https://doi.org/10.1016/1352-2310(94)90402-2)
- Katata, G., Hayashi, K., Ono, K., Nagai, H., Miyata, A., & Mano, M. (2013). Coupling atmospheric ammonia exchange process over a rice paddy field with a multi-layer atmosphere-soil-vegetation model. *Agricultural and Forest Meteorology*, 180(June 2019), 1–21. <https://doi.org/10.1016/j.agrformet.2013.05.001>
- Kelble, C. R., Loomis, D. K., Lovelace, S., Nuttle, W. K., Ortner, P. B., Fletcher, P., ... Boyer, J. N. (2013). The EBM-DPSER Conceptual Model: Integrating Ecosystem Services into the DPSIR Framework. *PLoS ONE*, 8(8). <https://doi.org/10.1371/journal.pone.0070766>
- Kelleghan, D. B., Hayes, E. T., Everard, M., & Curran, T. P. (2019). Mapping ammonia risk on sensitive habitats in Ireland. *Science of the Total Environment*, 649, 1580–1589. <https://doi.org/10.1016/j.scitotenv.2018.08.424>
- Kelleghan, D. B., Hayes, E. T., Everard, M., Keating, P., Lesniak-Podsiadlo, A., & Curran, T. P. (2021a). Atmospheric ammonia and nitrogen deposition on Irish Natura 2000 sites: Implications for Irish agriculture. *Atmospheric Environment*, 261(July), 118611. <https://doi.org/10.1016/j.atmosenv.2021.118611>
- Kelleghan, D. B., Hayes, E. T., Everard, M., Keating, P., Lesniak-Podsiadlo, A., & Curran, T. P. (2021b). Atmospheric ammonia and nitrogen deposition on Irish Natura 2000 sites: Implications for Irish agriculture. *Atmospheric Environment*, 261(July), 118611. <https://doi.org/10.1016/j.atmosenv.2021.118611>
- Kern, M., & Simon, J. (2011). Chapter nineteen - Production of Recombinant Multiheme

- Cytochromes c in *Wolinella succinogenes*. In M. G. B. T.-M. in E. Klotz (Ed.), *Research on Nitrification and Related Processes, Part A* (Vol. 486, pp. 429–446). Academic Press.
<https://doi.org/https://doi.org/10.1016/B978-0-12-381294-0.00019-5>
- Kesik, M., Blagodatsky, S., Papen, H., & Butterbach-Bahl, K. (2006). Effect of pH, temperature and substrate on N₂O, NO and CO₂ production by *Alcaligenes faecalis* p. *Journal of Applied Microbiology*, 101(3), 655–667. <https://doi.org/10.1111/j.1365-2672.2006.02927.x>
- Kibet, L. C., Saporito, L. S., Allen, A. L., May, E. B., Kleinman, P. J. A., Hashem, F. M., & Bryant, R. B. (2014). A protocol for conducting rainfall simulation to study soil runoff. *Journal of Visualized Experiments*, (86), 1–14. <https://doi.org/10.3791/51664>
- Kim, J., Bauer, H., Dobovičnik, T., Hitzengerger, R., Lottin, D., Ferry, D., & Petzold, A. (2015). Assessing optical properties and refractive index of combustion aerosol particles through combined experimental and modeling studies. *Aerosol Science and Technology*, 49(5), 340–350. <https://doi.org/10.1080/02786826.2015.1020996>
- Kim, N. K., Kim, Y. P., & Kang, C.-H. (2011). Long-term trend of aerosol composition and direct radiative forcing due to aerosols over Gosan: TSP, PM₁₀, and PM_{2.5} data between 1992 and 2008. *Atmospheric Environment*, 45(34), 6107–6115.
<https://doi.org/https://doi.org/10.1016/j.atmosenv.2011.08.051>
- Klein, S. (2006). Measurement of Ammonium by Ion Chromatography In High Sodium Concentration. *The Journal of Undergraduate Research*, 4.
- Klemetsson, L., Von Arnold, K., Weslien, P., & Gundersen, P. (2005). Soil CN ratio as a scalar parameter to predict nitrous oxide emissions. *Global Change Biology*, 11(7), 1142–1147.
<https://doi.org/10.1111/j.1365-2486.2005.00973.x>
- Kluizenaar, Y. De, & Farrell, E. P. (2000). *Ammonia Monitoring in Ireland-A Full Year of Monitoring*.
- Kouznetsov, R., & Sofiev, M. (2012). A methodology for evaluation of vertical dispersion and

- dry deposition of atmospheric aerosols. *Journal of Geophysical Research Atmospheres*, 117(1), 1–19. <https://doi.org/10.1029/2011JD016366>
- Kruit, R. J. W., van Pul, W. A. J., Sauter, F. J., van den Broek, M., Nemitz, E., Sutton, M. A., ... Holtslag, A. A. M. (2010). Modeling the surface-atmosphere exchange of ammonia. *Atmospheric Environment*, 44(7), 945–957. <https://doi.org/10.1016/j.atmosenv.2009.11.049>
- Krupa, S. . (2003). Effects of atmospheric ammonia (NH₃) on terrestrial vegetation: a review. *Environmental Pollution*, 124(2), 179–221. [https://doi.org/10.1016/S0269-7491\(02\)00434-7](https://doi.org/10.1016/S0269-7491(02)00434-7)
- Kulshrestha, U. (2017). Assessment of Atmospheric Emissions and Depositions of Major Nitrogen Species in Indian Region. In *The Indian Nitrogen Assessment: Sources of Reactive Nitrogen, Environmental and Climate Effects, Management Options, and Policies* (pp. 427–444). Elsevier. <https://doi.org/10.1016/B978-0-12-811836-8.00026-4>
- Labiadh, M., Bergametti, G., Kardous, M., Perrier, S., Grand, N., Attoui, B., ... Marticorena, B. (2013). Soil erosion by wind over tilled surfaces in South Tunisia. *Geoderma*, 202–203, 8–17. <https://doi.org/10.1016/J.GEODERMA.2013.03.007>
- Le Roux, G., Hansson, S. V., & Claustres, A. (2016). Chapter 3 - Inorganic Chemistry in the Mountain Critical Zone: Are the Mountain Water Towers of Contemporary Society Under Threat by Trace Contaminants? In G. B. Greenwood & J. F. B. T.-D. in E. S. P. Shroder (Eds.), *Mountain Ice and Water* (Vol. 21, pp. 131–154). Elsevier. <https://doi.org/https://doi.org/10.1016/B978-0-444-63787-1.00003-2>
- Leinert, S., McGovern, F., & Jennin. (2008). *New Transboundary Air Pollution Monitoring Capacity for Ireland. EPA ERC (Environmental Research Centre)*. Johnstown Castle.
- Leip, A., Achermann, B., Billen, G., Bleeker, A., Bouwman, A., de Vries, W., ... Winiwarter, W. (2011). Chapter 16: Integrating nitrogen fluxes at the European scale. *The European*

- Nitrogen Assessment*, 345–376. <https://doi.org/10.129/2003GB002060>.
- Leip, A., Billen, G., Garnier, J., Grizzetti, B., Lassaletta, L., Reis, S., ... Westhoek, H. (2015). Impacts of European livestock production: Nitrogen, sulphur, phosphorus and greenhouse gas emissions, land-use, water eutrophication and biodiversity. *Environmental Research Letters*, 10(11). <https://doi.org/10.1088/1748-9326/10/11/115004>
- Li, C., Frolking, S., & Butterbach-Bahl, K. (2005). Carbon sequestration in arable soils is likely to increase nitrous oxide emissions, offsetting reductions in climate radiative forcing. *Climatic Change*, 72(3), 321–338. <https://doi.org/10.1007/s10584-005-6791-5>
- Liao, N., Jiang, L., Li, J., Zhang, L., Zhang, J., & Zhang, Z. (2019). Effects of Freeze-Thaw cycles on phosphorus from sediments in the middle reaches of the Yarlung Zangbo river. *International Journal of Environmental Research and Public Health*, 16(19). <https://doi.org/10.3390/ijerph16193783>
- Lohmann, U. (2015). AEROSOLS | Aerosol–Cloud Interactions and Their Radiative Forcing. In G. R. North, J. Pyle, & F. B. T.-E. of A. S. (Second E. Zhang (Eds.), *Encyclopedia of Atmospheric Sciences* (Second Edi, pp. 17–22). Oxford: Academic Press. <https://doi.org/https://doi.org/10.1016/B978-0-12-382225-3.00052-9>
- Lohmann, Ulrike, Luond, F., Mahrt, F., Lohmann, U., Luond, F., & Mahrt, F. (2016). Cloud droplet formation and Köhler theory. In *An Introduction to Clouds* (pp. 155–185). Cambridge University Press. <https://doi.org/10.1017/cbo9781139087513.007>
- Loosmore, G. A., & Cederwall, R. T. (2004). Precipitation scavenging of atmospheric aerosols for emergency response applications: Testing an updated model with new real-time data. *Atmospheric Environment*, 38(7), 993–1003. <https://doi.org/10.1016/j.atmosenv.2003.10.055>
- Loubet, B., Sutton, M. A., Milford, C., & Cellier, P. (2001). Investigation of the interaction between sources and sinks of atmospheric ammonia in an upland landscape using a

- simplified dispersion-exchange model. *Journal of Geophysical Research*, 106, 183–195.
- Lovett, G. M. (1994). Atmospheric Deposition of Nutrients and Pollutants in North America. *Ecological Applications*, 4(4), 629–650.
- Mariraj Mohan, S. (2016). An overview of particulate dry deposition: measuring methods, deposition velocity and controlling factors. *International Journal of Environmental Science and Technology*, 13(1), 387–402. <https://doi.org/10.1007/s13762-015-0898-7>
- Martin, N. A., Ferracci, V., Cassidy, N., Hook, J., Battersby, R. M., di Meane, E. A., ... Seitler, E. (2019). Validation of ammonia diffusive and pumped samplers in a controlled atmosphere test facility using traceable Primary Standard Gas Mixtures. *Atmospheric Environment*, 199(February 2018), 453–462. <https://doi.org/10.1016/j.atmosenv.2018.11.038>
- Martin, S. T., Hung, H.-M., Park, R. J., Jacob, D. J., Spurr, R. J. D., Chance, K. V., & Chin, V. (2003). Effects of the physical state of tropospheric ammonium-sulfate-nitrate particles on global aerosol direct radiative forcing. *Atmospheric Chemistry and Physics Discussions*, 3(5), 5399–5467. <https://doi.org/10.5194/acpd-3-5399-2003>
- Martins, H., Monteiro, A., Ferreira, J., Gama, C., Ribeiro, I., Borrego, C., & Miranda, A. I. (2015). The role of ammonia on particulate matter pollution over Portugal. *International Journal of Environment and Pollution*, 57(3/4), 215–226. <https://doi.org/10.1504/IJEP.2015.074505>
- Massad, R.-S., & Loubet, B. (Eds.). (2013). *Review and Integration of Biosphere-Atmosphere Modelling of Reactive Trace Gases and Volatile Aerosols*. Versailles: Springer. <https://doi.org/10.1007/978-94-017-7284-6>
- Massad, R. S., Loubet, B., Tuzet, A., & Cellier, P. (2008). Relationship between ammonia stomatal compensation point and nitrogen metabolism in arable crops: Current status of knowledge and potential modelling approaches. *Environmental Pollution*, 154(3), 390–403. <https://doi.org/10.1016/j.envpol.2008.01.022>

- McGarry, S. J., O'Toole, P., & Morgan, M. A. (1987). Effects of Soil Temperature and Moisture Content on Ammonia Volatilization from Urea-Treated Pasture and Tillage Soils. *Irish Journal of Agricultural Research*, 26(2/3), 173–182. Retrieved from <http://www.jstor.org/stable/25556191>
- McLauchlan, K. K. (2006). Effects of soil texture on soil carbon and nitrogen dynamics after cessation of agriculture. *Geoderma*, 136(1–2), 289–299. <https://doi.org/10.1016/j.geoderma.2006.03.053>
- McMurry, P. H., & Wilson, J. C. (1983). Droplet phase (heterogeneous) and gas phase (homogeneous) contributions to secondary ambient aerosol formation as functions of relative humidity. *Journal of Geophysical Research*, 88(C9), 5101–5108. <https://doi.org/10.1029/JC088iC09p05101>
- McNeil, V. H., & Cox, M. E. (2000). Relationship between conductivity and analysed composition in a large set of natural surface-water samples, Queensland, Australia. *Environmental Geology*, 39(12), 1325–1333. <https://doi.org/10.1007/s002549900033>
- Meng, X., Wu, Y., Pan, Z., Wang, H., Yin, G., & Zhao, H. (2019). Seasonal characteristics and particle-size distributions of particulate air pollutants in Urumqi. *International Journal of Environmental Research and Public Health*, 16(3). <https://doi.org/10.3390/ijerph16030396>
- Menut, L., & Bessagnet, B. (2010). Atmospheric composition forecasting in Europe. *Annales Geophysicae*, 28(1), 61–74. <https://doi.org/10.5194/angeo-28-61-2010>
- Met Éireann. (n.d.). Major Weather Events. Retrieved from <https://www.met.ie/climate/major-weather-events>
- Michalski, R., Pecyna-Utylska, P., & Kernert, J. (2021). Determination of ammonium and biogenic amines by ion chromatography. A review. *Journal of Chromatography A*, 1651, 462319. <https://doi.org/10.1016/j.chroma.2021.462319>
- Milford, C., Theobald, M., Nemitz, E., & Sutton, M. A. (2001). Dynamics of Ammonia Exchange

- in Response to Cutting and Fertilising in an Intensively-Managed Grassland. *Water, Air & Soil Pollution*, 5, 167–176.
- Miller, B. G., & Miller, B. G. (2017). The Effect of Coal Usage on Human Health and the Environment. *Clean Coal Engineering Technology*, 105–144. <https://doi.org/10.1016/B978-0-12-811365-3.00003-X>
- Miller, B., & Miller, B. (2015). Sulfur oxides formation and control. *Fossil Fuel Emissions Control Technologies*, 197–242. <https://doi.org/10.1016/B978-0-12-801566-7.00004-X>
- Misra, P. K., Chan, W. H., Chung, D., & Tang, A. J. S. (1985). Scavenging ratios of acidic pollutants and their use in long-range transport models. *Atmospheric Environment (1967)*, 19(9), 1471–1475. [https://doi.org/10.1016/0004-6981\(85\)90284-7](https://doi.org/10.1016/0004-6981(85)90284-7)
- Moody, J. L., & Galloway, J. N. (1988). Quantifying the relationship between atmospheric transport and the chemical composition of precipitation on Bermuda. *Tellus B*, 40 B(5), 463–479. <https://doi.org/10.1111/j.1600-0889.1988.tb00117.x>
- Morán, M., Ferreira, J., Martins, H., Monteiro, A., Borrego, C., & González, J. A. (2016). Ammonia agriculture emissions: From EMEP to a high resolution inventory. *Atmospheric Pollution Research*, 7(5), 786–798. <https://doi.org/10.1016/j.apr.2016.04.001>
- Mount, G. H., Rumburg, B., Havig, J., Lamb, B., Westberg, H., Yonge, D., ... Kincaid, R. (2002). Measurement of atmospheric ammonia at a dairy using differential optical absorption spectroscopy in the mid-ultraviolet. *Atmospheric Environment*, 36(11), 1799–1810. [https://doi.org/https://doi.org/10.1016/S1352-2310\(02\)00158-9](https://doi.org/https://doi.org/10.1016/S1352-2310(02)00158-9)
- Mukherjee, A., & Agrawal, M. (2017). World air particulate matter: sources, distribution and health effects. *Environmental Chemistry Letters*, 15(2), 283–309. <https://doi.org/10.1007/s10311-017-0611-9>
- Muralikrishna, I. V., & Manickam, V. (2017). *Analytical Methods for Monitoring Environmental Pollution. Environmental Management*. <https://doi.org/10.1016/b978-0-12-811989->

- Nawrot, T. S., Torfs, R., Fierens, F., De Henauw, S., Hoet, P. H., Van Kersschaever, G., ... Nemery, B. (2007). Stronger associations between daily mortality and fine particulate air pollution in summer than in winter: Evidence from a heavily polluted region in western Europe. *Journal of Epidemiology and Community Health*, 61(2), 146–149. <https://doi.org/10.1136/jech.2005.044263>
- Nemitz, E., Sutton, M. A., Gut, A., San, R., Husted, S., & Schjoerring, J. K. (2000). Sources and sinks of ammonia within an oilseed rape canopy. *Agricultural and Forest Meteorology*, 105, 385–404.
- Ng, J. F., Ahmed, O. H., Jalloh, M. B., Omar, L., Kwan, Y. M., Musah, A. A., & Poong, K. H. (2022). Soil Nutrient Retention and pH Buffering Capacity Are Enhanced by Calciprill and Sodium Silicate. *Agronomy*, 12(1), 1–24. <https://doi.org/10.3390/agronomy12010219>
- Nikolov, N., & Zeller, K. (2006). Efficient retrieval of vegetation leaf area index and canopy clumping factor from satellite data to support pollutant deposition assessments. *Environmental Pollution*, 141(3), 539–549. <https://doi.org/10.1016/j.envpol.2005.08.059>
- Norman, M., Spirig, C., Wolff, V., Trebs, I., Flechard, C., Wisthaler, A., ... Neftel, A. (2009). Intercomparison of ammonia measurement techniques at an intensively managed grassland site (Oensingen, Switzerland). *Atmospheric Chemistry and Physics*, 9(8), 2635–2645. <https://doi.org/10.5194/acp-9-2635-2009>
- Nowak, J. B., Neuman, J. A., Bahreini, R., Brock, C. A., Middlebrook, A. M., Wollny, A. G., ... Fehsenfeld, F. C. (2010). Airborne observations of ammonia and ammonium nitrate formation over Houston, Texas. *Journal of Geophysical Research Atmospheres*, 115(22), 1–12. <https://doi.org/10.1029/2010JD014195>
- Okubo, M., & Kuwahara, T. (2020). Chapter 2 - Emission regulations. In M. Okubo & T. B. T.-N. T. for E. C. in M. D. E. Kuwahara (Eds.) (pp. 25–51). Butterworth-Heinemann.

<https://doi.org/https://doi.org/10.1016/B978-0-12-812307-2.00002-X>

- Pacyna, J. M. (2008). Atmospheric Deposition. In *Encyclopedia of Ecology* (pp. 275–285). Academic Press. <https://doi.org/10.1016/B978-008045405-4.00258-5>
- Palmer, J., Thorburn, P. J., Biggs, J. S., Dominati, E. J., Probert, M. E., Meier, E. A., ... Parton, W. (2017). Nitrogen cycling from increased soil organic carbon contributes both positively and negatively to ecosystem services in wheat agro-ecosystems. *Frontiers in Plant Science*, 8(May). <https://doi.org/10.3389/fpls.2017.00731>
- Pan, B., Lam, S. K., Mosier, A., Luo, Y., & Chen, D. (2016). Ammonia volatilization from synthetic fertilizers and its mitigation strategies: A global synthesis. *Agriculture, Ecosystems and Environment*, 232, 283–289. <https://doi.org/10.1016/j.agee.2016.08.019>
- Parsons, T. R., Maita, Y., & Lalli, C. M. (1984). *A Manual of Chemical and Biological Methods for Seawater Analysis*. Elmsford, N.Y.: Pergamon Press. <https://doi.org/https://doi.org/10.1016/C2009-0-07774-5>
- Parush, A. (2015). Conceptual Design: An Overview of the Methodology. *Conceptual Design for Interactive Systems*, 77–78. <https://doi.org/10.1016/B978-0-12-419969-9.00012-7>
- Pathak, R. K., Wu, W. S., & Wang, T. (2009). Summertime PM_{2.5} ionic species in four major cities of China: nitrate formation in an ammonia-deficient atmosphere. *Atmospheric Chemistry and Physics*, 9(5), 1711–1722. <https://doi.org/10.5194/acp-9-1711-2009>
- Pearson, J., & Stewart, G. R. (1993). The deposition of atmospheric ammonia and its effects on plants. *New Phytologist*, 125(2), 283–305. <https://doi.org/10.1111/j.1469-8137.1993.tb03882.x>
- Pedersen, J., Nyord, T., Feilberg, A., & Labouriau, R. (2021). Analysis of the effect of air temperature on ammonia emission from band application of slurry. *Environmental Pollution*, 282, 117055. <https://doi.org/10.1016/J.ENVPOL.2021.117055>
- Petetin, H., Sciare, J., Bressi, M., Gros, V. rie, Rosso, A., Sanchez, O., ... Beekmann, M. (2016).

- Assessing the ammonium nitrate formation regime in the Paris megacity and its representation in the CHIMERE model. *Atmospheric Chemistry and Physics*, 16(16), 10419–10440. <https://doi.org/10.5194/acp-16-10419-2016>
- Phillips, S. B., Arya, S. P., & Aneja, V. P. (2004). Ammonia flux and dry deposition velocity from near-surface concentration gradient measurements over a grass surface in North Carolina. *Atmospheric Environment*, 38(21), 3469–3480. <https://doi.org/10.1016/j.atmosenv.2004.02.054>
- Pleim, J. E., Bash, J. O., Walker, J. T., & Cooter, E. J. (2013). Development and evaluation of an ammonia bidirectional flux parameterization for air quality models. *Journal of Geophysical Research: Atmospheres*, 118(9), 3794–3806. <https://doi.org/10.1002/jgrd.50262>
- Pleim, J. E., Ran, L., Appel, W., Shephard, M. W., & Cady-Pereira, K. (2019). New Bidirectional Ammonia Flux Model in an Air Quality Model Coupled With an Agricultural Model. *Journal of Advances in Modeling Earth Systems*, 11(9), 2934–2957. <https://doi.org/10.1029/2019MS001728>
- Pohl, C., Rey, M., Jensen, D., & Kerth, J. (1999). Determination of sodium and ammonium ions in disproportionate concentration ratios by ion chromatography. *Journal of Chromatography A*, 850(1–2), 239–245. [https://doi.org/10.1016/S0021-9673\(99\)00002-3](https://doi.org/10.1016/S0021-9673(99)00002-3)
- Pollution and Pollution Prevention. (2011). *Handbook of Pollution Prevention and Cleaner Production: Best Practices in the Agrochemical Industry*, 25–79. <https://doi.org/10.1016/B978-1-4377-7825-0.00002-9>
- Poskitt, J. (2017). CEH ALPHA ® Sampler User Instructions.
- Pryor, S. C., & Klemm, O. (2004). Experimentally derived estimates of nitric acid dry deposition velocity and viscous sub-layer resistance at a conifer forest. *Atmospheric Environment*, 38(18), 2769–2777. <https://doi.org/10.1016/j.atmosenv.2004.02.038>
- Pulselli, F. M. (2008). Global Warming Potential and the Net Carbon Balance. In S. E. Jørgensen

- & B. D. B. T.-E. of E. Fath (Eds.) (pp. 1741–1746). Oxford: Academic Press.
<https://doi.org/https://doi.org/10.1016/B978-008045405-4.00112-9>
- Pulselli, F. M., & Marchi, M. B. T.-R. M. in E. S. and E. S. (2015). Global Warming Potential and the Net Carbon Balance☆. Elsevier. <https://doi.org/https://doi.org/10.1016/B978-0-12-409548-9.09526-9>
- Quirós, R. (2003). The relationship between nitrate and ammonia concentrations in the pelagic zone of lakes. *Limnetica*, 22(1–2), 37–50. <https://doi.org/10.23818/limn.22.03>
- Randall, D. A., Albrecht, B., Cox, S., Johnson, D., Minnis, P., Rossow, W., & Starr, D. O. (1996). On Fire at Ten. In R. Dmowska & B. B. T.-A. in G. Saltzman (Eds.) (Vol. 38, pp. 37–177). Elsevier. [https://doi.org/https://doi.org/10.1016/S0065-2687\(08\)60020-5](https://doi.org/https://doi.org/10.1016/S0065-2687(08)60020-5)
- Rey, M. A., Pohl, C. A., Jagodzinski, J. J., Kaiser, E. Q., & Riviello, J. M. (1998). A new approach to dealing with high-to-low concentration ratios of sodium and ammonium ions in ion chromatography. *Journal of Chromatography A*, 804(1–2), 201–209. [https://doi.org/10.1016/S0021-9673\(97\)01271-5](https://doi.org/10.1016/S0021-9673(97)01271-5)
- Rinnan, R., Michelsen, A., Bååth, E., & Jonasson, S. (2007). Fifteen years of climate change manipulations alter soil microbial communities in a subarctic heath ecosystem. *Global Change Biology*, 13(1), 28–39. <https://doi.org/10.1111/j.1365-2486.2006.01263.x>
- Roberts, S. D., Harrington, C. A., & Terry, T. A. (2005). Harvest residue and competing vegetation affect soil moisture, soil temperature, N availability, and Douglas-fir seedling growth. *Forest Ecology and Management*, 205(1), 333–350. <https://doi.org/https://doi.org/10.1016/j.foreco.2004.10.036>
- Rochette, P., Angers, D. A., Chantigny, M. H., Gasser, M. O., MacDonald, J. D., Pelster, D. E., & Bertrand, N. (2013). NH₃ volatilization, soil NH₄⁺ concentration and soil pH following subsurface banding of urea at increasing rates. *Canadian Journal of Soil Science*, 93(2), 261–268. <https://doi.org/10.4141/CJSS2012-095>

- Rosenfeld, D. (2018). Cloud-Aerosol-Precipitation Interactions Based of Satellite Retrieved Vertical Profiles of Cloud Microstructure. In T. Islam, Y. Hu, A. Kokhanovsky, & J. B. T.-R. S. of A. Wang Clouds, and Precipitation (Eds.), *Remote Sensing of Aerosols, Clouds and Precipitation* (pp. 129–152). Elsevier. <https://doi.org/https://doi.org/10.1016/B978-0-12-810437-8.00006-2>
- Rothe, A., Huber, C., Kreutzer, K., & Weis, W. (2002). Deposition and soil leaching in stands of Norway spruce and European beech: Results from the Höglwald research in comparison with other European case studies. *Plant and Soil*, 240(1), 33–45. <https://doi.org/10.1023/A:1015846906956>
- Roy, A., Chatterjee, A., Ghosh, A., Das, S. K., Ghosh, S. K., & Raha, S. (2019). Below-cloud scavenging of size-segregated aerosols and its effect on rainwater acidity and nutrient deposition: A long-term (2009–2018) and real-time observation over eastern Himalaya. *Science of The Total Environment*, 674, 223–233. <https://doi.org/10.1016/J.SCITOTENV.2019.04.165>
- Rusydi, A. F. (2018). Correlation between conductivity and total dissolved solid in various type of water: A review. *IOP Conference Series: Earth and Environmental Science*, 118(1). <https://doi.org/10.1088/1755-1315/118/1/012019>
- Saalidong, B. M., Aram, S. A., Otu, S., & Lartey, P. O. (2022). Examining the dynamics of the relationship between water pH and other water quality parameters in ground and surface water systems. *PLoS ONE*, 17(1 1). <https://doi.org/10.1371/JOURNAL.PONE.0262117>
- Sammur-Bonnici, T. (2008). Complexity theory. In *Wiley Encyclopedia of Management* (Vol. 12, p. 336). John Wiley & Sons, Ltd. <https://doi.org/10.1136/bmj.39602.443785.47>
- Sanhueza, E. (2001). Hydrochloric acid from chlorocarbons: A significant global source of background rain acidity. *Tellus, Series B: Chemical and Physical Meteorology*, 53(2), 122–132. <https://doi.org/10.3402/tellusb.v53i2.16568>

- Santachiara, G., Prodi, F., & Belosi, F. (2013). Atmospheric aerosol scavenging processes and the role of thermo- and diffusio-phoretic forces. *Atmospheric Research*, 128, 46–56. <https://doi.org/10.1016/J.ATMOSRES.2013.03.004>
- Sapek, A. (2013). Ammonia emissions from non-agricultural sources. *Polish Journal of Environmental Studies*, 22(1), 63–70. [https://doi.org/10.1016/S1352-2310\(99\)00362-3](https://doi.org/10.1016/S1352-2310(99)00362-3)
- Saylor, R., Myles, L., Sibble, D., Caldwell, J., & Xing, J. (2015). Recent trends in gas-phase ammonia and PM_{2.5} ammonium in the Southeast United States. *Journal of the Air & Waste Management Association*, 65(3), 347–357. <https://doi.org/10.1080/10962247.2014.992554>
- Schiferl, L. D., Heald, C. L., Nowak, J. B., Holloway, J. S., Neuman, J. A., Bahreini, R., ... Murphy, J. G. (2014). An investigation of ammonia and inorganic particulate matter in California during the CalNex campaign. *Journal of Geophysical Research: Atmospheres*, 119(4), 1883–1902. <https://doi.org/10.1002/2013JD020765>
- Schindlbacher, A., Zechmeister-Boltenstern, S., & Butterbach-Bahl, K. (2004). Effects of soil moisture and temperature on NO, NO₂, and N₂O emissions from European forest soils. *Journal of Geophysical Research D: Atmospheres*, 109(17), 1–12. <https://doi.org/10.1029/2004JD004590>
- Schmohl, A., Miklos, A., & Hess, P. (2020). Detection of ammonia by photoacoustic spectroscopy with semiconductor lasers. *Optical Society of America*, 41(9), 1815–1823.
- Scholz, M., & Scholz, M. (2006). Organic effluent. *Wetland Systems to Control Urban Runoff*, 15–18. <https://doi.org/10.1016/B978-044452734-9/50007-4>
- Schrader, F., Brümmer, C., Flechard, C. R., Kruit, R. J. W., Van Zanten, M. C., Zöll, U., ... Erisman, J. W. (2016). Non-stomatal exchange in ammonia dry deposition models: Comparison of two state-of-the-art approaches. *Atmospheric Chemistry and Physics*, 16(21), 13417–13430. <https://doi.org/10.5194/acp-16-13417-2016>
- Schwab, J. J., Li, Y., Bae, M. S., Demerjian, K. L., Hou, J., Zhou, X., ... Pryor, S. C. (2007). A

- laboratory intercomparison of real-time gaseous ammonia measurement methods. *Environmental Science and Technology*, 41(24), 8412–8419. <https://doi.org/10.1021/es070354r>
- Scott, B. C. (1981). Sulfate Washout Ratios in Winter Storms. *Journal Of Applied Meteorology*, 20(6), 619–625. [https://doi.org/10.1175/1520-0450\(1981\)020<0619:SWRIWS>2.0.CO;2](https://doi.org/10.1175/1520-0450(1981)020<0619:SWRIWS>2.0.CO;2)
- Seigneur, C. (2019). *Air Pollution: Concept, Theory and Application*. (Belin/Humensis, Ed.). Cambridge: Cambridge University Press. <https://doi.org/10.1017/9781108674614>
- Shober, A. L., & Taylor, R. (2015). Nitrogen Cycling in Agriculture, 4. Retrieved from <http://cdn.extension.udel.edu/wp-content/uploads/2015/09/26184951/N-Cycling-in-Agriculture.pdf>
- Silvern, R. F., Jacob, D. J., Kim, P. S., Marais, E. A., Turner, J. R., Campuzano-Jost, P., & Jimenez, J. L. (2017). Inconsistency of ammonium-sulfate aerosol ratios with thermodynamic models in the eastern US: A possible role of organic aerosol. *Atmospheric Chemistry and Physics*, 17(8), 5107–5118. <https://doi.org/10.5194/acp-17-5107-2017>
- Sim Tang, Y., Braban, C. F., Dragosits, U., Simmons, I., Leaver, D., Van Dijk, N., ... Sutton, M. A. (2018). Acid gases and aerosol measurements in the UK (1999-2015): Regional distributions and trends. *Atmospheric Chemistry and Physics*, 18(22), 16293–16324. <https://doi.org/10.5194/acp-18-16293-2018>
- Singh, S. P., Satsangi, G. S., Khare, P., Lakhani, A., Maharaj Kumari, K., & Srivastava, S. S. (2001). Multiphase measurement of atmospheric ammonia. *Chemosphere - Global Change Science*, 3(1), 107–116. [https://doi.org/https://doi.org/10.1016/S1465-9972\(00\)00029-5](https://doi.org/https://doi.org/10.1016/S1465-9972(00)00029-5)
- Skiba, U., Drewer, J., Tang, Y. S., van Dijk, N., Helfter, C., Nemitz, E., ... Sutton, M. A. (2009). Biosphere-atmosphere exchange of reactive nitrogen and greenhouse gases at the NitroEurope core flux measurement sites: Measurement strategy and first data sets. *Agriculture, Ecosystems and Environment*, 133(3–4), 139–149.

<https://doi.org/10.1016/j.agee.2009.05.018>

Skjøth, C. A., & Geels, C. (2013). The effect of climate and climate change on ammonia emissions in Europe. *Atmospheric Chemistry and Physics*, 13(1), 117–128. <https://doi.org/10.5194/acp-13-117-2013>

Skjøth, C. A., Geels, C., Berge, H., Gyldenkaerne, S., Fagerli, H., Ellermann, T., ... Hertel, O. (2011). Spatial and temporal variations in ammonia emissions- a freely accessible model code for Europe. *Atmospheric Chemistry and Physics*, 11(11), 5221–5236. <https://doi.org/10.5194/acp-11-5221-2011>

Smith, E., Gordon, R., Bourque, C., Campbell, A., Générmont, S., Rochette, P., & Mkhabela, M. (2009). Simulated management effects on ammonia emissions from field applied manure. *Journal of Environmental Management*, 90(8), 2531–2536. <https://doi.org/https://doi.org/10.1016/j.jenvman.2009.01.012>

Snider, G., Weagle, C. L., Murdymootoo, K. K., Ring, A., Ritchie, Y., Stone, E., ... Martin, R. V. (2016). Variation in global chemical composition of PM_{2.5}: emerging results from SPARTAN. *Atmospheric Chemistry and Physics*, 16(15), 9629–9653. <https://doi.org/10.5194/acp-16-9629-2016>

Solórzano, L. (1968). Determination of ammonia in natural waters by the phenolhypochlorite method. *Limnology and Oceanography*, 14, 799–801.

Speight, J. G., & Speight, J. G. (2017). Industrial Inorganic Chemistry. *Environmental Inorganic Chemistry for Engineers*, 111–169. <https://doi.org/10.1016/B978-0-12-849891-0.00003-5>

Squizzato, S., Masiol, M., Brunelli, A., Pistollato, S., Tarabotti, E., Rampazzo, G., & Pavoni, B. (2013). Factors determining the formation of secondary inorganic aerosol: A case study in the Po Valley (Italy). *Atmospheric Chemistry and Physics*, 13(4), 1927–1939. <https://doi.org/10.5194/acp-13-1927-2013>

State of Alaska Department of Environmental Conservation. Standard Operating Procedure :

- Laboratory Gravimetric Analysis of Air Quality Filter Samples (2017).
- Stavrakou, T., Müller, J. F., Boersma, K. F., Van Der A., R. J., Kurokawa, J., Ohara, T., & Zhang, Q. (2013). Key chemical NO_x sink uncertainties and how they influence top-down emissions of nitrogen oxides. *Atmospheric Chemistry and Physics*, 13(17), 9057–9082. <https://doi.org/10.5194/acp-13-9057-2013>
- Stevenson, F. J., & Cole, M. A. (1999). *Cycles of Soil (Carbon, Nitrogen Phosphorus Sulfur, Micronutrients)*. New York: Wiley.
- Sutton, M. A., Miners, B., Tang, Y. S., Milford, C., Wyers, G. P., Duyzer, J. H., & Fowler, D. (2001). Comparison of low cost measurement techniques for long-term monitoring of atmospheric ammonia. *Journal of Environmental Monitoring*, 3(5), 446–453. <https://doi.org/10.1039/b102303a>
- Sutton, M. A., Schjorring, J. K., & Wyers, G. P. (1995). Plant-atmosphere exchange of ammonia. *Philosophical Transactions - Royal Society of London, A*, 351(1696), 261–278. <https://doi.org/10.1098/rsta.1995.0033>
- Sutton, M. A., Tang, Y. S., Miners, B., & Fowler, D. (2001). A New Diffusion Denuder System for Long-Term, Regional Monitoring of Atmospheric Ammonia and Ammonium. *Air-Surface Exchange of Gases and Particles (2000)*, 145–156. https://doi.org/10.1007/978-94-010-9026-1_15
- Sutton, M.A., Moncrieff, J. B., & Fowler, D. (1992). Deposition of atmospheric ammonia to moorlands. *Environmental Pollution*, 75(1), 15–24. [https://doi.org/10.1016/0269-7491\(92\)90051-B](https://doi.org/10.1016/0269-7491(92)90051-B)
- Sutton, M.A., Nemitz, E., Erisman, J. W., Beier, C., Bahl, K. B., Cellier, P., ... Reis, S. (2007). Challenges in quantifying biosphere–atmosphere exchange of nitrogen species. *Environmental Pollution*, 150(1), 125–139. <https://doi.org/10.1016/J.ENVPOL.2007.04.014>

- Sutton, M.A., Pitcairn, C. E. R., & Fowler, D. (1993). The Exchange of Ammonia Between the Atmosphere and Plant Communities. *Advances in Ecological Research*, 24, 301–393. [https://doi.org/10.1016/S0065-2504\(08\)60045-8](https://doi.org/10.1016/S0065-2504(08)60045-8)
- Sutton, Mark A., Reis, S., Riddick, S. N., Dragosits, U., Nemitz, E., Theobald, M. R., ... de Vries, W. (2013). Towards a climate-dependent paradigm of ammonia emission and deposition. *Philosophical Transactions of the Royal Society B: Biological Sciences*, 368(1621). <https://doi.org/10.1098/rstb.2013.0166>
- Tang, Y. S., Simmons, I., van Dijk, N., Di Marco, C., Nemitz, E., Dämmgen, U., ... Sutton, M. A. (2009). European scale application of atmospheric reactive nitrogen measurements in a low-cost approach to infer dry deposition fluxes. *Agriculture, Ecosystems and Environment*, 133(3–4), 183–195. <https://doi.org/10.1016/j.agee.2009.04.027>
- Tang, Y S, Stephens, A., Simmons, I., Poskitt, J. P., Warwick, A., Farrand, P., ... Braban, C. F. (2017). DELTA System.
- Tang, Yuk S., Braban, C. F., Dragosits, U., Dore, A. J., Simmons, I., Van Dijk, N., ... Sutton, M. A. (2018). Drivers for spatial, temporal and long-term trends in atmospheric ammonia and ammonium in the UK. *Atmospheric Chemistry and Physics*, 18(2), 705–733. <https://doi.org/10.5194/acp-18-705-2018>
- Tao, W.-K., & Matsui, T. (2015). NUMERICAL MODELS | Cloud-System Resolving Modeling and Aerosols. In G. R. DitionNorth, J. Pyle, & F. B. T.-E. of A. S. (Second E. Zhang (Eds.), *Encyclopedia of Atmospheric Sciences* (Second Edi, pp. 222–231). Oxford: Academic Press. <https://doi.org/https://doi.org/10.1016/B978-0-12-382225-3.00511-9>
- Teagasc. (n.d.). Agriculture in Ireland. Retrieved from <https://www.teagasc.ie/rural-economy/rural-economy/agri-food-business/agriculture-in-ireland/>
- Teagasc. (2011). *Teagasc grazing guide*.
- Teagasc. (2020). Agricultural Emissions- greenhouse gases and ammonia. Retrieved from

- <https://www.teagasc.ie/publications/2020/agricultural-emissions---greenhouse-gases-and-ammonia.php#:~:text=They are not greenhouse gases,fertiliser applications and grazing animals.>
- Teepe, R., Brumme, R., & Beese, F. (2000). Nitrous oxide emissions from frozen soils under agricultural, fallow and forest land. *Soil Biology and Biochemistry*, 32(11–12), 1807–1810. [https://doi.org/10.1016/S0038-0717\(00\)00078-X](https://doi.org/10.1016/S0038-0717(00)00078-X)
- Thomas, D. H., Rey, M., & Jackson, P. E. (2002). Determination of inorganic cations and ammonium in environmental waters by ion chromatography with a high-capacity cation-exchange column. *Journal of Chromatography A*, 956(1–2), 181–186. [https://doi.org/10.1016/S0021-9673\(02\)00141-3](https://doi.org/10.1016/S0021-9673(02)00141-3)
- Tobias, C., & Neubauer, S. C. (2019). Chapter 16 - Salt Marsh Biogeochemistry—An Overview. In G. M. E. Perillo, E. Wolanski, D. R. Cahoon, & C. S. B. T.-C. W. Hopkinson (Eds.) (pp. 539–596). Elsevier. <https://doi.org/https://doi.org/10.1016/B978-0-444-63893-9.00016-2>
- Tonitto, C., Woodbury, P. B., & McLellan, E. L. (2018). Defining a best practice methodology for modeling the environmental performance of agriculture. *Environmental Science & Policy*, 87, 64–73. <https://doi.org/10.1016/J.ENVSCI.2018.04.009>
- Tricker, R., Tricker, S., Tricker, R., & Tricker, S. (1999). Pollutants and contaminants. *Environmental Requirements for Electromechanical and Electronic Equipment*, 158–194. <https://doi.org/10.1016/B978-075063902-6.50010-3>
- Tucker, W. G. (2000). Overview of PM_{2.5} sources and control strategies. *Fuel Processing Technology*, 65, 379–392. [https://doi.org/10.1016/S0378-3820\(99\)00105-8](https://doi.org/10.1016/S0378-3820(99)00105-8)
- U.S.EPA. (2017). Criteria Air Pollutants. Retrieved from https://19january2017snapshot.epa.gov/criteria-air-pollutants_.html
- United Nations Food and Agriculture Organization. (n.d.). Driver-Pressure-State-Impact-Response Framework (DPSIR). Retrieved from <https://www.fao.org/land-water/land/land->

[governance/land-resources-planning-toolbox/category/details/en/c/1026561/](https://doi.org/10.1016/j.landusepol.2016.05.011)

- Vallero, D. A., & Letcher, T. M. (2013). Chapter 8 - Climate. In D. A. Vallero & T. M. B. T.-U. E. D. Letcher (Eds.) (pp. 183–220). Boston: Elsevier.
[https://doi.org/https://doi.org/10.1016/B978-0-12-397026-8.00008-2](https://doi.org/10.1016/B978-0-12-397026-8.00008-2)
- van Breemen, N., & van Dijk, H. F. G. (1988). Ecosystem effects of atmospheric deposition of nitrogen in The Netherlands. *Environmental Pollution*, 54(3–4), 249–274.
[https://doi.org/10.1016/0269-7491\(88\)90115-7](https://doi.org/10.1016/0269-7491(88)90115-7)
- Van Damme, M., Clarisse, L., Dammers, E., Liu, X., Nowak, J. B., Clerbaux, C., ... Coheur, P. F. (2015). Towards validation of ammonia (NH₃) measurements from the IASI satellite. *Atmospheric Measurement Techniques*. <https://doi.org/10.5194/amt-8-1575-2015>
- Van der Swaluw, E., Asman, W. A. H., van Jaarsveld, H., & Hoogerbrugge, R. (2011). Wet deposition of ammonium, nitrate and sulfate in the Netherlands over the period 1992-2008. *Atmospheric Environment*, 45(23), 3819–3826.
<https://doi.org/10.1016/j.atmosenv.2011.04.017>
- Van Oss, R., Duyzer, J., & Wyers, P. (1998). The influence of gas-to-particle conversion on measurements of ammonia exchange over forest. *Atmospheric Environment*, 32(3), 465–471. [https://doi.org/10.1016/S1352-2310\(97\)00280-X](https://doi.org/10.1016/S1352-2310(97)00280-X)
- van Zelm, R., Huijbregts, M. A. J., den Hollander, H. A., van Jaarsveld, H. A., Sauter, F. J., Struijs, J., ... van de Meent, D. (2008). European characterization factors for human health damage of PM₁₀ and ozone in life cycle impact assessment. *Atmospheric Environment*, 42(3), 441–453. <https://doi.org/10.1016/J.ATMOSENV.2007.09.072>
- Vardoulakis, S., Fisher, B. E. A., Gonzalez-Flesca, N., & Pericleous, K. (2002). Model sensitivity and uncertainty analysis using roadside air quality measurements. *Atmospheric Environment*, 36(13), 2121–2134. [https://doi.org/10.1016/S1352-2310\(02\)00201-7](https://doi.org/10.1016/S1352-2310(02)00201-7)
- Vayenas, D. V., Takahama, S., Davidson, C. I., & Pandis, S. N. (2005). Simulation of the

- thermodynamics and removal processes in the sulfate-ammonia-nitric acid system during winter: Implications for PM $<inf>2.5</inf>$ control strategies. *Journal of Geophysical Research Atmospheres*, 110(7), 1–11. <https://doi.org/10.1029/2004JD005038>
- Venkatram, A., & Du, S. (2003). TURBULENT DIFFUSION. *Encyclopedia of Atmospheric Sciences*, 2455–2466. <https://doi.org/10.1016/B0-12-227090-8/00441-3>
- Venkatram, A., & Du, S. (2015). TURBULENCE & MIXING | Turbulent Diffusion. *Encyclopedia of Atmospheric Sciences: Second Edition*, 277–286. <https://doi.org/10.1016/B978-0-12-382225-3.00441-2>
- Vet, R., Artz, R. S., Carou, S., Shaw, M., Ro, C. U., Aas, W., ... Reid, N. W. (2014). A global assessment of precipitation chemistry and deposition of sulfur, nitrogen, sea salt, base cations, organic acids, acidity and pH, and phosphorus. *Atmospheric Environment*. <https://doi.org/10.1016/j.atmosenv.2013.10.060>
- Von Bobruzki, K., Braban, C. F., Famulari, D., Jones, S. K., Blackall, T., Smith, T. E. L., ... Nemitz, E. (2010). Field inter-comparison of eleven atmospheric ammonia measurement techniques. *Atmospheric Measurement Techniques*, 3(1), 91–112. <https://doi.org/10.5194/amt-3-91-2010>
- Walker, J., Spence, P., Kimbrough, S., & Robarge, W. (2008). Inferential model estimates of ammonia dry deposition in the vicinity of a swine production facility. *Atmospheric Environment*, 42(14), 3407–3418. <https://doi.org/https://doi.org/10.1016/j.atmosenv.2007.06.004>
- Walker, J. T., Robarge, W. P., Shendrikar, A., & Kimball, H. (2006). Inorganic PM_{2.5} at a U.S. agricultural site. *Environmental Pollution*, 139(2), 258–271. <https://doi.org/10.1016/J.ENVPOL.2005.05.019>
- Wang, B., Yu, F., Teng, Y., Cao, G., Zhao, D., & Zhao, M. (2022). A SEEC Model Based on the DPSIR Framework Approach for Watershed Ecological Security Risk Assessment: A Case

- Study in Northwest China. *Water (Switzerland)*, 14(1). <https://doi.org/10.3390/w14010106>
- Wang, J., & Ogawa, S. (2015). Effects of meteorological conditions on PM_{2.5} concentrations in Nagasaki, Japan. *International Journal of Environmental Research and Public Health*, 12(8), 9089–9101. <https://doi.org/10.3390/ijerph120809089>
- Wang, P. K. (2002). Scavenging and Transportation of Aerosol Particles by Ice Crystals in Clouds. In *Ice Microdynamics* (pp. 152–196). San Diego: Academic Press. <https://doi.org/https://doi.org/10.1016/B978-012734603-8/50029-6>
- Warneck, P. (1988). *Chemistry of the Natural Atmosphere*. San Diego: Academic Press.
- Wayne, R. P. (2000). *Chemistry of Atmospheres* (Third). New York: Oxford University Press.
- West, J. J., Pilinis, C., Nenes, A., & Pandis, S. N. (1998). Marginal direct climate forcing by atmospheric aerosols. *Atmospheric Environment*, 32(14), 2531–2542. [https://doi.org/https://doi.org/10.1016/S1352-2310\(98\)00003-X](https://doi.org/https://doi.org/10.1016/S1352-2310(98)00003-X)
- Wichink Kruit, R. J., Aben, J., de Vries, W., Sauter, F., van der Swaluw, E., van Zanten, M. C., & van Pul, W. A. J. (2017). Modelling trends in ammonia in the Netherlands over the period 1990–2014. *Atmospheric Environment*, 154, 20–30. <https://doi.org/10.1016/j.atmosenv.2017.01.031>
- Widdison, P. E., & Burt, T. P. (2008). Nitrogen Cycle. In S. E. Jørgensen & B. D. B. T.-E. of E. Fath (Eds.) (pp. 2526–2533). Oxford: Academic Press. <https://doi.org/https://doi.org/10.1016/B978-008045405-4.00750-3>
- Wolf, C., Stephan, A., Fendt, S., & Spliethoff, H. (2017). Measuring gaseous HCl emissions during pulverised co-combustion of high shares of straw in an entrained flow reactor. *Energy Procedia*, 120, 246–253. <https://doi.org/10.1016/j.egypro.2017.07.174>
- Wriedt, G., Spindler, J., Neef, T., Meißner, R., & Rode, M. (2007). Groundwater dynamics and channel activity as major controls of in-stream nitrate concentrations in a lowland catchment system? *Journal of Hydrology*, 343(3–4), 154–168.

<https://doi.org/10.1016/j.jhydrol.2007.06.010>

- Wu, J.-Z., Ge, D.-D., Zhou, L.-F., Hou, L.-Y., Zhou, Y., & Li, Q.-Y. (2018). Effects of particulate matter on allergic respiratory diseases. *Chronic Diseases and Translational Medicine*, 4(2), 95–102. <https://doi.org/10.1016/j.cdtm.2018.04.001>
- Wu, Yanan, Liu, J., Zhai, J., Cong, L., Wang, Y., Ma, W., ... Li, C. (2018). Comparison of dry and wet deposition of particulate matter in near-surface waters during summer. *PLoS One*, 13(6), e0199241/1-e0199241/15. <https://doi.org/10.1371/journal.pone.0199241>
- Wu, Yihua, Walker, J., Schwede, D., Peters-Lidard, C., Dennis, R., & Robarge, W. (2009). A new model of bi-directional ammonia exchange between the atmosphere and biosphere: Ammonia stomatal compensation point. *Agricultural and Forest Meteorology*, 149(2), 263–280. <https://doi.org/https://doi.org/10.1016/j.agrformet.2008.08.012>
- Yang, Q., Easter, R. C., Campuzano-Jost, P., Jimenez, J. L., Fast, J. D., Ghan, S. J., ... Wisthaler, A. (2015). Aerosol transport and wet scavenging in deep convective clouds: A case study and model evaluation using a multiple passive tracer analysis approach. *Journal of Geophysical Research: Biogeosciences*, 120(3), 693–706. <https://doi.org/doi:10.1002/2014JG002832>
- Yao, Z., Zhang, W., Wang, M., Chen, J., Shen, Y., Wei, Y., ... Zeng, H. (2015). Tunable diode laser absorption spectroscopy measurements of high-pressure ammonium dinitramide combustion. *Aerospace Science and Technology*, 45, 140–149. <https://doi.org/https://doi.org/10.1016/j.ast.2015.05.003>
- Yi, Y., Cao, Z., Zhou, X., Xue, L., & Wang, W. (2018). Formation of aqueous-phase secondary organic aerosols from glycolaldehyde and ammonium sulfate/amines: A kinetic and mechanistic study. *Atmospheric Environment*, 181, 117–125. <https://doi.org/10.1016/J.ATMOENV.2018.03.021>
- Zang, L., Wang, Z., Zhu, B., & Zhang, Y. (2019). Roles of relative humidity in aerosol pollution

- aggravation over central China during wintertime. *International Journal of Environmental Research and Public Health*, 16(22). <https://doi.org/10.3390/ijerph16224422>
- Zhang, C. J., Shen, J. P., Sun, Y. F., Wang, J. T., Zhang, L. M., Yang, Z. L., ... He, J. Z. (2017). Interactive effects of multiple climate change factors on ammonia oxidizers and denitrifiers in a temperate steppe. *FEMS Microbiology Ecology*, 93(4), 1–11. <https://doi.org/10.1093/femsec/fix037>
- Zhang, L., Brook, J. R., & Vet, R. (2003). A revised parameterization for gaseous dry deposition in air-quality models. *Atmospheric Chemistry and Physics*, 3(6), 2067–2082. <https://doi.org/10.5194/acp-3-2067-2003>
- Zhang, L., Wright, L. P., & Asman, W. A. H. (2010a). Bi-directional air-surface exchange of atmospheric ammonia: A review of measurements and a development of a big-leaf model for applications in regional-scale air-quality models. *Journal of Geophysical Research Atmospheres*, 115(20). <https://doi.org/10.1029/2009JD013589>
- Zhang, L., Wright, L. P., & Asman, W. A. H. (2010b). Bi - directional air - surface exchange of atmospheric ammonia : A review of measurements and a development of a big - leaf model for applications in regional - scale air - quality models. *Journal of Geophysical Research*, 115, D20310. <https://doi.org/10.1029/2009JD013589>
- Zhang, Y., Seigneur, C., Seinfeld, J. H., Jacobson, M., Clegg, S. L., & Binkowski, F. S. (2000). A comparative review of inorganic aerosol thermodynamic equilibrium modules: similarities, differences, and their likely causes. *Atmospheric Environment*, 34(1), 117–137. [https://doi.org/https://doi.org/10.1016/S1352-2310\(99\)00236-8](https://doi.org/https://doi.org/10.1016/S1352-2310(99)00236-8)
- Zöll, U., Brümmer, C., Schrader, F., Ammann, C., Ibrom, A., Flechard, C. R., ... Kutsch, W. L. (2016). Surface-atmosphere exchange of ammonia over peatland using QCL-based eddy-covariance measurements and inferential modeling. *Atmospheric Chemistry and Physics*, 16(17), 11283–11299. <https://doi.org/10.5194/acp-16-11283-2016>

List of Publications

Bowditch, E., Santopuoli, G., Neroj, B., Svetlik, J., Tominlson, M., Pohl, V., ... João C. (2021). Application of Climate-Smart Forestry – Forest Manager Response to the Relevance of European Definition and Indicators. <http://dx.doi.org/10.2139/ssrn.4038212>

Gómez-Gener, L., Siebers, A. R., Arce, M. I., Arnon, S., Bernal, S., Bolpagni, R., Datry, T., Gionchetta, G., Gossart, H., Mendoza-Lera, C., Pohl, V., ... Zoppini, A. (2021). Towards an improved understanding of biogeochemical processes across surface-groundwater interactions in intermittent rivers and ephemeral streams. *Earth-Science Reviews*, 220. <https://doi.org/10.1016/j.earscirev.2021.103724>

Pohl V., Gilmer A., O'Connor D., McGovern E., Byers V., (Paper in preparation) Ammonia cycling and emerging inorganic secondary fine particulate matter-a review

Pohl V., Gilmer A., O'Connor D. (2018) The role of nitrogen in climate change and agriculture, Environ

Pohl V., Gilmer A., O'Connor D., McGovern E., Byers V. (2018) Hydrology in practice-anthropogenic effects on water quality, National Hydrology Conference

Pohl V., Gilmer A., O'Connor D., McGovern E., Byers V., (2019) The role of nitrogen in climate change and agriculture, Environ

Pohl V., Gilmer A., O'Connor D., McGovern E., Byers V., (2019) Ammonia pollutant effects on terrestrial systems: A simulation model, Second Ecology and Evolution Conference Ireland

Pohl V., Gilmer A., O'Connor D., McGovern E., Byers V., (2019) Fine particulate matter: A critical link between air quality and sustainable management?, Irish Academy of Management Conference

List of Employability and Discipline Skills

To date, the following employability and discipline skills have been attained:

Employability:

1. Data Visualisation
2. Research Methods

Discipline:

1. Classical Mechanics and Thermodynamics
2. Applied Mathematical Modelling in Environment, Food and Health